SEARCH FOR THE NOVEL PROTEIN MARKERS THAT MAY ALLOW EARLY DIAGNOSIS OF BREAST CANCER BY USING COMPARATIVE SEROLOGICAL PROTEOME ANALYSIS OF BREAST CANCER TISSUES

A THESIS SUBMITTED TO THE
GRADUATE SCHOOL OF NATURAL AND APPLIED SCIENCES
OF
KOCAELI UNIVERSITY

BY

KÜBRA KARAOSMANOĞLU YÖNETEN

IN PARTIAL FULFILLMENT OF THE REQUIREMENTS
FOR
THE DEGREE OF DOCTOR OF PHILOSOPHY
IN
BIOMEDICAL ENGINEERING

KOCAELI 2020

SEARCH FOR THE NOVEL PROTEIN MARKERS THAT MAY ALLOW EARLY DIAGNOSIS OF BREAST CANCER BY USING COMPARATIVE SEROLOGICAL PROTEOME ANALYSIS OF BREAST CANCER TISSUES

A THESIS SUBMITTED TO
GRADUATE SCHOOL OF NATURAL AND APPLIED SCIENCES
OF
KOCAELI UNIVERSITY

BY

KÜBRA KARAOSMANOĞLU YÖNETEN

IN PARTIAL FULFILLMENT OF THE REQUIREMENTS
FOR
THE DEGREE OF DOCTOR OF PHILOSOPHY
IN
BIOMEDICAL ENGINEERING

Prof. Dr. Murat KASAP
Supervisor, Kocaeli University .....

Prof. Dr. Serdar KÜÇÜK
Jury member, Kocaeli University .....

Assoc. Prof. Dr. Bekir ÇÖL
Jury member, Muğla Sıtkı Koçman University .....

Prof. Dr. Nihat Zafer UTKAN
Jury member, Kocaeli University .....

Prof. Dr. Berna SARIYAR AKBULUT
Jury member, Marmara University .....

Thesis Defense Date: 27.01.2020

DEDICATION AND ACKNOWLEDGEMENT

I would like to express my deepest gratitude to my supervisor Prof. Murat KASAP for his valuable guidance, encouragement and endless support throughout this research. He has patiently shared his valuable life and work experiences with me, and this has made a priceless contribution to me in making decisions and directing my life. It was a priceless opportunity to meet and work with him.

I would like to express my deep gratitude to Assoc.Prof. Gürler AKPINAR, for his continuous guidance with supporting ideas throughout this research. He has been a second supervisor to me throughout my thesis. He guided and helped me not only in the scientific field but also in all the difficulties that I faced during the doctoral process.

I would like to thank Prof. Nihat Zafer UTKAN for his valuable insights and guidance throughout this research. I would also like to state my gratitude to Prof. Nihat Zafer UTKAN, Op.Dr. Abdullah Güneş and their assistants for the provision of biological materials to the research. This work could not be completed without their contributions.

I appreciate the members of my thesis committee, Assoc.Prof. Bekir Çöl and Prof. Serdar KÜÇÜK for their time and contribution to improve my thesis. I would also like to thank the jury member, Prof. Berna SARIYAR AKBULUT, for her contribution to this thesis and for her time.

I would like to express my deep appreciation and special thanks to my dear friends, Dr. Gülşah YILAN, Eylül Ece İŞLEK CAMADAN, Mehin ZÜLFİGAROVA, Dr. Abula AYIMUGU, and Mehmet SARIHAN, for their friendship, and their endless and priceless support throughout the years. I am also grateful to my other laboratory members, Assist. Prof. Aylin KANLI and Merve Gülsen Bal, for their help and friendship.

I would like to express my deepest love and gratitude to my beloved husband for his endless support and love. I would like to express my deepest love and appreciation to my family for their presence. They have always been with me with their love, support, and faith. I could not be able to complete this thesis without them.

Financial support has been provided by the Scientific and Technological Research Council of Turkey (TUBITAK) under the grant number of 117S218 and Kocaeli University Scientific Research Unit under the grant number of 2018/123.

January-2020 Kübra KARAOSMANOĞLU YÖNETEN

CONTENTS

LIST OF FIGURES

LIST OF TABLES

SYMBOLS AND ABBREVIATIONS

μ : micro
MΩ : Megaohm

Abbreviations

2-DE : Two-dimensional electrophoresis
AKR1C2 : Aldo-keto reductase family 1 member C2
Ambic : Ammonium bicarbonate
ACN : Acetonitrile
AUC : Area under the curve
BC : Breast cancer
CA : Cancer antigen
CA1 : Carbonic anhydrase 1
cCBB : Colloidal Coomassie Brilliant Blue
CCDC13 : Coiled-coil domain protein 13
CEA : Carcinoembryonic antigen
CHO : Chinese hamster ovary
CKs : Cytokeratins
CLU : Clusterin
Cs : Control sera
CsC : Control sera with control tissue proteins
CsT : Control sera with tumour tissue proteins
DP : Dental pulp
DIGE : Difference gel electrophoresis
DTT : Dithiothreitol
ELISA : Enzyme-linked immunosorbent assay
EEF2 : Elongation factor 2
EEFG1 : Elongation factor 1-gamma
ER : Estrogen receptor
E-SERPA : Enhanced-serological proteome analysis
FA : Formic acid
FBS : Fetal bovine serum
FDR : False discovery rate
FPR : False-positive rate
FFAs : Free fatty acids
GAPDH : Glyceraldehyde-3-phosphate dehydrogenase
GPD1 : Glycerol-3-phosphate dehydrogenase 1
H4C1 : Histone H4
HPLC : High-performance liquid chromatography
HeLa : Human cervical cancer cells
HER2 : Human epidermal growth factor receptor 2
HR : Hazard ratio

HRP : Horseradish peroxidase
HSPD1 : 60 kDa heat shock protein
HSP90AA1 : Heat shock protein 90-alpha
IAA : Iodoacetamide
IDC : Invasive ductal carcinoma
IEF : Isoelectric focusing
IF : Immunofluorescence
IHC : Immunohistochemistry
IPG : Immobilized pH gradient
kDa : kilo Dalton
KRT8 : Keratin type II cytoskeletal 8
KRT19 : Keratin type I cytoskeletal 19
kV : kilo Volt
LDH : L-lactate dehydrogenase
LumA : Luminal A
LumB : Luminal B
MAG : Monoacylglycerol
MAGL : Monoacylglycerol lipase
MALDI-TOF : Matrix-assisted laser desorption ionization-time of flight
MCF-7 : Human breast adenocarcinoma cells
MIF : Macrophage migration inhibitory factor
MSC : Mesenchymal stem cells
MS/MS : Tandem mass spectrometry
nLC-MS/MS : nano-liquid chromatography-mass spectrometry
PBS : Phosphate-buffered saline
PCA : Principal Component Analysis
PCL : Primary breast adenocarcinoma cells
PDIA1 : Protein disulfide-isomerase
PK : Pyruvate kinase
PMFs : Peptide mass fingerprints
POSTN : Periostin
PPIA : Peptidyl prolyl cis/trans isomerase A
PR : Progesterone receptor
Ps : Patient sera
PsC : Patient sera with control tissue proteins
PsT : Patient sera with tumour tissue proteins
PTMs : Post-translational modifications
ROC : Receiver Operating Characteristic
RT-PCR : Reverse transcription-polymerase chain reaction
SDS-PAGE : Sodium dodecyl sulphate-polyacrylamide gel electrophoresis
SFRS3 : Splicing factor serine/arginine-rich 3
SH-SY5Y : Human neuroblastoma cells
TAAs : Tumour-associated antigens
TAG : Triacylglycerol
TBS-T : Tris-buffered saline-tween 20
TCA : Tricarboxylic acid cycle
TCGA : The Cancer Genome Atlas
TEMED : Tetramethylethylenediamine
TFA : Trifluoroacetic acid

TN	: Triple-negative
TNBC	: Triple-negative breast cancer
TNM	: Tumour node metastasis
TNR	: True-negative rate
TPR	: True-positive rate
TUBA1C	: alpha-tubulin
UPR	: Unfolded protein response
WB	: Western blotting

MEME KANSER DOKULARINDA KARŞILAŞTIRMALI SEROLOJİK PROTEOM ANALİZİ YAPARAK MEME KANSERİNİN ERKEN TANISINDA KULLANILABİLECEK POTANSİYEL BİYOMARKER MOLEKÜLLERİN ARAŞTIRILMASI

ÖZET

Erken teşhis için uygun tanı araçlarının bulunmaması nedeniyle meme kanseri (MK) insidansı ve mortalite oranları artmaktadır. Proteomik tabanlı çalışmalar ile meme kanserinin erken tanısı ve etkili tedavi yöntemleri için yeni hedefler sunulabilir. Bu çalışmanın amacı, MK tanısına izin verebilecek diagnostik veya prognostik biyobelirteçler keşfetmektir. BC dokuları, bunlara karşılık gelen sağlıklı dokular ve serum örnekleri toplandı ve meme kanseri alt tiplerine ayrıldı. Deneysel yaklaşım olarak, iki boyutlu jel elektroforezi (2-DE) ve floresans jel elektroforezi (DIGE) ile birleştirilmiş matriks destekli lazer desorpsiyonu/iyonizasyonu kütle spektrometresi (MALDI-TOF/TOF) ve serolojik proteom analizi (E-SERPA) ile birleştirilmiş nano sıvı kromatografisi-kütle spektrometresi (n-LC-MS/MS) kullanıldı. Önerilen biyobelirteçlerin prognostik ve diagnostik özelliklerini değerlendirmek için ELISA kullanıldı. Ekspresyon seviyelerinde değişiklik görülen proteinler ile yapılan biyoistatistiksel analizler, GPD1 ve MAGL'ın biyobelirteçler olarak diagnostik ve/veya prognostik özelliklerini kanıtladı. Alfa-tubulin (TUBA1C), siklofilin A (PPIA), histon H4 (H4C1), klasterin (CLU), periostin (POSTN), makrofaj göç inhibitör faktörü (MIF), splicing faktörü serin/arginin açısından zengin 3 (SFRS3) ve coiled coil domain protein 13 (CCDC13), E-SERPA analizi ile tümöre özgü antijenik proteinler olarak tanımlandı. Burada sunulan çalışma, BC alt tiplerinin proteomunda meydana gelen değişiklikleri analiz etmiştir. Bulgular, triaçilgliserol metabolizması ve BC-alt tipleri arasındaki ilişkiye vurgu yaparak ve iki kilit protein olan GPD1 ve MAGL'da meydana gelen değişiklikleri detaylandırdı. SFRS3 ve POSTN proteinlerinin ekspresyon seviyelerindeki belirgin farklılık, MK alt tiplerinde doğrulandı. Bu çalışma, BC metabolizması hakkındaki bilgimizi genişletmemizi ve diagnostik ve/veya prognostik biyobelirteç olma potansiyeli yüksek biyobelirteçler önermemizi sağladı.

Anahtar Kelimeler: Biyomarker Arayışı, Geliştirilmiş-Serolojik Proteome Analizi, MALDI-TOF/TOF, Meme Kanseri Proteomiği, nLC-MS/MS.

SEARCH FOR THE NOVEL PROTEIN MARKERS THAT MAY ALLOW EARLY DIAGNOSIS OF BREAST CANCER BY USING COMPARATIVE SEROLOGICAL PROTEOME ANALYSIS OF BREAST CANCER TISSUES

ABSTRACT

Breast cancer (BC) incidence and mortality rates have been increasing due to the lack of appropriate diagnostic tools for early detection. Proteomics-based studies may provide novel targets for the early diagnosis of BC and efficient treatments. The aim of this study was to discover potential diagnostic/prognostic biomarkers for BC. BC tissues, their corresponding healthy counterparts, and sera samples were collected and subtyped. Two-dimensional gel electrophoresis (2-DE) and difference gel electrophoresis (DIGE) coupled to matrix-assisted laser desorption/ionization mass spectrometry (MALDI-TOF/TOF) and enhanced-serological proteome analysis (E-SERPA) coupled to nano-liquid chromatography-mass spectrometry (nLC-MS/MS) were used as the experimental approaches. ELISA was used to assess the prognostic and diagnostic values of the proposed biomarkers. Biostatistical analyses performed with differentially regulated proteins, GPD1 and MAGL, presented high evidence for their diagnostic and/or prognostic values as biomarkers. Alpha-tubulin (TUBA1C), cyclophilin A (PPIA), histone H4 (H4C1), clusterin (CLU), periostin (POSTN), macrophage migration inhibitory factor (MIF), splicing factor serine/arginine-rich 3 (SFRS3), glyceraldehyde-3-phosphate dehydrogenase (GAPDH) and coiled-coil domain-containing protein 13 (CCDC13) were identified as tumour-associated antigens (TAAs) by E-SERPA assay. The work presented here analysed the changes occurring in the proteome of BC subtypes. The findings emphasized the relationship between triacylglycerol (TAG) metabolism and BC-subtypes and detailed the changes occurring in two key proteins, GPD1 and MAGL. Significant regulation in expression levels of SFRS3 and POSTN was verified in BC subtypes. This work allowed us to extend our knowledge of BC metabolism and propose biomarkers that have high potentials to become diagnostic and/or prognostic biomarkers.

Keywords: Biomarker Discovery, Breast Cancer Proteomics, Enhanced-Serological Proteome Analysis, MALDI-TOF/TOF, nLC-MS/MS.

INTRODUCTION

Despite major advances in health sciences, breast cancer (BC) is still one of the most life-threatening diseases for women. Unfortunately, BC mortality rates have been drastically increasing around the world reaching up to 522.000 deaths in 2017 alone [1]. Luckily, however, not all women who have BC expire. In fact, the overall survival rate is highly dependent on the stage of cancer. For the early-detected and localized tumours (stage I and II), the chance of survival can reach up to 80-90%, while for the late-detected tumours (stage III and IV) the survival rate drops dramatically to as low as 24% [1]. Similarly, when 5-year survival rates were analysed, 92% of stage 0 patients are not affected by the disease [2]. While this rate for stage II patients is 75%, it goes down to 13% in stage IV patients [2]. Overall, these numbers are indicative of the significance of early BC diagnosis and getting appropriate cancer treatment to prevent deaths.

The early diagnosis of BC is dependent on two different tests. One of the tests relies on physical examination and imaging of the breast tissue by a physician or the patient herself. If any suspicious lump is detected, an image of the breast via mammography may be examined to assess the presence of the tumour [3]. The other test may be performed directly on the biopsy material taken from the breast tissue or on the serum sample of the suspected BC patient. For BC, the CA 15-3 (Cancer antigen 15-3), CA 27-29, carcinoembryonic antigen (CEA), estrogen receptor (ER), progesterone receptor (PR), human epidermal growth factor 2 (HER2) are currently the most commonly used biomarkers in the clinic [4]. Each biomarker is a reporter of the special status of breast tumour. For example, CA 15-3 and CA 27-29 are glycoproteins encoded by the genes of the MUC family [5, 6]. Their levels are increased in sera of BC patients, thus representing valuable markers for BC prognosis and therapy monitoring. However, none of these biomarkers is useful for the early diagnosis of BC [7]. Recent efforts to find a biomarker or a group of biomarkers for the early BC detection were not successful, although some novel prognostic biomarkers were proposed [8].

There is an immediate need for a specific BC biomarker or a biomarker panel. Therefore, the aim of this thesis was to search for a novel BC-associated biomarker. A unique approach was designated based on the fact that antibodies were produced by the host's body against a protein that is aberrantly produced in cells. In this context, proteins that are released by the cancer cells can stimulate the immune system and cause the production of autoantibodies. We enhanced an experimental design by purifying autoantibodies and coupling them to magnetic beads so that tumour cell free-extract could be used to capture the antigenic proteins that caused the autoantibody production. Finally, our design allowed us to elute the target proteins of the immune system, tumour-associated antigenic proteins, and identify them via nano-liquid chromatography-mass spectrometry (nLC-MS/MS) analysis.

Venn diagrams were used to demonstrate the presence of antigenic proteins which stimulated the production of autoantibodies by the hosts' immune system. Overall, we were able to identify 9 proteins that were specifically captured by the autoantibodies purified from the serum pool of the BC patients. Those proteins were, namely, alpha-tubulin (TUBA1C), cyclophilin A (PPIA), histone H4 (H4C1), clusterin (CLU), periostin (POSTN), macrophage migration inhibitory factor (MIF), splicing factor serine/arginine-rich 3 (SFRS3), glyceraldehyde-3-phosphate dehydrogenase (GAPDH), and coiled-coil domain-containing protein 13 (CCDC13). Not only the expression differences between the tumour and control protein pools but also the differences among BC tumour subtypes and their corresponding control protein pools were determined by Western Blot analysis (WB). Differential regulations in SFRS3, POSTN, and PPIA were clearly demonstrated. Those proteins displayed significant increases in their expression levels in the tumour tissues in comparison to their corresponding controls. Regulations in TUBA1C, CLU, MIF, and H4C1 were less significant, although noticeable. There was no regulation in the expression level of GAPDH, although GAPDH was selectively captured by the BC patients' autoantibodies.

Two-dimensional gel electrophoresis (2-DE) and difference gel electrophoresis (DIGE) coupled to matrix-assisted laser desorption/ionisation-time of flight mass spectrometry-time of flight (MALDI-TOF/TOF) approaches were performed to understand BC metabolism in detail. Enzyme-linked immunosorbent assay (ELISA)

and WB analyses were used to verify the changes occurring at the protein expression levels. Bioinformatics analyses performed with differentially regulated proteins highlighted the changes occurring in expression levels of glycerol-3-phosphate dehydrogenase 1 (GPD1) and monoacylglycerol lipase (MAGL). The findings emphasized the relationship between triacylglycerol (TAG) metabolism and BC-subtypes and detailed the changes occurring in two key proteins, GPD1 and MAGL. Biostatistical analysis has proved the high diagnostic values of GPD1 and MAGL for BC-associated biomarkers.

1. LITERATURE REVIEW

1.1. BC: Histopathology and Classification

Cancer is a complex disease that is caused by the cells growing uncontrollably. The uncontrolled cell growth is known to be caused by the accumulated mutations in multiple cellular regulatory systems [9]. The accumulation of abnormal cells constitutes a mass of tissue called "tumour". A tumour can have benign (non-cancerous) or malign (cancerous) characteristics. Benign tumours do not invade the surrounding tissue and do not spread to the other parts of the body. Malign tumours, unlike benign tumours, have the ability to invade the surrounding healthy tissues (invasion) and spread to the other parts of the body (metastasis) through lymphatic or circulatory systems [9].

In BC, malignant tumours originate from the cells in the breast. In general, breast tumours are malignancies of epithelial cells of mammary glands that are called "carcinomas" and 90% of all human cancers are carcinomas [9]. Breast carcinomas are classified into two groups based on the place where they occur in the breast. If they occur in the ductal tissue, they are named as "ductal carcinoma" and if they occur in the lobules, they are called "lobular carcinoma" (Figure 1.1., (Memorial Sloan Kettering Cancer Center).

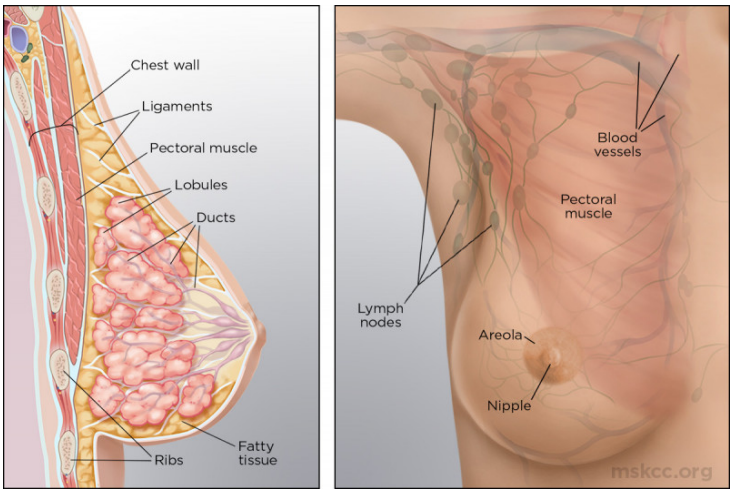

Figure 1.1. The anatomy of the breast

The carcinomas are also classified based on their invasion properties. If they invade the basement membrane, breast carcinomas are called “invasive carcinoma”. If not, they are called “*in situ* carcinoma” [10]. Overall, BC has a comprehensive variety of morphological features, distinct immunohistochemical profiles and histopathological subtypes causing them to display specific clinical courses and outcomes [11]. The histopathological classification of invasive BC based on the recommendations made by Foote and Steward is presented in Table 1.1. [10].

Table 1.1. Classification of invasive BC

No.	Types of breast disease	Incidence (%)
I	Paget’s disease	
II	Invasive ductal carcinoma	
	A. Adenocarcinoma	80
	B. Medullary carcinoma	4
	C. Mucinous carcinoma	2
	D. Papillary carcinoma	2
	E. Tubular carcinoma	2
III.	Invasive lobular carcinoma	10
IV.	Rare cancers (adenoid cystic, squamous cell, apocrine)	

BC classification is important in order to obtain information about the clinical course of the disease and its outcome and to choose the best treatment strategy. In addition to the mentioned classification approaches above, BC can be categorized into sub-categories based on different criteria to determine the stage of the disease. For instance, the traditional approach determines the categories using parameters such as tumour size, lymph node involvement and metastasis. This classification system is called TNM (tumour, node, metastasis) classification and was first presented by Pierre Denoix [12]. The TNM system has been widely accepted around the world and has guided the treatment strategies, enabled the follow-up of the treatment and the prognosis of the disease. Although the TNM classification along with the hormone receptor expression status determined by immunohistochemistry (IHC) provides some benefits, the underlying biology and clinical behaviour of BC subtypes remain elusive [13]. Hence, there have been serious efforts to generate novel classification systems for better clinical outcomes. These efforts resulted in extensive profiling of the DNA, microRNA, and ultimately allowed the creation of BC subtypes [14]. In 2000, it has been shown by Perou et al. that differential gene

expression patterns of BC tumours account for the heterogeneity among breast carcinomas. A molecular classification system has been proposed for BC using the differences in gene expression levels [15]. Based on their system, BC was classified into subgroups, namely "Luminal", "HER2-enriched", "Basal-like" and "Normal breast-like" subtype. Each subtype displays differences in its incidence rate, prognostic properties, response to treatment, preferential metastasis to organs, and recurrence or disease-free survival outcomes [16, 17]. This subtype-based classification system has been used by the St. Gallen International Expert Consensus panel for systemic BC therapies since 2011 [13]. However, a detailed full genetic analysis of BC requires a high budget and extensive resources. Thus, surrogate definitions of the subtype based on semiquantitative IHC scoring of ER, PR, and *in situ* hybridization tests for HER2 overexpression have been proposed [18]. This system called "Molecular classification" and provides the basis for new methods to be used in "personalized" prognostic and predictive tests [19]. The classification system used in this study was the one that was proposed in St. Gallen Consensus in 2013 [13, 18] (Table 1.2.).

Table 1.2. Surrogate definitions of the intrinsic subtypes of BC

	IHC status			
Intrinsic subtype	**ER**	**PR**	**HER2**	**Ki-67 (%)**
Luminal A	+	+	-	<15
	+	-	-	<15
	-	+	-	<15
Luminal B	+	+	-	≥15
	+	-	-	≥15
	-	+	-	≥15
Luminal B-like HER2+	+	+	+	≥15
	+	-	+	≥15
	-	+	+	≥15
TNBC (triple-negative breast cancer)	-	-	-	any
HER2-enriched	-	-	over-expressed	any

(HER2-negative: score 1, score 2; HER2-positive: score 3).

1.2. Global and Regional Statistical Data on the Incidence of BC

According to the data released by the American Cancer Society in 2013, BC is the second leading cause of cancer-related death among women, after lung cancer, in the USA. According to the estimations made by the American Cancer Society, in 2015, approximately 231,840 American women will be diagnosed with BC and there will be 40,290 BC deaths in the USA [20]. In 2019, the number of new cases of BC among women is expected to increase to 331,530, and the number of deaths from BC will increase to 41,760.

In Europe, the scenario is similar to the USA. The incidence rate for BC was reported to be 562,500 in 2018 [21]. It is estimated that 1 in 8 women in the EU will develop BC before the age of 85 [22].

Although Turkey is a Eurasian country, due to its distinct social texture, the BC-related data is different from the European countries. In Turkey, one out of every 4 women diagnosed with cancer has BC. BC was identified to be the most common type of cancer in women with an incidence rate of 43.8 per hundred thousand (Based on the data published by Turkish Ministry of Health's report in September 2018, data for 2015). According to Turkey Cancer Statistics, 44.5% of women diagnosed with BC are between 50-69 years of age, while 40.6% are in the 25-49 age range (Turkish Ministry of Health, data for 2015).

The early diagnosis of BC is one of the most effective ways of reducing deaths from BC. So far, there are no easy to perform genetic or biochemical tests that have been developed for the early diagnosis of BC. The presence of biomarker proteins used by different laboratories in the diagnosis and treatment of BC has been reported in the literature [23]. However, none of these biomarkers is helpful in the early diagnosis of BC. Therefore, there is an urgent need for a biomarker protein or protein panel to allow the early BC diagnosis. The biomarker or the biomarker panel identified may also help the prognosis of the disease, help physicians to estimate whether the patient would develop drug resistance or not and would allow the determination of treatment options. Although there are many published studies regarding biomarker discovery for BC, the absence of such biomarker in clinical use shows that the search for BC biomarkers has not yet reached to its ultimate goal.

1.3. BC Risk Factors

BC risk factors can be grouped into 4 categories. (1) Demographic Factors: Being a woman is the greatest risk factor for BC. The risk of developing BC in woman increases with increasing age. The risk of developing BC in a woman's life span is reported to be 1 in 6 when non-invasive BC is considered and 1 in 8 when invasive BC is considered [24]. The geographical features of the region where the patient lives are also among the demographic factors. (2) Reproductive History: Increased exposure to estrogen increases the risk of developing BC. This is particularly the case with early menarche (age 11 and under) and late menopause (age 55 and later) [25]. Also, the first labour at a late age or being nulliparous women can increase the risk of BC [26]. Lactation is known to reduce the risk of miscarriage or infertility. But the relation of lactation with BC has not been demonstrated. (3) Genetic/familial factors: Several genes that lead to the inheritance of susceptibility to BC have been identified. Among these genes, mutations in the BRCA1/BRCA2, TP53 and pTEN are important [27]. Family history is also a risk factor for BC. Presence of BC in first-degree relatives increases the risk of BC by 1.8 times. (4) Environmental factors: Environmental factors such as socioeconomic status, exercise, radiation exposure esp. to the chest area, hormone replacement therapy, oral contraceptive use, nutritional disorders (such as eating with fatty foods), alcohol consumption and smoking increase the risk of BC [24].

In addition to these factors, some other factors can be considered as risk factors. For example, the increase in body mass index (>30 kg/m2), the presence of breast lesions, previous BC history, dense breast tissue structure, the number of breast biopsy, the use of NSAID group drugs, and even working at night shifts are among the risk factors [29]. However, when the risk factors of BC are taken into consideration, only “being a woman” and“ age ”factors, are directly linked to BC.

1.4. Screening, Diagnosis and Treatment Methods Used in BC

BC is a disease that has a high chance of survival when diagnosed at early stages of cancer. When 5-year survival rates were examined, it was determined that 92% of the patients with stage 0 were not affected by the disease [2]. While this rate is 75% in stage II patients, it decreases to 13% in stage IV patients. Therefore, early detection

of BC is highly important for the treatment of the disease. Routine breast examinations of asymptomatic women who have no complaints of breast pain and mass detection are of great importance for the early diagnosis of BC. Routine breast examination for women esp. over the age of 40 involves mammography, the annual examination by a physician, and monthly self-examination.

If routine controls raise suspicion for BC or if a woman complains about a lump or pain in the breast, then the use of mammography, ultrasonography or magnetic resonance imaging is required [29]. Currently, mammography appears to be the most effective method for the diagnosis of BC. The specificity of mammography is high for patients with fatty breast tissue, whereas it is low for patients with high breast density. In addition to mammography, ultrasonography is used to ascertain the diagnosis of BC patients with higher density breast tissue [29].

Not all breast masses are cancerous 'malign'. Some breast tissues may naturally contain small lumps which undergo biopsy. Laboratory tests on these lumps are performed to reveal the characteristics of the lumps and tell us whether they are non-cancerous 'benign' or malignant tumour tissues. Statistics imply that one-quarter of the breast tumours are malignant tumours that cause BC [30]. The stages of malignant tumours may be determined by evaluating their clinicopathological properties which are based on the tumour size (T1-4), the association of lymph nodes (N1-3) and the existence of distant metastases (M0-1) [31]. These clinicopathological properties are also used to grade the malignant tumours and are often stated in the patient's reports.

Several different approaches have been used to treat BC, such as surgery, radiation treatment (adjuvant or neoadjuvant), endocrine therapy and chemotherapy [32]. For many years, chemotherapy has been the most widely used approach for BC treatment, although it was non-targeted with almost no specificity. Over the past twenty years, specific targeted treatment strategies have evolved depending on the hormone receptor status of the tumour tissue (ER, PR) and expression of the HER2 receptor [33, 34]. Hormone receptor-positive BC tumours express ER and/or PR, and approximately 60% of all BC cases are hormone receptor-positive [34]. ER/PR+ tumours are called "Luminal" and their prognosis is more convenient [14]. Drugs

such as tamoxifen or raloxifene targeting the endocrine system are preferred to treat this subtype [18]. HER-2/neu is over-expressed in approximately 20% of all BC cases. HER2+ tumours respond to Trastuzumab (Herceptin), an inhibitory monoclonal antibody which targets HER2 receptor [14, 18]. Approximately 20% of BC cases lack the expression of ER, PR, and HER-2/neu. These tumours are subtyped as triple-negative (TN) tumours [35, 36]. Since TN tumours suffer from the absence of known drug targets, their prognosis is poor and are often treated by chemotherapy [37, 38].

The subtyping of BC is further detailed when genomic array analyses were considered into account. Based on the analysis of array data, several distinct molecular subtypes of BC were determined. Those subtypes, namely, are luminal A, luminal B, basal, normal breast-like, and HER-2-enriched [15, 39]. Despite the detailed analysis of molecular subtypes, there are still BC subtypes that do not meet the current subtyping criteria. This is mainly because BC is a highly heterogeneous disorder [31]. The future of BC treatment should rely on the development of more personalized treatment strategies that would cause a decrease in morbidity and mortality rates. This is only possible if novel drugs with reduced side effects are developed. Development of novel drugs with reduced side effects requires the discovery of novel target molecules. The discovery of novel tumour markers and drug target molecules are now possible with the availability of omics technologies.

1.5. BC Biomarkers in Clinic

Biomarkers are biochemical indicators that indicate a physiological condition or development of disease [40]. However, an evolved definition of a biomarker has been suggested by the World Health Organization that “A biomarker is any substance, structure or process that can be measured in the body or its products and influence or predict the incidence of outcome or disease.” [41, 42].

According to the areas of utilization, biomarkers can be classified into three main categories; diagnostic, prognostic, and predictive [43]. Diagnostic biomarkers are the markers used to detect the presence of a disease. Prognostic biomarkers are the markers used to track the changes in disease status, the likelihood of recurrence, and the aggression of the tumour. Predictive biomarkers are used to identify patients who

are most likely to respond to the treatment options. Thus, the drug that the patient's body responds can be determined or designed [43]. Biomarkers can be proteins (circulating proteins in plasma or serum, tissue proteins) [44-50], autoantibodies [51-55], microRNAs [56-62], methylated nucleic acids [63-68], lipids [69, 70] and metabolites [71-73].

Serum tumour markers are soluble molecules that are released into the bloodstream by cancer cells or the other cells of the tumour environment [74]. Quantifying the amount of these biomarkers in the patients' blood or serum and correlating the data with the diagnosis and prognosis of the disease is a non-invasive and cost-effective approach [75]. In general, an ideal biomarker should have the following features: (1) should be specific and sensitive for a specific type of tumour (2) should help early diagnosis of the disease (3) provide information about the treatment options (4) provide information about the prognosis of the disease (5) should help to determine the efficacy of the initial treatment (6) should provide hints about the possibility of drug resistance [6, 76, 77].

Many serum markers have been used for the prognosis or prediction of BC, but the ones used to date have not met the expectations for BC screening, early detection or diagnosis [78-80]. The most commonly used BC marker proteins are: CEA, MUC-1 protein, CA 15-3, and CA 27-29, tissue polypeptide antigen, tissue polypeptide specific antigen, circulating cytokeratins (CKs), CK 19 fragment, HER2, ER, PR, urokinase plasminogen activator, plasminogen activator inhibitor 1 [6, 80-85]. P53, cathepsin D, cyclin E and nestin are also used in the screening of BC but they do not have sufficient evidence to be routinely used in clinical practice due to their lack of specificity and sensitivity [77, 86].

1.6. Serum Autoantibodies and BC

Autoantibodies were discovered in 1955 when it was realized that tumour cells could stimulate the immune system against cancer and cause the production of autoantibodies [87]. Later on, the cause for the stimulation was found to be due to the overexpression of tumour-associated proteins, misfolding, partial degradation of proteins, synthesis of the mutant proteins, or alterations in intracellular trafficking of the proteins by the tumour cells [88, 89]. The proteins causing the production of

autoantibodies released from the tumour cells or the cells present in the tumour microenvironment are called Tumour-Associated Antigens (TAAs). After the discovery of autoantibodies and TAAs, interest in this area has considerably increased. It was realized that autoantibodies are indeed developed against various cancer types by the host immune systems [89]. What is more significant about the autoantibodies is that they begin to circulate in the serum as soon as they are being produced, which sometimes occur way before the onset of disease symptoms [90, 91].

Identification of TAAs may allow the early detection of cancer and the elucidation of molecular events occurring at different stages of cancer [92]. The characteristics of TAAs that can be used in the early diagnosis of cancer can be summarized as follows:

- Can be detected in non-symptomatic stages of cancer.
- Serum concentrations can reach to considerably high levels.
- Stable and have a long half-life of up to 7 days which makes sample collection easier and more reliable.

In the literature, TAA panels have been described and used to identify different types of cancers. Those TAAs include c-myc, p53, cyclin-B, p62, Koc, and IMPI [93-95]. Experimental approaches used for the identification of TAAs are presented in Figure 1.2 [89]. Table 1.3 lists the promising potential biomarker proteins for BC and the technologies used for their discoveries [81].

1.7. The Use of Proteomics Technologies in BC Research

The discovery and clinical application of novel tumour markers for cancer screening, diagnosis, and prognosis became one of the main focuses of cancer research [96]. Proteomics, in that sense, has revolutionized the area of cancer research and raised the hopes of finding novel tumour markers and drug targets that would help to fight against various types of cancers [97]. Tissue biopsies, body fluids (plasma, serum, nipple aspirate) and cell lines are the attractive sources for proteomics-based biomarker discovery studies [98]. Identification of differentially regulated proteins isolated from tumour tissues allows the discovery of TAAs and leads to the unveiling of the information about cancer metabolism.

MS-based proteomics approaches in the cancer research area includes gel electrophoresis (1D-PAGE, 2D-PAGE, 2D-DIGE), liquid chromatography (LC/MALDI, LC-MS, LC-MS/MS), 2D-LC or MudPIT, LC-ESI-MS, MS (ESI-MS, MALDI-MS, SELDI-MS) combined with mass analyzers (Q MS, TOF MS, FTICR MS, MALDI-TOF MS, SELDI-TOF MS, ESI-MS/MS) [96].

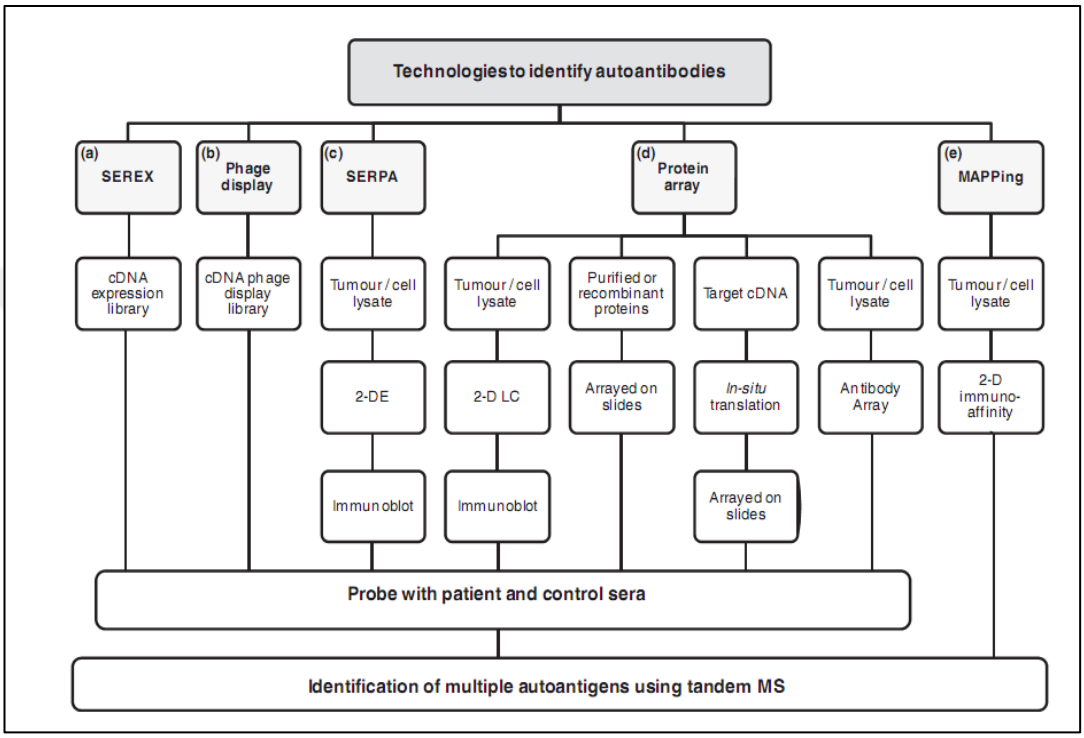

Figure 1.2. Experimental approaches used to identify autoantibodies and their target antigens

The biomarkers discovered by the above proteomics approaches are verified using specific antibodies. The verification methods utilizing antibodies include WB, ELISA, IHC, tissue microarray, forward-phase protein array and reverse-phase protein array [99].

The development of innovative MS-based proteomic technologies and strategies to deeply investigate the cancer cell proteome have revealed a list of potential biomarkers [117]. Some of those studies and discovered potential biomarkers are listed in Appendices Table A.

Table 1.3. List of promising potential biomarker proteins for BC diagnosis

Biomarker	The technology used for discovery	Type	Reference
RS/DJ-1	Immune response	Autoantibody	[100]
P53	Immune response	Autoantibody	[101-104]
Hsp60	Immune response	Autoantibody	[105, 106]
Hsp90	Immune response	Autoantibody	[107, 108]
Mucin-associated	Immune response	Autoantibody	[106, 109-111]
CA 15-3	Serum profiling	Serum protein	[112, 113]
Alpha-2-HS glycoprotein	Nipple aspirate	Ductal protein	[114]
Lipophylline B	Nipple aspirate	Ductal protein	[114]
Beta-globulin	Nipple aspirate	Ductal protein	[114]
Hemopexin	Nipple aspirate	Ductal protein	[114]
Vitamin-D binding protein	Nipple aspirate	Ductal protein	[114]
Topo2alfa	Serum profiling	Protein leaking into serum	[115]
EGFR	Serum profiling	Protein leaking into serum	[115]
Bcl2	Serum profiling	Protein leaking into serum	[115]
MGMT	Serum profiling	Protein leaking into serum	[115]
COX2	Serum profiling	Protein leaking into serum	[115]
Osteopontin	Serum profiling	Protein leaking into serum	[115]

RS-DJ1: Parkinson protein 7, MGMT: O6-Methylguanine-DNA methyltransferase, HSP60: heat shock protein 60, HSP90: heat shock protein 90, EGFR: epidermal growth factor receptor, Bcl2: B-cell lymphoma 2, COX2: Cyclooxygenase 2.

2. MATERIALS AND METHODS

Required components of the buffers and solutions used in this study were included in Appendices Table B1.

2.1. Ethical Approval

This study was approved by the Ethics Committee of Kocaeli University (approval numbers: KOU KAEK 2015/274 and KU GOKAEK 2018/49). Informed consents approved by the institutional ethics committee were obtained from each patient.

2.2. Procurement and Storage of the Tissues

The BC tumour and corresponding healthy tissues were collected from the patients who were diagnosed with BC at Kocaeli University Medical School General Surgery Department and underwent lumpectomy or mastectomy between the years of 2015 and 2017. Immediately after the removal, the breast tissues were washed with ice-cold wash buffer, snap-frozen in liquid nitrogen and stored at -80°C. Blood samples were collected from each patient (n=100) before the surgery, and healthy volunteers (n=20). Collected blood samples were centrifuged at 2000 x g for 10 minutes at room temperature. Serum was separated and stored at -80ºC until analysis.

2.3. Patients' Characteristics

One hundred female BC patients aged between 30-80 years old and diagnosed with invasive ductal carcinoma (IDC) and infiltrative ductal carcinoma were selected, and incorporated into this study. The patients did not receive prior treatment such as endocrine therapy and/or chemotherapy. Clinical parameters of BC patients can be found in Table 2.1.

2.4. Molecular Subtyping of Tumour Samples

Molecular subtyping of tumour samples was performed at Kocaeli University Medical School Pathology department by analysing expressions of ER, PR, HER2,

and Ki-67 proteins. In addition to the mentioned proteins, CK5/6 expression levels of eight patients were also analysed at Kocaeli University Medical School Pathology Department. The expressions of these proteins were evaluated using routine immunohistochemical methods [117]. Based on the expression patterns, the tumour tissues were grouped into five different subtypes, namely Luminal A (ER+ and/or PR+, HER2-, Ki-67<15%); Luminal B (HER2-) (ER+ and/or PR+, HER2-, Ki-67≥15%); Luminal B-like (HER2+) (ER+ and/or PR+, HER2+, Ki-67≥15%); HER2-enriched (ER-, PR-, HER2+); TNBC (ER-, PR-, HER2-) (Table I) [13,18]. In overall, Luminal A (LumA), Luminal B (LumB), Luminal B-like HER2+, HER2-enriched, and TNBC groups consisted of 34, 33, 14, 8, and 11 patients, respectively (Table 2.1.). The control group consisted of 100 samples obtained from healthy breast tissue of BC patients. Detailed information on clinical parameters of BC patients was provided in Appendices Table B2.

Table 2.1. Clinical parameters of BC patients

	BC patients (n)
Molecular subtype	
Luminal A	34
Luminal B	33
Luminal B-like HER2+	14
TNBC	11
HER2-enriched	8
Clinical variables	
Histological tumour type	
Invasive ductal carcinoma	93
Infiltrative ductal carcinoma	7
TNM staging*	
I	13
II	63
III	22
IV	2
Tumour grade**	
1	17
2	56
3	27

* American Joint Committee On Cancer. AJCC Cancer Staging Manual, 6th ed. New York: Springer, 2002, p: 227-228.
** Bloom HJ, Richardson WW. Histological grading and prognosis in breast cancer; A study of 1409 cases of which 359 have been followed for 15 years. British Journal of Cancer. 1957. 11 (3): 359–77.
Scarff RW and Torloni H. Histological typing of breast tumours., International histological classification of tumours, 2(2) World Health Organization, Geneva. 1968. pp. 13-20.

2.5. Preparation of Protein Extracts

Tissue samples were thawed on ice and minced into small pieces (<1.00 mm) and centrifuged for 5 min at 10.000 x g to remove the blood and wash solution. Approximately 200 µl extraction/rehydration buffer was added onto 0.15 g minced tissues and homogenized with Scilogex homogenizer (Rocky hill, CT, USA) for about 10 s at 20000rpm, on ice. Further homogenization was achieved with a bead-beater (Blut blender, Next Advance, Troy, NY, USA) using 0.2-0.8 mm stainless steel beads. The homogenates were centrifuged for 15 min at 10.000 x g to obtain a crude supernatant which was further centrifuged for 45 min at 15.000 x g to obtain a clear protein extract. Protein concentrations were determined by a modified Bradford assay (Bio-Rad, Hercules, CA, USA). After protein extraction, tumour tissue protein extracts and control tissue protein extracts of BC subtypes were pooled into 10 groups and each group was named according to its subtype (e.g. LA tumour pool, LA control pool). For tumour versus control experiments, every five subtypes from the tumour and the control pools were pooled into two groups and named as "tumour pool" and "control pool", respectively. Serum samples of BC patients were also pooled in the same manner as protein extracts were pooled. Serum samples belonged to healthy volunteers (n=20) were also pooled and named as "control sera pool".

2.6. Protein Normalization with a House-keeping Protein

25 µg of protein from BC subtypes and the control protein pool was separated on SDS-PAGE gels and transferred onto nitrocellulose membranes. Actin was selected as the house-keeping protein and the blot was probed with an anti-β-actin antibody. Bands were visualized with an enhanced chemiluminescence detection system (Bio-Rad, USA). ImageJ (https://imagej.nih.gov/ij/index.html) was used for the calculation of band intensities of actin. Protein concentrations in the pools were then recalculated based on the band intensity ratios.

2.7. 2-DE Analysis

Protein extracts (500 µg) were loaded onto 11 cm non-linear pH 3-10 immobilized pH gradient (IPG) strips (Bio-Rad, USA) by passive rehydration. First dimension separation based on isoelectric points was performed with a Protean isoelectric

focusing (IEF) cell (Bio-Rad, USA) using the following conditions: 20 min at 250 V with rapid ramp, 2 h at 4000 V with slow ramp, and 8000 V with rapid ramp until a total of 25.000 V/h was reached, at 20°C. Following IEF, strips were washed with equilibration buffer I for 15 min and then with equilibration buffer II for 15 min at room temperature. Second dimension separation based on molecular weights was achieved by SDS-PAGE (sodium dodecyl sulphate-polyacrylamide gel electrophoresis) (12%) using Criterion Dodeca gel running system (Bio-Rad, USA). Gels were stained with colloidal Coomassie Brilliant Blue (cCBB) and visualized by VersaDoc4000 MP (Bio-Rad, USA) using QuantityOne software (Version 4.6.7, Bio-Rad, USA).

2.8. DIGE Analysis

Protein extracts were pooled in equal amounts and were labelled with CyDye minimal fluors using the CyDye™ DIGE Fluor Minimal Labeling Kit (GE Healthcare, Chicago, IL, USA). The experiments were carried out in dark. In brief, 50 µg protein sample was used in each experiment. The pH of the extracts was adjusted to 8.5 before labelling and protein pools were incubated with the Cy2, Cy3, and Cy5 dyes at 4°C for 30 min. Labelling reactions were stopped by adding 10 mM L-lysine. 2X sample buffer was added to the labelled protein samples and the labelled samples were combined to perform the routine 2-DE experiment.

2.9. Analysis of 2-DE and DIGE Gel Images

The cCBB-stained 2-DE gels were analysed with PDQuest Advance 2-DE Analysis Software (Version 8.0.1 build 055, Bio-Rad, USA) which provided the tools for spot intensity calibration, spot detection, and background subtraction. Two separate gels were run for each pooled group to minimize the experimental variation. Stain speckles were filtered and the standardized areas of interest from all gels were warped and matched. The quantity of each spot was normalized by the total valid spot intensity using the linear regression model. The statistical significance of image analysis was determined by the Student's t-test (statistical level of $p<0.05$ was considered significant). Protein spots with differences in their expressions more than 2-fold were selected and excised from the gels using ExQuest Spotcutter (Bio-Rad, USA). DIGE gels were also visualized with VersaDoc MP4000 (Bio-Rad, USA)

using three different light sources. After automatic spot detection by using PDQuest Advance Analysis Software, spots were manually revised with edition tools to prevent mismatches. Spot picking was performed using a preparative 2-DE gel. The preparative gel was aligned with the DIGE reference image to outline the spots of interest selected during DIGE analysis. All selected spots were excised as described above.

2.10. Cell Culture

CHO (Chinese hamster ovary cells), SH-SY5Y (human neuroblastoma cells), HeLa (human cervical cancer cells) and MCF-7 (human breast adenocarcinoma cells) cell lines were purchased from ATCC (Manassas, VA, USA). DP (dental pulp)-derived mesenchymal stem cells (MSCs) was purchased from Kocaeli University Stem Cell Research Center (KOGEM, Kocaeli, Turkey). The cells were cultured in DMEM low-glucose medium supplemented with 10% fetal bovine serum (FBS), 100 µg/ml penicillin/streptomycin and 2 mM L-glutamine at 37°C in a humidified 5% CO2 atmosphere (All supplements were from Lonza, Basel, Switzerland). Primary breast adenocarcinoma cells (PCL) were isolated using a commercial kit (Cancer Cell Isolation Kit, Thermo Scientific, USA) from a TNBC tissue sample and grown in DMEM high-glucose medium supplemented with 10% heat-inactivated FBS, 100 µg/ml penicillin-streptomycin, 2 mM L-glutamine, and human epidermal growth factor (EGF; 10ng/ml) at 37°C in a humidified 5% CO2 atmosphere. Confluent cells (70-80%) were washed with phosphate-buffered saline (PBS) three times and removed from the plates by scraping. The cell pellet was formed by centrifugation at 1500 x g for 10 min at 4°C. Mammalian protein extraction reagent (M-PER, Thermo Scientific, USA) containing protease inhibitor cocktail (Roche, Indianapolis, IN, USA) was added over each cell pellet and cells were homogenized with a bead-beater using 0.2-0.6 mm stainless steel beads. The soluble protein fraction was obtained by centrifugation at 10.000 x rpm for 10 min and 15.000 x rpm for 45 min at 4°C. Protein concentrations were measured as described above. Protein extracts were stored at −80°C after snap-frozen in liquid nitrogen.

2.11. Immunofluorescence (IF) Microscopy

Cells were grown on culture plates containing 12 mm poly-D-lysine-coated coverslips (Corning, Corning, NY, USA) for IF microscopy. Cells on coverslips were fixed with 3% formaldehyde and permeabilized with PBS containing 0.5% Triton X-100. Anti-GPD1 and anti-MAGL antibodies (Santa Cruz Biotech., USA) were used at a dilution of 1:100. Goat anti-mouse Texas Red antibody (T-6390; Thermo Scientific, USA) was used as the secondary antibody with a dilution of 1:100. The nuclei were stained with DAPI (Molecular Probes, Eugene, OR, USA) (0.5% in PBS) and coverslips were mounted on glass slides using Mowiol®. Cells were observed with an inverted Olympus CKX41 microscope (Olympus, Tokyo, Japan) with appropriate filters. Images were processed using ImageJ software and localization of the proteins was assessed.

2.12. Determination of Serum GPD1 Levels via ELISA

Serum GPD1 levels were determined using a commercially available ELISA kit following the instructions provided by the manufacturer (#MBS9344172, MyBioSource, USA). In brief, the positions for the standards and the blank were assigned to the wells of the ELISA plate and 50 µL from each standard, sample and the diluent (as blank) was added to each corresponding assigned well. 100 µL horseradish peroxidase (HRP)-conjugate reagent was added to each well and the plate was covered and incubated at 37 ° C for 60 minutes. All wells were washed 4 times and 50 µL of Chromogen A and 50 µL of Chromogen B solutions were added to each well and incubated at 37°C in the dark for 10 minutes. At the end of the incubation, 50 µL of stop solution was added to each well to stop the reaction and optical density was read at 450 nm within 15 minutes. Protein concentrations were determined using the optical density of known standards.

2.13. Determination of Serum MAGL Levels via ELISA

Serum MAGL levels were determined using a commercially available ELISA kit following the instructions provided by the manufacturer (#MBS167556, MyBioSource, USA). In brief, the positions for the standards and the blank were assigned to the wells of the ELISA plate and 50 µL from each standard, 40 µL of

sample and 10 µL of anti-MAGL antibody were added to each corresponding assigned well. 50 µL of streptavidin-HRP was added to each well and the plate was covered and incubated at 37°C for 60 minutes. All wells were washed 5 times for 1 min each and 50 µL of substrate solution A and substrate solution B were added to each well and incubated at 37°C and 10 min in the dark. 50 µL of stop solution was added to each well and optical density was read at 450 nm within 10 minutes. Protein concentrations were determined using the optical density of known standards.

2.14. Enhanced-Serological Proteome Analysis (E-SERPA)

2.14.1. Determination and optimization of the antigen-capture conditions used in E-SERPA

E-SERPA assay consisted of several experimental steps. The steps of E-SERPA included (1) antiboy purification, (2) antibody coupling to the magnetic beads, (3) autoantigen capture and (4) elution of the captured antigens. Each step required optimization to efficiently capture and identify the target protein (antigen). At this point, it is important to note that optimization of E-SERPA assay conditions was only possible with the availability of a purified highly specific antibody and its purified antigen. In here, a purified in-house produced antibody (Clone 1D11G8) that specifically recognized and bound to human CK-MB protein as the antigen was used. This antibody was produced in Kocaeli Univesity Antibody Production Laboratory during a project that was supported by MARKA (Project no: TR42/13/GPD/1). Commercially available CK-MB protein was bought from Lee Biosciences (MA, USA). The optimized conditions were mentioned below with the letters in parentheses. For the optimization of one variable, all of the other variables were kept constant in optimization experiments.

- Determination of binding buffer (Variable C): Variable C was optimized to select a suitable buffer for E-SERPA assay which allows the formation of autoantibody/autoantigen complex and reduces non-specific binding.
- The amount of pure CK-MB protein (amount of antigen in optimization experiments) (Variable G, was only used in optimization experiments): Variable G was optimized to determine the efficiency of the method.

- The amount of antigen (Breast tissue protein extract) (Variable F): The amount of antigen was optimized to obtain the sufficient amount of antigenic proteins which allow them to be identified by mass spectrometric analysis.
- The volume of antibody-coupled magnetic beads (Variable A): Variable A was optimized to increase the amount of captured antigen.
- The amount of antibody coupled magnetic beads (Variable B): Variable B was optimized to obtain saturated magnetic beads before incubation with antigens and to increase the amount of captured antigen.
- Incubation time for the formation of antibody/antigen complex (Variable D): Incubation time was optimized for the efficient formation of the antibody/antigen complex.
- Incubation temperature for the formation of antibody/antigen complex (Variable E): Variable E was optimized for the efficient formation of the antibody/antigen complex.
- Elution method (Variable H): Elution method was optimized to separate antigens from the antibody/antigen complex at maximum yield and to ensure their identification in protein identification step.

Throughout the optimization experiments, the results of the optimized conditions were presented by various methods. Of these methods, SDS-PAGE and WB were used to demonstrate that CK-MB protein interacted with CKMB antibody. MALDI-TOF/TOF and LC-MS/MS were used to demonstrate that CK-MB protein was successfully captured and identified by MS analysis.

2.14.2. Antibody purification

Antibodies from the tumour and control sera pools were purified via NGC Chromatography system (Bio-Rad, USA) using HiTrap Protein G, HP column (#17-0404, GE Healthcare, USA). Briefly, sera samples were diluted with the binding buffer for antibody purification. The column was equilibrated with the binding buffer before the sample application. Unbound materials were washed away with 10 column volumes of binding buffer. Bound proteins were eluted with elution buffer in 0.5 mL fractions. Neutralization buffer was immediately added to the fractions to obtain neutral pH.

2.14.3. Antibody coupling

Dynabeads® Antibody Coupling Kit (#14311D, Thermo Fisher Scientific, Massachusetts, ABD) was used for the coupling of antibodies to the magnetic beads following the instructions provided by the manufacturer. In brief, purified antibodies were bound to dry Dynabeads® M-270 Epoxy magnetic beads on a roller at 37°C overnight using C1 and C2 buffers supplied by the manufacturer (Dilution: 30 µg antibody/mg bead). Unbound and/or non-specific materials were removed by repeated washing steps. Antibody-coupled beads were then collected using a magnetic stand and resuspended in SB buffer supplied by the manufacturer. The final bead concentration used in immune capture experiments were 10 mg antibody-coupled bead/mL.

2.14.4. Autoantigen capture

Commercially available buffer (IP buffer, #87787, Thermo Scientific, USA) was used for the preparation of immune complexes and the washing steps during immune capturing. Patient sera-coupled beads (Ps) from BC patients and control sera-coupled beads (Cs) from healthy donors were used to capture antigenic proteins from the protein extracts prepared from the tumour (PsT and CsT, respectively) and control tissues (PsC and CsC, respectively). 100 µL antibody-coupled beads (Ps or Cs) were incubated with 4 mg of tissue protein extracts in 1 mL IP buffer on a rocking platform at 4ºC for overnight. Unbound proteins were removed by washing the immune complexes with 500 µL IP buffer three times and ultrapure water once. Immune complexes were prepared as follows:

(1) Ps was incubated with the proteins extracted from BC tumour tissues (PsT). This complex was formed to capture the autoantigens.
(2) Ps was incubated with the proteins extracted from control tissues (PsC). This complex was formed as the control to determine false positives.
(3) Cs was incubated with the proteins extracted from BC tumour tissues (CsT). This complex was formed as the control to determine non-specific immune captures.

(4) Cs was incubated with the proteins extracted from control tissues (CsC). This complex was formed as the control to determine non-specifically captured antigens in.

(5) Ps (only the coupled beads). This complex was formed to eliminate the impurities that may have coupled to the beads and to eliminate the antibodies that were co-eluted with the antigen (negative control).

(6) Cs (only the coupled beads). This complex was formed to eliminate the impurities that may have coupled to the beads and to eliminate the antibodies that were co-eluted with the antigen (negative control).

2.14.5. Elution of captured antigens

To elute immune-captured antigenic proteins from the autoantibody-coupled beads, 50 mM ammonium bicarbonate (Ambic) containing 6 mM dithiothreitol (DTT) was directly added onto the beads. The antigenic proteins were then eluted by incubating the beads at 95ºC.

2.15. In-gel Tryptic Digestion

In-gel tryptic digestion was performed using the in-gel tryptic digestion kit (Thermo Fisher Scientific, USA) according to the instructions provided by the manufacturer. The digested peptides were then desalted and concentrated using C18 ZipTips (Millipore, Burlington, MA, USA). Peptides were eluted with a matrix solution and were spotted onto the MALDI target plate.

2.16. In-solution Tryptic Digestion

In-solution digestion was performed according to the manufacturer's instructions using ‘in-solution tryptic digestion and guanidination kit (#89895, Thermo Fisher Scientific, USA). The protocol can be briefly summarized as follows: 0.025-10 µg protein sample was added to 15 µL 50 mM Ambic and 1.5 µL 100 mM DTT mixture. The volume was completed to 27 µL and incubated at 95ºC for 5 min. Iodoacetamide (IAA) was added to the protein sample with 10 mM final concentration and incubated in the dark for 20 min. 1 µL of 100ng/µL trypsin was added to the protein sample and incubated for 3 hours at 37ºC. 1 µL of 100ng/µL trypsin was more added

to the peptide mixture and incubated overnight at 30ºC. After incubation, the solution was vacuum concentrated to dryness and the peptides were dissolved in 0.1% formic acid (FA) for the nLC-MS/MS analysis.

2.17. Tandem Mass Spectrometry (MS/MS)

2.17.1. MALDI-TOF/TOF analysis

Peptide-mass fingerprints (PMFs) were collected using AB SCIEX TOF/TOF 5800 instrument (AB Sciex, Framingham, MA, USA). The TOF spectra were recorded in the positive ion reflector mode with a mass range from 400 to 2000 Da. Each spectrum was the cumulative average of 200 laser shots. Ten of the strongest peaks of the MS spectrums per spot were chosen for MS/MS analysis.

2.17.2. Nano-liquid chromatography-mass spectrometry (nLC-MS/MS) analysis

The peptides were analysed by nLC-MS/MS using an Ultimate 3000 RSLC nanosystem (Dionex, Thermo Scientific, USA) coupled to a Q Exactive mass spectrometer (Thermo Scientific, USA). The entire system was controlled by Xcalibur 4.0 software (Thermo Fisher Scientific, USA).

High-performance liquid chromatography (HPLC) separation was performed using mobiles phases A and B. Digested peptides were pre-concentrated and desalted on trap column. Then the peptides were transferred to an Acclaim PepMap RSLC C18 analytical column (75 µmx15 cmx2 µm, 100 Å diameter, Thermo Scientific, USA). The gradient for separation was 6-20% B in 45 min, 20-40% B in 30 min, 40-90% B in 15 min, 90% in 30 min, 90-6% B in 5 min and 6% B for 10 min with the flow rate of 300 nL/min. Full scan MS spectra were acquired with the following parameters: resolution 70.000, scan range 400-2000 m/z, target automatic gain control "AGC" 3×10^6, maximum injection time 60 ms, spray voltage 2.3 kV. MS/MS analysis was performed by data-dependent acquisition selecting the top ten precursor ions. The instrument was calibrated using a standard positive calibrant (LTQ Velos ESI Positive Ion Calibration Solution 88323, Pierce, USA) prior to each analysis.

2.18. MS/MS Data Analysis

2.18.1. MALDI-TOF/TOF data analysis

All PMFs were searched in the MASCOT database (Matrix Science, Boston, MA, USA) using ProteinPilot software 4.0.8085 revision 148085 (AB Sciex, Framingham, MA, USA). Search parameters included; human as taxonomy, trypsin as the enzyme, ±50 ppm as the precursor tolerance, ±0.4 Da as the MS/MS fragment tolerance, and carbamidomethyl and MetOxidation as the variable modifications. Only hits with $p<0.05$ value were accepted for protein determination.

2.18.2. nLC-MS/MS data analysis

Raw data were analysed with Proteom Discoverer 2.2 (Thermo Scientific, USA) software for protein identification and the following parameters were used: peptide mass tolerance 10 ppm, MS/MS mass tolerance 0.2 Da, mass accuracy 2 ppm, tolerant miscarriage 1, minimum peptide length 6 amino acids, fixed changes cysteine carbamidomethylation, unstable changes methionine oxidation and asparagine deamination. The minimum number of peptides identified for each protein was considered to be 2 and obtained data were searched in the Uniprot/Swissprot database.

2.19. WB Analysis

Proteins were separated by SDS-PAGE (12%) and transferred onto a nitrocellulose membrane (GE Healthcare, Chicago, IL, USA) using a Trans-Blot SD Semi-Dry Transfer Cell (Bio-Rad, USA). The membrane was blocked in TBS-T (Tris-buffered saline-Tween 20) containing 5% non-fat dry milk for 1 h at room temperature and washed with TBS-T for three times before incubation with a primary antibody diluted in TBS-T for 1 h at room temperature or overnight at 4°C (See Appendices Table B3 for primary antibodies used throughout the study). The membrane was then washed three times with TBS-T and incubated with appropriate HRP-labelled secondary antibodies (goat anti-mouse #170-5047, goat anti-rabbit #170-5046, Bio-Rad, USA) for 1 h at room temperature with 1:10.000 dilution). Following subsequent three washes with TBS-T, protein bands were visualized with an enhanced chemiluminescence detection system (Bio-Rad, USA). Membranes were

stripped using Restore™ WB stripping buffer (#21059, Thermo Scientific, USA) when necessary. Either QuantityOne (Bio-Rad, USA) or ImageJ (https://imagej.nih.gov/ij/index.html) was used for the relative quantitative assessments of the band intensities.

2.20. Bioinformatics Analysis

STRING analysis (https://string-db.org) was carried out using the UniProt accession numbers of the regulated proteins. The search engine option was set to "multiple proteins by names/identifiers" and the organism was specified as *Homo sapiens*. The retrieved proteins were manually checked to assure that they were all correctly retrieved from the database. The whole-genome analysis was the preferred choice. The setting tab was used to change the stringency of the analysis. The parameters for STRING search included interaction score of medium confidence, the selected maximum number of interactors for the 1st and 2nd shells of no more than 5 interactors, active interaction sources of text mining, experiments, databases, co-expression, neighbourhood, gene fusion and co-occurrence. The hits considered in this study had False Discovery Rates (FDR) smaller then 1e-04.

DAVID analysis (version 6.8; David Bioinformatics Resources, https://david.ncifcrf.gov) was carried out using the UniProt accession numbers of the regulated proteins. Principal component analysis (PCA) was performed using the add-in statistical software XLSTAT (Addinsoft, New York, NY, USA). Average spot intensities were exported from PDQuest Advance as tab delaminated Excel data. Missing intensities were estimated using mean mode approach in XLSTAT and descriptive statistics and correlations were calculated. Venn diagrams were created using the online available tool [118].

2.21. Statistical Analysis

2-DE and WB experiments were performed in duplicate. When it was required quantitative results were expressed as means±standard deviation. The p-values were calculated using one-way analysis of variance "ANOVA" or Student t-tests in XLSTAT. All p-values<0.05 were considered statistically significant. Only

significant hits, as defined by the MASCOT probability analysis ($p<0.05$), were accepted.

2.22. Statistical Analysis for ELISA

Statistical analyses were carried out using R (Version 3.5.3). All variables were expressed as mean±standard deviation. The Mann-Whitney U test was applied to determine the statistical significance of the differences between groups. Spearman's rank correlation test was used to evaluate the correlations between groups. In all analyses, p-values less than 0.05 were considered as statistically significant.

2.22.1. Evaluation of the diagnostic performance of the biomarkers

The diagnostic performance of a biomarker was determined through sensitivity and specificity metrics, and the Receiver Operating Characteristic (ROC) curve. Using serum levels of proteins, true-positive rate (TPR), true-negative rate (TNR), and false-positive rate (FPR) were calculated and used to construct the ROC curve. The optimal cut-off level for biomarker quantification was calculated by the Youden index.

2.22.2. Evaluation of the prognostic performance of the biomarkers

The prognostic capabilities of the biomarkers were identified by using BC RNA-Seq dataset obtained from The Cancer Genome Atlas (TCGA) and survival analysis via SurvExpress validation tool [119]. In SurvExpress, the samples were partitioned into low- and high-risk groups according to their prognostic index. The prognostic capabilities of the biomarkers were characterized through Kaplan-Meier plots using the overall survival times of patients, the log-rank test, and the hazard ratio (HR).

3. RESULTS

3.1. Preparation of Protein Pools

SDS-PAGE gels were run to assess the quality and the quantity of each protein extract after measurement of protein concentrations (See Appendices Figure C1 for SDS-PAGE gel images). In terms of quality, each sample displayed distinct bands without any evidence of smear indicating that the protein extracts required no further clean up (Figure 3.1A). WB analysis was performed using the anti-β-actin antibody to ensure equal protein loading [120]. ImageJ software was used to determine the normalization coefficient. The band intensities were measured by performing densitometric analysis on ImageJ software. The protein pools were accurately recreated based on WB quantification results (Figure 3.1.B).

3.2. The Comparative 2-DE Analysis Revealed 13 Proteins That Were Differentially Regulated in the Tumour Groups Compared to the Control Group

Well-resolved and reproducible 2-DE gels were produced and subjected to spot detection (Figure 3.2.). An average of 750 spots per analytical gel was detected. The overall mean coefficient for spot matching was 24%, indicating that the protein distribution patterns among the gels were highly similar. Protein spots that significantly differed in expression (more than 2-fold) were selected and identified by MALDI-TOF/TOF analysis. In Figure 3.3., proteins spots labelled with Uniprot accession numbers indicate the positions of the identified protein spots on a representative gel.

The changes in spot intensities were compared for each tumour protein pool in comparison to the control pool (e.g., Luminal A versus control or Luminal B versus control), while comparisons between tumour groups (e.g., Luminal A versus Luminal B) were not considered in this study. Lists of the identified proteins with their respective MALDI scores and their corresponding regulation ratios among the

tumour groups over the control group are given in Appendices Table D1 and D2, respectively.

A Venn diagram was created using the accession numbers of differentially regulated proteins in each comparative analysis (tumour groups versus the control group) (Figure 3.4.). Thirteen shared proteins were differentially regulated in each tumour group in comparison to the control (Appendices Figure E1). Those proteins were elongation factor 2 (EEF2), 60 kDa heat shock protein (HSPD1), heat shock protein 90-alpha (HSP90AA1), MAGL, pyruvate kinase (PK), protein disulphide isomerase (PDIA1), elongation factor 1-gamma (EEFG1), L-lactate dehydrogenase B chain (LDH-B), carbonic anhydrase 1 (CA1), aldo-keto reductase family 1 member C2 (AKR1C2), GPD1, keratin type II cytoskeletal 8 (KRT8), and keratin type I cytoskeletal 19 (KRT19).

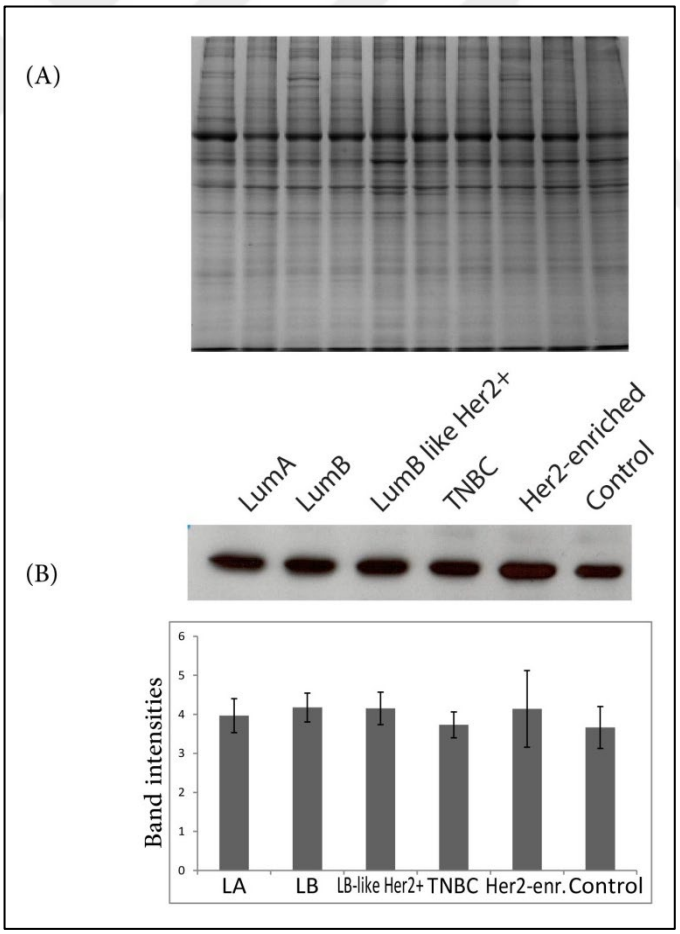

Figure 3.1. Assessment of the quality (A) and quantity (B) of protein extracts

When regulation ratios of these thirteen proteins were analysed, MAGL, LDH-B, CA1, AKR1C2 and GPD1 displayed low expression levels while EEF2, HSPD1, HSP90AA1, PKM, PDIA1, EEFG1, KRT8 and KRT19 displayed high expression levels in tumour groups in comparison to the control group.

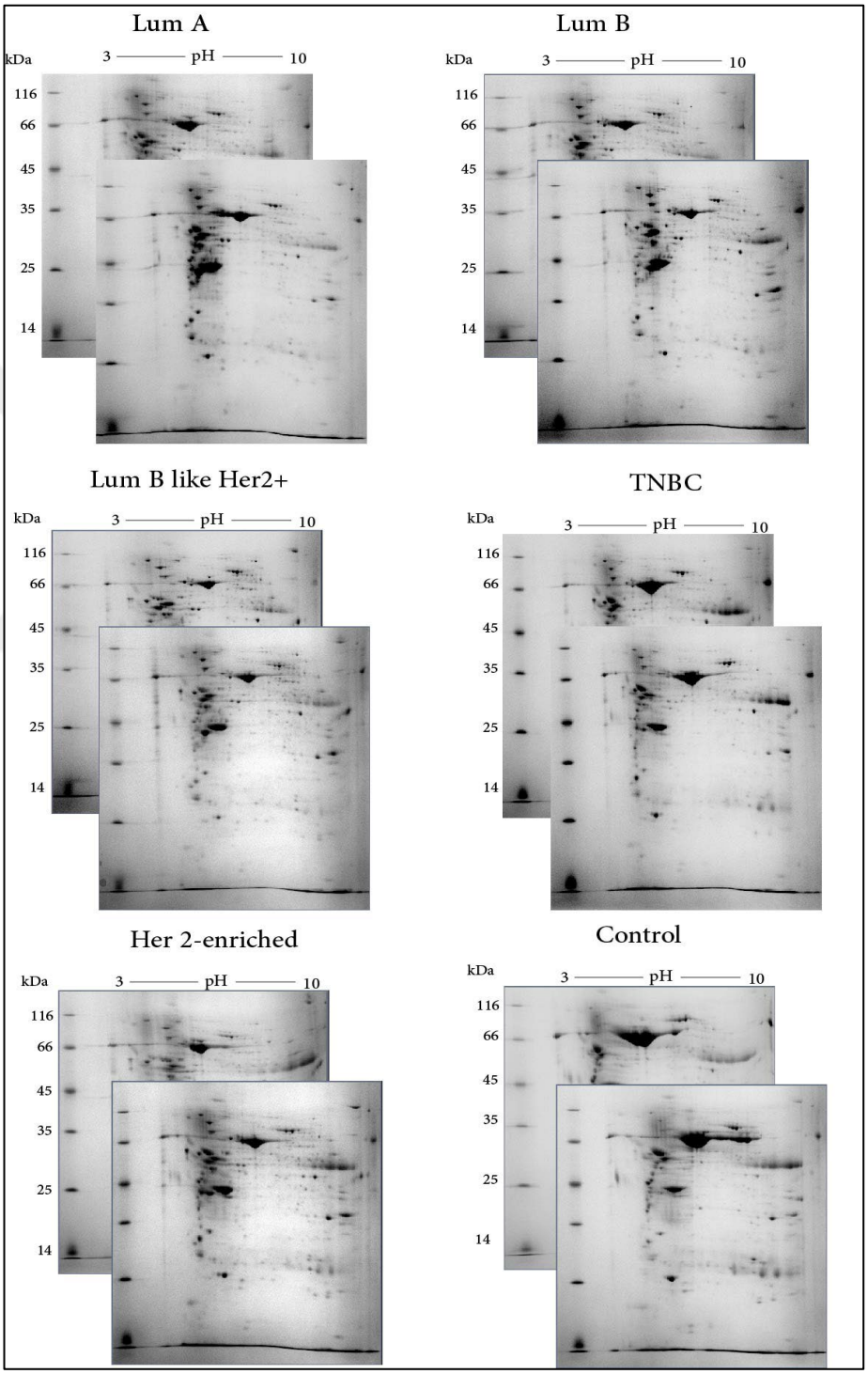

Figure 3.2. Images of the 2-DE gels for tumour and control groups

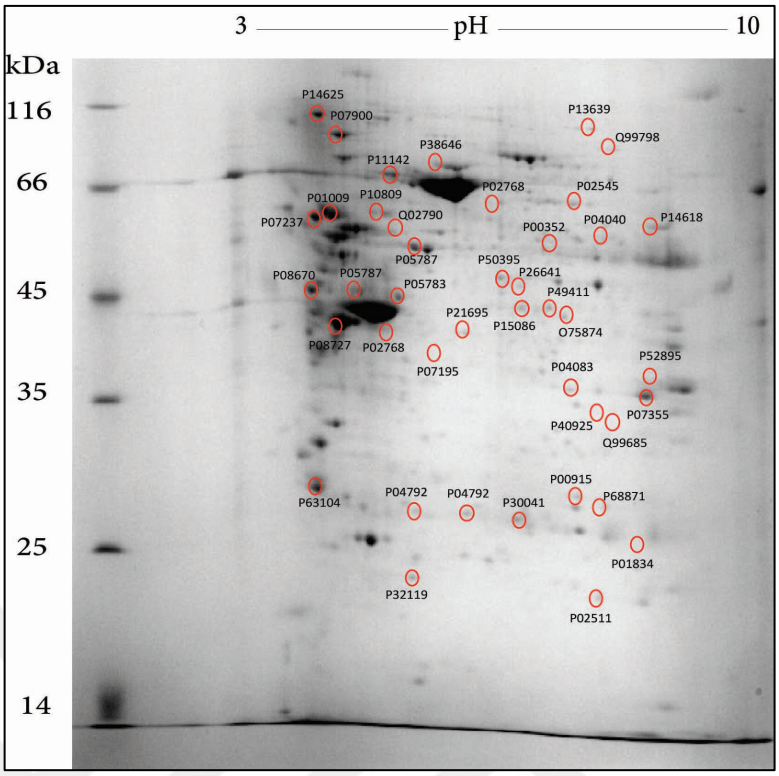

Figure 3.3. A representative image showing excised spots on a 2-DE gel

3.3. Comparative DIGE Analysis Revealed 5 Proteins Down-regulated in Tumour Tissues Compared to the Control Group

For DIGE analysis, a separate protein pool representing each tumour subtype was formed. This protein pool was then compared with the control protein pool. Pooled protein extracts from the tumour and control samples were labelled with Cye3 and Cye5, respectively. The internal control mix (Cye2-labeled), used for normalization, was formed by mixing equal amounts of protein from the tumour and control pools. In Figure 3.5., representative image for all three Cye dye gel images and the superimposed image of all three labelled gels were shown (Images were pseudo-coloured). Based on the 2-fold change criteria, differentially regulated proteins were detected and identified by MALDI-TOF/TOF (Appendices Table D3).

GPD1 received our attention since it was highly down-regulated in the tumour tissues in comparison to control tissues in the DIGE experiment with a similar trend observed in 2-DE experiments. Analysis of the regulation ratios indicated down-regulation of four other proteins in addition to the up-regulated ones but the up-

regulated and the other down-regulated proteins except MAGL were not closely associated in terms of their metabolic roles. On the other hand, MAGL was selected as the second most important differentially regulated protein since it is involved in TAG metabolism like GPD1. In other words, both proteins directed our attention to the changes in lipid metabolism and verification experiments were performed for both GPD1 and MAGL [121].

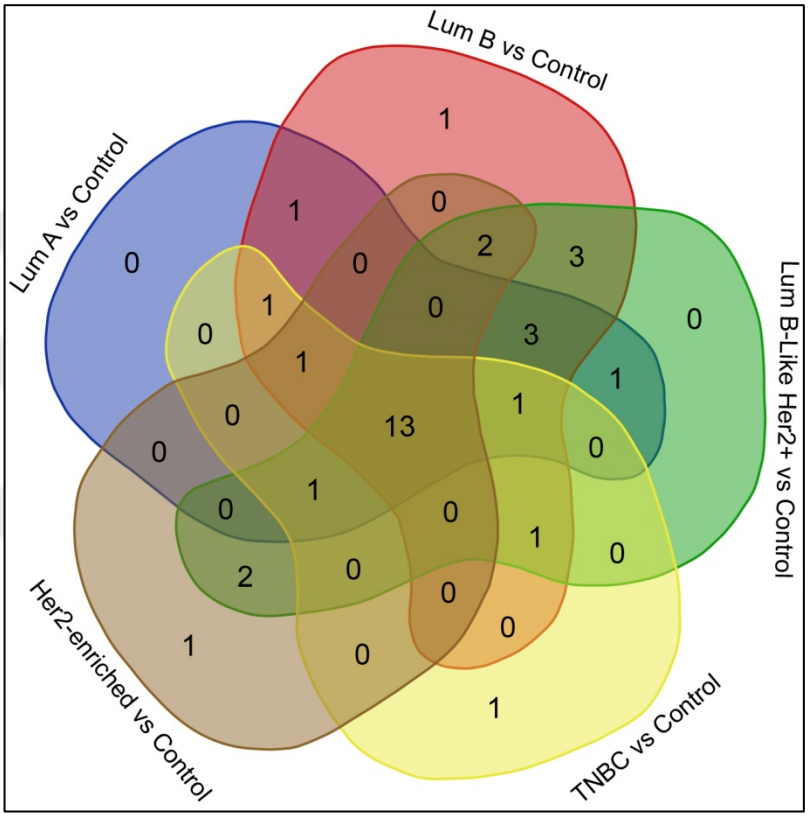

Figure 3.4. Venn diagram representing differentially regulated proteins

3.4. WB Analysis Verified the Changes in GPD1 and MAGL Protein Levels

The protein pools from the tumour and the control groups were analysed by WB using the anti-GPD1 and anti-MAGL monoclonal antibodies. The band intensities were measured by performing densitometric analysis using ImageJ software. The results indicated low expression levels of both proteins in the tumour pools in comparison to the control, verifying the findings of 2-DE and DIGE experiments. Moreover, comparisons among the tumour groups revealed that the TNBC group had the lowest level of GPD1 and MAGL expression, while the other tumour groups

displayed similar GPD1 expression levels (GPD1: >1000-fold difference, p=0.03; MAGL: >100-fold difference, p=0.04) (Figure 3.6.).

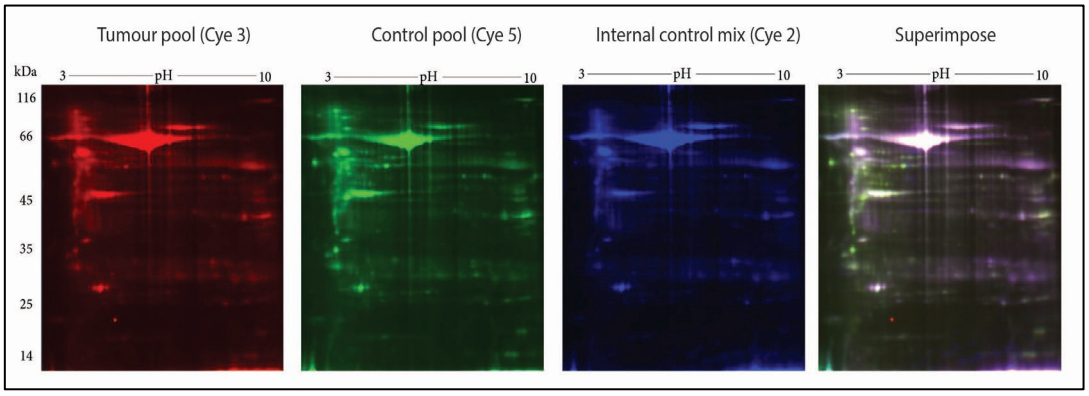

Figure 3.5. Representative images of DIGE gels used for comparative analysis of the tumour and control group

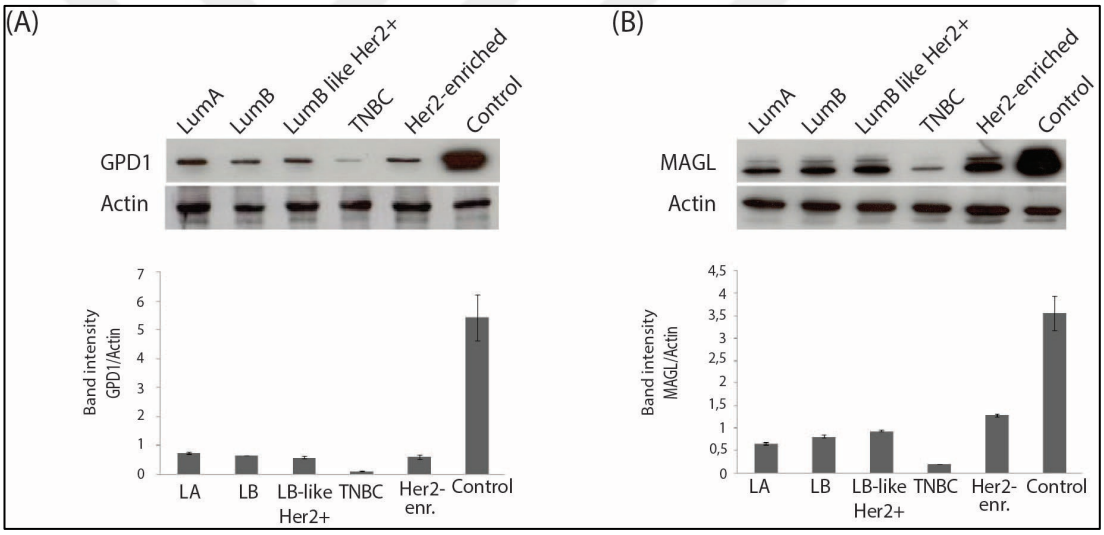

Figure 3.6. WB analysis of the tumour groups and the control group using anti-GPD1 (A) and anti-MAGL antibody (B)

3.5. GPD1 Protein Levels Varied among the TNBC Samples

To further determine the variation in GPD1 expression levels among individual patients in the tumour groups, eight samples from each tumour subtype were selected and subjected to WB analyses. The blot was stripped and re-probed with an anti-β-actin antibody for normalization of the expression levels. The band intensities were measured with the QuantityOne software (Figure 3.7.). Except for the five samples of TNBC and three samples of the $HER2^{+}$ group, GPD1 expression was detected in each sample at a similar level in each subtype. However, GPD1 levels in each sample

belonging to tumour groups were always lower than the GPD1 levels in the control group. For the samples belonging to the TNBC group, 5 out of 8 samples displayed extremely low/non-detectable the GPD1 expression and WB experiments were repeated to screen all the available TNBC samples (n=11). The results indicated that nearly half of the TNBC samples had non-detectable GPD1 expression.

Each control sample belonging to the TNBC group (peripheral healthy breast tissues collected from the same TNBC patients) was also subjected to WB analyses to assess the changes in GPD1 levels (Figure 3.8A). Two out of 11 control samples also displayed statistically significant low GPD1 levels (p<0.05).

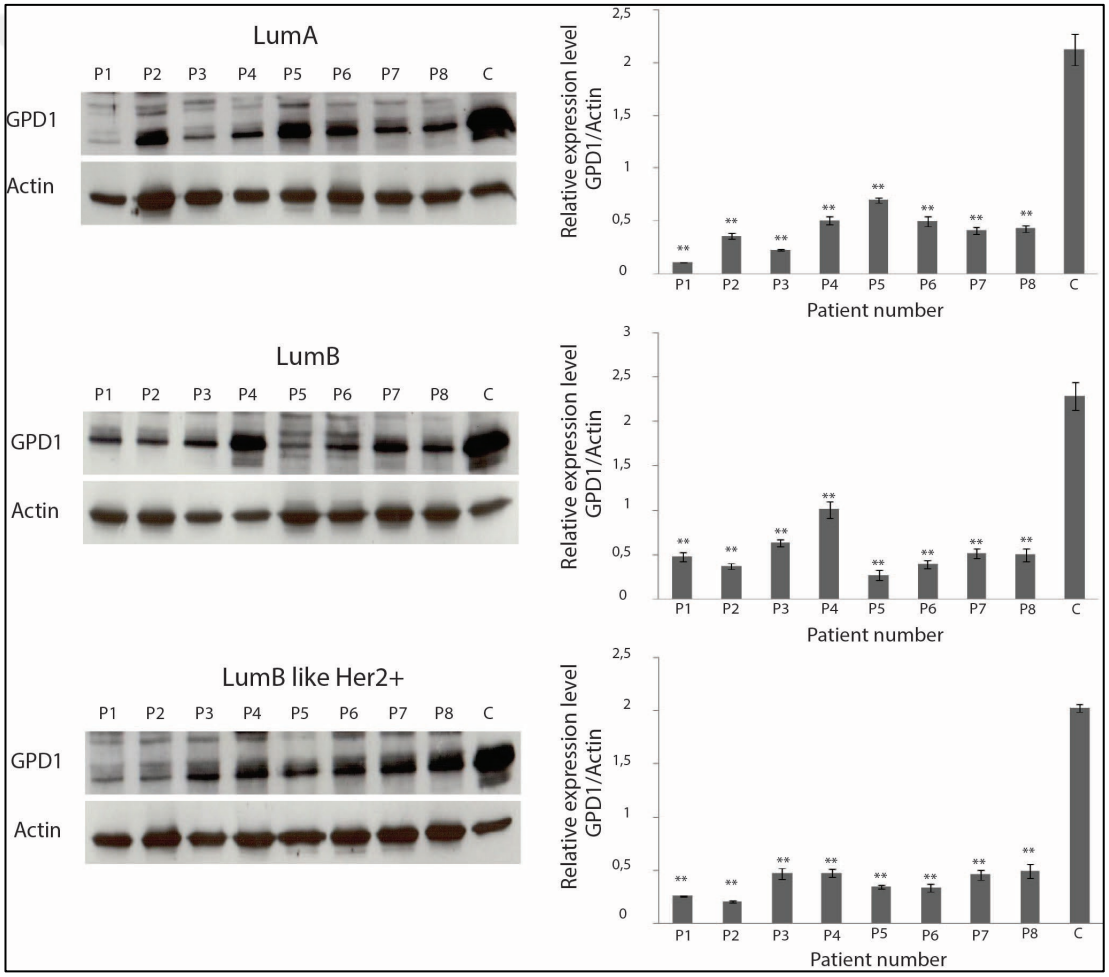

Figure 3.7. The expression level of GPD1 in each tumour group and the control group

(Explanation for Figure 3.7: The letters "P" and "C" designate the patient number and the control pool formed by control tissue protein extracts of all individuals, respectively. *p<0.05 and **p<0.01 vs. control pool).

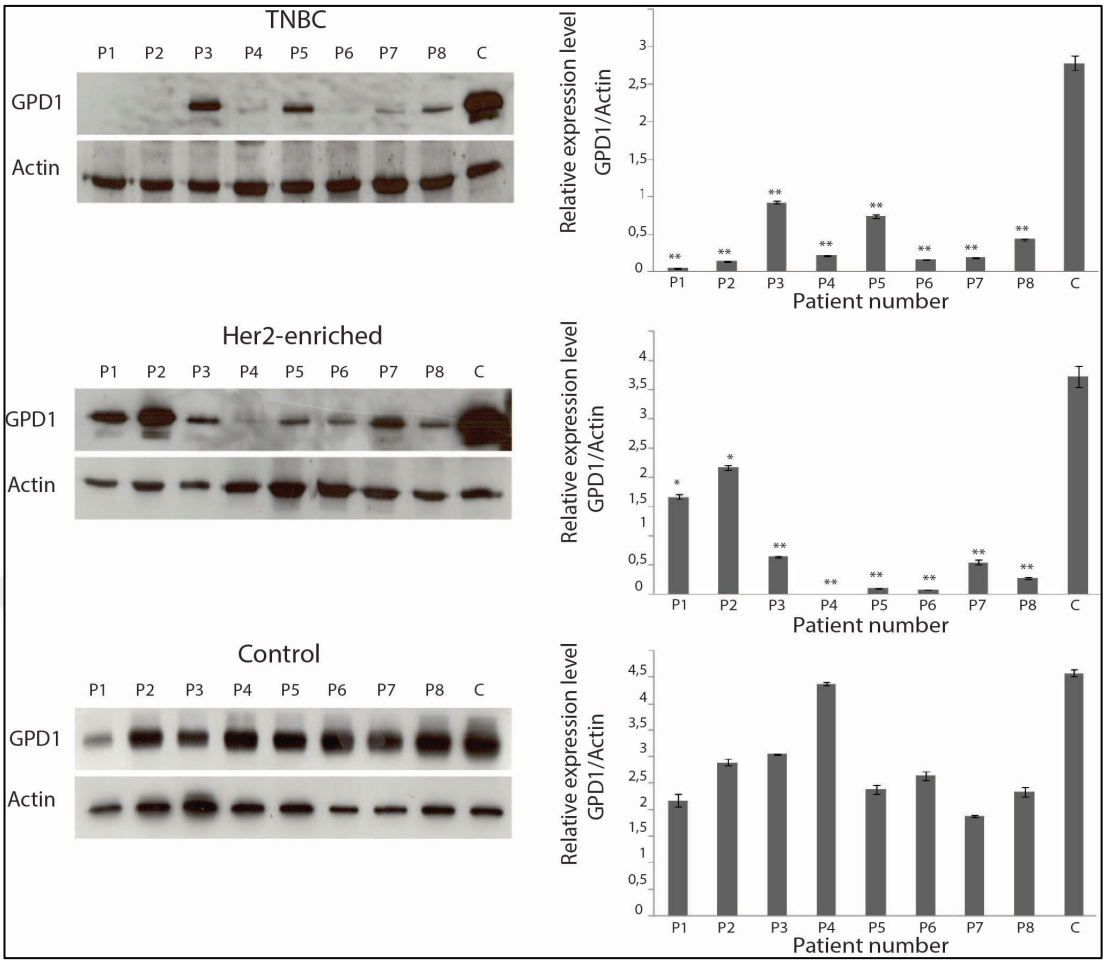

Figure 3.7 (Continues). The expression level of GPD1 in each tumour group and the control group

(Explanation for Figure 3.7: The letters "P" and "C" designate the patient number and the control pool formed by control tissue protein extracts of all individuals, respectively. *p<0.05 and **p<0.01 vs. control pool).

Based on these findings, all TNBC samples (n=11) were selected for further analysis by WB using the anti-MAGL antibody to determine the variation in expression levels of MAGL among individual patients in the TNBC subtype. Two samples (P2 and P9) displayed relatively low levels of MAGL expression, while repeated WB experiments using all the TNBC samples confirmed the findings and indicated that one-fifth of the TNBC group displayed low-level MAGL expression.

Each control sample belonging to the TNBC group was also subjected to WB analyses to assess the changes in MAGL levels. One out of the 11 control samples (P9) displayed a low level of MAGL expression. The corresponding tumour sample of P9 also displayed a low level of MAGL expression (Figure 3.8B.).

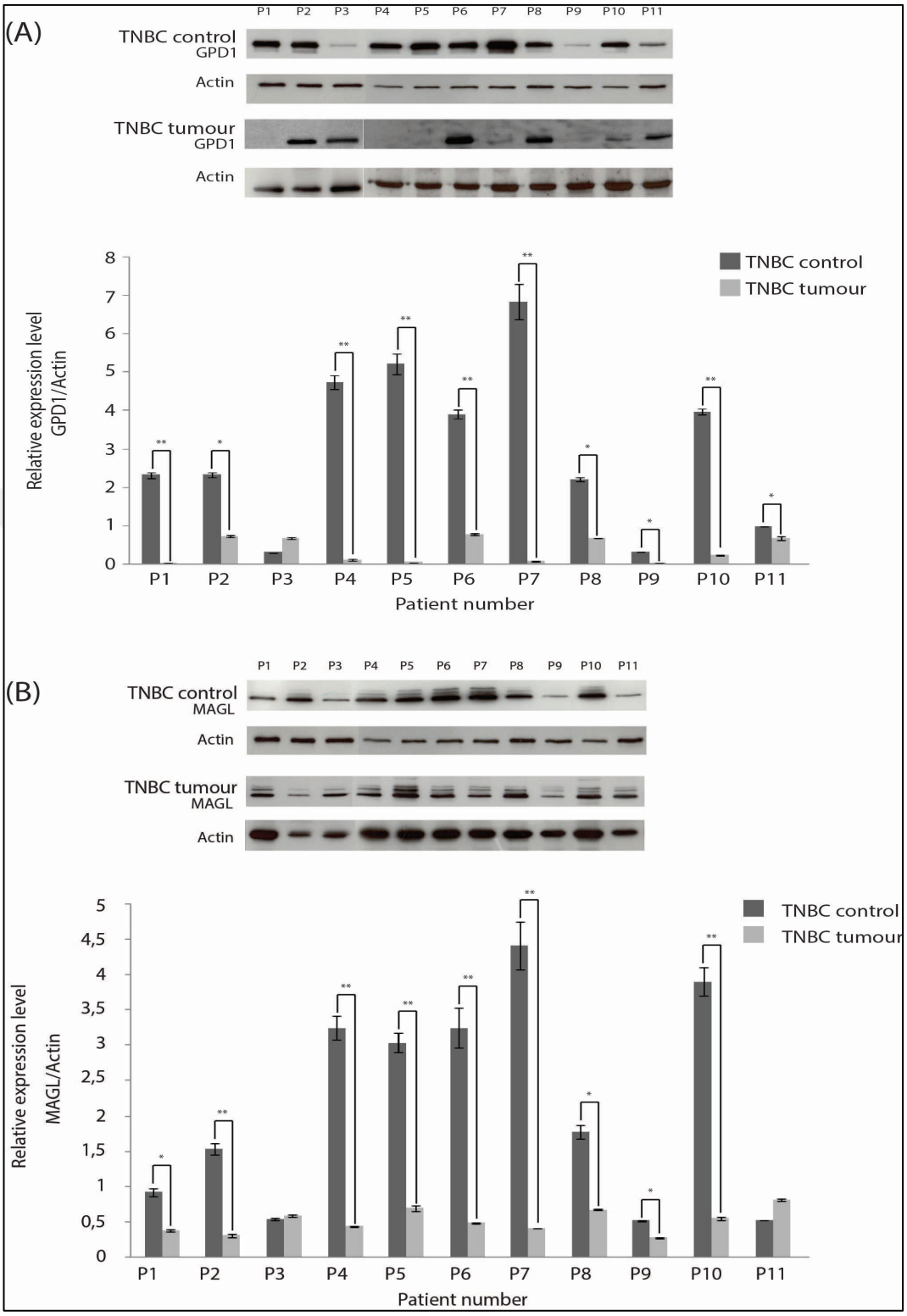

Figure 3.8. GPD1 (A) and MAGL (B) expression levels of TNBC patients

(Explanation for Figure 3.8: *p<0.05 and **p<0.01 vs. TNBC controls. Data presented as mean±SD, n=3).

3.6. PCA of the Tumour Groups and the Control Group

Taking 2-DE spot intensities on every replicate tumour group and the control group, the variations were projected onto a two-dimensional space. Therefore, we were able to determine which groups were similarly contributing to the variance and which groups appeared in a separate region (Figure 3.9.). PCA succeeded to differentiate the tumour groups from the control group. PCA also provided the evidence for the separation of TNBC from the other BC subtypes, which was indicative of variation in their respective protein expression profiles.

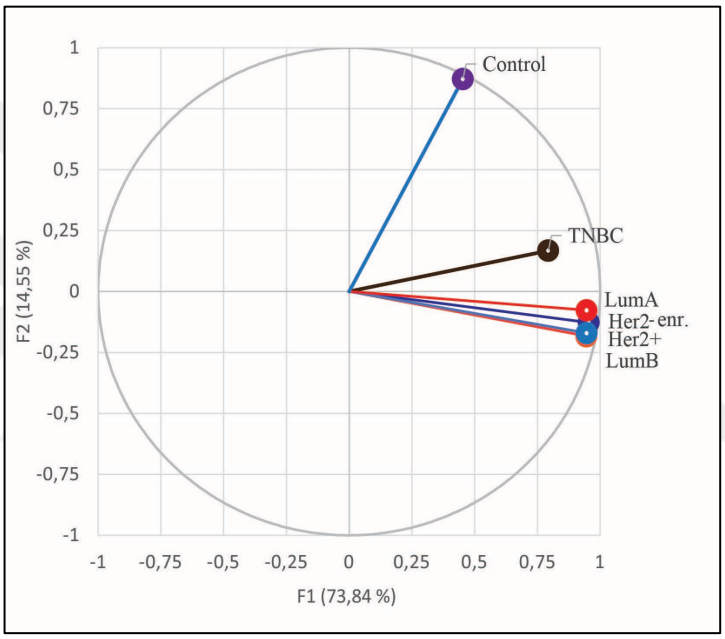

Figure 3.9. PCA of BC tumour groups and the control group

3.7. Comparative DIGE Analysis for the GPD1-positive and GPD1-negative TNBC Samples

Analysis of the WB results revealed two subgroups with different GPD1 expression levels in the TNBC group. The first group consisted of the samples with low/non-detectable GPD1 expression ($GPD1^-$) and the second group with moderate GPD1 expression ($GPD1^+$). This finding led us to perform DIGE analysis to compare $GPD1^+$ and $GPD1^-$ samples at the proteome level. Pooled protein extracts from the GPD1+ and GPD1- samples were labelled with Cye5 and Cye3, respectively. The internal control mix (Cye2-labeled), used for normalization, was formed by mixing

equal amounts of protein from the GPD1+/- pools (Figure 3.10.). Based on the 2-fold change criteria, differentially regulated proteins were detected and identified by MALDI-TOF/TOF. 16 proteins displayed regulation in their expression levels (Appendices Table D4).

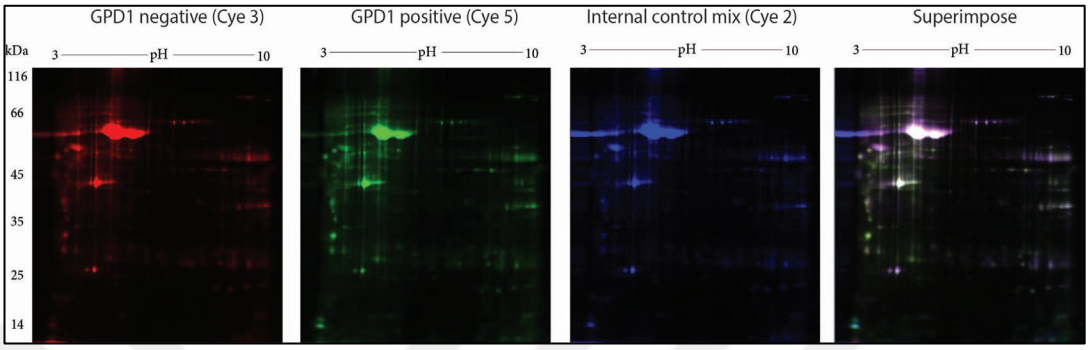

Figure 3.10. Representative images of DIGE gels used for comparative analysis of GPD1$^{+/-}$ group

3.8. GPD1 and MAGL Expression in Different Cell Lines

The expression levels of GPD1 and MAGL were further examined in CHO, SH-SY5Y, HeLa, DP, MCF-7 and PCL cell lines *in vitro*. All cell lines expressed both proteins when cultured. Among the cell lines, the lowest expression level of GPD1 was observed in the primary PCL cells which were obtained from a TNBC patient. The low GPD1 expression level in this sample was in agreement with our previous findings and demonstrated that TNBC samples either lacked or had a low level of GPD1 expression (Figure 3.11A.). As to MAGL, its expression levels fluctuated among the cell lines (Figure 3.11A.).

The expressions of the two proteins in the cell lines were also confirmed by IF. Results showed a uniform cytoplasmic distribution of both proteins within the cells (red colour) (Figure 3.11B.).

3.9. Serum GPD1 Levels Discriminated Patients with TNBC Subtype from the Others

Serum GPD1 levels were determined in BC subtypes by ELISA. For this purpose, serum samples were used to create serum pools as described in materials and methods section. The results demonstrated that except the TNBC subtype, serum

GPD1 levels in BC subtypes were similar to the levels measured in the control serum pool (Figure 3.12.). The TNBC subtype displayed significantly high serum GPD1 levels.

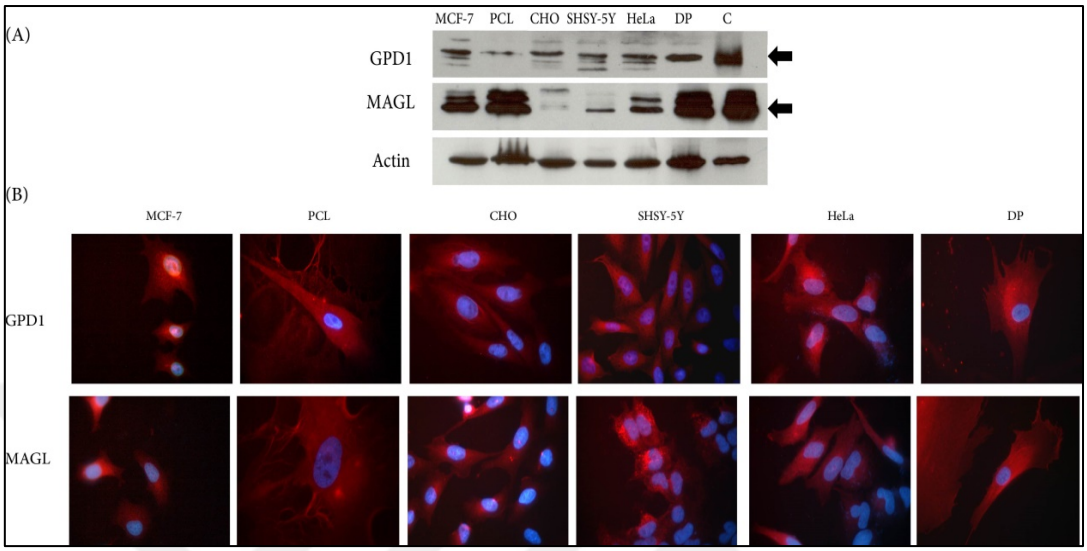

Figure 3.11. GPD1 and MAGL expression in different cell lines were assessed by WB (A) and IF (B)

To further investigate serum GPD1 levels in the individual samples (n=11) of TNBC subtype, serum samples that used to create the TNBC serum pool were subjected to ELISA. The serum pool created from the serum samples of healthy individuals (n=20) was also used as the control group. Determination of GPD1 levels in the individual TNBC serum samples showed that serum GPD1 levels were at similar levels in the majority of the samples (an average of 3.04 ng/mL) and were lower compared to the control group (Figure 3.13.). However, GPD1 levels displayed significantly higher levels than the other individuals and the control group in some serum samples (P3, P5, and P11 individuals), which eventually caused the TNBC subtype to display high GPD1 levels.

The TNBC individuals with high serum GPD1 levels (P3, P5, and P11) were labelled as the outliers during biostatistical analyses and were not included for the data set. This prevented the deflection of the results or underestimation of the possible significant findings. With the refined input data, a significantly lower GPD1 level in the serum samples of TNBC patients were detected in comparison to other BC subtypes (Table 3.1.). The differences in expression levels between TNBC and each subtype were all statistically significant with HER2-enriched ($p=4.73\times10^{-5}$), LumA

($p=5.46\times10^{-6}$), LumB ($p=8.34\times10^{-5}$), LumB-like HER2+ (p=0,0206), and Control ($p=1.10\times10^{-3}$). In addition, the expression levels of LumB-like HER2+ group was statistically lower when compared to LumA ($p=8.59\times10^{-4}$), LumB ($p=2.47\times10^{-3}$), HER2-enriched ($p=3.70\times10^{-3}$), and Control (p=0.023) groups (Figure 3.14.).

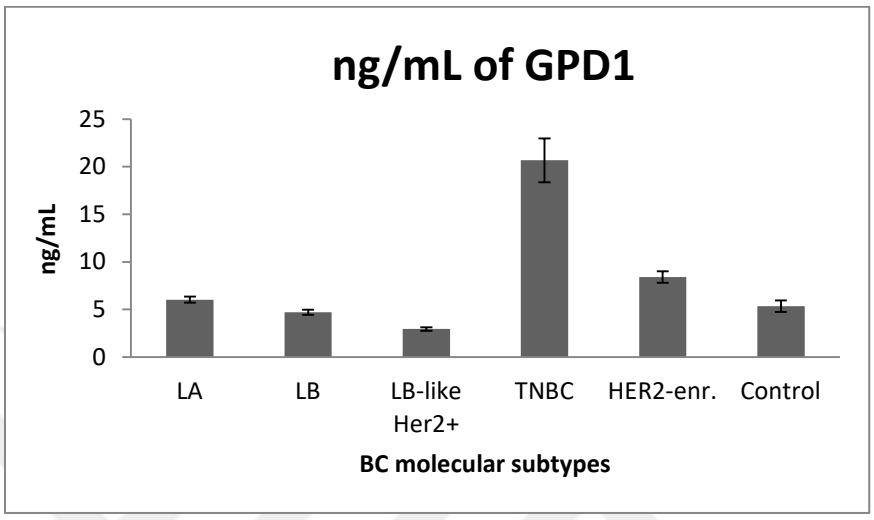

Figure 3.12. ELISA results showing serum GPD1 levels in BC subtypes

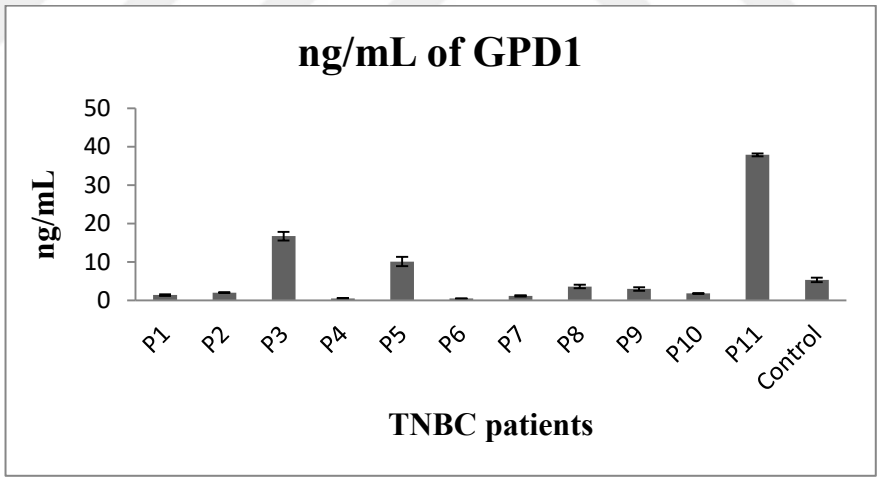

Figure 3.13. ELISA results showing serum GPD1 levels in TNBC individuals

Table 3.1. Serum GPD1 levels in BC subtypes and the control group (mean±standard deviation)

Subtype	LumA	LumB	LumB-like HER2+	TNBC	HER2-enriched	Control
GPD1 expression (ng/ml)	6.04±0.38	4.72±0.32	2.95±0.22	1.77±1.11	8.41±0.75	5.36± 0.75

On the other hand, there was no statistically significant difference among other subtypes. Evaluation of the tissue and serum levels of GPD1 revealed that serum GPD1 levels well correlated with the tissue GPD1 expression levels in BC subtypes and displayed relatively lower expression levels than the control group. There was no correlation between the tissue and serum GPD1 levels among the individual samples of TNBC subtype.

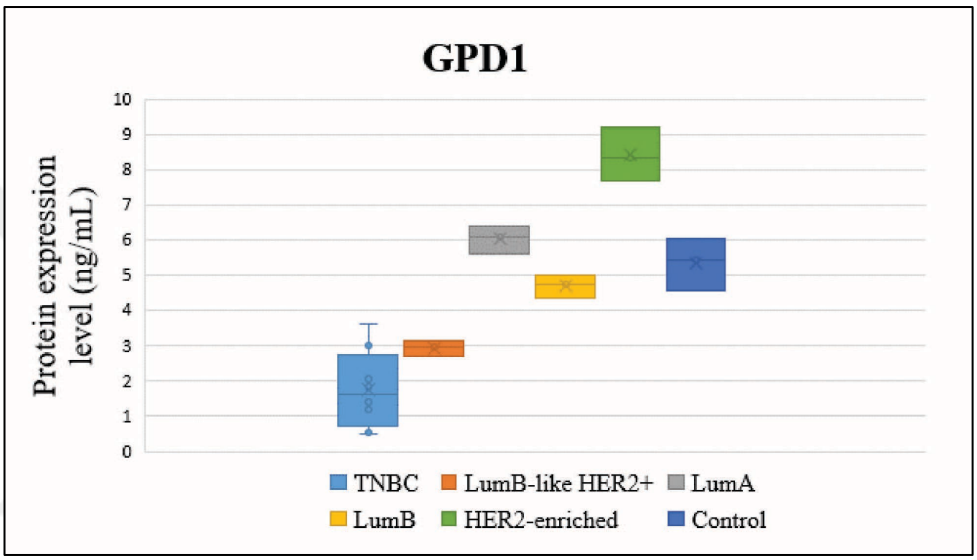

Figure 3.14. The comparative analysis of the serum GPD1 protein levels among BC subtypes

3.10. Serum MAGL Protein Levels Discriminated Healthy Individuals from BC Subtypes Regardless of the Subtype

Serum MAGL levels were determined in BC subtypes by ELISA. Serum samples were used to create serum pools as described in materials and methods section. The results demonstrated that serum MAGL levels in all BC subtypes were significantly lower than the control pool (Figure 3.15.). The lowest MAGL level was observed in the TNBC serum pool while the control group had the highest MAGL level. The results of serum MAGL levels in TNBC individuals are shown in Figure 3.16. According to the results, the serum level of MAGL in the TNBC subtype varied among the individuals. Serum MAGL levels of 2 individuals (P2 and P6) were the same as the control group, whereas all the other 9 individuals (73% of the TNBC individuals) had lower levels of MAGL than those in the control group.

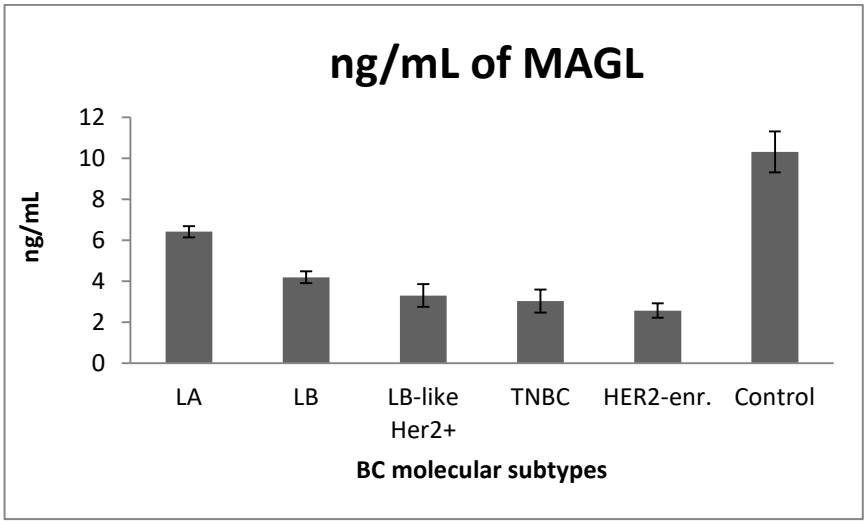

Figure 3.15. The results of the ELISA assay showing serum MAGL levels in the BC subtypes

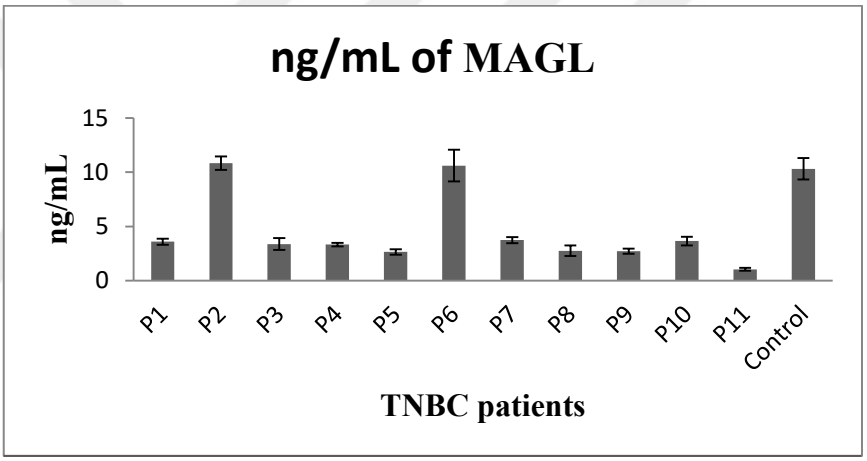

Figure 3.16. The results of the ELISA assay showing serum MAGL levels in TNBC individuals

The comparative analysis of the serum MAGL levels among BC subtypes and healthy individuals indicated a significantly higher MAGL level in the healthy individuals in comparison to the serum levels observed in all BC subtypes (Table 3.2.) (Figure 3.17.). The difference in serum MAGL levels between the healthy subjects and each subtype were statistically significant with TNBC ($p=0.024$), LumA ($p=0.0245$), LumB ($p=0.0087$), LumB-like HER2+ ($p=0.0027$), and HER2-enriched ($p=0.0041$). The findings pointed out that serum MAGL levels correlated with the tissue MAGL expression levels in BC subtypes.

Table 3.2. Serum MAGL levels in the BC subtypes and the control group (mean±standard deviation)

Subtype	LumA	LumB	LumB-like HER2-	TNBC	HER2-enriched	Control
MAGL level (ng/ml)	6.41±0.34	4.19±0.35	3.30±0.68	3.03±0.69	2.57±0.43	10.31±1.22

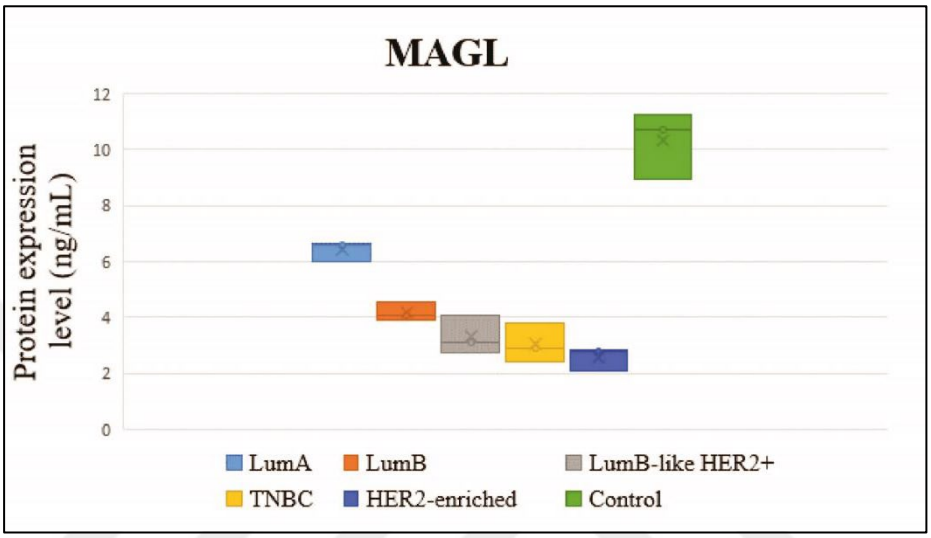

Figure 3.17. The comparative analysis of the MAGL serum levels among BC subtypes

3.11. Co-evaluation of Serum Protein and mRNA Levels of GPD1 and MAGL

3.11.1. Serum GPD1 protein level was more predictive in discriminating TNBC patients than GPD1 mRNA level

Using the mRNA expression data from TCGA (BC dataset with 155 TNBC, 74 HER2, 507 LumA, 191 LumB and 34 Control), the mRNA expression levels of GPD1 in each subtype were evaluated (Figure 3.18.). A profile similar to the serum GPD1 levels was observed in GPD1 mRNA expression levels in BC patients. However, when in-group comparisons using the mRNA expression levels were made among the subtypes, the differences were significant for only TNBC vs. LumA ($p=6.22\times10\text{-}24$) and TNBC vs. Control ($p=3.81\times10\text{-}14$). There was no statistically significant difference among other subtypes except LumA vs. LumB ($p=1.50\times10\text{-}25$) and LumB vs. control ($p=4.79\times10\text{-}14$).

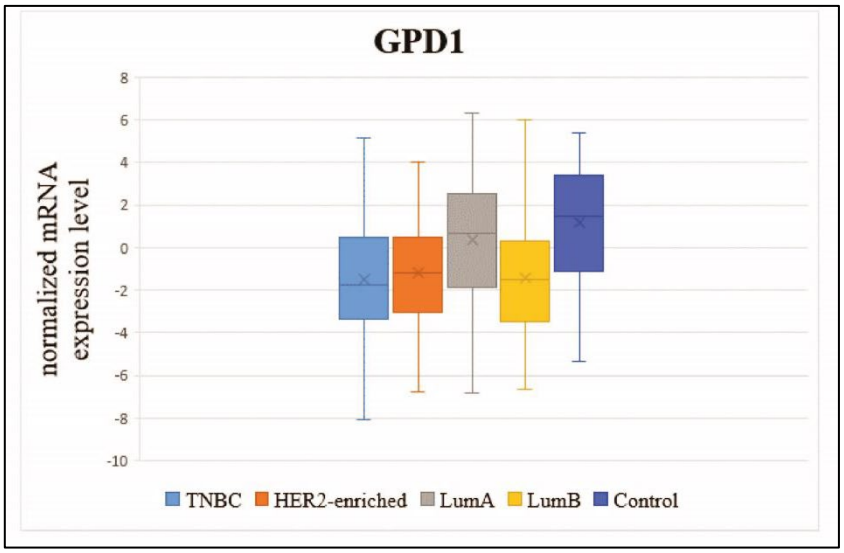

Figure 3.18. Normalized mRNA expression levels of GPD1 among BC subtypes

3.11.2. Serum MAGL level instead of mRNA level was more predictive in discriminating TNBC patients

Using the mRNA expression data from TCGA (BC dataset with 155 TNBC, 74 HER2, 507 LumA, 191 LumB and 34 Control), the mRNA expression levels of MAGL in each subtype were evaluated (Figure 3.19.). Both protein and mRNA expressions are the lowest in TNBC and highest in the control group. But the differences were not significantly clear.

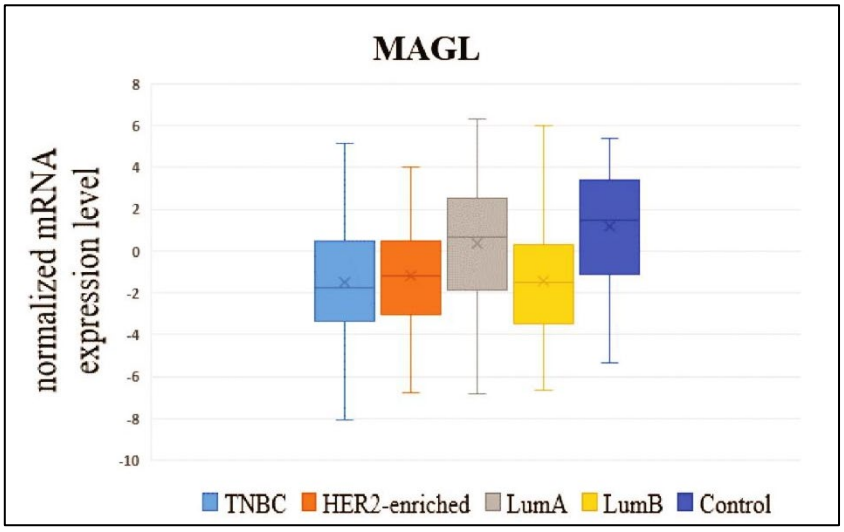

Figure 3.19. Normalized mRNA expression levels of MAGL among BC subtypes

3.12. The Diagnostic Values of GPD1 and MAGL as Biomarkers

3.12.1. Reduced serum GPD1 level acted as a potential diagnostic biomarker for TNBC

To assess the performance of GPD1 protein expression as a diagnostic biomarker in distinguishing TNBC patients from the patients belonging to the other subtypes, ROC curve and area under the curve (AUC) analyses were used (Figure 3.20.). The ROC analysis showed that the AUC was 0.948 (95% CI: 0.928-0.968, p<10-3). The optimal cut-off value determined by the Youden index was 3.18 ng/mL, and the sensitivity and specificity were 95.0% and 77.5%, respectively (Figure 3.21.). In other words, patients with GPD1 level less than 3.18 ng/ml can be diagnosed as TNBC with 95% sensitivity and of 77.5% specificity.

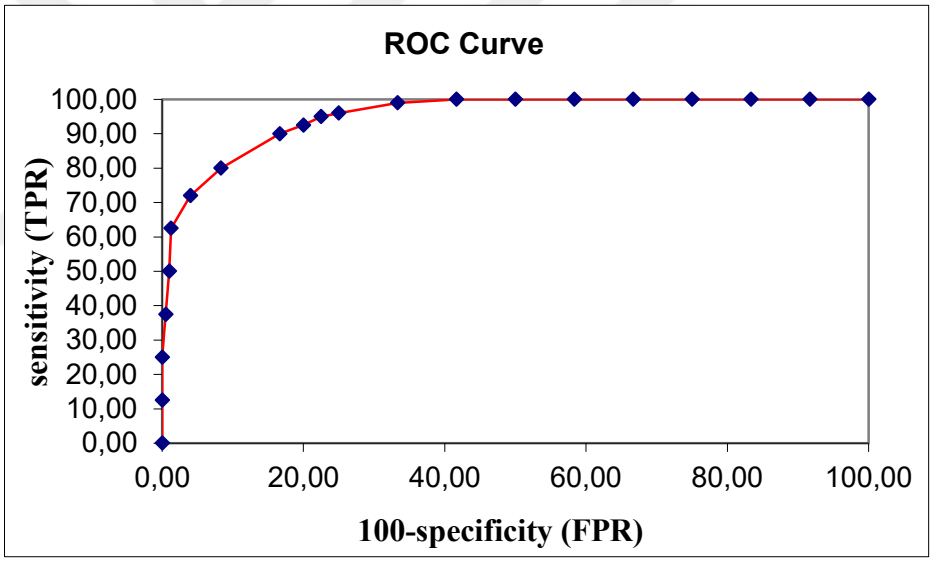

Figure 3.20. ROC curve and AUC to assess the performance of GPD1 as a diagnostic biomarker

3.12.2. Reduced serum MAGL level acted as a potential diagnostic biomarker for BC

To assess the performance of the serum MAGL level as a diagnostic biomarker in distinguishing healthy individuals from the BC patients, ROC curve and AUC analyses were employed (Figure 3.22.). The ROC analysis showed that the AUC was 0.980 (95% CI: 0.968-0.992, $p<10^{-3}$).

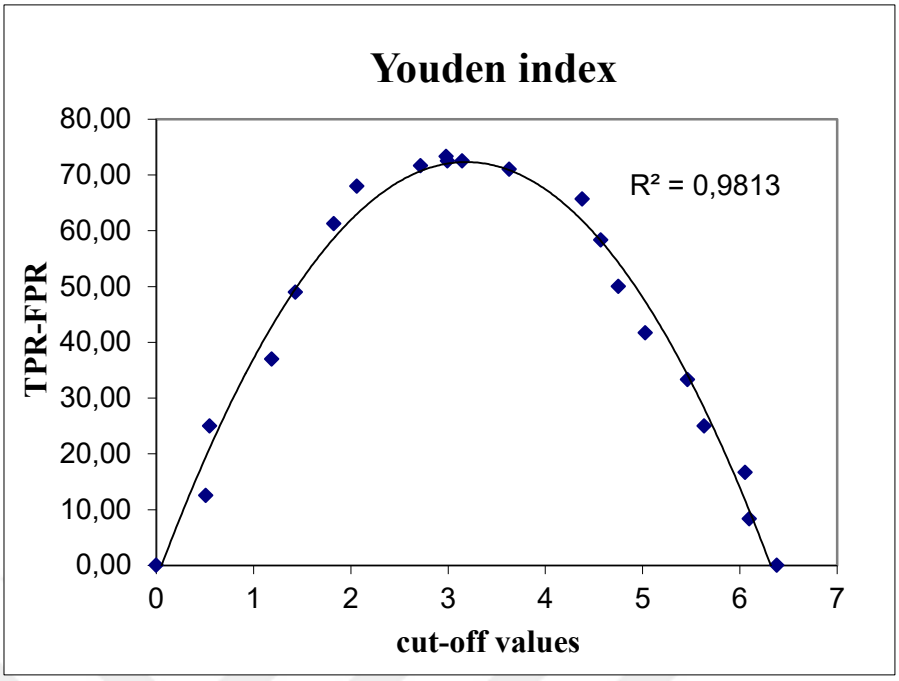

Figure 3.21. Sensitivity and specificity for GPD1 protein using Youden index

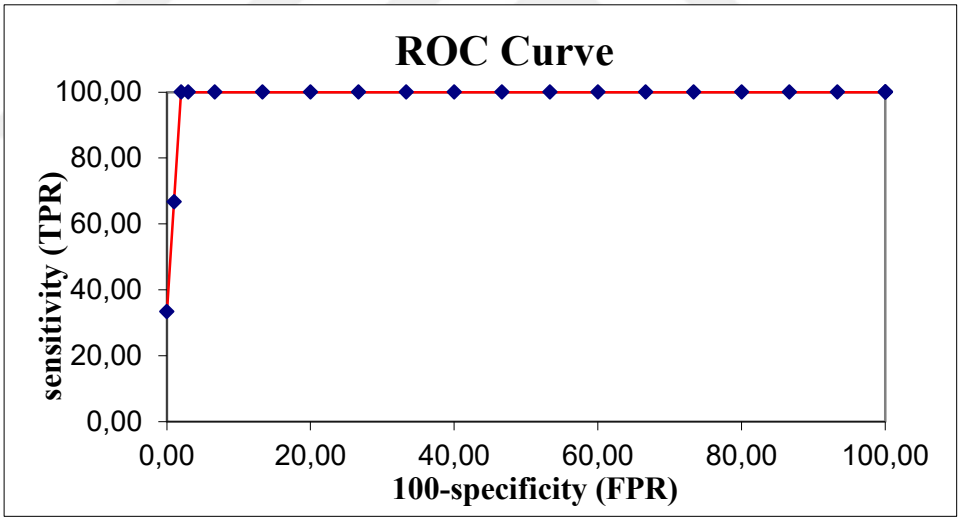

Figure 3.22. ROC curve and AUC to assess the performance of MAGL as a diagnostic biomarker

The optimal cut-off value determined by the Youden index was 7.23 ng/mL (Figure 3.23.), and the sensitivity and specificity were 100.0% and 98.5%, respectively. In other words, subjects with serum MAGL levels higher than 7.23 ng/mL can be considered as healthy with 100% sensitivity and 98.5% specificity.

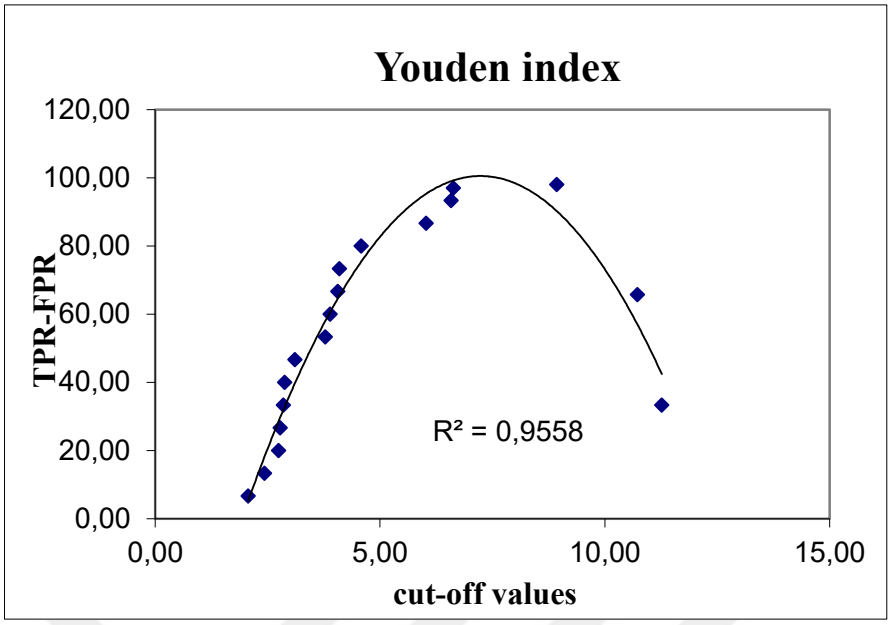

Figure 3.23. Sensitivity and specificity for MAGL protein using Youden index

3.13. The Prognostic Values of GPD1 and MAGL as Biomarkers

3.13.1. Elevated GPD1 protein level was correlated with poor prognosis of BC

To further explore the value of GPD1 in the prognosis of BC, patients' outcomes were analyzed through Kaplan-Meier survival estimator. GPD1 mRNA data obtained from TCGA was used to partition the samples into two risk groups displaying low GPD1 and high GPD1 levels (Figure 3.24.). The group with higher GPD1 gene expression levels received a poor prognosis compared to the low-risk group with lower GPD1 levels. (log-rank p=0.065 and HR=1.38) (Figure 3.25.).

3.13.2. Elevated MAGL protein level was correlated with poor prognosis of BC

To further explore the value of MAGL in the prognosis of BC, patients' outcomes were analyzed through Kaplan-Meier survival estimator. MAGL mRNA data obtained from TCGA was used to partition the samples into two risk groups displaying low MAGL and high MAGL levels (Figure 3.26.). The group with higher MAGL gene expression levels received a poor prognosis compared to the low-risk group with lower MAGL levels (log-rank p=2.2×10-4 and HR=1.93) (Figure 3.27.).

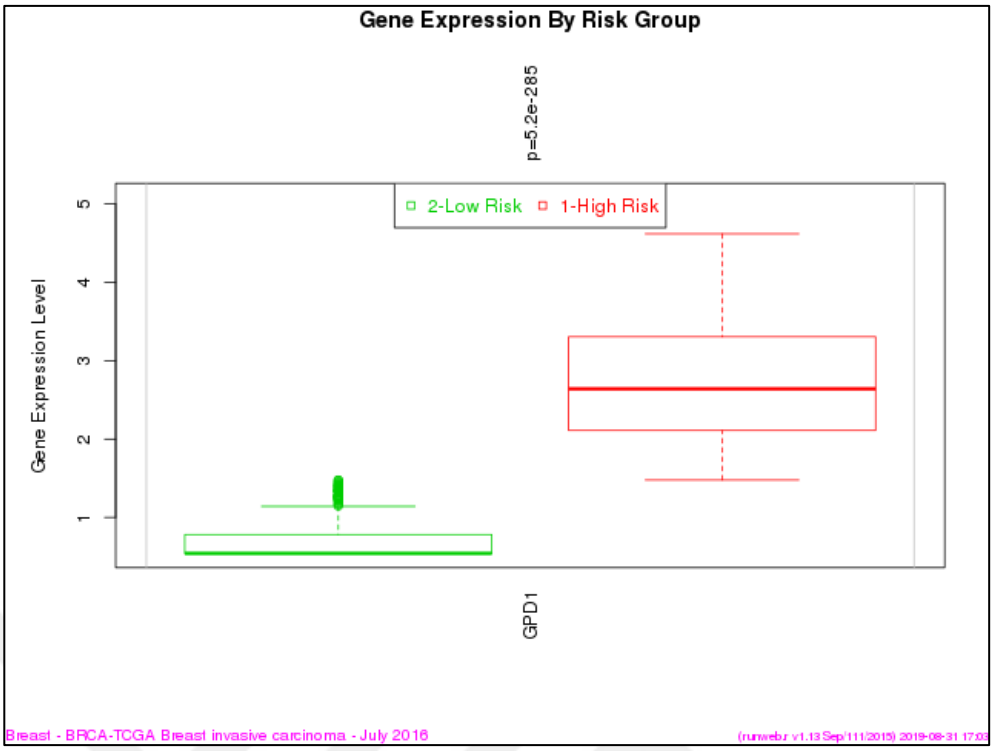

Figure 3.24. Box blot graph representing low- and high-risk groups for GPD1

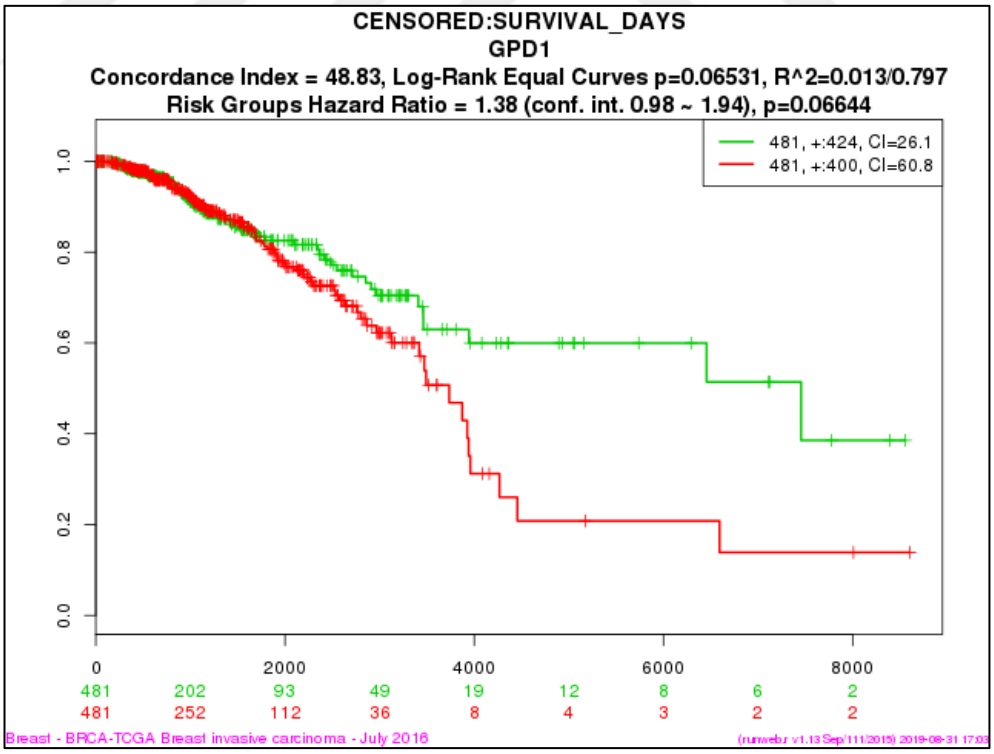

Figure 3.25. Correlation between GPD1 mRNA expression levels and disease outcome in BC

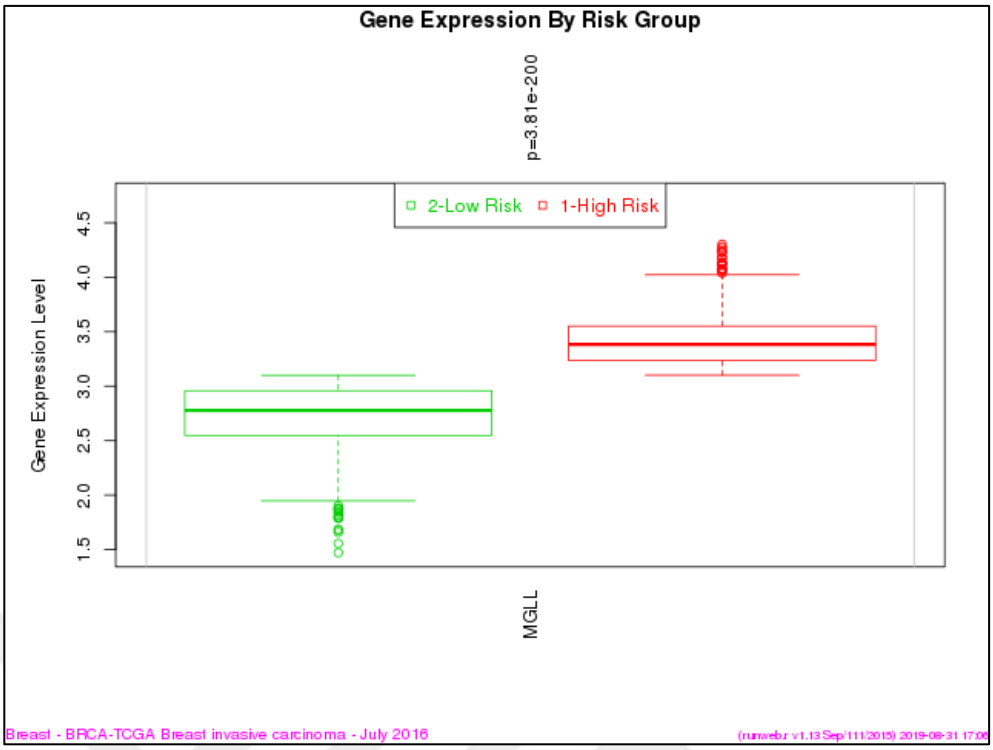

Figure 3.26. Box blot graph representing low- and high-risk groups for MAGL

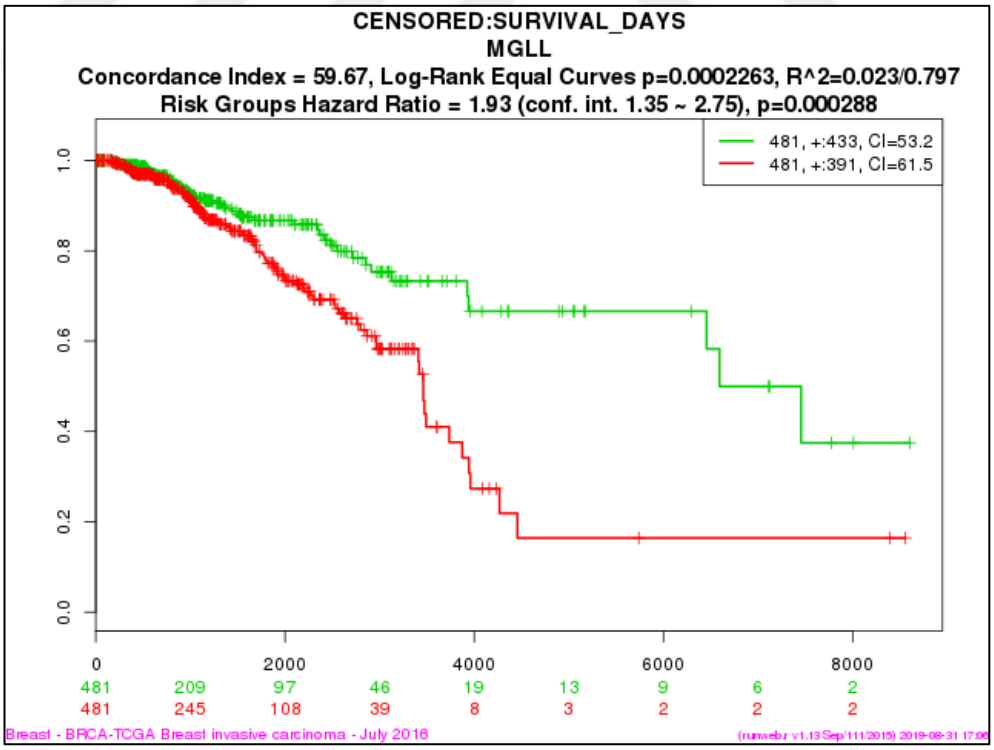

Figure 3.27. Correlation between MAGL mRNA expression levels and disease outcome in BC

3.14. Identification of BC-associated Autoantigenic Proteins via E-SERPA Assay

3.14.1. Optimized conditions of E-SERPA assay

Antigen binding affinity can vary between different antibodies. Moreover, the antibodies raised against the same antigen in the same species can vary in their binding affinity, stability and pI. Therefore, it is hard to optimize an efficient condition for the coupling of antibodies. E-SERPA assay consisted of antibody purification, antibody coupling to the magnetic beads, antigen capture and elution steps. Thus, each step was optimized to efficiently capture the target proteins, TAAs.

Optimization results can be summarized as follow:

- Determination of binding buffer (Variable C): The highest specificity was achieved when IP buffer (Thermo Scientific, USA) was used in immune capture experiments.
- The amount of pure CK-MB protein (Variable G): The sensitivity of immune capturing was 1 ng of CK-MB per 10 mg ab-coupled bead/mL.
- The amount of antigen (Breast tissue protein extract) (Variable F): In optimization experiments, the amount of breast tissue protein extract did not affect the formation of CK-MB antibody/antigen complex. In actual experiments, 4 mg breast tissue protein extract was used to obtain and identify antigens.
- The volume of antibody-coupled magnetic beads (Variable A): 100 µL of antibody-coupled magnetic beads were sufficient to achieve efficient antigen capturing. Thus 100 µL antibody-coupled magnetic beads were used in each experiment.
- The amount of antibody coupled magnetic beads (Variable B): Although 6 µg antibody per mg of beads was sufficient for coupling, the amount of antibody was used as 30 µg per mg beads to achieve full saturation and to prevent non-specific binding.
- Incubation time (Variable D): Maximum captured antigen was achieved by overnight incubation.

- Incubation temperature (Variable E): Maximum captured antigen was achieved at 4ºC.
- Elution method (Variable H): To comply with in-solution tryptic digestion protocol, the antigen elution was performed at 95ºC with a buffer containing 50 mM Ambic and 10 mM DTT. Tryptic digestion on the magnetic beads led to an increase in the number of identified proteins, however, the majority of the eluted proteins were from IgGs which can hamper the identification of antigens. Therefore, the eluted antigens were digested separately without the magnetic beads.

The details of the results of optimization experiments were presented in Appendices Figure F1-F6.

3.14.2. Purification of autoantibodies from serum samples

Affinity chromatography was used for the purification of autoantibodies from sera. A representative image showing the elution profile from a purification was presented in Figure 3.28. Flowthrough and elution fractions were subjected to SDS-PAGE and the gels were stained with cCBB. Imaging of the SDS-PAGE gels revealed that the autoantibodies present in the serum were separated from the albumin and other serum proteins and successfully purified (Figure 3.29.).

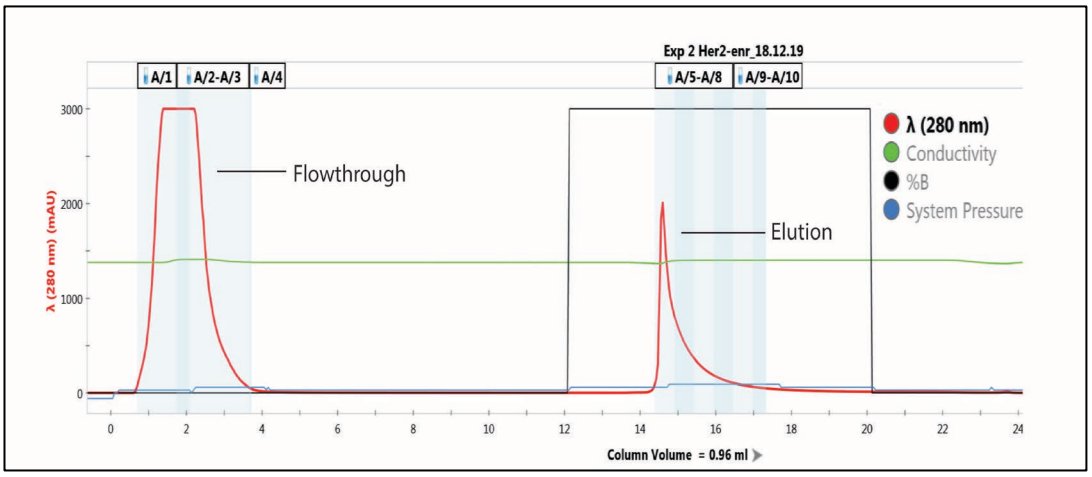

Figure 3.28. A representative image depicting chromatogram of autoantibody purification

3.14.3. Preparation of antibody/antigen complexes

To perform immune capture experiments, protein extracts prepared from BC tissues representing all BC subtypes (LumA, LumB, LumB-like HER2+, TNBC and HER2-enriched) were used to create a protein pool and this pool was labelled as the tumour group. Similarly, a control protein pool was also created from the protein extracts prepared from the corresponding healthy breast tissues and this pool was labelled as the control group.

Serum samples of all BC patients were pooled in equal volume and named as patient sera "Ps" and serum from healthy individuals (n=20) were pooled in equal volume and named as control sera "Cs". Autoantibodies were purified from these serum pools and coupled to magnetic beads as described in the materials and methods section. Then six different immune capture experiments were set as Ps, PsT, PsC, Cs, CsT, CsC. PsC, CsC and CsT were set as the control experiments. Ps and Cs were set as negative control experiments. Only PsT was selected as the group which identified TAAs (the tumour tissues proteins that reacted with the purified autoantibodies from Ps).

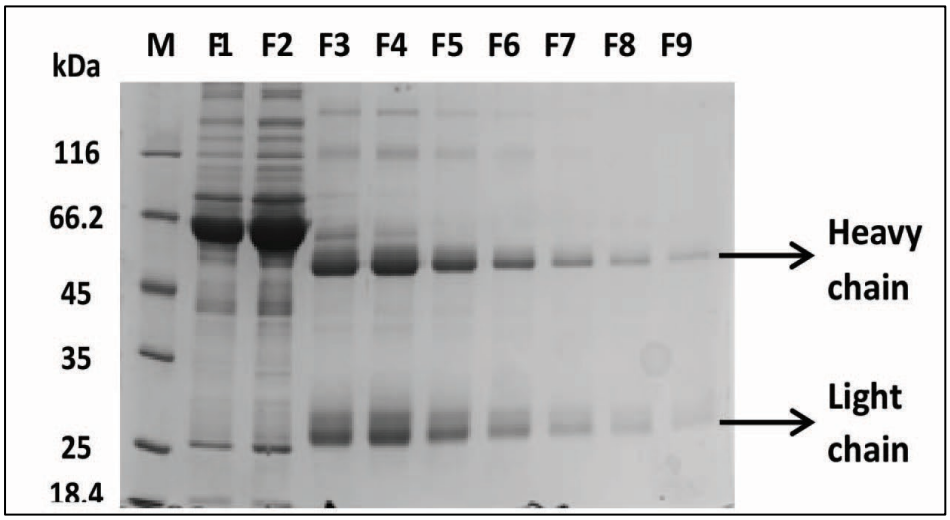

Figure 3.29. A representative SDS-PAGE gel image of the purified autoantibodies from a serum sample

(The abbreviations represent; M, marker (#26610, Thermo Scientific, USA); F1 and F2, flowthroughs; F3-F9, purified autoantibodies).

3.14.4. Elucidation of TAAs

3.14.4.1. Identification of TAAs via nLC-MS/MS analysis

E-SERPA assay was performed to elucidate TAAs by comparing the tumour group with the control group. Identified proteins of the control groups (PsC, CsT and CsC) were excluded, and the number of identified proteins only in PsT was designated and named as 'exclusive PsT'. Then, identified proteins of the negative control groups were excluded from the list of identified proteins in exclusive PsT. This group was labelled as TAAs and a total of 64 proteins were identified (Figure 3.30.).

To evaluate the obtained data, the same proteins with different accession numbers, fragment proteins belonging to an identified protein and some serum proteins were excluded from the list of identified proteins. Finally, evaluation of the results revealed the presence of 9 TAAs in PsT (Table 3.3.). Those proteins were, namely, GAPDH, TUBA1C, PPIA, CLU, MIF, SFRS3, POSTN, H4C1 and CCDC13.

The list of the identified proteins belonged to "Ps, PsT, PsC, Cs, CsT and CsC" was presented in Appendices Table G1-G6, respectively.

Table 3.3. The list of the identified TAAs

No.	Master	Accession	Description	Coverage [%]	# Peptides	# Unique Peptides	MW [kDa]	calc. pI
1	MP	P10909	Clusterin	3	1	1	52,5	6,27
2	MP	Q8IYE1	Coiled-coil domain-containing protein 13	2	1	1	80,8	8,84
3	MP	P04406	Glyceraldehyde-3-phosphate dehydrogenase	4	1	1	36	8,46
4	MP	P62805	Histone H4	19	2	2	11,4	11,36
5	MP	I4AY87	Macrophage migration inhibitory factor (Fragment)	8	1	1	12,5	7,88
6	MP	A8K486	Peptidyl-prolyl cis-trans isomerase	5	1	1	18	6,9
7	MP	B2R6F3	Splicing factor arginine/serine-rich 3	13	1	1	19,3	11,65
8	MPC	B1ALD9	Periostin	2	1	1	90,1	7,94
9	MPC	Q9BQE3	Tubulin alpha-1C chain	3	1	1	49,9	5,1

(MP: master protein, MPC: master protein candidate, MW: molecular weight, calc. pI: calculated isoelectric point)

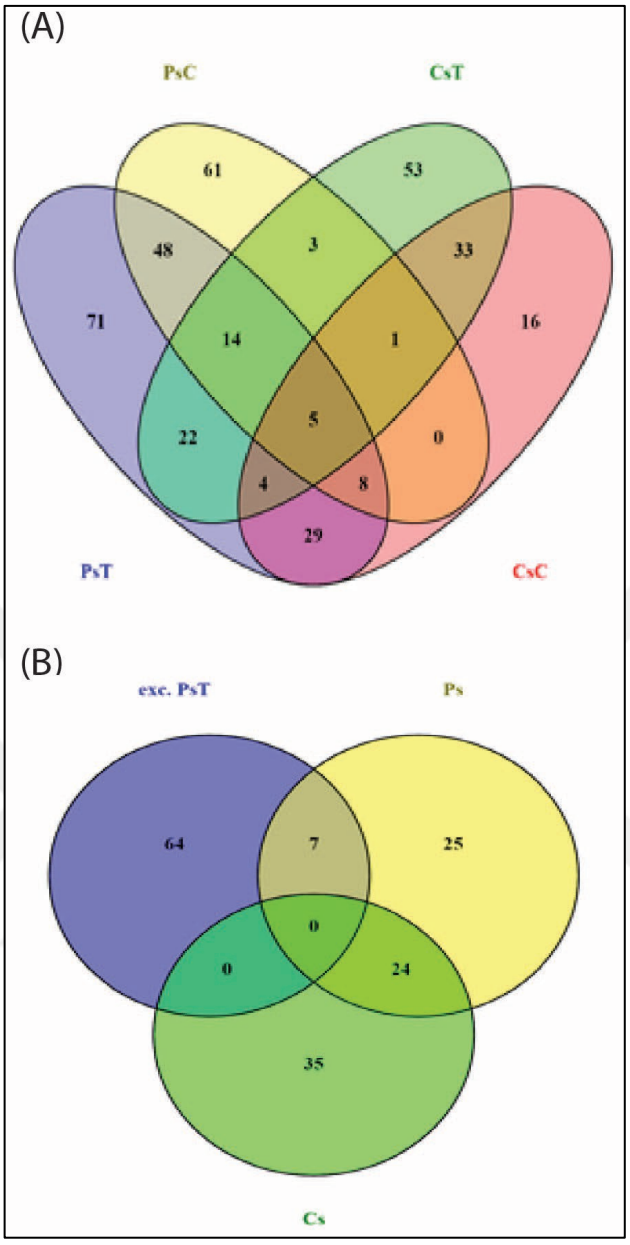

Figure 3.30. Venn diagram showing the number of identified proteins by E-SERPA analysis

3.14.4.2. Evaluation of the tissue expression levels of TAAs via WB

The relative tissue expression levels of TAAs were elucidated by comparing the tumour group prepared from the tumour protein extracts with the control group prepared from the control protein extracts. The changes in the expression levels of these proteins and also determined in the pools prepared from protein extracts of BC tumour subtypes and their corresponding controls. Protein expression levels were normalized using anti-β-actin antibody (Figure 3.31.). The band intensities of TAAs

and β-actin were measured by the Quantity software and relative expression levels were represented in graphs (Figure 3.32.).

Among the identified TAAs, four of the proteins, POSTN, SFRS3, PPIA, and H4C1, were showed higher expression levels in the tumour groups when compared to control groups. The proteins displaying relatively high expression levels in the control group were CLU, TUBA1C, and MIF. Expression of GAPDH was similar in the tumour and the control groups, and also in all BC subtypes and their respective controls.

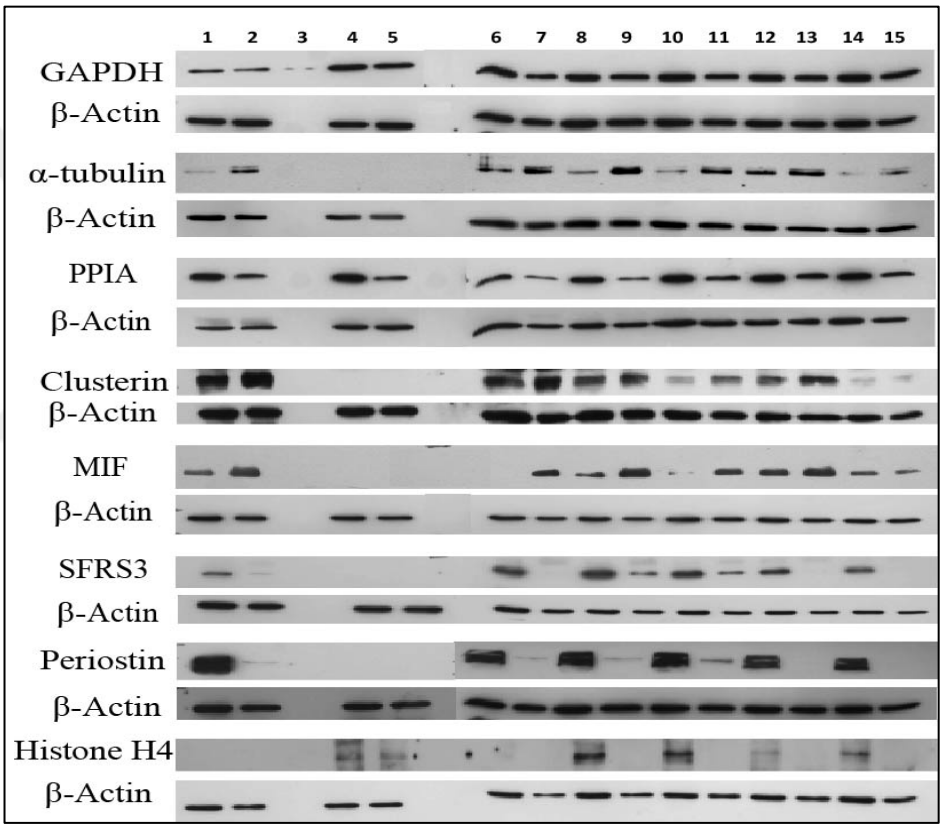

Figure 3.31. Evaluation of the tissue expression levels of TAAs by WB analysis

(Explanation for Figure 3.31: The numbers 1-15 designate the following: (1) tumour tissue protein pool, (2) control tissue protein pool, (3) negative control, (4) MCF-7 cell extract, (5) MCF-12A cell extract, (6) LA tumour protein pool, (7) LA control protein pool, (8) LB tumour protein pool, (9) LB control protein pool, (10) LB-like HER2+ tumour protein pool, (11) LB-like HER2+ control protein pool, (12) TNBC tumour protein pool, (13) TNBC control protein pool, (14) HER2-enriched tumour protein pool, (15) HER2-enriched control protein pool).

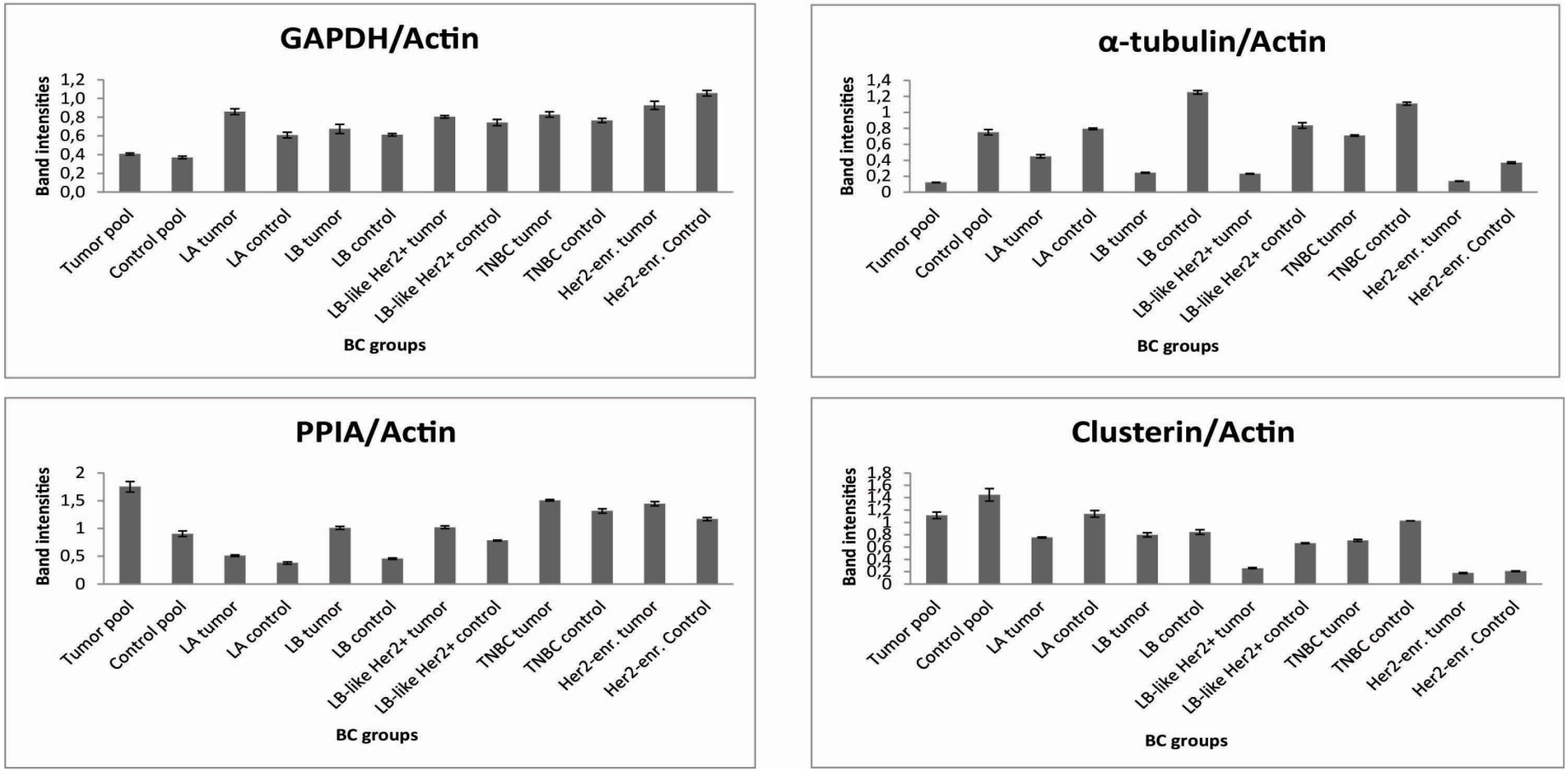

Figure 3.32. The graphs representing relative expression levels of TAAs

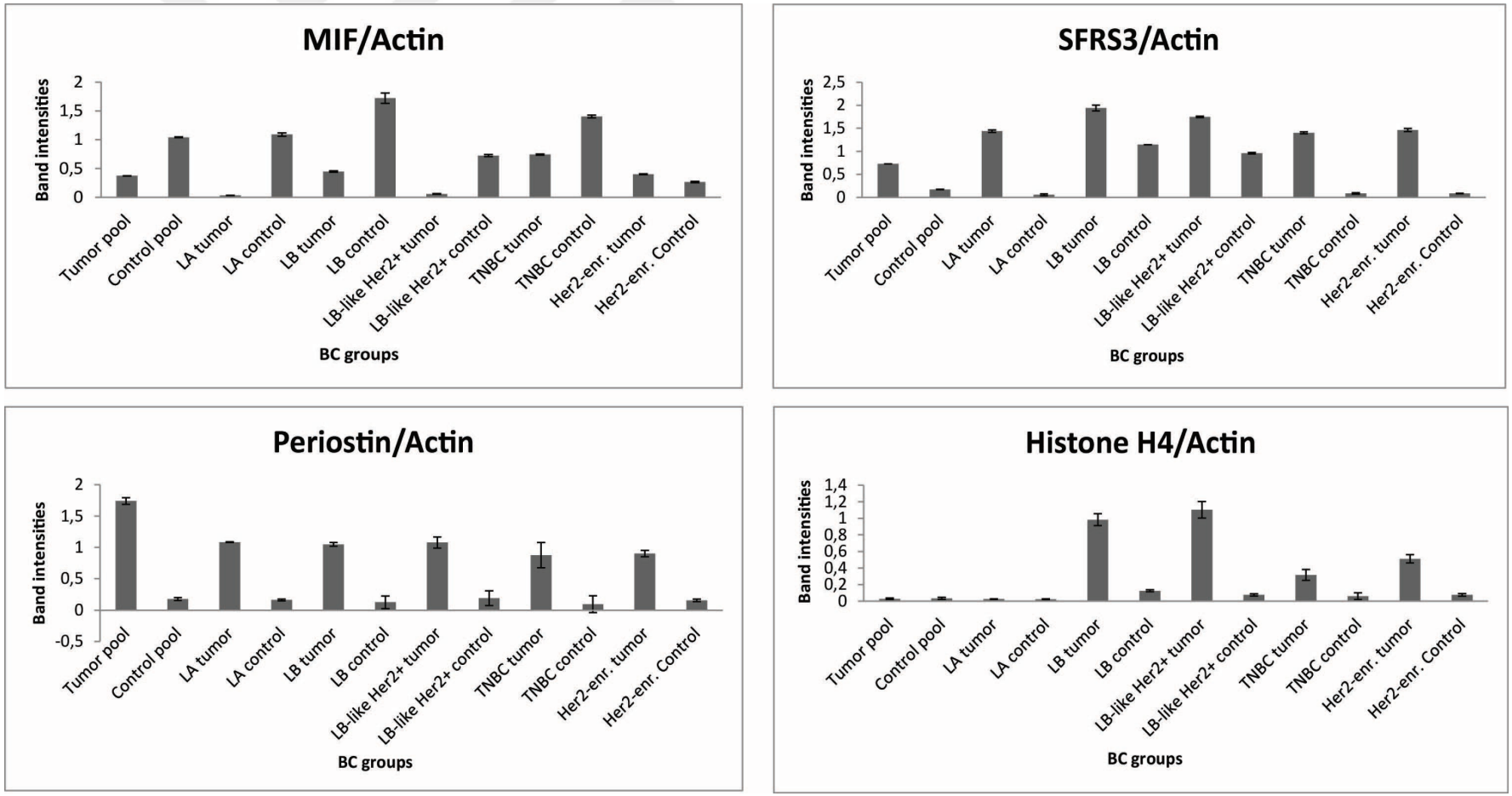

Figure 3.32 (Continues). The graphs representing relative expression levels of TAAs

4. DISCUSSION

4.1. Evaluation of Proteins Identified by 2-DE and DIGE Approaches

2-DE and DIGE-coupled to MALDI-TOF/TOF analyses allowed us to elucidate and identify several differentially regulated proteins in the breast tumours in comparison to their respective control tissues. Using bioinformatics tools and relevant software, the differentially regulated proteins were linked to metabolic events, which might be associated with the metabolic changes occurring in breast tumour cells.

Differentially regulated proteins identified in conventional 2-DE experiments were subjected to STRING analysis. The analysis created an interactome which led to the pathways associated with protein folding and unfolded protein response (UPR) (Figure 4.1A.). STRING analysis of the differentially regulated proteins determined by DIGE also confirmed the findings of 2-DE, pointing to the pathways associated with protein folding and UPR (Figure 4.1B.). Similar to our findings, Pozniak et al. reported changes in protein levels associated with UPR [122]. In their study, formalin-fixed paraffin-embedded BC tissue samples were analyzed and down-regulation of UPR-related proteins was found in tumours compared to the control tissue. UPR activation indicates the presence of cellular stress related to endoplasmic reticulum due to accumulation of unfolded or misfolded proteins [123]. Sustained over-activation of the UPR has also been implicated in several different human solid tumours [124-128]. In general, UPR is expected in solid tumours because human solid tumours contain areas of pure vascular perfusion that causes insufficient blood circulation, severe oxygen and glucose deprivations in the tumour microenvironment. UPR is expected to protect the tumour cells in response to adverse conditions [129]. It has been demonstrated that in anti-estrogen-treated cancer cells, and in cells that increased protein production and secretion, UPR activation is mild and protective [130]. UPR activation has also been linked to the inhibition of chemosensitivity to drugs [131]. Therefore, markers of UPR activation may provide clinical relevance for BC therapeutic approaches.

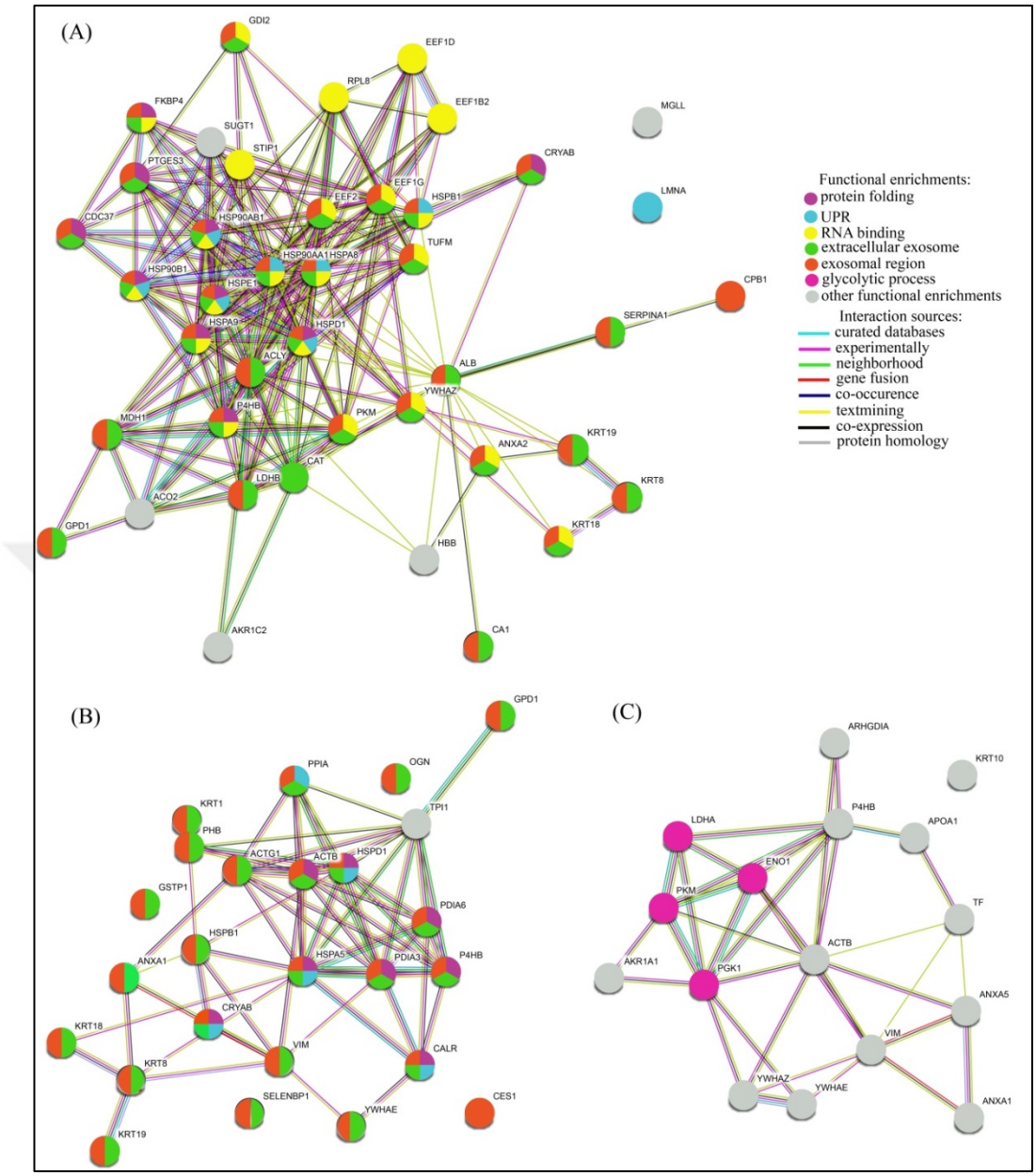

Figure 4.1. STRING analysis of the differentially regulated proteins identified via 2-DE (A), DIGE (B), and DIGE for $GPD1^{+}$ and $GPD1^{-}$ groups (C)

Some of the differentially regulated proteins of this study can be linked to carbon metabolism. Those proteins include aconitate hydratase (Q99798), malate dehydrogenase (P40925), PK (P14618) and LDH-B (P07195). It has been long known that cancer cells can reprogram their central carbon metabolism and maintain the elevated level of glycolysis to sustain their energy needs and convert glucose to lactate [132-135]. During this conversion, PK catalyses the last step of glycolysis converting phosphoenolpyruvate to pyruvate. Pyruvate is then converted to lactate by LDH to provide sufficient reducing power for energy production [136]. In our study,

we observed up-regulation in PK in all BC subtypes in comparison to the control. The up-regulation of PK in cancer cells can be linked to higher cell proliferation ability and increased anabolic functions [137, 138]. In literature, there is evidence indicating that the expression of LDH isoforms differs in healthy and cancerous tissues. LDH-A is the isoenzyme which plays the key role in regulating glycolysis in tumour cells and carcinomatous tissues possess high LDH-A isoform [139, 140, 141]. However, the LDH isoform identified in this study was LDH-B (48% sequence coverage). So far, there was no report emphasizing the changes occurring at LDH-B levels. To the best of our knowledge, this is the first study reported regulation in LDH-B levels in all subtypes of BC.

The role of lipid metabolism has been conferred to explain the aggressive properties of malignant cancers [142]. In the literature, dysregulated core enzymes in lipid metabolism and their contribution to the cancer cell migration, invasion and metastasis have been well established [142-144]. The genes involved in cellular fatty acid uptake and *de novo* lipogenesis are amplified in metastatic tumours and fatty acid synthesis plays an important role in cancer pathogenesis [145, 146]. The liberated stored fatty acids and the newly synthesized fatty acids are rapidly incorporated into neutral-lipid and phospholipid stores. Here, two differentially regulated proteins, namely MAGL and GPD1 helped us to establish an association between triglyceride metabolism and BC.

GPD1 is a member of the NAD+-dependent dehydrogenase family and plays a critical role in carbohydrate and lipid metabolism by catalysing the reversible conversion of dihydroxyacetone phosphate “DHAP” and reduced nicotinamide adenine dinucleotide “NADH” to glycerol-3-phosphate and NAD+ [147, 148]. Based on the Human Protein Atlas, GPD1 expression can be detected in most malignant tumours including renal and hepatocellular carcinomas, malignant gliomas and prostate cancers (http://v15.proteinatlas.org/ENSG00000167588-GPD1/cancer).

The relative expression levels of GPD1 among 20 different cancer types indicate that GPD1 is moderately expressed in BC tissues compared to other cancer types. In the present study, we found that GPD1 was highly down-regulated in all BC subtypes in comparison to the control. Also, the lowest GPD1 expression was detected in the

TNBC subtype. In fact, in some TNBC samples, GPD1 expression could not be detected at all. This was in line with a recent study by Zhou et al. demonstrating that the mRNA expression level of GPD1 was found to be significantly down-regulated in BC patients [149]. The same study revealed several important findings including higher GPD1 expression levels in receptor (ER and PR) positive and HER2 negative subtypes, shorter survival time in patients with low GPD1 expression, prognostic GPD1 value for ER-positive tumours, significant down-regulation at GPD1 mRNA levels in BC cell lines and significant down-regulation in GPD1 protein levels in BC cell lines and tissues [149]. In the present study, we have observed similar GPD1 protein expression levels in all BC subtypes, except the TNBC. Luminal A displayed the highest GPD1 expression at the protein level. The lowest level of GPD1 protein expression was observed in TNBC samples, implicating that not only HER2 reactivity but also ER/PR positivity is associated with GPD1 expression levels. Analysis of GPD1 expression levels in each sample revealed some variation among the individual samples, mainly in TNBC and HER2+ groups. This variability is an expected result considering the heterogeneous nature of BC subtypes. BC is a heterogeneous disease that differs greatly among different patients (inter-tumour heterogeneity) and even within the same tumour sample (intra-tumour heterogeneity) [150]. Some of the samples in the TNBC group had either no or barely detectable GPD1 expression; thus, TNBC samples were suggested to be divided into two different groups, $GPD1^{+}$ and $GPD1^{-}$.

TNBC represents 12-15% of all BCs [151]. Its molecular heterogeneity is reflected in a significantly different clinical outcome among other subtypes. Mostly, this subtype is much more aggressive causing distant metastasis [152]. Therefore, it is necessary to establish a detailed classification for the TNBC subtype. Statistically, high percentages of TNBC belong to the basal-like BC group which has a high mitotic index and high histological grade [153, 154]. Basal-like BC is identified by a variety of immunohistochemical markers, such as cytokeratins (CK5, CK6, CK14 or CK17), EGFR, SMA, p-cadherin, p63 or c-kit antigen [155]. Herein, we were curious about whether GPD1 negative or positive samples represented the basal-like BC. Using CK5/6 expressions in eight of those samples, the coherence between CK5/6 and GPD1 expressions were evaluated (Table 4.1.). Except for one sample, there was an

inverse correlation between CK5/6 status and GPD1 expression levels in TNBC individuals. Samples which lacked GPD1 expression had positive IHC staining for CK5/6, while the samples which expressed GPD1 were negative for CK5/6 staining. This finding indicated that GPD1 may be a good candidate biomarker to differentiate basal-like BC from other TNBC subtypes [154].

Table 4. 1. Tissue and serum levels of GPD1 and MAGL, and tissue CK5/6 status

Patient #	Staining pattern for CK5/6	CK5/6 status	Tissue GPD1 expression	Serum GPD1 level	Tissue MAGL expression	Serum MAGL level
P1	20%-strong	positive	-	low	+	low
P2	negative	negative	+	low	Low	high
P3	NT*	NT*	+	high	+	low
P4	20%-strong	positive	-	low	+	low
P5	60%-strong	positive	-	high	+	low
P6	<10%-weak	negative	+	low	+	high
P7	80%-strong	positive	-	low	+	low
P8	NT*	NT*	+	low	+	low
P9	NT*	NT*	-	low	Low	low
P10	negative	negative	+	low	+	low
P11	20%-strong	positive	+	high	+	low

The results of comparative DIGE experiments with $GPD1^{+}$ and $GPD1^{-}$ samples revealed the presence of 16 differentially regulated proteins. STRING analysis with the differentially regulated proteins indicated a significant change in the glycolytic process (FDR of 8.56e-05) (Figure 4.1C). The glycolytic proteins that displayed down-regulation in $GPD1^{+}$ samples in comparison to $GPD1^{-}$ samples were LDH, PK, phosphoglycerate kinase 1 and alpha-enolase. The heterogenic complex nature of TNBC may likely require flexible cell metabolism in which non-enzymatic functions of most glycolytic enzymes may offer important contributions [156]. Future studies should consider whether the changes in the levels of these glycolytic enzymes may help TNBC cells to sustain their growth.

It is known that *de novo* fatty acid synthesis is significantly increased in tumour cells. On the other hand, normal cells are primarily taken fatty acids from dietary sources [146, 157]. MAGL is an enzyme of fatty acid metabolism and responsible for the breakdown of monoacylglycerols (MAGs) to free fatty acids (FFAs) [158]. MAGL is

best recognized for its role in degrading endogenous 2-arachidonoylglycerol in the brain and the peripheral tissues [158]. It is considered to be one of the key enzymes which regulate the network of FFAs in numerous aggressive tumours such as colorectal cancer, neuroblastoma and nasopharyngeal carcinoma [159-161]. In our study, we have identified MAGL as one of the regulated proteins in BC subtypes. Our 2-DE results demonstrated that MAGL was down-regulated in all BC subtypes in comparison to the control. More specifically, the TNBC subtype showed the lowest MAGL expression compared to the other BC subtypes. This finding supported the fact that tumour cells use *de novo* fatty acid synthesis rather than hydrolysis of neutral lipid stores. However, Nomura et al. demonstrated a compelling result for lipid metabolism in tumour cells that MAGL was highly expressed in aggressive human cancer cells and primary tumours [162]. They stated that increased aggressiveness of cancer cells requires increased lipid synthesis by the lipolytic pathway to liberate stored fatty acids by MAGL. Aggressive cell lines displayed much greater in vitro migration and in vivo tumour growth rates in comparison to their non-aggressive counterparts. Moreover, inhibition of MAGL demonstrated that aggressive cancer cells display highly elevated MAG activity, most of which comes from the MAGL enzyme. Blocking MAGL by either siRNA or an inhibitor reduced in vitro migration, invasion, and cell survival under serum deprivation; while over-expression of MAGL in non-aggressive cancer cells increased their pathogenicity. The work by Nomura et al. opened a way to investigate whether MAGL could be a potential therapeutic target and prognostic indicator for various cancer types [158]. Contrary to the results by Nomura et al., our study demonstrated a decrease in the MAGL expression level in the tumour tissues compared to their corresponding control tissues. This conundrum cannot be explained with the current knowledge about the known function of MAGL. The complex interplay between oncogenic signalling and lipid metabolism and the large spectrum of lipid functions at both the cellular and organismal level require a more detailed understanding of the alterations in lipid metabolism in cancer. A possible reason to explain the controversy between our data and that reported by Nomura et al. could be that they performed activity-based proteomic analysis and did not monitor the changes in MAGL protein levels while we performed non-functional proteomic analysis and only determined the changes in MAGL protein levels. MAGL overexpression causes a significant

reduction in MAGs and elevation in FFAs [158]. Based on this knowledge, we propose that the *in vivo* aggressiveness of cancer cells depends on the level of MAGs rather than the level of FFAs. However, currently, there is no supporting data for our proposal in the literature. Despite the recent research indicating the relationship between MAGL and the tumour progression, the mechanism of pro-tumour activity of MAGL is still unknown. The data presented here raised a point for MAGL to be a candidate therapeutic target and prognostic indicator for BC. Histological examination of tissue samples may be useful for clinical application of MAGL for BC diagnosis and subtyping. It may be worth investigating the changes in serum levels of MAGL to develop a more reliable and convenient clinical test for BC diagnosis and prognosis.

4.2. GPD1 and MAGL Can Be Useful BC Biomarkers

The aim of this study was to identify BC-associated biomarkers. With the use of gel-based mass spectrometric approaches, the roles of GPD1 and MAGL proteins in BC metabolism and their contributions to cancer metabolism have been discussed and they were proposed as the potential biomarkers for BC. To strengthen our proposal that GPD1 and MAGL were BC-associated biomarkers, their serum levels were also determined by ELISA. The comparative analysis of the serum GPD1 and MAGL levels among the BC subtypes indicated a significantly lower expression level in TNBC when compared to other BC subtypes. This finding was in agreement with the findings of 2-DE and WB analyses.

Most of the BC markers in use today have low sensitivity and specificity. For example, CEA, one of the most commonly used biomarkers, has a sensitivity of 95% with 15% specificity [163]. Similarly, CA 15-3, soluble form of MUC-1 protein and widely used serum marker for BC, has a sensitivity of 95% with 23% specificity [163]. In here, patients with GPD1 protein expression level less than 3.18 ng/mL can be diagnosed as TNBC with 95% sensitivity 77.5% specificity. The ELISA results indicated that the serum GPD1 showed higher diagnostic performance for BC patients compared to the ones used in clinics today. These findings were also in agreement with the transcriptome data extracted from TCGA. However, monitoring the serum GPD1 levels rather than mRNA levels was more predictive in

distinguishing BC patients with TNBC subtype. The prognostic role of GPD1 in BC patients was analyzed through Kaplan-Meier survival analysis using mRNA expression data. Patients with higher GPD1 gene expression levels received a poor prognosis compared to the low-risk group with lower GPD1 levels. Although GPD1 have high potential as a diagnostic biomarker for BC, its prognostic potential does not represent the same. The comparative analysis of the serum MAGL levels among BC subtypes and healthy subjects indicated a significantly higher level in the control group. When the serum levels were compared with the MAGL mRNA levels, it was observed that serum MAGL level was more predictive in discriminating the healthy subjects from BC patients. According to ROC analysis results, subjects with MAGL protein expression level higher than 7.23 ng/mL can be determined as healthy with 100% sensitivity 98.5% specificity. This data shows that MAGL has high potential as a diagnostic biomarker for BC.

4.3. Immunoproteomics Led to the Identification of TAAs

Immunoproteomics is a widely used technique where the target proteins are captured by the autoantibodies that bound to a solid matrix [164]. In this study, proteins extracted from BC tumour tissues were used as the target proteins and antibodies purified from the serum samples of BC patients were used as the autoantibodies to capture BC-associated antigenic proteins. In general, autoantigens are in much lower amounts than autoantibodies and hard to capture and identify [164]. Therefore, a powerful technique, called E-SERPA, was used to capture TAAs. The captured antigenic proteins were then identified by nLC-MS/MS analysis. Evaluation of the nLC-MS/MS results revealed the presence of 9 TAAs (only in PsT). Those proteins were, namely, GAPDH, TUBA1C, PPIA, CLU, MIF, SFRS3, POSTN, H4C1 and CCDC13. Expressions of these proteins in BC tumour and control pools were investigated by WB. The WB analysis was extended to cover the pools of BC subtypes as well. Among these proteins, the expressions of SFRS3 and POSTN were significantly upregulated in all BC subtypes compared to their corresponding controls. PPIA and H4C1 are the other upregulated proteins with less significance. Contrary to that, expressions of CLU, MIF and TUBA1C were higher in the control tissues compared to the tumour tissues. The GAPDH expression was nearly the same

in all BC subtypes and their corresponding controls. The expression of CCDC13 was not determined in the tumour and control tissues.

POSTN, also designated as an osteoblast-specific factor, is a 93 kDA matricellular glycoprotein secreted by cancer-associated fibroblasts [165, 166]. It has roles in the promotion of cancer initiation and progression [167, 168]. Its overexpression has been stated in a wide range of cancer types, including BC, glioblastoma, colon, gastric, and pancreatic cancer [169-175]. Also, overexpression of POSTN in epithelial cells of BC is associated with poor survival rates [165, 176]. The relationship between the expression of POSTN in the prognosis of BC and cancer stem cells have been studied by Lambert et al. in basal-like BC [177]. They found that POSTN was highly expressed in basal-like stem cells and associated with reduced survival rates. In addition, knockdown of POSTN revealed that POSTN expression was required for cells to maintain cancer stem cell phenotypes. In another study, Vardaki et al. [178] used mammary epithelial carcinoma cells lines to picture their exosomal protein profiles. LC-MS/MS analysis of exosomes revealed that the majority of the exosomal proteins have functions in adhesion and migration. The highly enriched proteins in exosomes were integrin and POSTN. They validated their *in vitro* findings in the extracellular vesicles of plasma of 14 BC patients and hypothesized that accumulation of POSTN in exosomes help cells to maintain cancer stem cells properties. In here, POSTN has been identified as TAA by nLC-MS/MS. This finding supported the current knowledge that POSTN is expressed at higher levels in BC epithelial cells than in healthy tissues. In this study, the tissue expression level of POSTN was significantly higher in the tumour tissues than the controls as demonstrated by WB. POSTN expression was also significantly high in all BC subtypes implying that the higher levels of POSTN expression were irrespective of BC subtypes. It is important to note here that POSTN could be a sensitive tissue-based diagnostic biomarker since there was almost no expression of POSTN in the control tissues.

SFRS3 is the smallest member of the serine/arginine-rich protein family [179]. SFSR members have roles in RNA metabolism including regulation of transcription and alternative splicing of precursor mRNA [180-181]. 95% of the human genes are alternatively spliced [182] and misregulation of alternative splicing has been linked

to diseases including a wide variety of cancers [183-185]. Stickeler et al. have studied the role of precursor mRNA splicing in human malignancies using the *in vivo* mouse model of mammary development and tumorigenesis [186]. They found that the expression levels of serine/arginine-rich proteins are regulated in mammary adenocarcinomas. Kurokawa et al. studied SFRS3 knockdown in colon cancer [187]. They found that knockdown of SFRS3 induced G1 arrest and apoptosis and stated that SFRS3 can have an essential role in tumour growth. Knockdown of SRSF3 has been studied by other researchers and they also stated the role of SFRS3 in the apoptosis of cancer cells [188, 189]. Overexpression of SFRS3 has been stated in human ovarian cancer [179]. The researchers suggested that SFRS3 is a regulator in DNA repair in ovarian tumour cells and SFRS3 overexpression is necessary for ovarian tumour cell survival and growth. In here, SFRS3 has been identified as the target protein for the immune system. Analysis of the tissue expression levels showed that there was no detectable level of SFRS3 expression in the control pools. SFRS3 expression was detected in each BC subtype. The relative tumour tissue expression levels of SFSR3 compared to their control groups were higher in TNBC and HER2-enriched subtypes. The role of SFRS3 in alternative splicing may cause tumour cells to grow in BC, especially in the aggressive TNBC subtype.

PPIA mediates normal and malignant mammary gland differentiation by regulating the Jak2/Stat5 pathway [190]. It is a cytosolic protein known to bind to the immunosuppressive drug cyclosporine A [191]. Its expression in various cancers such as pancreatic, lung and oral squamous has been stated by different studies. [192-194]. PPIA expression also contributes to the proliferation of vascular endothelial cells [195]. In a study, Theuerkorn et al. stated that the overexpression of PPIA in tumour cells can lead to cell transformation by suppressing apoptosis [196]. This data was stated in former research which studied the growth of endometrial carcinoma HEC-1-B cells. They showed that the growth of tumour cells was inhibited by the down-regulation of PPIA and PPIA induced apoptosis in endometrial tumour cells [197]. Fujioka et al. investigated the paclitaxel resistance in MCF-7 human BC cells and its paclitaxel-resistant subclone (MCF-7/PTX) using gel-based proteomics approaches [198]. They found that paclitaxel-resistant cells showed overexpression of PPIA compared to normal MCF-7 cells. siRNA-mediated knockdown of PPIA

caused the resistant cells to be sensitive to the drug. They hypothesized that PPIA had roles in regulatory cell death metabolism and paclitaxel resistance. Based on their findings, PPIA was suggested to be a prognostic biomarker. In here, PPIA was identified as TAA in BC, and its overexpression in cancer cells was confirmed by the presented results. The tissue expression level of PPIA was higher in all BC subtypes compared to their corresponding controls. But the tumour tissue expression levels compared to their control groups were higher in TNBC and HER2-enriched subtypes.

Histone proteins, H2A, H2B, H3 and H4, are highly conserved proteins that constitute the core component of the nucleosome [199]. They have roles in the regulation of gene expression by stimulating the encoding of epigenetic information [200]. The identified histone family member in here was H4C1. Histones and their variants can undergo changes by different post-translational modifications (PTMs), such as methylation, acetylation, glycation and ubiquitination [201]. PTMs have important roles in the regulation of cellular events by creating various stimuli in the cell [202]. Some histone PTMs are linked to a wide range of cancers, including BC [203, 204]. Perri et al. studied the histone PTMs in BC cell lines using gel-based MS and identified 85 histone PTMs [199]. They found that H1 tyrosine phosphorylation levels were high in BC cell lines compared to the non-cancerous cell line and proposed Focal adhesion kinase as a candidate for H1 tyrosine phosphorylation. Taken into consideration that Focal adhesion kinase is overexpressed in BC and contributes to its tumourigenesis, they suggested that H1 tyrosine phosphorylation can be novel PTM which drives breast tumorigenesis [199]. It is known that glycosylation of proteins plays critical roles in the regulation of protein structure [205], signal transduction [206], cell-cell and cell-environment interactions [207], immune responses [208, 209], and cancer progression [210]. Zheng et al. studied *in vitro* and *in vivo* histone glycation and revealed a regulation mechanism for DJ-1, a histone deglycase. DJ-1 has a key role in recovering glycosylation-induced damage in cells [201]. They showed that BC tumours expressed high levels of DJ-1 and had strong histone glycation, especially in basal cells. In this study, H4C1 was identified as TAA in BC. The relative tumour tissue expression levels of H4C1 compared to

their control groups were higher in Luminal B and Luminal B-like HER2+ than TNBC and HER2-enriched subtypes.

CLU protein is a heterodimeric chaperon-like glycoprotein [211]. It possesses multiple functions in lipid transport, membrane recycling, cell adhesion, and programmed cell death [211]. Three different proteins are the products of CLU gene: nuclear CLU "nCLU" which promotes cell death, secreted CLU "sCLU" which prevents cell death, and cytoplasmic CLU "cCLU" with multiple functions [211-213]. Based on its different roles and locations, expression of CLU protein was down-regulated in several cancer types displaying a pro-apoptotic role and was up-regulated in several cancer types displaying a suppressor role in apoptosis [214-216]. Ranney et al. studied the role CLU in BC using MDA-MB-231 and MDA-MB-435S cells lines and found that after DNA damage, the intrinsic apoptotic pathway was suppressed by CLU by limiting cytochrome release [212]. Suppression of apoptosis had a negative effect on chemotherapy and reduced its effectiveness. Wang et al. determined the CLU expression profiles of TNBC patients who had neoadjuvant therapy before surgery by comparing tumour and stromal stainings using immunohistochemical staining approach [217]. Based on the results, CLU expression profiles were differed in tumour and non-tumourous cells; while CLU was expressed only in the lobules in the lobules of non-cancerous tissue, and the staining was homogenous and membranous in the tumour tissue. CLU expression in tumours does not correlate well with the treatment outcome. However, stromal CLU expression was shown to be significantly associated with neoadjuvant therapy in TNBC patients. They concluded that CLU expression is important in cancer progression. In here, CLU protein was identified as TAA by the E-SERPA method. Further analysis of CLU expression in the tumour and control tissues of BC subtypes showed that the control tissues had higher levels of expression than the tumour tissues. The lowest CLU expression was detected in HER2-enriched subtype. Considering the pro-apoptotic role of CLU when it is being down-regulated, we might predict that CLU-associated cellular pathways are regulated to encourage apoptosis in all BC subtypes. Further research may correlate the down-regulation of CLU with its pro-apoptotic function in BC subtypes.

MIF is a homotrimer, pro-inflammatory cytokine and a multifunctional protein. It has multiple effects on immune cells, inflammation and cancer [218]. There are two forms of MIF, intracellular and extracellular [219]. Thongwatchara et al. investigated the protein expression levels of BC patients with axillary lymph node metastasis and node-negative breast carcinoma using gel-based LC-MS/MS. They found that MIF was down-regulated in the metastatic axillary lymph node. Avalos-Navarro et al. investigated the plasma levels of 150 BC patients and 60 healthy volunteers and found that MIF expression levels in plasma were significantly high in BC patients compared to controls [218]. There are other studies investigated MIF serum levels in various types of cancers including BC and they all reported a significant increase in MIF levels compared to the levels observed in healthy volunteers [220-227]. Xu et al. used showed tissue microarray technology and showed that MIF is overexpressed in BC patients at the mRNA level [221]. They stated that 30% of the patients showed high MIF expression in their tumour tissue. The high MIF expression level showed a significantly worse disease-free survival compared to low levels. The overall conclusion of Xu et al. was that MIF could be a therapeutic target in BC. Using gene array technology, Burnett et al. studied the role of tumour-associated macrophages in tumour progression in MCF-7 cells, tamoxifen-treated MCF-7 cells and MCF-7 cells co-cultured with macrophages [228]. They reported the presence of two forms of MIF as extracellular and intracellular in co-cultured MCF-7 cells. The observation was linked to the covalent modification of one form. They commented that MIF of macrophages, down-regulated, can be protective for cancer cells and MIF in cancer cells, up-regulated, can be adaptive. The two forms of MIF, intracellular or extracellular expression, was also reported in human BC tissues by Verjans et al. [229]. In our study, MIF was identified by nLC-MS/MS as TAA. In contrast, the tissue expression levels of MIF was higher in control tissues than the BC subtypes. It can be inferred from the studies mentioned above that the role of MIF in BC has different effects on metabolism, and needs to be explored in detail.

TUBA1C is a structural protein and an important component of the cytoskeleton. An important part of cytoskeleton consists of microtubules formed by polymerization of alpha- and beta-tubulin [230]. Based on their critical functions in cell division and various cellular functions, tubulins draw attention as tumour targets for cancer

therapy [231]. The role of tubulins in cancer metabolism have been investigated through altering tubulin structure via microtubule stabilizers and destabilizers. Sakchaisri et al. identified a novel antimitotic agent named STK899704 that binds to tubulin and inhibits its polymerization which eventually leads to cell death and causes cell cycle arrest during mitosis. STK899704 was found to be inhibited the tumour growth via suppressing the proliferation of cancer cells of various origins (skin, bone, breast, colon, lung, prostate, stomach, brain and liver). STK899704 was then proposed as a novel tubulin-depolymerizing and a potential anti-cancer agent [231]. Other natural or chemically synthesized compounds that affect tubulin polymerization and thus cancer progression were reported in the literature. For instance, resveratrol displayed an anti-cancer activity via inhibition of tubulin polymerization [230]. In their study, Mu et al. identified stromal proteins of the tumour microenvironment [232]. Ingenuity Pathway Analysis with differentially regulated proteins showed that cancer is the main disease that linked to the regulated proteins by biological functions. Tubulin destabilization is not restricted only to the use of exogenous compounds. PTMs can also destabilize tubulin polymerization and affect cellular viability [233-235]. Liao et al. reported that acetylation of alpha-tubulin leads to apoptosis of cancer cells [236, 237]. APOC1P1-3 could bind to tubulin and decrease α-tubulin acetylation. This leads to the inactivation of caspase-3 and finally to inhibition of apoptosis. This study demonstrates that overexpression of APOC1P1-3 can inhibit BC apoptosis [238]. In here, TUBA1C was identified as a TAA and captured in BC tumour tissues. Hence, the expression level of TUBA1C was higher in the control groups of BC subtypes compared to tumour tissues. At first, this observation might appear obscure since tubulin was solely captured by the autoantibodies purified from the patients' sera. However, it should be kept in mind that the property of being a TAA has no relation with its tissue concentration. A protein with low tissue concentration may well have an antigenic property and vice versa.

GAPDH is the key enzyme of glycolysis and serves to break down glucose for energy [239]. Although GAPDH is a key housekeeping enzyme and expressed constitutively in cells, it actively involves in cancer metabolism. The uncontrollable growth of cancer cells prevents them to use aerobic respiration and utilize the

tricarboxylic acid cycle (TCA) effectively [132]. Even if the cancer cells are able to perform aerobic respiration, the limited oxygen availability in the tumour microenvironment prevents the TCA cycle to work. The tumour cells then have to solely rely on the glycolytic pathway to meet their energy requirement. In tumour cells, the glycolytic enzymes perform not only their housekeeping duties but also different roles in the cell. Many cytoplasmic metabolic enzymes are known to be relocated into the nucleus and performed other duties rather than their catalytic activities, a phenomenon called moonlighting [240]. For instance, several glycolytic enzymes including hexokinase, phosphoglucose isomerase, glyceraldehyde triphosphate dehydrogenase and GAPDH were shown to moonlight. In here, GAPDH was identified as a TAA. Several studies related to GAPDH were examined in many cancers. Elkhalfi et al. studied the expression of GAPDH in cervix, breast and prostate tumours [241]. Using immunohistochemical approaches, they showed that in all tumour types, GAPDH was overexpressed mainly in the nucleus and spread throughout the cell. Besides, in benign tissues, it was mainly expressed in the membrane and/or cytoplasm. This was a notable finding since GAPDH is known to be a cytosolic protein in healthy cells. They speculated that GAPDH may perform an unknown function in the nucleus and the nuclear form of GAPDH may be different than the cytosolic form. More relevant to our study, Revillion et al. studied the expression of GAPDH in MCF-7 human mammary epithelial cells in the presence of oestradiol and the primary BCs [242]. Quantitive results of reverse transcription-polymerase chain reaction (RT-PCR) showed that GAPDH gene expression was inversely correlated with the oestradiol levels in primary BCs, whereas in MCF-7 human BC cells GAPDH expression was induced by oestradiol. As a result, they concluded that GAPDH is associated with cell proliferation and tumourigenesis in BC. In here, GAPDH was among the identified TAAs. The expression levels of GAPDH were monitored by WB analysis. The results showed that GAPDH expression levels were nearly equal in all BC subtypes and their corresponding controls. This finding was notable since GAPDH was solely captured by the autoantibodies purified from the patients' sera. It is possible that the cellular form of GAPDH that induces autoantibody production by the host is much different than the well-known cytoplasmic form of GAPDH. It is even likely that GAPDH is secreted into the bloodstream via the tumour cells after a vigorous modification. All

these possibilities are needed to be searched for. It can be hypothesized that not the amount of GAPDH in the cells but the localization of it causes the immune response and lead to the production of autoantibodies against GAPDH.

CCDC13 is a centrosomal protein which functions in the formation of primary cilia and genome stability [243]. Although there are not many cancer-related studies about CCDC13, there are studies including other members of the protein family. In a study, Hu et al. studied the expression of CCDC34 in oesophageal squamous cell carcinoma using the immunohistochemical technique in 100 cancer cases and 80 cases of corresponding control tissues [244]. They stated an up-regulation of CCDC34 protein in oesophageal squamous cell carcinoma and associated the expression with tumour progression, angiogenesis, and poor survival rates. The effect of CCDC8 expression on cancer cell invasion and metastasis were investigated for the first time by Jiang et al. in non-small cell lung cancer [245]. Using immunohistochemical staining, they determined CCDC8 expression in 147 tumours and 30 adjacent control tissues. They showed that CCDC8 expression was significantly low in cancer cells and commended that invasion and metastasis of lung cancer cells may be suppressed by CCDC8 expression. In overall, they suggested CCDC8 protein as a therapeutic target for non-small cell lung cancer. In here, CCDC13 was identified among the TAAs. The aberrant expression of CCDC13 may have stimulated the immune system in BC patients.

5. CONCLUSION AND FUTURE WORK

5.1. Conclusion

The quest to find a biomarker for early detection of BC continues. The biomarkers in use today are either not specific or do not allow early detection of BC. The classical radiological scans and the other clinical approaches do not appear to be powerful and convenient enough to allow early detection. In the late few years, novel biomarker candidates have emerged but they also suffered from sensitivity and specificity issues and do not have the potential to satisfy the needs of the early diagnosis of BC [246-248]. Gene/protein signatures are proposed as biomarker panels but they stay inadequate due to their high cost and availability. Lack of success to find a biomarker for early detection lies in the complexity of pathways that transform cells into the cancerous state. Understanding the complex interplay among these pathways will ultimately lead to the discovery of a simple and effective biomarker/biomarker panel. However, this requires a detailed analysis of the genome, transcriptome, metabolome and proteome. The work presented here analysed the changes occurring in proteome profiles of BC subtypes with respect to their healthy counterparts. Two different approaches were used throughout the study. The first approach utilized the tools of conventional 2-DE and DIGE approaches and elucidated 13 proteins whose level displayed significant changes in the tumour tissues in comparison to the controls. Subsequent bioinformatics analysis of the regulated proteins revealed the importance of TAG metabolism in BC and directed us to the identified proteins, namely GPD1 and MAGL. WB analysis was then performed to investigate the expression levels of these proteins in BC subtypes and control group. The results implied that GPD1 and MAGL did have a great potential to become tissue-based diagnostic and/or prognostic BC biomarkers and can readily differentiate TNBC subtype from the other subtypes. However, the tissue-based biomarkers are less practical to be used in clinics and thus, we were urged to see if the changes in the expression levels of GPD1 and MAGL were reflected onto the serum. For this reason, we analyzed the serum GPD1 and MAGL levels using ELISA assay. Statistical analysis of the

ELISA results provided strong evidence that GPD1 acts as a diagnostic biomarker in distinguishing TNBC patients from other subtypes (the sensitivity of 95% and specificity of 77.5%). In addition, MAGL can be a diagnostic biomarker in distinguishing healthy subjects from BC patients (sensitivity of 100% and specificity of 98.5%). Due to the limited availability of the clinical data regarding the patients used in this study, we were not able to estimate the prognostic value of these two proteins. However, the elucidation of the prognostic values of these two proteins was possible at the transcriptome level using the RNAseq data from the TCGA database. The statistical analysis could not generate strong evidence for prognostic values of GPD1 and MAGL. We concluded that GPD1 and MAGL might be proposed as non-invasive diagnostic biomarkers with high sensitivity and specificity for BC.

The second approach used here was called E-SERPA. In this approach, we purified antibodies produced by the hosts' immune system and used them to capture TAAs. The captured antigenic proteins were then identified by nLC-MS/MS. Similar versions of this approach were used in the literature but none of those was performed as elaborately as ours since we spent a great deal of time to optimize binding and elution steps. The E-SERPA experiments generated a vast amount of data which we processed and evaluated. In the end, 9 proteins were labelled as the TAAs. Commercial antibodies against these proteins were then used to investigate the expression levels in tumour and control tissues. Except for GAPDH, they were all differentially regulated in the tumour tissues in comparison to the controls. Bioinformatics analysis with these antigenic proteins using freely-available databases and software did not produce a significant metabolic pathway, molecular event or a biological process which we may scrutinize further. However, literature search with each protein indicated that those proteins were previously associated with either BC or other cancer types and worthy of further investigation.

In conclusion, the herein presented study significantly contributed to the current BC literature by proposing novel BC-associated putative protein biomarkers that were discovered using the state-of-the-art technologies e.g. 2-DE coupled to MALDI-TOF/TOF and E-SERPA coupled to nLC-MS/MS. Some of these novel biomarker candidates are worthy of further investigation and may well find their places in clinical practice as diagnostic tools.

5.2. Future Work

The experiments carried out in this study generated a list of BC-associated biomarker candidates with high confidence. However, the generated data has little strength to propose that these candidate biomarker proteins may readily be used in clinics. To put them in clinical use, multi-centred large cohort studies ought to be carried out. Also, the determination of serum levels of identified TAAs in BC subtypes may add valuable information to the literature.

Due to financial limitations, the specificities of the biomarkers discovered here were only assessed in BC. We do not know, however, if these proteins are also differentially regulated in other cancer types. Future work may be carried out to study the possible changes in the expression levels of these biomarker candidates to determine a BC-specific biomarker protein.

As a new treatment option for cancer in the last decade, immunotherapy uses patients' immune system to eliminate tumour cells and provides a new way to eradicate cancer by leveraging or stimulating the immune system [249]. Therapeutic vaccination is a type of immunotherapy and an alternative approach to fight against cancer. The main obstacle of tumour vaccines is the need for the identification of TAAs to be used in vaccine development [249]. To provide and maintain the specificity of immunotherapy, TAAs must be identified and the therapeutic potential of TAAs must be addressed. In this way, the immunogenicity of the discovered biomarker candidates can be studied in detail. Such future studies should focus on PTMs since PTMs induce an immune response in the body by generating a neo-epitope to the major histocompatibility complex or T-cell receptors which eventually induce the production of autoantibodies [89, 250]. Autoantigens representing different PTMs are the targets of the immune system. Thus, the PTMs which add antigenic characteristics to the putative biomarkers should be determined by MS-based technologies. Glycosylation is a type of PTM and glycoproteins are membrane-bound or membrane-associated proteins which act as drug targets in various diseases including cancer. In BC, most of the identified biomarkers are glycoproteins displaying different antigenic characteristics. For instance, CEA, HER2, MUC-1, and P-glycoprotein are hyperglycosylated antigens in BC [251]. In this study, among the identified antigens, POSTN and CLU are glycoproteins. In

addition, PPIA and H4C1 proteins are known to be glycosylated in several cancer types. To propose TAAs as drug targets, therapeutic efficacy and immunogenicity of the proteins must be studied. In addition, cell membrane proteome representing most of the glycoproteins of the cells can be investigated in BC tumour tissues and/or BC cell lines to propose drug targets.

REFERENCES

[1] Society A.C., Breast Cancer Facts & Figures 2017-2018, American Cancer Society, https://www.cancer.org/content/dam/cancer-org/research/cancer-factsand statistics/breast-cancer-facts-and-figures/breast-cancer-factsand-figures-2017-2018.pdf, (Access time: January 2019).

[2] Woodward WA., Strom E.A., Tucker S.L., McNeese M.D., Perkins G.H., Schechter N.R., Singletary S.E., Theriault R.L., Hortobagyi G.N., Hunt K.K., Buchholz T.A., Changes in the 2003 American Joint Committee on Cancer Staging for Breast Cancer Dramatically Affect Stage-Specific Survival, *J Clin Oncol*, 2003, **21**(17), 3244-3248.

[3] Provencher L., Hogue J.C., Desbiens C., Poirier B., Poirier E., Boudreau D., et al., Is Clinical Breast Examination Important for Breast Cancer Detection?, *Curr Oncol*, 2016, **23**(4), 332-339.

[4] Duffy M.J., Harbeck N., Nap M., Molina R., Nicolini A., Senkus E., et al., Clinical Use of Biomarkers in Breast Cancer: Updated Guidelines from the European Group on Tumour Markers (EGTM), *Eur J Cancer*, 2017, **75**, 284-298.

[5] Cole K.D., He H.J., Wang L., Breast Cancer Biomarker Measurements and Standards, *Proteomics Clin Appl*, 2013, **7**(1-2), 17-29.

[6] Kabel A.M., Tumour Markers of Breast Cancer: New Prospectives, *Journal of Oncological Science*, 2017, **3**(1), 5-11.

[7] Frenette P.S., Thirlwell M.P., Trudeau M., Thomson D.M., Joseph L. and Shuster J.S., The Diagnostic Value of CA 27-29, CA 15-3, Mucin-like Carcinoma Antigen, Carcinoembryonic Antigen and CA 19-9 in Breast and Gastrointestinal Malignancies, *Tumour Biol*, 1994, **15**(5), 247-254.

[8] Nicolini A., Ferrari P., Duffy M.J., Prognostic and Predictive Biomarkers in Breast Cancer: Past, Present and Future, *Semin Cancer Biol*, 2017, **52**(1), 56-73.

[9] Cooper G.M., *The Cell: A Molecular Approach, The Development and Causes of Cancer*, 2nd ed., Sinauer Associates, Sunderland (MA), 2000.

[10] Bland K.I., Copeland E.M., Klimberg S., Gradishar W.J., *The Breast: Comprehensive Management of Benign and Malignant Diseases*, 5 ed., Elsevier, ISBN-10: 0323359558, 2017.

[11] Makki J., Diversity of Breast Carcinoma: Histological Subtypes and Clinical Relevance, *Clin Med Insights Pathol*, 2015, **8**, 23–31.

[12] Denoix P.F., Enquete Permanent Dans les Centres Anticancereux, *Bull Inst Nat Hyg*, 1946, **1**, 70.

[13] Cho N., Molecular Subtypes and Imaging Phenotypes of Breast Cancer, *Ultrasonography*, 2016, **35**(4), 281-288.

[14] Cancer Genome Atlas Network, Comprehensive Molecular Portraits of Human Breast Tumours, *Nature,* 2012, **490**(7418), 61-70.

[15] Perou C.M., Sorlie T., Eisen M.B., Rijn M., Jeffrey S.S., Rees C.A., et al., Molecular Portraits of Human Breast Tumours, *Nature*, 2000, **406**, 747-752.

[16] Sorlie T., Perou C.M., Tibshirani R., Aas T., Geisler S., Johnsen H., et al., Gene Expression Patterns of Breast Carcinomas Distinguish Tumour Subclasses with Clinical Implications, *Proc Natl Acad Sci*, 2001, **98**, 10869-10874.

[17] Parker J.S., Mullins M., Cheang M.C., Leung S., Voduc D., Vickery T., et al., Supervised Risk Predictor of Breast Cancer Based on Intrinsic Subtypes, *J Clin Oncol*, 2009, **27**, 1160-1167.

[18] Goldhirsch A., Winer E.P., Coates A.S., Gelber R.D., Piccart-Gebhart M., Thurlimann B., et al., Personalizing the Treatment of Women with Early Breast Cancer: Highlights of the St Gallen International Expert Consensus on the Primary Therapy of Early Breast Cancer 2013, *Ann Oncol*, 2013, **24**, 2206-2223.

[19] Fragomeni S.M., Sciallis A., Jeruss J.S., Molecular Subtypes and Local-Regional Control of Breast Cancer, *Surg Oncol Clin N Am*, 2018, **27**(1), 95–120.

[20] Siegel R., Ma J., Zou Z., Jemal A., Cancer Statistics, *CA Cancer J Clin*, 2014, *64*, 9–29.

[21] Ferlay J., Colombet M., Soerjomataram I., Mathers C., Parkin DM., Piñeros M., et al., Estimating the Global Cancer Incidence and Mortality in 2018: GLOBOCAN Sources and Methods, *Int J Cancer*, 2019, **144**(8), 1941-1953.

[22] Curado M.P., Edwards B., Shin H.R., Storm H., Ferlay J., Heanue M., Boyle P., *Cancer Incidence in Five Continents Vol. IX*, IARC Scientific Publications No. 160, IARC Press, Lyon, 2007.

[23] Pultz B.A., Cordero da Luz F.A., Rogério de Faria P., Oliveira A.P.L., Agenor de Araújo R., Silva M.J.B., Far Beyond the Usual Biomarkers in Breast Cancer: A Review, *Journal of Cancer*, 2014, **5**(7), 559-571.

[24] Ozbas S., Boylu S., Soyder A., Meme Kanserinde Risk Faktörleri, Editors: Ozmen V., Canturk Z., Celik V., Guler N., Kapkac M., Koyuncu A., Muslumanoglu M., Utkan Z., *MHDF Meme Hastalıları Kitabı*, 1st ed., Gunes Kitabevi, Ankara, 151-154, 2012.

[25] Surakasula A., Nagarjunapu G.C., Raghavaiah K.V., A Comparative Study of Pre- and Post-Menopausal Breast Cancer: Risk Factors, Presentation, Characteristics and Management, *J Res Pharm Pract*, 2014, **3**, 12-8.

[26] Majeed W., Aslam B., Javed I., Khaliq T., Muhammad F., Ali A., Raza A., Breast Cancer: Major Risk Factors and Recent Developments in Treatment, *Asian Pac J Cancer Prev*, 2014, **15**, 3353-8.

[27] O'Brien K.M., Cole S.R., Engel L.S., Bensen J.T., Poole C., Herring A.H., Millikan R.C., Breast Cancer Subtypes and Previously Established Genetic Risk Factors: A Bayesian Approach, *Cancer Epidemiol Biomarkers Prev*, 2013, **23**, 84-97.

[28] Dumalaon-Canaria J.A., Hutchinson A.D., Prichard I., Wilson C., What Causes Breast Cancer? A Systematic Review of Causal Attributions among Breast Cancer Survivors and How These Compare to Expert-Endorsed Risk Factors, *Cancer Causes Control*, 2014, **25**, 771-85.

[29] Weber E.S., Questions & Answers about Breast Cancer Diagnosis, *The American Journal of Nursing*, 1997, **97**(10), 34-38.

[30] Ferlay J., Shin H.R., Bray F., et al., Estimates of Worldwide Burden of Cancer in 2008: GLOBOCAN 2008, Int J Cancer, 2010, 127(12), 2893–917.

[31] Anjum F., Razvi N., Masood A.M., Breast Cancer Therapy: A Mini Review, *MOJ Drug Design Development & Therapy*, 2017, **1**(2), 00006.

[32] Lukaszewicz K., Wtorek J., Bujnowski A., Skokowski J., Monitoring of Breast Tissue Thermo-Ablation by Means of Impedance Measurements, *J Physics Conference Series*, 2010, **224**, 1-4.

[33] Carlson R.W., Allred D.C., Anderson B.O., Burstein H.J., Carter W.B., Edge S.B., et al., Breast Cancer Clinical Practice Guidelines in Oncology, *J Natl Compr Canc Netw*, 2009, **7**(2), 122-92.

[34] Buzdar A.U., Role of Biologic Therapy and Chemotherapy in Hormone Receptor- and HER2-positive Breast Cancer, *Ann Oncol*, 2009, **20**(6), 993-9.

[35] Slamon D.J, Leyland-Jones B., Shak S., Fuchs H., Paton V., Bajamonde A., et al., Use of Chemotherapy Plus a Monoclonal Antibody Against HER2 for Metastatic Breast Cancer that Overexpresses HER2, *N Engl J Med*, 2001, **344**, 783–792.

[36] Anders C.K., Carey L.A., Biology, Metastatic Patterns, and Treatment of Patients with Triple-Negative Breast Cancer, *Clin Breast Cancer*, 2009, **9**(Suppl 2), S73–S81.

[37] Tan D.S., Marchio C., Jones R.L, Savage K., Smith I.E., Dowsett M., et al., Triple Negative Breast Cancer: Molecular Profiling and Prognostic Impact in Adjuvant Anthracycline Treated Patients, *Breast Cancer Res Treat*, 2008, **111**(1), 27-44.

[38] Yanovich G., Agmon H., Harel M., Sonnenblick A., Peretz T., Geiger T., Clinical Proteomics of Breast Cancer Reveals a Novel Layer of Breast Cancer Classification, *Cancer Res*, 2018, **78**(20), 6001-6010.

[39] Sotiriou C., Pusztai L., Gene-expression Signatures in Breast Cancer, *N Engl J Med*, 2009, **360**(8), 790-800.

[40] Institute of Medicine: Micheel C.M., Nass S.J., Omenn G.S., *Evolution of Translational Omics: Lessons Learned and the Path Forward*, The National Academies Press, Washington DC, 2012.

[41] Lassere M.N., The Biomarker-Surrogacy Evaluation Schema: A Review of the Biomarker-surrogate Literature and a Proposal for a Criterion-based, Quantitative, Multidimensional Hierarchical Levels of Evidence Schema for Evaluating the Status of Biomarkers as Surrogate Endpoints, *Statistical Methods in Medical Research*, 2008, **17**(3), 303–40.

[42] World Health Organization & International Programme on Chemical Safety., *Biomarkers in Risk Assessment: Validity and Validation*, World Health Organization, Geneva, 2001.

[43] Goossens N., Nakagawa S., Sun X., Hoshida Y., Cancer Biomarker Discovery and Validation, *Transl Cancer Res*, 2015, **4**(3), 256–269.

[44] Levenson V.V., Biomarkers for Early Detection of Breast Cancer: What, When, and Where?, *Biochim Biophys Acta*, 2007, **1770**(6), 847-56.

[45] Attallah A.M., El-Far M., Omran M.M., Abdallah S.O., ElDesouky M.A., El-Dosoky I., et al., Circulating Levels and Clinical Implications of Epithelial Membrane Antigen and Cytokeratin-1 in Women with Breast Cancer: Can Their Ratio Improve the Results?, *Tumour Biol*, 2014, **35**(11), 10737-45.

[46] Ma J., Kong Y., Nan H., Qu S., Fu X., Jiang L., et al., Pleiotrophin as a Potential Biomarker in Breast Cancer Patients, *Clin Chim Acta*, 2017, **466**, 6-12.

[47] Lu M., Ju S., Shen X., Wang X., Jing R., Yang C., et al., Combined Detection of Plasma miR-127-3p and HE4 Improves the Diagnostic Efficacy of Breast Cancer, *Cancer Biomark*, 2017, **18**(2), 143-8.

[48] Lawicki S., Zajkowska M., Glazewska E.K., Bedkowska G.E., Szmitkowski M., Plasma Levels and Diagnostic Utility of VEGF, MMP-9, and TIMP-1 in the Diagnosis of Patients with Breast Cancer, *Onco Targets Ther*, 2016, **9**, 911-9.

[49] Garczyk S., Von Stillfried S., Antonopoulos W., Hartmann A., Schrauder M.G., Fasching P.A., et al., AGR3 in Breast Cancer: Prognostic Impact and Suitable Serum-based Biomarker for Early Cancer Detection, *PLoS One*, 2015, **10(**4), e0122106.

[50] Song D., Yue L., Zhang J., Ma S., Zhao W., Guo F., et al., Diagnostic and Prognostic Significance of Serum Apolipoprotein C-I in Triple-negative Breast Cancer Based on Mass Spectrometry, *Cancer Biol Ther*, 2016, **17**(6), 635-47.

[51] Wang-Johanning F., Li M., Esteva F.J., Hess K.R., Yin B., Rycaj K., et al., Human Endogenous Retrovirus Type K Antibodies and mRNA as Serum Biomarkers of Early-Stage Breast Cancer, *Int J Cancer*, 2014, **134**(3), 587-95.

[52] Dong X., Yang M., Sun H., Lu J., Zheng Z., Li Z., et al., Combined Measurement of CA 15-3 with Novel Autoantibodies Improves Diagnostic Accuracy for Breast Cancer, *Onco Targets Ther*, 2013, **6**, 273-9.

[53] Kostianets O., Shyyan M., Antoniuk S.V., Filonenko V., Kiyamova R., Panel of SEREX-Defined Antigens for Breast Cancer Autoantibodies Profile Detection, *Biomarkers*, 2017, **22**(2), 149-56.

[54] Gupta P., Suman S., Mishra M., Mishra S., Srivastava N., Kumar V., et al., Autoantibodies against TYMS and PDLIM1 Proteins Detected as Circulatory Signatures in Indian Breast Cancer Patients, *Proteomics Clin Appl*, 2016, **10**(5), 564-73.

[55] Lacombe J., Mange A., Jarlier M., Bascoul-Mollevi C., Rouanet P., Lamy P.J., et al., Identification and Validation of New Autoantibodies for the Diagnosis of DCIS and Node Negative Early-Stage Breast Cancers, *Int J Cancer*, 2013, **132**(5), 1105-13.

[56] Ng E.K., Li R., Shin V.Y., Jin H.C., Leung C.P., Ma E.S., et al., Circulating microRNAs as Specific Biomarkers for Breast Cancer Detection, *PLoS One*, 2013, **8**(1), e53141.

[57] Mar-Aguilar F., Mendoza-Ramirez J.A., Malagon-Santiago I., Espino-Silva P.K., Santuario-Facio S.K., Ruiz-Flores P., et al., Serum Circulating microRNA Profiling for Identification of Potential Breast Cancer Biomarkers, *Dis Markers*, 2013, **34**(3), 163-9.

[58] Shimomura A., Shiino S., Kawauchi J., Takizawa S., Sakamoto H., Matsuzaki J., et al., Novel Combination of Serum microRNA for Detecting Breast Cancer in the Early Stage, *Cancer Sci*, 2016, **107**(3), 326-34.

[59] Chan M., Liaw C.S., Ji S.M., Tan H.H., Wong C.Y., Thike A.A., et al., Identification of Circulating microRNA Signatures for Breast Cancer Detection, *Clin Cancer Res*, 2013, **19**(16), 4477-87.

[60] Schwarzenbach H., Milde-Langosch K., Steinbach B., Muller V., Pantel K., Diagnostic Potential of PTEN-targeting miR-214 in the Blood of Breast Cancer Patients, *Breast Cancer Res Treat*, 2012, **134**(3), 933-41.

[61] Zhang L., Xu Y., Jin X., Wang Z., Wu Y, Zhao D., et al., A Circulating miRNA Signature as a Diagnostic Biomarker for Non-invasive Early Detection of Breast Cancer, *Breast Cancer Res Treat*, 2015, **154**(2), 423-34.

[62] Lyng M.B., Kodahl A.R., Binder H., Ditzel H.J., Prospective Validation of a Blood-based 9-miRNA Profile for Early Detection of Breast Cancer in a Cohort of Women Examined by Clinical Mammography, *Mol Oncol*, 2016, **10**(10), 1621-6.

[63] Ye M., Huang T., Ying Y., Li J., Yang P., Ni C., et al., Detection of 14-3-3 Sigma Promoter Methylation as a Noninvasive Biomarker Using Blood Samples for Breast Cancer Diagnosis, *Oncotarget*, 2017, **8**(6), 9230-42.

[64] Swellam M., Abdelmaksoud M.D., Sayed Mahmoud M., Ramadan A., Abdel-Moneem W., Hefny M.M., Aberrant Methylation of APC and RARbeta2 Genes in Breast Cancer Patients, *IUBMB Life*, 2015, **67**(1), 61-68.

[65] Yang R., Stocker S., Schott S., Heil J., Marme F., Cuk K., et al., The Association Between Breast Cancer and S100P Methylation in Peripheral Blood by Multicenter Case-control Studies, *Carcinogenesis*, 2017, **38**(3), 312-20.

[66] Yang R., Pfutze K., Zucknick M., Sutter C., Wappenschmidt B., Marme F., et al., DNA Methylation Array Analyses Identified Breast Cancer-associated HYAL2 Methylation in Peripheral Blood, *Int J Cancer*, 2015, **136**(8), 1845-55.

[67] Heyn H., Carmona F.J., Gomez A., Ferreira H.J., Bell J.T., Sayols S., et al., DNA Methylation Profiling in Breast Cancer Discordant Identical Twins Identifies DOK7 as Novel Epigenetic Biomarker, *Carcinogenesis*, 2013, **34**(1), 102-8.

[68] Cordero F., Ferrero G., Polidoro S., Fiorito G., Campanella G., Sacerdote C., et al., Differentially Methylated microRNAs in Prediagnostic Samples of Subjects Who Developed Breast Cancer in the European Prospective Investigation into Nutrition and Cancer (EPIC-Italy) Cohort, *Carcinogenesis*, 2015, **36**(10), 1144-53.

[69] Chen X., Chen H., Dai M., Ai J., Li Y., Mahon B., et al., Plasma Lipidomics Profiling Identified Lipid Biomarkers in Distinguishing Early-stage Breast Cancer from Benign Lesions, *Oncotarget*, 2016, **7**(24), 36622-31.

[70] Zhang Y., Song L., Liu N., He C., Li Z., Decreased Serum Levels of Free Fatty Acids Are Associated with Breast Cancer, *Clin Chim Acta*, 2014, **437**, 31-37.

[71] Hadi N.I., Jamal Q., Iqbal A., Shaikh F., Somroo S., Musharraf S.G., Serum Metabolomic Profiles for Breast Cancer Diagnosis, Grading and Staging by Gas Chromatography-Mass Spectrometry, *Sci Rep*, 2017, **7**(1), 1715.

[72] Jove M., Collado R., Quiles J.L., Ramirez-Tortosa M.C., Sol J., Ruiz Sanjuan M., et al., A Plasma Metabolomic Signature Discloses Human Breast Cancer. *Oncotarget*, 2017, **8**(12), 19522-33.

[73] Wang Q., Sun T., Cao Y., Gao P., Dong J., Fang Y., et al., A Dried Blood Spot Mass Spectrometry Metabolomic Approach for Rapid Breast Cancer Detection, *Onco Targets Ther*, 2016, **9**, 1389-98.

[74] Kilpatrick E.S., Lind M.J., Appropriate Requesting of Serum Tumour Markers, *BMJ*, 2009, **339**, 3111.

[75] Marrugo-Ramírez J., Mir M., Samitier J., Blood-Based Cancer Biomarkers in Liquid Biopsy: A Promising Non-invasive Alternative to Tissue Biopsy, *Int. J Mol Sci*, 2018, **19**, 2877.

[76] Banegas M.P., Bird Y., Moraros J., King S., Prapsiri S., Thompson B., Breast Cancer Knowledge, Attitudes, and Early Detection Practices in United States-Mexico Border Latinas, *J Women's Health*, 2012, **21**(1), 101-107.

[77] Marić P., Ozretić P., Levanat S., Oresković S., Antunac K., Beketić-Oresković L., Tumour Markers in Breast Cancer Evaluation of Their Clinical Usefulness, *Coll Antropol*, 2011, **35**(1), 241-247.

[78] Mirabelli P., Incoronato M., Usefulness of Traditional Serum Biomarkers for Management of Breast Cancer Patients, *BioMed Research International*, 2013, **2013**, 685641.

[79] Tang S.S., Gui G.P., Biomarkers in the Diagnosis of Primary and Recurrent Breast Cancer, *Biomark Med*, 2012, **6**(5), 567-85.

[80] Katchman B.A., Patriotis C., Anderson K.S., State-of-the-Science in Organ-Specific Biomarker Research, Breast Cancer, Editors: Srivastava S., *Biomarkers in Cancer Screening and Early Detection*, 1st ed., John Wiley & Sons, Inc., UK, 77-92, 2017.

[81] Misek D.E., Kim E.H., Protein Biomarkers for the Early Detection of Breast Cancer, *Int J Proteomics*, 2011, 343582.

[82] Zeidan B.A., Townsend P.A., Garbis S.D., Copson E., Cutress RI., Clinical Proteomics and Breast Cancer, *Surgeon*, 2015, **13**(5), 271-8.

[83] Ross J.S., Linette G.P., Stec J., Clark E., Ayers M., Leschly N., et al., Breast Cancer Biomarkers and Molecular Medicine, *Expert Rev Mol Diagn*, 2003, **3**(5), 573-85.

[84] Donepudi M.S., Kondapalli K., Amos S.J., Venkanteshan P., Breast Cancer Statistics and Markers, *J Cancer Res Ther*, 2014, **10**(3), 506-11.

[85] Duffy M.J., Serum Tumour Markers in Breast Cancer: Are They of Clinical Value?, *Clin Chem*, 2006, **52**(3), 345-51.

[86] Loke S.Y., Gek Lee A.S., The Future of Blood-based Biomarkers for the Early Detection of Breast Cancer, *European Journal of Cancer*, 2018, **92**, 54-68.

[87] Baldwin R.W., Immunity to Transplanted Tumour: The Effect of Tumour Extracts on the Growth of Homologous Tumours in Rats, *Br J Cancer*, 1955, **9**(4), 646-51.

[88] Finn O.J., Immune Response as a Biomarker for Cancer Detection and a Lot More, *N Engl J Med*, 2005, **353**, 1288–1290.

[89] Tan H.T., Low J., Lim S.G., Chung M.C., Serum Autoantibodies as Biomarkers for Early Cancer Detection, *FEBS J*, 2009, **276**, 6880-904.

[90] Hanash S., Harnessing Immunity for Cancer Marker Discovery, *Nat Biotechnol*, 2003, **21**, 37-8.

[91] Anderson K.S., LaBaer J., The Sentinel within: Exploiting the Immune System for Cancer Biomarkers, *J Proteome Res*, 2005, **4**, 1123-33.

[92] Caron M., Choquet-Kastylevsky G., Joubert-Caron R., Cancer Immunomics Using Autoantibody Signatures for Biomarker Discovery, *Mol Cell Proteomics*, 2007, **6**, 1115-22.

[93] Zhang J.Y., Chan E.K., Peng X.X., Lu M., Wang X., Mueller F., Tan E.M, Autoimmune Responses to mRNA Binding Proteins p62 and Koc in Diverse Malignancies, *Clin Immunol*, 2001, **100**, 149-56.

[94] Zhang J.Y., Casiano C.A., Peng X.X., Koziol J.A., Chan E.K., Tan E.M., Enhancement of Antibody Detection in Cancer Using Panel of Recombinant Tumour-associated Antigens, *Cancer Epidemiol Biomarkers Prev*, 2003, **12**, 136-43.

[95] Tan E.M., Zhang J., Autoantibodies to Tumour-associated Antigens: Reporters from the Immune System, *Immunol Rev*, 2008, **222**, 328-40.

[96] Khadir A., Tiss A., Proteomics Approaches towards Early Detection and Diagnosis of Cancer, *J Carcinogene Mutagene*, **S14**, 002.

[97] Cho W.C.S., Contribution of Oncoproteomics to Cancer Biomarker Discovery, *Mol Cancer*, 2007, **6**, 25.

[98] Mardamshina M., Geiger T., Next-Generation Proteomics and Its Application to Clinical Breast Cancer Research, *Am J Pathol*, 2017, **187**(10), 2175-2184.

[99] Mazur M.G., Pyatchanina T.V., The Use of Proteomic Technologies in Breast Cancer Research, *Exp Oncol*, 2016, **38**(3), 146-57.

[100] Le Naour F., Misek D.E., Krause M.C., et al., Proteomics-based Identification of RS/DJ-1 as a Novel Circulating Tumour Antigen in Breast Cancer, *Clinical Cancer Research*, 2001, **7**(11), 3328–3335.

[101] Lenner P., Wiklund F., Emdin S.O., Arnerlöv C., Eklund C., Hallmans G., et al., Serum Antibodies Against p53 in Relation to Cancer Risk and Prognosis

in Breast Cancer: A Population-based Epidemiological Study, *British Journal of Cancer*, 1999, **79**(5-6), 927–932.

[102] Soussi T., p53Antibodies in the Sera of Patients with Various Types of Cancer: A Review, *Cancer Research*, 2000, **60**(7), 1777–1788.

[103] Angelopoulou K., Yu H., Bharaj B., Giai M., Diamandis E.P., p53 Gene Mutation, Tumour p53 Protein Overexpression, and Serum p53 Autoantibody Generation in Patients with Breast Cancer, *Clinical Biochemistry*, 2000, **33**(1), 53–62.

[104] Kuli´c A., Sirotkovi´c-Skerlev M., Jelisavac-´Cosi´c S., Herceg D., Kovaˇc Z., Vrbanec D., Anti-p53 Antibodies in Serum: Relationship to Tumour Biology and Prognosis of Breast Cancer Patients, *Medical Oncology*, 2010, **27**(3), 887–893.

[105] Desmetz C., Bibeau F., Boissi`ere F., Bellet V., Rouanet P., Maudelonde T., et al., Proteomics-based Identification of HSP60 as a Tumour-Associated Antigen in Early Stage Breast Cancer and Ductal Carcinoma *in situ*, *Journal of Proteome Research*, 2008, **7**(9), 3830–3837.

[106] Desmetz C., Bascoul-Mollevi C., Rochaixetal P., Identification of a New Panel of Serum Autoantibodies Associated with the Presence of *in situ* Carcinoma of the Breast in Younger Women, *Clinical Cancer Research*, 2009, **15**(14), 4733– 4741.

[107] Conroy S.E., Gibson S.L., Brunstrom G., Isenberg D., Luqmani Y., Latchman D.S., Autoantibodies to 90 kD Heat-shock Protein in Sera of Breast Cancer Patients, *The Lancet*, 1995, **345**(8942), 126.

[108] Conroy S.E., Sasieni P.D., Fentiman I., Latchman D.S., Autoantibodies to the 90 kDa Heat Shock Protein and Poor Survival in Breast Cancer Patients, *European Journal of Cancer,* 1998, **34**(6)6, 942.

[109] Von Mensdorff-Pouilly S., Gourevitch M.M., Kenemans P., et al., Humoral Immune Response to Polymorphic Epithelial Mucin (MUC-1) in Patients with Benign and Malignant Breast Tumours, *European Journal of Cancer*, 1996, **32**(8), 1325–1331.

[110] Von Mensdorff-Pouilly S., Verstraeten A.A., Kenemans P., Snijdewint F.G., Kok A., Van Kamp G.J., et al., Survival in Early Breast Cancer Patients Is Favorably Influenced by a Natural Humoral Immune Response to Polymorphic Epithelial Mucin, *Journal of Clinical Oncology*, 2000, **18**(3), 574–583.

[111] Blixt O., Bueti D., Burford B., Allen D., Julien S., Hollingsworth M., et al., Autoantibodies to Aberrantly Glycosylated MUC 1inearly Stage Breast Cancer Are Associated with a Better Prognosis, *Breast Cancer Research*, 2011, **13**(2), 25.

[112] Duffy M.J., CA 15-3 and Related Mucins as Circulating Markers in Breast Cancer, *Annals of Clinical Biochemistry*,**1999**, 36(5), 579–586.

[113] Duffy M.J., Evoy D., McDermott E.W., CA 15-3: Uses and Limitation as a Biomarker for Breast Cancer, *Clinica Chimica Acta*, 2010, **411**(23-24), 1869–1874.

[114] Pawlik T.M., Hawke D.H., Liu Y., Krishnamurthy S., Fritsche H., Hunt K.K., Kuerer H.M., Proteomic Analysis of Nipple Aspirate Fuid from Women with Early-stage Breast Cancer Using Isotope-Coded Affinity Tags and Tandem Mass Spectrometry Reveals Differential Expression of Vitamin D Binding Protein, *BMC Cancer*, 2006, **6**(68).

[115] Chan D., Soo-Chin L., Serial Changes in Expression of Proteins in Response to Neoadjuvant Chemotherapy in Breast Cancer, Editors: Siregar Y., *Oncogene and Cancer: From Bench to Clinic*, 1st ed., IntechOpen, UK, 1-22, 2013.

[116] Luna C.J.A., Syed P., Sergelen K., Gyurján I., Weinhäusel A., The Current Status of Cancer Biomarker Research Using Tumour-associated Antigens for Minimal Invasive and Early Cancer Diagnostics, *J Proteomics*, 2012, **5**(76), 102-15.

[117] Williams S.L., Birdsong G.G., Cohen C., Siddiqui M.T., Immunohistochemical Detection of Estrogen and Progesterone Receptor and HER2 Expression in Breast Carcinomas: Comparison of Cell Block and Tissue Block Preparations, *Int J Clin Exp Pathol*, 2009, **2**(5), 476-480.

[118] Oliveros J.C., Venny. An Interactive Tool for Comparing Lists with Venn's Diagrams, Centro Nacional de Biotecnología, https://bioinfogp.cnb.csic.es/ tools/venny/ index.html, (Access time: 2017-2019).

[119] Aguirre-Gamboa R,, Gomez-Rueda H., Martínez-Ledesma E., Martínez-Torteya A., Chacolla-Huaringa R., Rodriguez-Barrientos A., Tamez-Peña J.G., Treviño V., SurvExpress: An Online Biomarker Validation Tool and Database for Cancer Gene Expression Data Using Survival Analysis, *PLoS One*, 2013, **8**(9), 74250.

[120] Ferguson R.E., Carroll H.P., Harris A., Maher E.R., Selby P.J., Banks R.E., Housekeeping Proteins: A Preliminary Study Illustrating Some Limitations as Useful References in Protein Expression Studies, *Proteomics*, 2005, **5**(2), 566-571.

[121] Saponaro C., Gaggini M., Carli F., Gastaldelli A., The Subtle Balance Between Lipolysis and Lipogenesis: A Critical Point in Metabolic Homeostasis, *Nutrients*, 2015, **7**(11), 9453-9474.

[122] Pozniak Y., Balint-Lahat N., Rudolph J.D., Lindskog C., Katzir R., Avivi C., et al., System-wide Clinical Proteomics of Breast Cancer Reveals Global Remodeling of Tissue Homeostasis, *Cell Syst*, 2016, **2**(3), 172-184.

[123] Mahdi A.A., Rizvi S.H., Parveen A., Role of Endoplasmic Reticulum Stress and Unfolded Protein Responses in Health and Diseases, *Indian J Clin Biochem*, 2016, **31**(2), 127-137.

[124] Fernandez P.M., Tabbara S.O., Jacobs L.K., Manning F.C., Tsangaris T.N., Schwartz A.M., Kennedy K.A., Patierno S.R., Overexpression of the Glucose-regulated Stress Gene GRP78 in Malignant but Not Benign Human Breast Lesions, *Breast Cancer Res Treat*, 2000, **59**(1), 15-26.

[125] Zhang J., Jiang Y., Jia Z., Li Q., Gong W., Wang L., et al., Association of Elevated GRP78 Expression with Increased Lymph Node Metastasis and Poor Prognosis in Patients with Gastric Cancer, *Clin Exp Metastasis*, 2006, **23**(7-8), 401-410.

[126] Shuda M., Kondoh N., Imazeki N., Tanaka K., Okada T., Mori K., et al., Activation of the ATF6, XBP1 and GRP78 Genes in Human Hepatocellular Carcinoma: A Possible Involvement of the ER Stress Pathway in Hepatocarcinogenesis, *J Hepatol*, 2003, **38**(5), 605-614.

[127] Scriven P., Brown N.J., Pockley A.G., Wyld L., The Unfolded Protein Response and Cancer: A Brighter Future Unfolding?, *J Mol Med*, 2007, **85**(4), 331-341.

[128] Uramoto H., Sugio K., Oyama T., Nakata S., Ono K., Yoshimastu T., et al., Expression of Endoplasmic Reticulum Molecular Chaperone GRP78 in Human Lung Cancer and Its Clinical Significance, *Lung Cancer*, 2005, **49**(1), 55-62.

[129] Koumenis C., Wouters B.G., Translating Tumour Hypoxia: Unfolded Protein Response (UPR)-dependent and UPR-independent Pathways, *Mol Cancer Res*, 2006, **4**(7), 423-436.

[130] Shapiro D.J., Livezey M., Yu L., Zheng X., Andruska N., Anticipatory UPR Activation: A Protective Pathway and Target in Cancer, *Trends Endocrinol Metab*, 2017, **27**(10), 731-741.

[131] Scriven P., Coulson S., Haines R., Balasubramanian S., Cross S., Wyld L., Activation and Clinical Significance of the Unfolded Protein Response in Breast Cancer, *Br J Cancer*, 2009, **101**(10), 1692-1698.

[132] Liberti M.V., Locasale J.W., Metabolism: A New Layer of Glycolysis, *Nat Chem Biol*, 2016, **12**(8), 577-578.

[133] Liberti M.V., Locasale J.W., The Warburg Effect: How Does It Benefit Cancer Cells?, *Trends Biochem Sci*, 2016, **41**(3), 211-218.

[134] Zhou W., Liotta L.A., Petricoin E.F., Cancer Metabolism: What We Can Learn from Proteomic Analysis by Mass Spectrometry, *Cancer Genomics Proteomics*, 2012, **9**(6), 373-381.

[135] Warburg O., Iron, the Oxygen-carrier of Respiration-ferment, *Science*, 1925, **61**(1588), 575-582.

[136] Gupta V., Bamezai R.N., Human Pyruvate Kinase M2: A Multifunctional Protein, *Protein Sci*, 2010, **19**(11), 2031-2044.

[137] Christofk H.R., Vander Heiden M.G., Harris M.H., Ramanathan A., Gerszten R.E., Wei R., et al., The M2 Splice Isoform of Pyruvate Kinase Is Important for Cancer Metabolism and Tumour Growth, *Nature*, 2008, **452**(7184), 230-233.

[138] Yao F., Zhao T., Zhong C., Zhu J., Zhao H., LDHA Is Necessary for the Tumourigenicity of Esophageal Squamous Cell Carcinoma, *Tumour Biol*, 2013, **34**(1), 25-31.

[139] Pan L.X., Xu J.N., Isaacson P.G., Cellular H- and M-type Lactate Dehydrogenase (LDH) Isoenzymes and Tumour Diagnosis: An Immunohistochemical Assessment, *J Pathol*, 1991, **163**(1), 53-60.

[140] Wong T.L., Che N., S., Reprogramming of Central Carbon Metabolism in Cancer Stem Cells, *Biochim Biophys Acta*, 2017, **1863**(7), 1728-1738.

[141] Miao P., Sheng S., Sun X., Liu J., Huang G., Lactate Dehydrogenase A in Cancer: A Promising Target for Diagnosis and Therapy, *IUBMB Life*, 2013, **65**(11), 904-910.

[142] Luo X., Cheng C., Tan Z., Li N., Tang M., Yang L., Cao Y., Emerging Roles of Lipid Metabolism in Cancer Metastasis, *Mol Cancer*, 2017, **16**(1), 76.

[143] Santos C.R., Schulze A., Lipid Metabolism in Cancer, *FEBS J*, 2012, **279**(15), 2610-2623.

[144] Ray U., Roy S.S., Aberrant Lipid Metabolism in Cancer Cells - The Role of Oncolipid-activated Signaling, *FEBS J*, 2018, **285**(3), 432-443.

[145] Kim H.Y., Lee K.M., Kim S.H., Kwon Y.J., Chun Y.J., Choi H.K., Comparative Metabolic and Lipidomic Profiling of Human Breast Cancer Cells with Different Metastatic Potentials, *Oncotarget*, 2016, **7**(41), 67111-67128.

[146] Menendez J.A., Lupu R., Fatty Acid Synthase and the Lipogenic Phenotype in Cancer Pathogenesis, *Nat Rev Cancer*, 2007, **7**(10), 763-777.

[147] Hopkinson D.A., Peters J., Harris H., Rare Electrophoretic Variants of Glycerol-3-Phosphate Dehydrogenase: Evidence for Two Structural Gene Loci (GPD1 and GPD2), *Ann Hum Genet*, 1974, **37**(4), 477-484.

[148] Menaya J., Gonzalez-Manchon C., Parrilla R., Ayuso MS., Molecular Cloning, Sequencing and Expression of a cDNA Encoding a Human Liver NAD-dependent Alpha-glycerol-3-phosphate Dehydrogenase, *Biochim Biophys Acta*, 19995, **1262**(1), 91-94.

[149] Zhou C., Yu J., Wang M., Yang J., Xiong H., Huang H., et al., Identification of Glycerol-3-phosphate Dehydrogenase 1 as a Tumour Suppressor in Human Breast Cancer, *Oncotarget*, 2017, **8**(60), 101309-101324.

[150] Turashvili G., Brogi E., Tumour Heterogeneity in Breast Cancer, *Front Med (Lausanne)*, 2017, **4**, 227.

[151] Boyle P., Triple-negative Breast Cancer: Epidemiological Considerations and Recommendations, *Ann Oncol*, 2012, **6**, 7-12.

[152] Rouzier R., Perou C.M., Symmans W.F., Ibrahim N., Cristofanilli M., Anderson K., et al., Breast Cancer Molecular Subtypes Respond Differently to Preoperative Chemotherapy, *Clin Cancer Res*, 2005, **11**(16), 5678-5685.

[153] Badowska-Kozakiewicz A.M., Budzik M.P., Immunohistochemical Characteristics of Basal-like Breast Cancer, *Contemp Oncol (Pozn)*, 2017, **20**(6), 436-443.

[154] Alluri P., Newman L.A., Basal-like and Triple-negative Breast Cancers: Searching for Positives among Many Negatives, *Surg Oncol Clin N Am*, 2014, **23**(3), 567-577.

[155] Rakha E.A., El-Sayed M.E., Reis-Filho J., Ellis I.O., Patho-biological Aspects of Basal-like Breast Cancer, *Breast Cancer Res Treat*, 2009, **113**(3), 411-422.

[156] Lincet H., Icard P., How Do Glycolytic Enzymes Favour Cancer Cell Proliferation by Nonmetabolic Functions?, *Oncogene*, 2015, **34**(29), 3751-3759.

[157] Medes G., Thomas A., Weinhouse S., Metabolism of Neoplastic Tissue. IV. A Study of Lipid Synthesis in Neoplastic Tissue Slices in vitro, *Cancer Res*, 1953, **13**(1), 27-29.

[158] Zhang J., Liu Z., Lian Z., Liao R., Chen Y., Qin Y., Wang J., et al., Monoacylglycerol Lipase: A Novel Potential Therapeutic Target and Prognostic Indicator for Hepatocellular Carcinoma, *Sci Rep*, 2016, **6**, 35784.

[159] Ye L., Zhang B., Seviour E.G., Tao K.X., Liu X.H., Ling Y., et al., Monoacylglycerol Lipase (MAGL) Knockdown Inhibits Tumour Cells Growth in Colorectal Cancer, *Cancer Lett*, 2011, **307**(1), 6-17.

[160] Matuszak N., Hamtiaux L., Baldeyroux B., Muccioli G.G., Poupaert J.H., Lansiaux A., Lambert D.M., Dual Inhibition of MAGL and Type II Topoisomerase by N-phenylmaleimides as a Potential Strategy to Reduce Neuroblastoma Cell Growth, *Eur J Pharm Sci*, 2012, **45**(3), 263-271.

[161] Hu W.R., Lian Y.F., Peng L.X., Lei J.J., Deng C.C., Xu M., et al., Monoacylglycerol Lipase Promotes Metastases in Nasopharyngeal Carcinoma, *Int J Clin Exp Pathol*, 2012, **7**(7), 3704-3713.

[162] Nomura D.K., Long J.Z., Niessen S., Hoover H.S., Ng S.W., Cravatt B.F., Monoacylglycerol Lipase Regulates a Fatty Acid Network that Promotes Cancer Pathogenesis, *Cel*l, 2010, **140**(1), 49-61.

[163] Huang C., Ye Z., Wan J., Liang J., Liu M., Xu X., Li L., Secreted Frizzled-Related Protein 2 Is Associated with Disease Progression and Poor Prognosis in Breast Cancer, *Dis Markers*, 2019, **3**, 6149381.

[164] Ganesan V., Schmidt B., Avula R., Cooke D., Maggiacomo T., Tellin L., et al., Immuno-proteomics: Development of a Novel Reagent for Separating Antibodies from Their Target Proteins, *Biochim Biophys Acta*, 2015, **1854**(6), 592-600.

[165] González-González L., Alonso J., Periostin: A Matricellular Protein with Multiple Functions in Cancer Development and Progression, *Front. Oncol*, 2018, **8**, 225.

[166] Ratajczak-Wielgomas K., Grzegrzolka J., Piotrowska A., Matkowski R., Wojnar A., Rys J., et al., Expression of Periostin in Breast Cancer Cells, *International Journal of Oncology*, 2017, **51**, 1300-1310.

[167] Xu X., Chang W., Yuan J., Han X., Tan X., Ding Y., et al., Periostin Expression in Intra-tumoural stromal Cells Is Prognostic and Predictive for Colorectal Carcinoma via Creating a Cancer-supportive Niche, *Oncotarget*, 2016, **7**, 798 –813.

[168] Oskarsson T., Massague J., Extracellular Matrix Players in Metastatic Niches, *EMBO J*, 2012, **31**, 254-256.

[169] Cui D., Huang Z., Liu Y., Ouyang G., The Multifaceted Role of Periostin in Priming the Tumour Microenvironments for Tumour Progression, *Cell Mol Life Sci*, 2017, **74**, 4287–4291.

[170] Bao S., Ouyang G., Bai X., Huang Z., Ma C., Liu M., et al., Periostin Potently Promotes Metastatic Growth of Colon Cancer by Augmenting Cell Survival via the AKT/PKB Pathway, *Cancer Cell*, 2004, **5**, 329 –339.

[171] Shi Y., Ping Y.F., Zhang X., Bian X.W., Hostile Takeover: Glioma Stem Cells Recruit TAMs to Support Tumour Progression, *Cell Stem Cell*, 2015, **16**, 219 –220.

[172] Zhang R., Yao R.R., Li J.H., Dong G., Ma M., Zheng Q.D., et al., Activated Hepatic Stellate Cells Secrete Periostin to Induce Stem Cell-like Phenotype of Residual Hepatocellular Carcinoma Cells After Heat Treatment, *Sci. Rep*, 2017, **7**, 2164.

[173] Malanchi I., Santamaria-Martínez A., Susanto E., Peng H., Lehr H.A., Delaloye J.F., Huelsken J., Interactions Between Cancer Stem Cells and Their Niche Govern Metastatic Colonization, *Nature*, 2011, **481**, 85-89.

[174] Wang Z., Ouyang G., Periostin: A Bridge Between Cancer Stem Cells and Their Metastatic Niche, *Cell Stem Cell*, 2012, **10**, 111-112.

[175] Zhang Y., Zhang G., Li .J, Tao Q., Tang W., The Expression Analysis of Periostin in Human Breast Cancer, *J Surg Res,* 2010, **160**, 102-106.

[176] Kim G.E., Lee J.S., Park M.H., Yoon J.H., Epithelial Periostin Expression Is Correlated with Poor Survival in Patients with Invasive Breast Carcinoma, *PLoS One*, 2017, **12**(11), e0187635.

[177] Lambert A.W., Wong C.K., Ozturk S., Papageorgis P., Raghunathan R., Alekseyev Y., et al., Tumour Cell-derived Periostin Regulates Cytokines That Maintain Breast Cancer Stem Cells, *Mol Cancer Res*, 2016, **14**(1), 103–13.

[178] Vardaki I., Ceder S., Rutishauser D., Baltatzis G., Foukakis T., Panaretakis T., Periostin Is Identified as a Putative Metastatic Marker in Breast Cancer-derived Exosomes, *Oncotarget*, 2016, **7**(46), 74966-78.

[179] He X., Zhang P., Serine/Arginine-rich Splicing Factor 3 (SRSF3) Regulates Homologous Recombination-mediated DNA Repair, *Molecular Cancer*, 2015, **14**, 158.

[180] Sen S., Talukdar I., Webster N.J., SRp20 and CUG-BP1 Modulate Insulin Receptor Exon 11 Alternative Splicing, *Mol Cell Biol*, 2009, **29**(3), 871–80.

[181] Galiana-Arnoux D., Lejeune F., Gesnel M.C., Stevenin J., Breathnach R., Del Gatto-Konczak F., The CD44 Alternative V9 Exon Contains a Splicing Enhancer Responsive to the SR Proteins 9G8, ASF/SF2, and SRp20, *J Biol Chem*, 2003, **278**(35), 32943–53.

[182] Pan Q., Shai O., Lee L.J., Frey B.J., Blencowe B.J., Deep Surveying of Alternative Splicing Complexity in the Human Transcriptome by High-throughput Sequencing, *Nat Genet*, 2008, **40**(12), 1413-5.

[183] He C., Zhou F., Zuo Z., Cheng H., Zhou R., A Global View of Cancer-specific Transcript Variants by Subtractive Transcriptome-wide Analysis, *PloS One*, 2009, **4**, e4732.

[184] Venables J.P., Klinck R., Bramard A., Inkel L., Dufresne-Martin G., Koh C., et al., Identification of Alternative Splicing Markers for Breast Cancer, *Cancer Res*, 2008, **68**, 9525–9531.

[185] Shapiro I.M., Cheng A.W., Flytzanis N.C., Balsamo M., Condeelis J.S., Oktay M.H., et al., An EMT-driven Alternative Splicing Program Occurs in Human Breast Cancer and Modulates Cellular Phenotype, *PLoS Genet*, 2011, **7**, e1002218.

[186] E., Kittrell F., Medina D., Berget S.M., Stage-specific Changes in SR Splicing Factors and Alternative Splicing in Mammary Tumourigenesis, *Oncogene*, 1999, **18**, 3574–3582.

[187] Kurokawa K., Akaike Y., Masuda K., Kuwano Y., Nishida K., Yamagishi N., et al., Downregulation of Serine/Arginine-rich Splicing Factor 3 Induces G1 Cell Cycle Arrest and Apoptosis in Colon Cancer Cells, *Oncogene*, 2014, **33**, 1407–1417.

[188] Jia R., Li C., McCoy J.P., Deng C.X., Zheng Z.M., SRp20 is a Proto-oncogene Critical for Cell Proliferation and Tumour Induction and Maintenance, *Int J Biol Sci*, 2010, **6**, 806–826.

[189] Anczukow O., Rosenberg A.Z., Akerman M., Das S., Zhan L., Karni R., et al., The Splicing Factor SRSF1 Regulates Apoptosis and Proliferation to Promote Mammary Epithelial Cell Transformation, *Nat Struct Mol Biol*, 2012, **19**, 220–228.

[190] Volker S.E., Hedrick S.E., Feeney Y.B., Clevenger C.V., Cyclophilin A Function in Mammary Epithelium Impacts JAK2/STAT5 Signaling, Morphogenesis, Differentiation, and Tumourigenesis in The Mammary Gland, *Cancer Res*. 2018, **78**(14), 3877–3887.

[191] Obchoei S., Wongkhan S., Wongkham C., Li M., Yao Q., Chen C., Cyclophilin A: Potential Functions and Therapeutic Target for Human Cancer, *Med Sci Monit*, 2009, **15**, 221-232.

[192] Shen J., Person M.D., Zhu J., Abbruzzese .J.L, Li D., Protein Expression Profiles in Pancreatic Adenocarcinoma Compared with Normal Pancreatic Tissue and Tissue Affected by Pancreatitis as Detected by Two-dimensional Gel Electrophoresis and Mass Spectrometry, *Cancer Res*, 2004, **64**, 9018–26.

[193] Howard B.A., Furumai R., Campa M.J., Rabbani Z.N., Vujaskovic Z., Wang X.F., et al., Stable RNA Interference-mediated Suppression of Cyclophilin A Diminishes Non-small-cell Lung Tumour Growth in vivo, *Cancer Res*, 2005, **65**, 8853–60.

[194] Nigro P., Pompilio G., Capogrossi M.C., Cyclophilin A: A Key Player for Human Disease, *Cell Death Dis*, 2013, **4**, e888.

[195] Satoh K., Matoba T., Suzuki J., O'Dell M., Nigro P., Cui Z., et al., Cyclophilin A Mediates Vascular Remodeling by Promoting Inflammation and Vascular Smooth Muscle Cell Proliferation, *Circulation*, 2008, **117**, 3088–98.

[196] Theuerkorn M., Fischer G., Schiene-Fischer C.. Prolyl cis/trans Isomerase Signalling Pathways in Cancer, *Curr Opin Pharmacol*, 2011, **4**, 281-7.

[197] Li Z.Y., Zhao X., Bai S.J., Wang Z., Chen L.J., Wei Y.Q., Huang C.H., Proteomics Identification of Cyclophilin A as a Potential Prognostic Factor and Therapeutic Target in Endometrial Carcinoma, *Mol Cell Proteomics*, 2008, **7**, 1810-1823.

[198] Fujıoka H., Sakai A., Tanaka S., Kimura K., Miyamoto A., Iwamoto M., Uchiyama K., Comparative Proteomic Analysis of Paclitaxel

Resistance-related Proteins in Human Breast Cancer Cell Lines, *Oncology Letters*, 2017, **13**, 289-295.

[199] Perri1 A.M., Agosti V., Olivo E., Concolino A., De Angelis M.T., Tammè L., et al., Histone Proteomics Reveals Novel Post-translational Modifications in Breast Cancer, *Aging*, 2019, **11**(23), 11722-11755.

[200] Byler S., Goldgar S., Heerboth S., Leary M., Housman G., Moulton K., Sarkar S., Genetic and Epigenetic Aspects of Breast Cancer Progression and Therapy, *Anticancer Res*, 2014, **34**, 1071–77.

[201] Zheng Q., Omans N.D., Leicher R., Osunsade A., Agustinus A.S., Finkin-Groner E., et al., Reversible Histone Glycation Is Associated with Disease-related Changes in Chromatin Architecture, *Nature Communications*, 2019, **10**, 1289.

[202] Bartholomew B., Regulating the Chromatin Landscape: Structural and Mechanistic Perspectives, *Annu Rev Biochem*, 2014, **83**, 671–696.

[203] Khan S.A., Reddy D., Gupta S., Global Histone Post-translational Modifications and Cancer: Biomarkers for Diagnosis, Prognosis and Treatment?, *World J Biol Chem*, 2015, **6**, 333–45.

[204] Elsheikh S.E., Green A.R., Rakha E.A., Powe D.G., Ahmed R.A., Collins H.M., et al., Global Histone Modifications in Breast Cancer Correlate with Tumour Phenotypes, Prognostic Factors, and Patient Outcome, *Cancer Res*, 2009, **69**, 3802–09.

[205] Shental-Bechor D., Levy Y., Folding of Glycoproteins: Toward Understanding the Biophysics of the Glycosylation Code, *Curr Opin Struct Biol*, 2009, **19**, 524-533.

[206] Haltiwanger RS., Regulation of Signal Transduction Pathways in Development by Glycosylation, *Curr Opin Struct Biol*, 2002, **12**, 593-598.

[207] Balog C.I., Mayboroda O.A., Wuhrer M., Hokke C.H., Deelder A.M., Hensbergen P.J., Mass Spectrometric Identification of Aberrantly Glycosylated Human Apolipoprotein C-III Peptides in Urine from *Schistosoma mansoni*-infected Individuals, *Mol Cell Proteomics*, 2010, **9**, 667-681.

[208] Rudd P.M., Elliott T., Cresswell P., Wilson I.A., Dwek R.A., Glycosylation and the Immune System, *Science*, 2001, **291**, 2370-2376.

[209] Bustamante J.J., Gonzalez L., Carroll C.A., Weintraub S.T., Aguilar R.M., Muñoz J., et al., O-glycosylated 24 kDa Human Growth Hormone Has a Mucin-like Biantennary Disialylated Tetrasaccharide Attached at Thr-60, *Proteomics*, 2009, **9**, 3474-3488.

[210] Varki A., Kannagi R., Toole B.P., Glycosylation Changes in Cancer, Editors: Varki A., Cummings R.D., Esko J.D., *Source Essentials of Glycobiology*, 2nd ed., Cold Spring Harbor Laboratory Press, NewYork, 44, 2009.

[211] Koltai T., Clusterin: A Key Player in Cancer Chemoresistance and Its Inhibition, *Onco Targets and Therapy*, 2014, **7**, 447–456.

[212] Ranney M.K., Ahmed I.S.A., Potts K.R., Craven R.J., Multiple Pathways Regulating the Anti-apoptotic Protein Clusterin in Breast Cancer, *Biochim Biophys Acta*, 2007, **1772**(9), 1103–1111.

[213] Zhang H., Kim J.K., Edwards C.A., Xu Z., Taichman R., Wang C.Y., Clusterin Inhibits Apoptosis by Interacting with Activated Bax, *Nat Cell Biol*, 2005, **7**, 909–915.

[214] So A., Sinnemann S., Huntsman D., Fazli L., Gleave M., Knockdown of the Cytoprotective Chaperone, Clusterin, Chemosensitizes Human Breast Cancer Cells Both in vitro and in vivo, *Mol Cancer Ther*, 2005, **4**, 1837–1849.

[215] Saffer H., Wahed A., Rassidakis G.Z., Medeiros L.J., Clusterin Expression in Malignant Lymphomas: A Survey of 266 Cases, *Mod Pathol*, 2002, **15**, 1221–1226.

[216] Lau S.H., Sham J.S., Xie D., Tzang C.H., Tang D., Ma N., et al., Clusterin Plays an Important Role in Hepatocellular Carcinoma Metastasis, *Oncogene*, 2006, **25**, 1242–1250.

[217] Wang Y., Brodsky A.S., Xiong J., Lopresti M.L., Yang D., Resnick M.B., Stromal Clusterin Expression PredictsmTherapeutic Response to Neoadjuvant Chemotherapy in Triple Negative Breast Cancer, *Clin Breast Cancer*, 2018, **18**(3), e373-379.

[218] Avalos-Navarro G., Muñoz-Valle J.F., Daneri-Navarro A., Quintero-Ramos A., Franco-Topete R.A., Morán-Mendoza A.J., et al., Circulating Soluble Levels of MIF in Women with Breast Cancer in the Molecular Subtypes: Relationship with TH17 Cytokine Profile, *Clinical and Experimental Medicine*, 2019, **19**, 385–391.

[219] Thongwatchara P., Promwikorn W., Srisomsap C., Chokchaichamnankit D., Boonyaphiphat P., Thongsuksai P., Differential Protein Expression in Primary Breast Cancer and Matched Axillary Node Metastasis, *Oncology Reports*, 2011, **26**, 185-191.

[220] Martinez L.M., Vallone V.B.F., Labovsky V., Choi H., Hofer E.L., Feldman L., et al., Changes in the Peripheral Blood and Bone Marrow from Untreated Advanced Breast Cancer Patients that Are Associated with the Establishment of Bone Metastases, *Clin Exp Metastasis*, 2014, **31**, 213-232.

[221] Xu X., Wang B., Ye C., Yao C., Lin Y., Huang X., et al., Overexpression of Macrophage Migration Inhibitory Factor Induces Angiogenesis in Human Breast Cancer, *Cancer Lett*, 2008, **261**, 147-157.

[222] Bando H., Matsumoto G., Bando M., Muta M., Ogawa T., Funata N., et al., Expression of Macrophage Migration Inhibitory Factor in Human Breast Cancer: Association with Nodal Spread, *Jpn J Cancer Res*, 2022, **93**, 389-396.

[223] Richard V., Kindt N., Decaestecker C., Gabius H.J., Laurent G., Noël J.C., Saussez S., Involvement of Macrophage Migration Inhibitory Factor and Its Receptor (CD74) in Human Breast Cancer, *Oncol Rep*, 2014, **32**, 523-529.

[224] Fersching D.M., Nagel D., Siegele B., Salat C., Heinemann V., Holdenrieder S., Stoetzer OJ., Apoptosis-related Biomarkers sFAS, MIF, ICAM-1 and PAI-1 in Serum of Breast Cancer Patients Undergoing Neoadjuvant Chemotherapy, *Anticancer Res*, 2012, **32**, 2047-2058.

[225] Meyer-Siegler K., Hudson P.B., Enhanced Expression of Macrophage Migration Inhibitory Factor in Prostatic Adenocarcinoma Metastases, *Urology*, 1996, **48**, 448-452.

[226] Kamimura A., Kamachi M., Nishihira J., Ogura S., Isobe H., Dosaka-Akita H., et al., Intracellular Distribution of Macrophage Migration Inhibitory Factor Predicts the Prognosis of Patients with Adenocarcinoma of the Lung, *Cancer*, 2000, **89**, 334-341.

[227] Bini L., Magi B., Marzocchi B., Arcuri F., Tripodi S., Cintorino M., et al., Protein Expression Profiles in Human Breast Ductal Carcinoma and Histologically Normal Tissue, *Electrophoresis*, 1997, **18**, 2832-2841.

[228] Burnett G., Weathersby D., Taylor T., Bremner T., Regulation of Inflammation- and Angiogenesis-related Gene Expression in Breast Cancer Cells and Co-cultured Macrophages, *Anticancer Research*, 2008, **28**, 2093-2100.

[229] Verjans E., Noetzel E., Bektas N., Schütz A.K., Lue H., Lennartz B., et al., Dual Role of Macrophage Migration Inhibitory Factor (MIF) in Human Breast Cancer, *BMC Cancer*, 2009, **9**, 230.

[230] Subedi L., Teli M.K., Lee J.H., Gaire B.P., Kim M., Kim S.Y., A Stilbenoid Isorhapontigenin as a Potential Anti-Cancer Agent against Breast Cancer through Inhibiting Sphingosine Kinases/Tubulin Stabilization, *Cancers*, 2019, **11**, 1947.

[231] Sakchaisri K., Kim S., Hwang J., Soung N.K., Lee K.H., Choi T.W., Anticancer Activity of a Novel Small Molecule Tubulin Inhibitor STK899704, *PLoSOne*, **12**(3), e0173311.

[232] Mu Y., Chen Y., Zhang G., Zhan X., Li Y., Liu T., et al., Identification of Stromal Differentially Expressed Proteins in the Colon Carcinoma by Quantitative Proteomics, *Electrophoresis*, 2013, **34**, 1679–1692.

[233] Janke C., The Tubulin Code: Molecular Components, Readout Mechanisms, and Functions, *J Cell Biol*, 2014, **206**, 461–472.

[234] Wloga D., Gaertig J., Post-translational Modifications of Microtubules, *J Cell Sci*, 2010, **123**, 3447–3455.

[235] Westermann S., Weber K., Post-translational Modifications Regulate Microtubule Function, *Nat Rev Mol Cell Biol*, 2003, **4**, 938–947.

[236] Zhu Q.Y., Wang Z., Ji C., Cheng L., Yang Y.L., Ren J., et al., C6-ceramide Synergistically Potentiates the Anti-tumour Effects of Histone Deacetylase Inhibitors via AKT Dephosphorylation and Alpha-tubulin Hyperacetylation both in vitro and in vivo, *Cell Death Dis*, 2011, **2**, 117.

[237] Howes S.C., Alushin G.M., Shida T., Nachury M.V., Nogales E., Effects of Tubulin Acetylation and Tubulin Acetyltransferase Binding on Microtubule Structure, *Mol Biol Cell*, 2014, **25**, 257.

[238] Liao X.H., Wang J.G., Li L.Y., Zhou D.M., Ren K.H., Jin Y.T., et al., Long Intergenic non-coding RNA APOC1P1-3 Inhibits Apoptosis by Decreasing α-tubulin Acetylation in Breast Cancer, *Cell Death and Disease*, 2016, **7**, 2236.

[239] Fothergill-Gilmore L.A., Pam M., Evolution of Glycolysis, *Journal of Progress in Biophysics and Molecular Biology*, 1993, **95**, 105-135.

[240] Boukouris A.E., Zervopoulos S.D., Michelakis E.D., Metabolic Enzymes Moonlighting in the Nucleus, Metabolic Regulation of Gene Transcription, *Trends Biochem Sci*, 2016, **41**(8), 712-730.

[241] Elkhalfi B., Senhaji N., Benomar H., Soukri A., Study of Glyceraldehyde-3-phosphate Dehydrogenase Expression in the Tumour Process of: Breast, Cervix and Prostate Cancers, *Advances in Biological Chemistry*, 2012, **2**, 335-340.

[242] ReÂ Villion F., Pawlowski V., Hornez L., Peyrat J.P., Glyceraldehyde-3-phosphate Dehydrogenase Gene Expression in Human Breast Cancer, *European Journal of Cancer*, 2000, **36**, 1038-1042.

[243] Staples C.J., Myers K.N., Beveridge R.D.D., Patil A.A., Howard A.E., Barone G., et al., CCDC13 is a Novel Human Centriolar Satellite Protein Required for Ciliogenesis and Genome Stability, *Journal of Cell Science*, 2014, **127**, 2910-2919.

[244] Hu D.D., Li P.C., He Y.F., Jia W., Hu B., Overexpression of Coiled-Coil Domain-Containing Protein 34 (CCDC34) and Its Correlation with Angiogenesis in Esophageal Squamous Cell Carcinoma, *Med Sci Monit*, 2018, **3**(24), 698-705.

[245] Jiang G.Y., Zhang X.P., Zhang Y., Xu H.T., Wang L., Li Q.C., Wang E.H., Coiled-coil Domain-containing Protein 8 Inhibits the Invasiveness and Migration of Non–small Cell Lung Cancer Cells, *Human Pathology*, 2016, **56**, 64-73.

[246] Jia Y, Chen Y, Wang Q, Jayasinghe U, Luo X, Wei Q, et al., Exosome: Emerging Biomarker in Breast Cancer, *Oncotarget*, 2017, **8**(25), 41717-41733.

[247] Sana M., and Malik H.J., Current and Emerging Breast Cancer Biomarkers, *J Cancer Res Ther*, 2015, **11**(3), 508-513.

[248] Weigel M.T., and Dowsett M., Current and Emerging Biomarkers in Breast Cancer: Prognosis and Prediction, *Endocr Relat Cancer*, 2010, **17**(4), 245-262.

[249] Locy H., Mey S., Mey W., Ridder M., Thielemans K., Maenhout S.K., Immunomodulation of the Tumor Microenvironment: Turn Foe Into Friend, *Front Immunol*, 2018, **9**, 2909.

[250] Ganesan V., Ascherman D.P., Minden J.S., Immunoproteomics Technologies in the Discovery of Autoantigens in Autoimmune Diseases, *BioMol Concepts*, 2016, **7**(2), 133–143.

[251] Criscitiello C., Tumour-associated Antigens in Breast Cancer, *British Journal of Cancer*, 1996, **74**, 63-68.

APPENDICES

Appendices A

Table A.1. List of biomarker discovery studies in proteomics

Material type	Test specimens	Proteomic approach	Identified proteins	Verification method	Candidate biomarkers	Reference
Tissue	19 HER2+ BC vs 15 TNBC	2D-DIGE, MALDI-TOF MS	34	WB, IHC	CK7, GAPDH, PGK1	Schulz et al., 2009
Tissue	18 ER+ BC vs adjacent benign tissue	2D-DIGE, MALDI-TOF MS	50	WB	PPIaseB, Rho-GDI α, TPM4	Weitzel et al., 2010
Tissue	9 ER+ BC vs 9 healthy tissue	GeLC-MS/MS	298	-	-	Cha et al., 2010
Tissue	3 ER+ vs 3 ER- BC	GeLC-MS/MS	236	IHC	Liprin- α1, β-arrestin-1, fascin, DAP5	Rezaul et al., 2010
Plasma	420 prediagnostic plasma from ER+ BC vs 420 controls	Depletion, nLC-MS/MS	57	ELISA	EGFR	Pitteri et al., 2010
Tissue	6 lymph node-positive vs 6 lymph node-negative TNBC	GeLC-MS/MS	339	WB, IHC	STAT1, CD74	Greenwood et al., 2011
Cell lines	6 Lapatinib-resistant HER2+ vs 6 Lapatinib-sensitive parental cells	Phosphoprotein enrichment, GeLC-MS/MS	20 tyrosin phosphorylation sites (differential)	microarray	LYN, LCK, FYN	Rexer et al., 2011
Cell lines	2 trastuzumab-resistant HER2+ vs 2 trastuzumab-sensitive parental cells	Phosphoprotein enrichment, SILAC, nLC-MS/MS	62 and 106 proteins with differential phosphorylation sites per cell line, 3 proteins with increased phosphorylation in both cell lines	WB, siRNA	WB: EGFR, HER4, CDCP1/Trask, FAK, PXN. SiRNA: MAPK1, PXN, FAM83A, EFS	Boyer et al., 2012
Plasma	420 prediagnostic plasma from ER+ BC vs 420 controls	Depletion, nLC-MS/MS	467	-	-	Amon et al., 2012
Plasma	14 TNBC vs 14 controls	Antibody microarray	93	Antibody microarray	DUSP9, EED, EFNA5, ITGB1, PPMT1	Li et al., 2012
Tissue	ER+ vs ER- BC	2D-PAGE, LC-LTQ/FTICR MS	11 differential glycoproteins	WB	A1- antitrypsin	Semaan et al., 2012

Table A.1 (Continues). List of biomarker discovery studies in proteomics

Material type	Test specimens	Proteomic approach	Identified proteins	Verification method	Candidate biomarkers	Reference
Tissue	4 chemosensitive ER+ vs 3 chemoresistant ER+ BC	Antibody microarray	45 differential	WB, IHC	14-3-3 theta/tau, tBID	Hodgkinson et al., 2012
Cell line secretome	3 luminal vs 3 basal vs 3 HER2+	2D LC-MS/MS	31 differential	Targeted MS	ABAT, PDZK1	Pavlou et al., 2013
Plasma	Infiltrative ductal BC: 107 women, healthy control group: 120	bidimensional nanoUPLC tandem nanoESI-MSE Ms (Label-free quantitative MS)	down-regulated proteins: 78 LumA, 87 LUM HER2+, 80 HER2+, 79 TNBC. Up-regulated proteins: 102 LumA, 68 LUM HER2+, 87 HER2+, 87 TNBC.	WB	Clusterin, Killin, IKBP1, IRX1, IRX4, IRX5	Correa et al., 2016
Serum	Sera samples from BC patients (112) and healthy control (35)	SEREX, ELISA	In IDC patients: autoantibodies to RAD50, NY-CO58, NY-ffIR-62, PARD3, SAP30BP, SPP1; in MBC patients to SAP30BP and SPP1; in ILC patients to PARD3, SAP30BP, and NY-BR-62.	RT-PCR	the expression profile of SPP1, PARD3, SAP30BP were determined by RT-PCR	Kostianets et al., 2016
Cell lines, BC adipose tissue	MCF7: Luminal A, ER+, PR+, HER2–; and MDA-MB-231: Basal, ER–/PR–/HER2–. Differentiated BC adipose tissue	LC coupled to LTQ-Orbitrap tandem MS (iTRAQ)	85 proteins in CAA-MCF-7 and 63 proteins in CAA-MDA-MB-231 were differentially regulated	WB	20 proteins in MCF-7 and 20 proteins in MDA-MB-231. Three proteins were selected for validation: NDRG1, PGK1 and TFF1.	Crake et al., 2019

Appendices B

Table B.1. Buffers and solutions used in the study

Section number	Buffer/solution name	Contents with final concentrations
2.2.	Wash buffer for tissues samples	10 mM Tris-HCl, 250 mM sucrose, pH 7.2
2.5.	DIGE extraction/rehydration buffer	30 mM Tris-HCl, 7 M urea, 2 M Thiourea, 4% w/v CHAPS (pH 8.5) (add 1% Tributylphosphine "TBP" and 1% pH3.10 ampholyte for rehydration)
2.6.	SDS-PAGE Separating Gel composition (12%)	375 mM Tris-HCl (pH 8.8), 12% (w/v) Acrylamide/bis-acrylamide solution, 0.1% (w/v) SDS, 0.1% APS, 0.05% (v/v) tetramethylethylenediamine (TEMED).
2.6.	SDS-PAGE Stacking Gel composition (4%)	125 mM Tris-HCl (pH 6.8), 4% (w/v) Acrylamide/bisacrylamide solution, 0.1% (w/v) SDS, 0.1% APS, 0.05% (v/v) TEMED.
2.6.	Acrylamide/bisacrylamide solution	30% (w/v) acrylamide, 0.8% (w/v) bisacrylamide (37.5:1 (w/w))
2.6.	6 X Loading Dye	0,5M Tris-HCl pH 6.8, Glycerol (99.7%), 10 % SDS, ß-Mercaptoethanol, 0.5% (w/v) Bromphenol blue
2.7.	Equilibration Buffer I	6 M Urea, 2% (w/v) SDS, 375 mM Tris-HCl (pH 8.8), 20% (v/v) Glycerol, 2% (w/v) DTT
2.7.	Equilibration Buffer II	6 M Urea, 2% (w/v) SDS, 375 mM Tris-HCl (pH 8.8), 20% (v/v) Glycerol, 2.5% (w/v) IAA
2.7.	Overlay Agarose	1% low melt agarose in SDS running buffer, a trace amount of bromophenol blue
2.8.	2X Sample Buffer (for Fluorescence Labelling)	8 M urea, 130 mM DTT, 4% w/v CHAPS, 2% w/w Ampholyte

Table B.1 (Continues). Buffers and solutions used in the study

Section number	Buffer/solution name	Contents with final concentrations
2.7.	SDS/2-D PAGE Running Buffer	25 mM Tris-HCl, 192 mM glycine, 0.1% SDS
2.9.	Gel fix solution	40% (v/v) Ethanol (99%), 10% (v/v) acetic acid (85%)
2.9.	Staining solution for CBB G-250	757 mM ammonium sulphate, 1.45 mM Coomassie Brilliant Blue, 10% phosphoric acid (v/v), 20% (v/v) methanol
2.14.2.	Binding Buffer (BB)	20 mM sodium phosphate, pH 7.0
2.14.2.	Elution buffer (EB)	0.1 M Glycine-HCl, pH 2.7
2.14.2.	Neutralization buffer (NB)	1 M Tris-HCl, pH 9.0
2.14.4.	IP buffer (#87788)	25 mM Tris-HCl, 0.15M NaCl, 0.001M EDTA, 1% NP-40, 5% glycerol; pH 7.4
2.15.	MALDI matrix solution	50% (v/v) acetonitrile (ACN), 0.1% (v/v) trifluoroacetic acid (TFA) and 10 mg/ml alpha-cyano-4-hydroxycinnamic acid
2.17.2.	Mobile phase A	0.1% FA in water
2.17.2.	Mobile phase B	80% ACN, 20% water, 0.1% FA
2.17.2.	Loading pump solution	98% water, 2% ACN (v/v), 0.05% TFA
2.19.	Western Blot Transfer Buffer	25 mM Tris-HCl, 192 mM glycine, 20% methanol (v/v), 1,3 mM SDS
2.19.	TBS-T	25 mM Tris-HCl, 150 mM NaCl, pH 7.2, 0.1% Tween20
2.19.	Blocking solution	5% dry milk powder in TBS-T
2.19.	Ponceau S staining buffer (0.1% (w/v))	1,5 mM Ponceau S, 0.5 mL Acetic acid (v/v)

All buffers/solutions have been prepared with 18.2 MΩ grade deionized water unless stated otherwise. All chemicals used for nLC-MS/MS were HPLC grade.

Table B.2. Detailed information on clinical parameters of patients

Luminal A subtype								
		IHC Status						
No.	**Patient code**	**ER (%)**	**PR (%)**	**HER2**	**Ki-67 (%)**	**Histological tumour type**	**TNM staging**	**Tumour grade**
1	**K1**	20	50	-	5	IDC	IIIA	2
2	**K7**	90	60	-	12	IDC	IIA	2
3	**K10**	90-95	90-95	-	3	IDC	IIA	2
4	**K13**	50	-	(+2)	6	IDC	IIB	1
5	**K16**	100	-	-	-	IDC	IIIA	2
6	**K17**	100	50	-	2	IDC	IIA	2
7	**K21**	80	80	-	4	IDC	IIA	1
8	**K23**	90	70	-	10	IDC infiltrative ductal	IIA	2
9	**K27**	80	-	-	8	IDC	IIB	1
10	**K40**	70	10	-	3	IDC	IA	1
11	**K43**	70	10	-	10	IDC	IIB	2
12	**K48**	80	90	-	2	IDC	IIA	1
13	**K49**	95	10	-	1	IDC	IA	1
14	**K55**	100	60	-	6	IDC	IA	1
15	**K58**	60	70	-	10	IDC	IIA	2
16	**D8**	60	80	(+1)	5	IDC	IIB	2
17	**D11**	70	70	(+1)	1	IDC	IA	1
18	**D14**	70	70	(+1)	5	IDC	IA	2
19	**D16**	90	90	(+2)	10	IDC	IIB	3
20	**D21**	90	90	-	10	IDC	IIA	1
21	**D28**	70	80	(+2)	10	IDC	IIIA	1
22	**D31**	80	50	(+2)	5	IDC	IIB	1
23	**D33**	80	50	-	5	IDC	IIA	1
24	**D43**	100	5	-	5	IDC	IIA	2
25	**D45**	80	80	(+2)	10	IDC	IIB	2
26	**D53**	90	80	-	10	IDC infiltrative ductal	IIIA	3
27	**D58**	100	5	-	8	IDC	IIB	2
28	**D66**	90	60	(+1)	10	IDC	IIIA	2
29	**D69**	75	80	-	3	IDC infiltrative ductal	IIA	3
30	**D70**	95	85	-	5	IDC	IA	1
31	**D74**	100	100	-	12	IDC	IIA	2
32	**D77**	95	98	-	8	IDC	IA	1
33	**D79**	70	90	-	10	IDC	IIIA	2
34	**D86**	80	80	-	5	IDC	IIA	2

Luminal B subtype								
		IHC Status						

Table B.2 (Continues). Detailed information on clinical parameters of patients

No.	Patient code	ER (%)	PR (%)	HER2	Ki-67 (%)	Histological tumour type	TNM staging	Tumour grade
1	**K6**	90	70	-	65	IDC	IA	2
2	**K11**	80	90	-	30	IDC	IIB	2
3	**K15**	100	70	-	30	IDC	IIA	3
4	**K18**	100	60	-	60	IDC	IIB	3
5	**K26**	95	5	-	36	IDC	IA	2
6	**K28**	80	5	-	40	IDC	IIB	2
7	**K32**	90	50	-	40	IDC	IIB	2
8	**K50**	70	90	-	19	IDC	IIA	2
9	**K56**	100	100	-	20	IDC	IIA	2
10	**D15**	80	80	(+1)	25	IDC	IIA	2
11	**D17**	80	70	(+1)	40	IDC	IIIA	3
12	**D22**	70	60	(+1)	40	IDC	IIA	2
13	**D24**	30	30	(+1)	65	IDC	IIA	2
14	**D30**	-	80	-	30	IDC	IIA	2
15	**D32**	100	100	(+1)	25	IDC	IIIC	2
16	**D35**	95	70	(+2)	35	IDC	IIA	2
17	**D38**	80	10	-	15	IDC	IIIA	2
18	**D39**	100	70	-	50	IDC	IIIC	3
19	**D41**	80	80	-	20	IDC	IIA	2
20	**D44**	90	90	-	25	IDC	IIA	2
21	**D49**	80	50	-	15	IDC	IIB	2
22	**D50**	95	5	-	20	IDC	IIB	2
23	**D51**	80	70	-	20	IDC	IIA	2
24	**D54**	80	50	-	20	IDC	IIA	2
25	**D55**	80	-	-	20	IDC	IIB	2
26	**D63**	80	90	-	30	IDC	IA	2
27	**D64**	90	-	-	20	IDC	IIA	1
28	**D65**	90	-	(+2)	30	IDC	IIIA	3
29	**D68**	90	70	-	20	IDC	IIA	2
30	**D72**	70	-	-	20	IDC	IIIA	2
31	**D73**	70	70	(+2)	46	IDC	IIIA	3
32	**D78**	90	90	-	25	IDC	IIA	2
33	**D80**	60	95	-	20	IDC	IIA	2

Luminal B-like HER2+ subtype

		IHC Status					
No.	**Patient code**	**ER (%)**	**PR (%)**	**HER2**	**Histological tumour type**	**TNM staging**	**Tumour grade**
1	**K2**	30	-	(+3)	IDC	IIA	2
2	**K19**	70	-	(+3)	IDC	IA	2
3	**K60**	100	-	(+3)	IDC	IA	2
4	**D3**	90	90	(+3)	IDC	IIB	2

Table B.2 (Continues). Detailed information on clinical parameters of patients

5	**D5**	70	10	(+3)	IDC	IIB	2
6	**D7**	90	90	(+3)	IDC	IIB	2
7	**D10**	100	70	(+3)	IDC	IIA	2
8	**D13**	90	80	(+3)	infiltrative ductal	IIIA	3
9	**D23**	-	5	(+3)	infiltrative ductal	IIA	3
10	**D27**	60	20	(+3)	IDC	IIB	3
11	**D48**	5	-	(+3)	IDC	IIIA	3
12	**D56**	80	80	(+3)	infiltrative ductal	IIIA	3
13	**D57**	100	70	(+3)	IDC	IIIA	2
14	**D83**	100	100	(+3)	IDC	IV	3

TNBC subtype

IHC Status

No.	**Patient code**	**ER (%)**	**PR (%)**	**HER2**	**CK 5/6**	**GPD1 exp.**	**Histological tumour type**	**TNM staging**	**Tumour grade**
1	**K8**	-	-	-	+	low	IDC	IIB	3
2	**K25**	-	-	-	-	high	IDC	IA	3
3	**K41**	-	-	-	+	low	IDC	IIA	2
4	**K47**	-	-	-	+	low	IDC	IIB	3
5	**K54**	-	-	-	-	high	IDC	IIA	3
6	**K57**	-	-	-	+	low	IDC	IIA	3
7	**D1**	-	-	(+2)	NT *	high	IDC	IIIA	2
8	**D12**	-	-	(+2)	NT *	low	IDC	IIIB	3
9	**D19**	-	-	-	-	high	infiltrative ductal	IIIA	3
10	**D71**	-	-	-	+	high	IDC	IIA	2
11	**D84**	-	-	(+2)	NT *	high	IDC	IIA	2

HER2-enriched subtype

IHC Status

No.	**Patient code**	**ER (%)**	**PR (%)**	**HER2**	**Histological tumour type**	**TNM staging**	**Tumour grade**
1	**K9**	-	-	(+3)	IDC	IIB	3
2	**K22**	-	-	(+3)	IDC	IIA	3
3	**K33**	-	-	(+3)	IDC	IIA	2
4	**D9**	-	-	(+3)	IDC	IIIB	3
5	**D26**	-	-	(+3)	IDC	IIIA	3
6	**D42**	-	-	(+3)	IDC	IV	1
7	**D61**	-	-	(+3)	IDC	IIA	1
8	**D76**	-	-	(+3)	IDC	IIIB	3

* NT: not tested.

Table B.3. Primary antibodies used for verification experiments

Antibody name	Gene name	Brand	Catalogue no.	Used dilution	Predicted molecular weight (kDa)
β-actin	ACTB	Santa Cruz Biotech.	sc-81178	1:1000	43
glycerol-3-phosphate dehydrogenase NAD+, cytoplasmic	GPD1	Santa Cruz Biotech.	sc-376219	1:750	38
monoglyceride lipase	MGLL, MAGL	Santa Cruz Biotech.	sc-398942	1:750	33
Glyceraldehyde-3-phosphate dehydrogenase	GAPH	Santa Cruz Biotech.	sc-365062	1/1000	37
Alpha-tubulin	TBA1A	Santa Cruz Biotech.	sc-8035	1/1000	55
Peptidyl-prolyl cis-trans isomerase A (Cyclophilin A)	PPIA/PPIaseA/CYPA	NOVUS Biologicals	H00005478-M01	1/500	15
Histone H4	H4C1	Abcam	ab10158	3 µg/mL	14
Clusterin	CLU	Santa Cruz Biotech.	sc-166907	1/2000	Precursor: 70. α/β: 36-39/34-36
Periostin	POSTN	Santa Cruz Biotech.	sc-398631	1/5000	84/74
Macrophage migration inhibitory factor	MIF	Santa Cruz Biotech.	sc-271631	1/250	13
Serine/arginine-rich-splicing factor 3	SRSF3	Thermo Sci.	33-4200	2 µg/mL	25
Splicing factor arginine/serine-rich 3	SFRS3	NOVUS Biologicals	NBP2-41316	1/250	19
Coiled-coil domain-containing protein 13	CCDC13	ORIGENE	AP50765PU-N	1/250	80

Appendices C

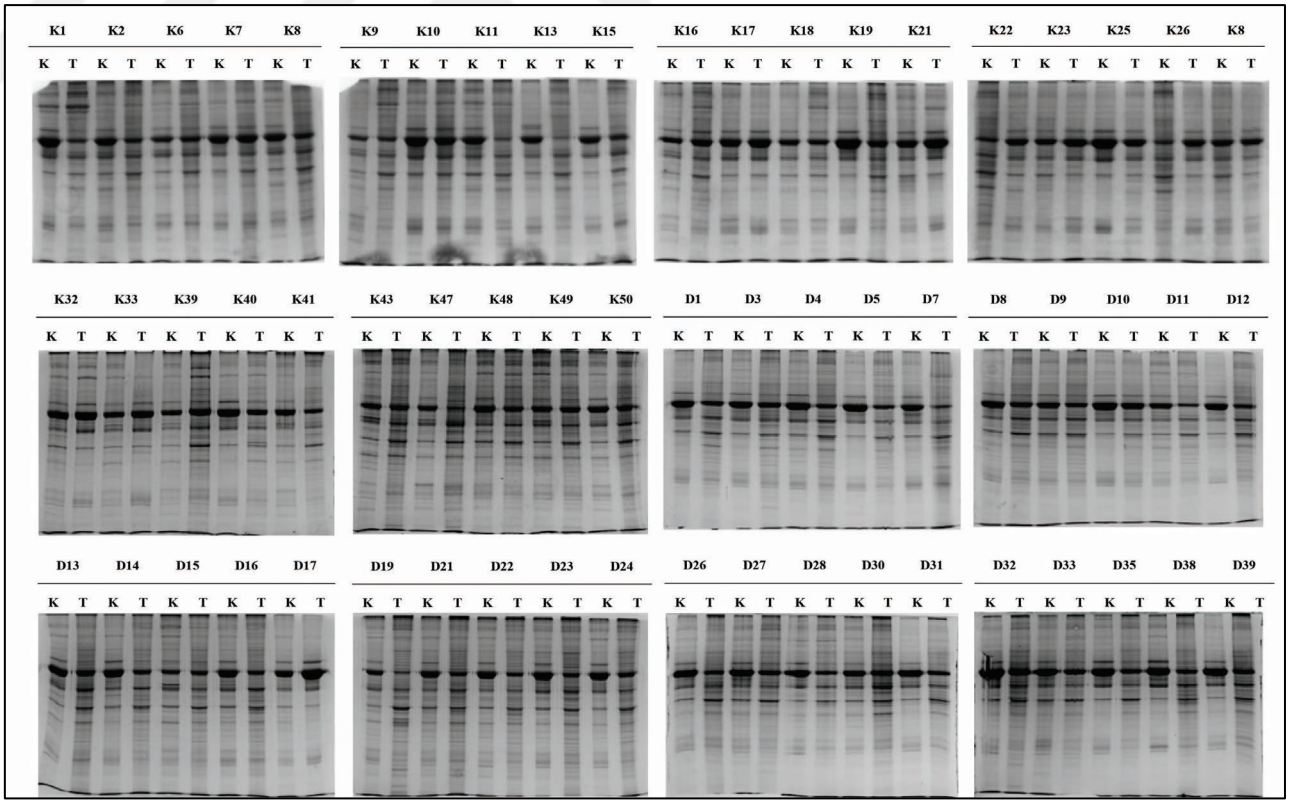

Figure C.1. SDS-PAGE images showing the quantity and quality of protein extracts from tumour and control tissues

(Explanation for Figure C.1: K1-K60 and D1-D76 designate patients' codes (top row). K designates healthy/control, and T designates tumour tissue protein extracts (bottom row)).

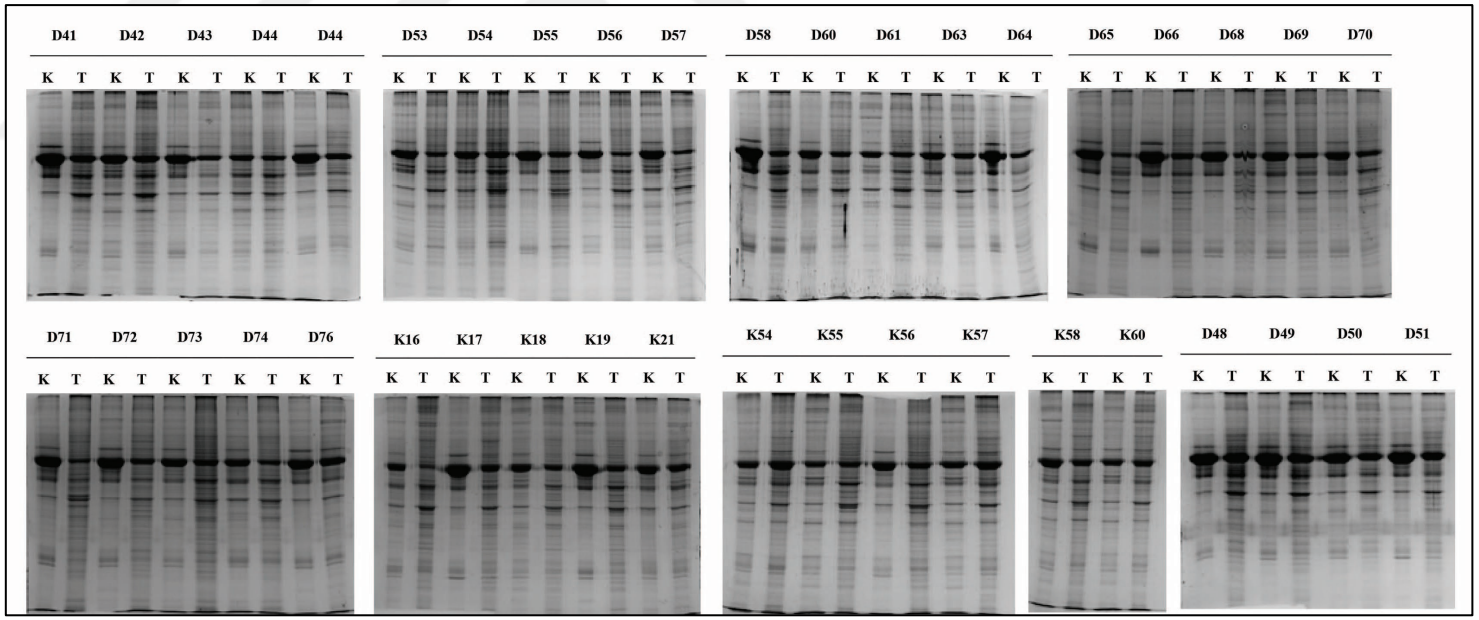

Figure C.1 (Continues). SDS-PAGE images showing the quantity and quality of protein extracts from tumour and control tissues

(Explanation for Figure C.1: K1-K60 and D1-D76 designate patients' codes (top row). K designates healthy and T designates tumour tissue protein extracts (bottom row)).

Appendices D

Table D.1. The list of differentially regulated proteins identified by 2-DE coupled to MALDI-TOF/TOF

No.	AC no.	Protein description	Protein mass	Protein score	Expect	Matches	Theoretical pI	Seq. cov. (%)
1	P02768	Serum albumin	69321	272	1.3e-023	37	5,92	37
2	P01009	Alpha-1-antitrypsin	46707	335	6.4e-030	37	5,37	55
3	P30041	Peroxiredoxin-6	25019	414	8.1e-038	31	6	75
4	P05787	Keratin, type II cytoskeletal 8	53671	594	8.1e-056	53	5,52	64
5	P32119	Peroxiredoxin-2	21878	366	5.1e-033	24	5,66	74
6	P07355	Annexin A2	38580	508	3.2e-047	38	7,57	58
7	P49411	Elongation factor Tu, mitochondrial	49510	337	4E-30	34	7,26	59
8	P63104	14-3-3 protein zeta/delta	27728	205	6.4e-017	28	4,73	61
9	P08670	Vimentin	53619	566	5.1e-053	52	5,06	60
10	P04792	Heat shock protein beta-1	22768	293	1E-25	23	5,98	67
11	P50395	Rab GDP dissociation inhibitor beta	50631	401	1.6e-036	45	6,11	62
12	P13639	Elongation factor 2	95277	301	1.6e-026	48	6,41	39
13	P08727	Keratin, type I cytoskeletal 19	44065	590	2e-055	45	5,04	69
14	P15086	Carboxypeptidase B	47338	381	1.6e-034	30	6,16	59
15	P10809	60 kDa heat shock protein, mitochondrial	61016	480	2E-44	41	5,7	49
16	P05783	Keratin, type I cytoskeletal 18	48029	563	1E-52	43	5,34	56
17	P02545	Lamin-A/C	74095	304	8.1e-027	42	6,57	47
18	Q02790	Peptidyl-prolyl cis-trans isomerase FKBP4	51722	153	1E-11	31	5,35	49
19	P14625	Endoplasmin	92411	373	1e-033	45	4,76	36
20	P07900	Heat shock protein HSP 90-alpha	84607	288	3.2e-025	42	4,94	49
21	P11142	Heat shock cognate 71 kDa protein	70854	341	1.6e-030	39	5,37	40
22	Q99685	Monoglyceride lipase	33240	183	1E-14	25	6,49	62

Table D.1 (Continues). The list of differentially regulated proteins identified by 2-DE coupled to MALDI-TOF/TOF

No.	AC no.	Protein description	Protein mass	Protein score	Expect	Matches	Theoretical pI	Seq. cov. (%)
23	Q99798	Aconitate hydratase, mitochondrial	85372	303	1E-26	36	7,36	39
24	P14618	Pyruvate kinase isozymes M1/M2	57900	269	2.6e-023	41	7,96	61
25	P07237	Protein disulfide-isomerase	57081	329	2.6e-029	34	4,76	49
26	P26641	Elongation factor 1-gamma	50087	132	1.3e-009	22	6,25	32
27	P00352	Retinal dehydrogenase 1	54827	92	1.2e-005	16	6,3	30
28	P38646	Stress-70 protein, mitochondrial	73635	80	0,00018	18	5,57	27
29	O75874	Isocitrate dehydrogenase [NADP] cytoplasmic	46630	325	6.4e-029	41	6,53	57
30	P07195	L-lactate dehydrogenase B chain	36615	269	2.6e-023	28	5,71	48
31	P00915	Carbonic anhydrase 1	28852	258	3.2e-022	20	6,59	70
32	P04083	Annexin A1	38690	521	1.6e-048	36	6,57	63
33	P02511	Alpha-crystallin B chain	20146	268	3.2e-023	23	6,76	51
34	P01834	Ig kappa chain C region	11602	120	0,00000002	10	5,58	88
35	P68871	Hemoglobin subunit beta	15988	211	1.6e-017	17	6,75	83
36	P52895	Aldo-keto reductase family 1 member C2	36712	209	2.6e-017	25	7,13	56
37	P21695	Glycerol-3-phosphate dehydrogenase [NAD+], cytoplasmic	37543	373	1E-33	37	5,81	75
38	P40925	Malate dehydrogenase, cytoplasmic	36403	204	8.1e-017	21	6,91	47
39	P04040	Catalase	59719	290	2e-025	28	6,9	38

Table D.2. The list of differentially regulated proteins and their regulation ratios among the tumour groups over the control group

No.	AC no.	SSP no.	Protein description	Luminal A *vs*. Control	Luminal B *vs*. Control	Luminal B-like HER2 + *vs*. Control	TNBC *vs*. Control	HER2-enriched *vs*. Control
1	P02768	5603	Serum albumin	NR	0,21	0,33	NR	NR
2	P01009	1504	Alpha-1-antitrypsin	NR	NR	0,29	NR	0,49
3	P30041	6001	Peroxiredoxin-6	NR	NR	NR	NR	NR
4	P05787	4505	Keratin, type II cytoskeletal 8	8,81	9,53	10,12	3,16	3,7
5	P32119	4002	Peroxiredoxin-2	NR	NR	NR	NR	NR
6	P07355	8104	Annexin A2	NR	NR	2,52	NR	2,81
7	P49411	6202	Elongation factor Tu, mitochondrial	2,84	3,13	2,02	NR	NR
8	P63104	1001	14-3-3 protein zeta/delta	3,26	NR	2,62	2,11	3,01
9	P08670	0204	Vimentin	NR	NR	NR	NR	NR
10	P04792	5002	Heat shock protein beta-1	NR	2,18	NR	NR	NR
11	P50395	5301	Rab GDP dissociation inhibitor beta	2,5	2,53	2,34	2,22	NR
12	P13639	7805	Elongation factor 2	3,12	5,93	10,41	3,23	4,39
13	P08727	2202	Keratin, type I cytoskeletal 19	14,74	12,07	10,26	3,12	5,57
14	P15086	6203	Carboxypeptidase B	5,24	7,4	NR	NR	NR
15	P10809	3602	60 kDa heat shock protein, mitochondrial	4,7	6,52	5,3	2,64	6,07
16	P05783	4201	Keratin, type I cytoskeletal 18	6,33	7,69	8,96	NR	NR
17	P02545	7602	Lamin-A/C	2,5	3,18	3,81	NR	NR
18	Q02790	4502	Peptidyl-prolyl cis-trans isomerase FKBP4	NR	4,69	4,18	0,26	NR
19	P14625	1801	Endoplasmin	2,38	2,59	NR	2,11	2,12

Table D.2 (Continues). The list of differentially regulated proteins and their corresponding regulation ratios among the tumour groups over the control group

No.	AC no.	SSP no.	Protein description	Luminal A *vs.* Control	Luminal B *vs.* Control	Luminal B-like HER2 + *vs.* Control	TNBC *vs.* Control	HER2-enriched *vs.* Control
20	P07900	1802	Heat shock protein HSP 90-alpha	5,14	6,58	4,01	3,11	4,81
21	P11142	3703	Heat shock cognate 71 kDa protein	NR	2,08	2,32	NR	2,71
22	Q99685	8110	Monoglyceride lipase	0,18	0,05	0,18	0,01	0,05
23	Q99798	8802	Aconitate hydratase, mitochondrial	NR	2,21	2,31	NR	NR
24	P14618	8603	Pyruvate kinase isozymes M1/M2	6,14	11,26	9,98	6,94	7,02
25	P07237	0504	Protein disulfide-isomerase	3,14	2,84	3,92	4,1	6,73
26	P26641	6302	Elongation factor 1-gamma	6,01	7,22	7,88	8,4	8,38
27	P00352	6502	Retinal dehydrogenase 1	NR	NR	NR	NR	NR
28	P38646	4708	Stress-70 protein, mitochondrial	NR	0,24	0,16	NR	2,69
29	O75874	7203	Isocitrate dehydrogenase [NADP], cytoplasmic	NR	NR	NR	NR	2,09
30	P07195	4109	L-lactate dehydrogenase B chain	0,03	0,01	0,04	0,01	0
31	P00915	7002	Carbonic anhydrase 1	0,35	0,21	0,34	0,19	0,4
32	P04083	6101	Annexin A1	NR	NR	NR	NR	NR
33	P02511	8012	Alpha-crystallin B chain	NR	0,45	0,4	NR	NR
34	P01834	8004	Ig kappa chain C region	0,27	0,21	NR	2,04	NR

Table D.2 (Continues). The list of differentially regulated proteins and their corresponding regulation ratios among the tumour groups over the control group

No.	AC no.	SSP no.	Protein description	Luminal A *vs.* Control	Luminal B *vs.* Control	Luminal B-like HER2 + *vs.* Control	TNBC *vs.* Control	HER2-enriched *vs.* Control
35	P68871	8006	Hemoglobin subunit beta	0,46	NR	0,26	NR	NR
36	P52895	8206	Aldo-keto reductase family 1 member C2	0,06	0,06	0,03	0,06	0,07
37	P21695	5101	Glycerol-3-phosphate dehydrogenase [NAD+], cytop.	0,06	0,06	0,02	0,001	0,03
38	P40925	7106	Malate dehydrogenase, cytoplasmic	NR	NR	NR	0,4	NR
39	P04040	8506	Catalase	NR	NR	NR	NR	NR

NR: Non-relevant (Indicates less than two-fold up/down-regulation).

Table D.3. The list of differentially regulated proteins identified by DIGE coupled to MALDI-TOF/TOF

No.	AC no.	Protein description	Protein mass	Protein score	Expect	Matches	Theoretical pI	Seq. cov. (%)
1	P09211	Glutathione S-transferase P	23341	68	0,0031	7	5,43	31
2	P04792	Heat shock protein beta-1	22768	214	8,1E-18	15	5,98	46
3	A6NL28	Putative tropomyosin alpha-3 chain-like protein	26253	97	0,0000039	5	4,47	24
4	P62258	14-3-3 protein epsilon	29155	80	0,0002	14	4,63	44
5	P01834	Ig kappa chain C region	11602	80	0,00019	6	5,58	76
6	P02511	Alpha-crystallin B chain	20146	68	0,0031	7	6,76	33
7	P60174	Triosephosphate isomerase	26653	66	0,0055	9	6,45	35
8	P35232	Prohibitin	29786	101	0,0000016	8	5,57	19
9	P62937	Peptidyl-prolyl cis-trans isomerase A	18001	138	3,2E-10	16	7,68	58
10	P63261	Actin, cytoplasmic 2	41766	92	1.4e-005	12	5,31	33
11	P05787	Keratin, type II cytoskeletal 8	53671	252	1.3e-021	24	5,52	45
12	P30101	Protein disulfide-isomerase A3	56747	147	4E-11	17	5,98	33
13	P05783	Keratin, type I cytoskeletal 18	48029	192	1.3e-015	22	5,34	30
14	P10809	60 kDa heat shock protein, mitochondrial	61016	95	0,0000069	12	5,70	22
15	P20774	Mimecan	33901	99	0,0000023	8	5,46	29
16	Q15084	Protein disulfide-isomerase A6	48091	151	1,6E-11	12	4,95	24
17	P08727	Keratin, type I cytoskeletal 19	44065	449	2.6e-041	29	5,04	46
18	P11021	78 kDa glucose-regulated protein	72288	190	2e-015	15	5,07	20
19	P08670	Vimentin	53619	209	2,6E-17	21	5,06	30
20	P07237	Protein disulfide-isomerase	57081	160	2E-12	12	4,76	22
21	P27797	Calreticulin	48112	116	0,000000051	12	4,29	25
22	P04083	Annexin A1	38690	266	5,1E-23	15	6,57	40

Table D.3 (Continues). The list of differentially regulated proteins identified by DIGE coupled to MALDI-TOF/TOF

No.	AC no.	Protein description	Protein mass	Protein score	Expect	Matches	Theoretical pI	Seq. cov. (%)
23	P04264	Keratin, type II cytoskeletal 1	65999	101	0,0000016	14	8,15	27
24	P60709	Actin, cytoplasmic 1	41710	96	0,0000049	9	5,29	16
25	P23141	Liver carboxylesterase 1	62841	76	0,00049	8	6,15	13
26	P21695	Glycerol-3-phosphate dehydrogenase [NAD+], cytoplasmic	37543	150	2e-011	22	5,81	43
27	Q13228	Selenium-binding protein 1	52358	114	0,000000081	15	5,93	20

Table D.4. The list of differentially expressed proteins of GPD1$^{+/-}$ group by DIGE coupled to MALDI-TOF/TOF

No.	AC no.	Protein description	Protein mass	Protein score	Expect	Matches	Theoretical pI	Seq. cov. (%)
1	P14618	Pyruvate kinase isozymes M1/M2	57900	178	3.2e-014	22	7,96	31
2	P06733	Alpha-enolase	47139	138	3.2e-010	18	7,01	28
3	P00558	Phosphoglycerate kinase 1	44586	119	2.6e-008	24	8,3	52
4	P04083	Annexin A1	38690	96	5e-006	22	6,57	46
5	P14550	Alcohol dehydrogenase [NADP+]	36550	90	1.9e-005	21	6,32	39
6	P00338	L-lactate dehydrogenase A chain	36665	65	0,0063	15	8,44	24
7	P02647	Apolipoprotein A-I	30759	81	0,00016	17	5,56	32
8	P08758	Annexin A5	35914	224	8.1e-019	24	4,94	43
9	P07237	Protein disulfide-isomerase	57081	161	1.6e-012	22	4,76	20
10	P08670	Vimentin	53619	133	1.0e-008	25	5,06	44
11	P13645	Keratin, type I cytoskeletal 10	58792	80	0,00022	21	5,13	24
12	P60709	Actin, cytoplasmic 1	41710	172	1.3e-013	26	5,29	44
13	P02787	Serotransferrin	77000	259	2.6e-022	47	6,81	45
14	P52565	Rho GDP-dissociation inhibitor 1	23193	152	1.3e-011	20	5,02	40
15	P63104	14-3-3 protein	27728	106	5.1e-007	20	4,73	43
16	P62258	14-3-3 protein epsilon	29155	69	0,0027	21	4,63	41

Appendices E

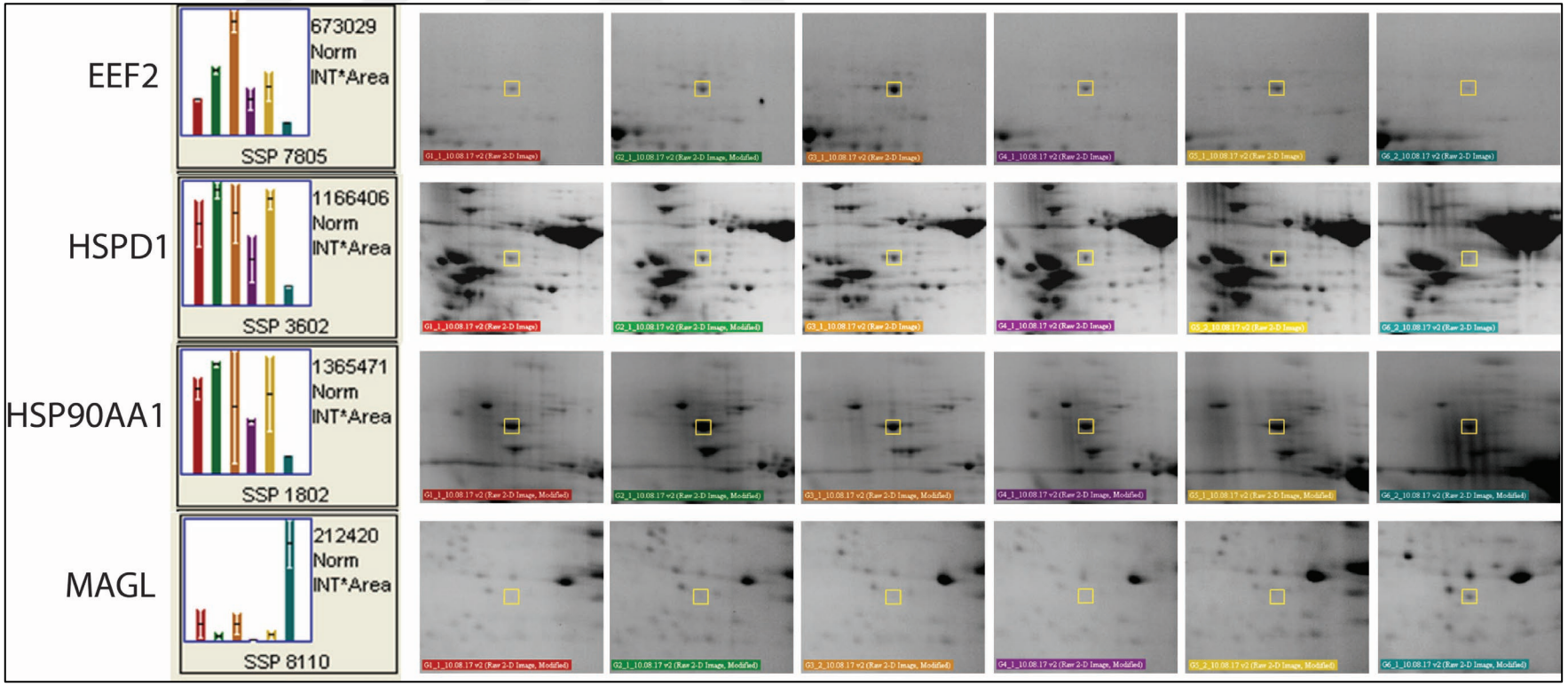

Figure E.1. The representative close-up images of the differentially regulated proteins

(Red line: Luminal A, green line: Luminal B, orange line: Luminal B-like HER2+, purple line: TNBC, yellow line: HER2-enriched, blue line: control group)

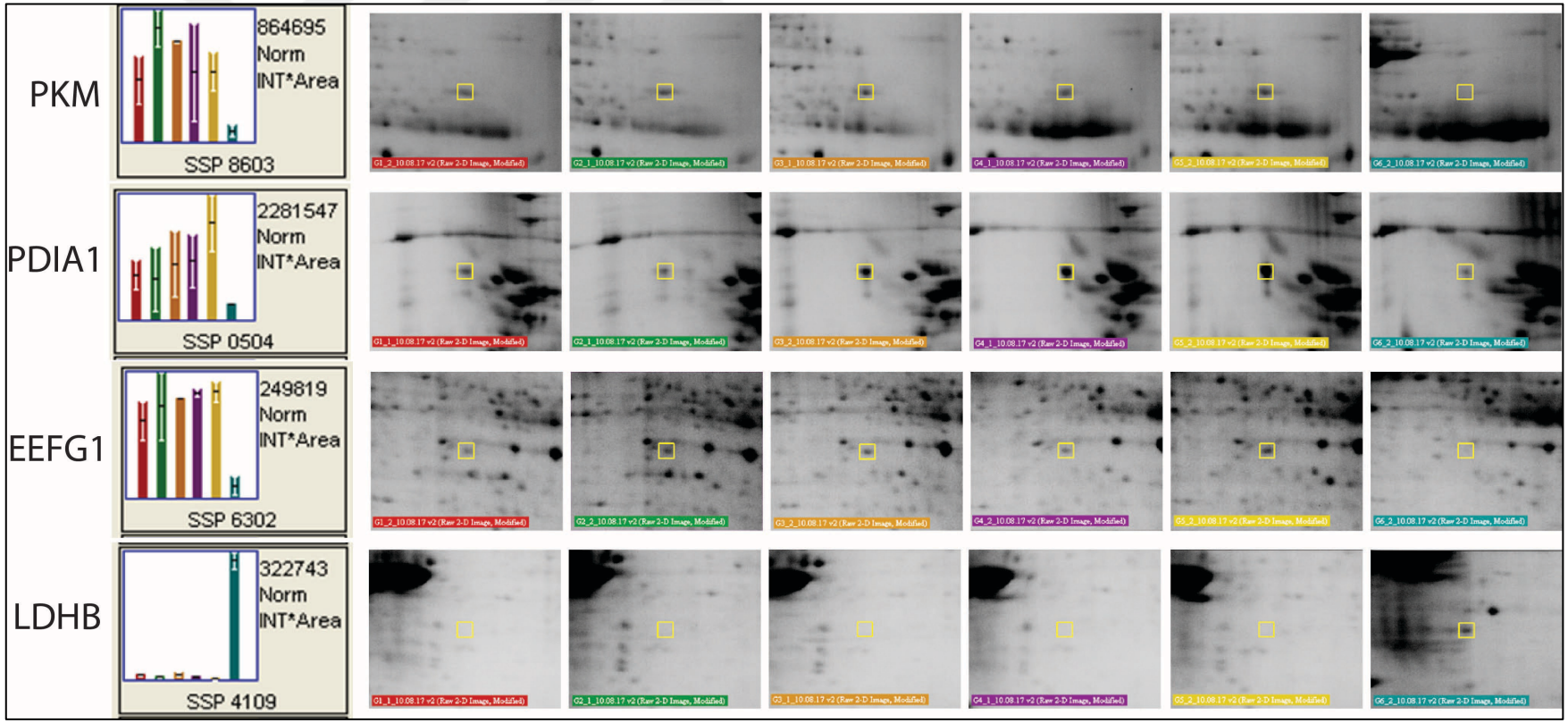

Figure E.1 (Continues). The representative close-up images of the differentially regulated proteins

(Red line: Luminal A, green line: Luminal B, orange line: Luminal B-like HER2+, purple line: TNBC, yellow line: HER2-enriched, blue line: control group)

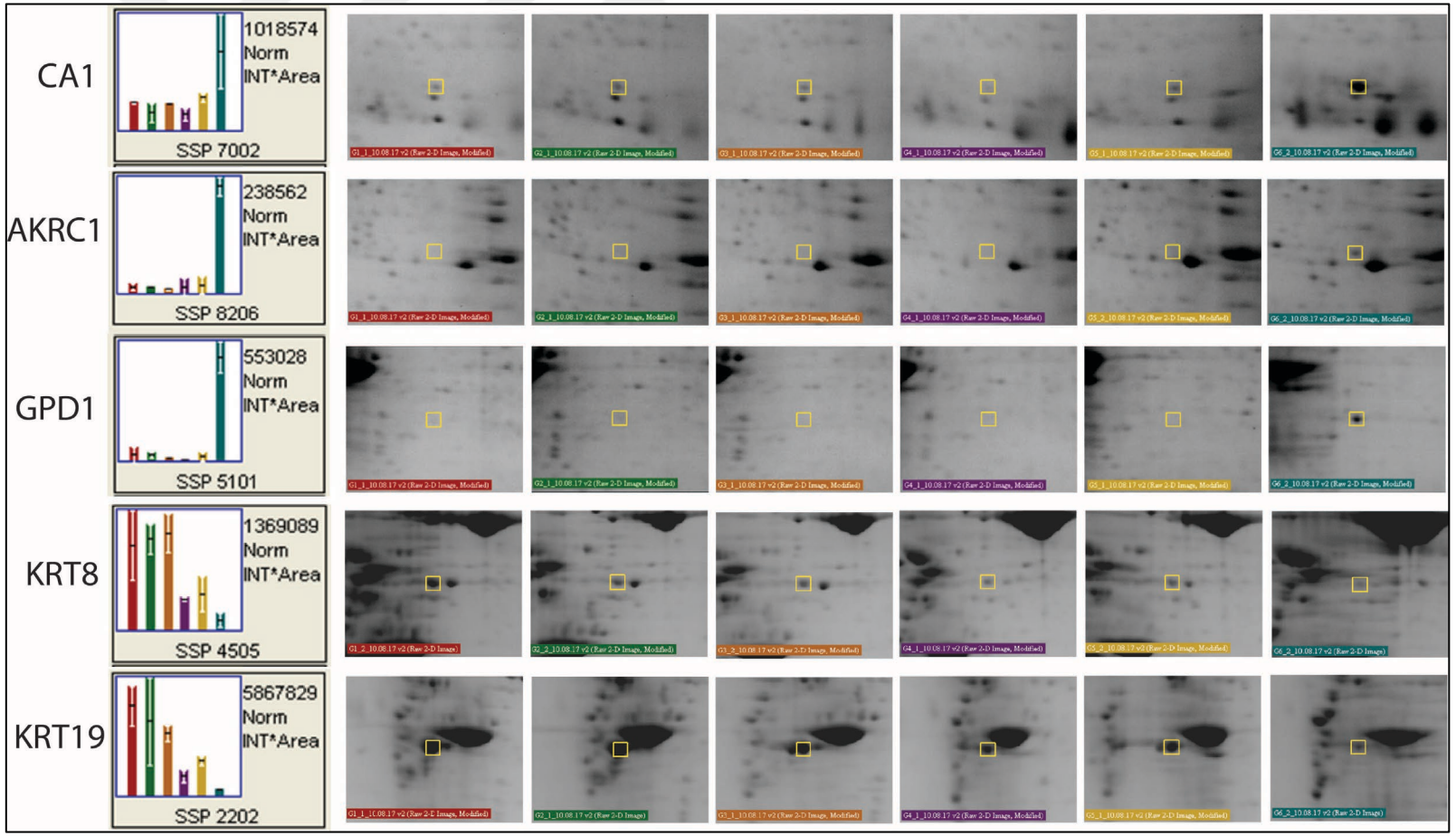

Figure E.1 (Continues). The representative close-up images of the differentially regulated proteins

(Red line: Luminal A, green line: Luminal B, orange line: Luminal B-like HER2+, purple line: TNBC, yellow line: HER2-enriched, blue line: control group)

Appendices F. Evaluation of optimization results of E-SERPA assay

Variable G

Optimization Setup for the Accuracy of the Method
An experimental setup was established using constants and variables stated in the table below to demonstrate that the method works accurately and specific to the antibody we used.

Table. Verification of accuracy of the E-SERPA binding assay using purified CK-MB antigen and in-house produced CK-MB antibody

		Experimental setup	
	Constants and variables	**I**	**II**
A	The amount of antibody coupled to 1 mg beads	6 µg	6 µg
B	The volume of antibody-coupled magnetic beads	20 µl	20 µl
C	Buffer solution	IPb	IPb
D	Incubation time (hour)	1	1
E	Incubation temperature	RT	RT
F	Antigen amount	200 µg	200 µg
G	**Amount of CK-MB protein**	**-**	**200 ng**
H	Elution method	2X LD	2X LD

Variables were stated in bold.
(IPb: Immunprecipitation buffer, RT: room temperature, LD: loading dye)

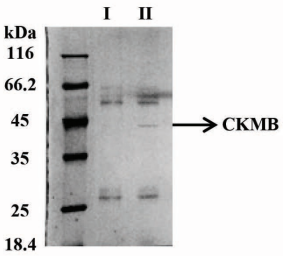

The molecular weight of band in the elution corresponded to the molecular weight of CK-MB protein indicating that E-SERPA assay was highly specific in capturing the protein of interest. The band was cut from the gel, identified by MALDI-TOF/TOF. The results confirmed that it indeed belonged to CK-MB.

Table. MALDI-TOF/TOF results

AC no.	Protein Accession	Protein Mass	Protein Score	Expect	Matches	Calc. pI	Seq. Cov. (%)	Best Protein Description
P06732	KCRM_HUMAN	43074	95	6.4e-006	16	6,77	29	Creatine kinase M-type
Ion score								
Observed	**Mr(expt)**	**Mr(calc)**	**ppm**	**Start**	**End**	**Miss**	**Ions**	**Peptide**
907.4847	906.4775	906.4811	-3.97	308	314	0	20	K.FEEILTR.L
1785.9253	1784.9180	1784.9520	-19.05	342	358	0	25	R.LGSSEVEQVQLVVDGVK.L
1994.9342	1993.9269	1993.9342	-3.63	321	341	0	12	R.GTGGVDTAAVGSVFDVSNADR.L

Figure F.1. E-SERPA optimization results for the accuracy of the method (Variable G)

Variable C

Optimization Setup for the Buffer Selection

An experimental setup was established using constants and variables stated in the table below to determine the appropriate buffer for E-SERPA method.

Table. Optimization conditions for buffer selection

		Experimental set-up	
	Constants and variables	**I**	**II**
A	The amount of antibody coupled to 1 mg beads	6 µg	6 µg
B	The volume of antibody-coupled magnetic beads	20 µl	20 µl
C	**Buffer solution**	**PBS**	**IPb**
D	Incubation time (hour)	1	1
E	Incubation temperature	RT	RT
F	Antigen amount	200 µg	200 µg
G	Amount of CK-MB protein	200 ng	200 ng
H	Elution method	2X LD	2X LD

Variables were stated in bold.
(PBS: Phosphate buffered saline)

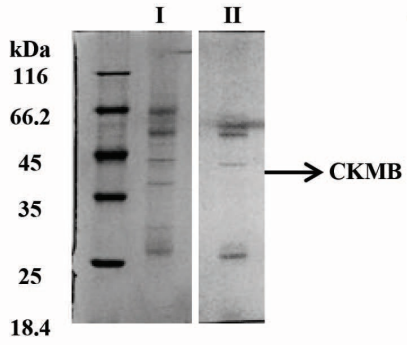

When PBS was used as the choice of buffer, several non-specific protein bands were observed on the gel. The IP buffer eliminated those non-specific bands and allowed the capture of the protein of interest, CK-MB. Therefore, the IP buffer was used throughout the E-SERPA experiments.

Figure F.2. E-SERPA optimization results for the selection of buffer (Variable C)

Variable A: According to the WB results, increasing the amount of antibody that coupled to magnetic beads did not increase the amount of captured antigen. Moreover, the yield was higher when 6 µg antibody was used for coupling. Therefore, it was decided that the coating of 1 mg magnetic beads with 6 µg antibody was sufficient for coupling.

		Experimental setup	
	Constants and variables		
A	**The amount of antibody coupled to 1 mg beads**	**6 µg**	**30 µg**
B	The volume of antibody-coupled magnetic beads	20 µl, 40 µl, 80 µl	20 µl, 40 µl, 80 µl
C	Buffer solution	IP	IP
D	Incubation time (hour)	1	1
E	Incubation temperature	RT	RT
F	Antigen amount	500 µg	500 µg
G	Amount of CK-MB protein	10 ng	10 ng
H	Elution method	2X LD	2X LD

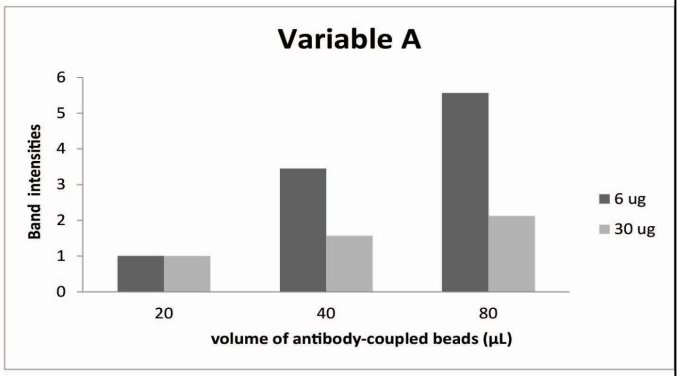

Variable B: According to the results of optimization experiments for variable B, the increase in the volume of antibody-coupled magnetic beads increased the amount of captured antigen.

		Experimental setup
	Constants and variables	
A	The amount of antibody coupled to 1 mg beads	6 µg
B	**The volume of antibody-coupled magnetic beads**	**20 µl, 40 µl, 80 µl, 160 µl**
C	Buffer solution	IP
D	Incubation time (hour)	1
E	Incubation temperature	RT
F	Antigen amount	500 µg
G	Amount of CK-MB protein	10 ng
H	Elution method	2X LD

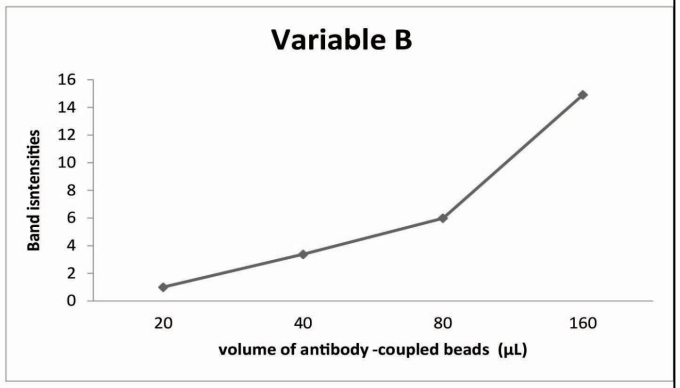

Figure F.3. E-SERPA optimization results for Variable A and B

Variable D: According to the results of optimization experiments for variable D, the increase in incubation time increased the amount of captured antigen up to 6 hours. Moreover, there is no difference between 6 hours and overnight incubation.

		Experimental setup
	Constants and variables	
A	The amount of antibody coupled to 1 mg beads	6 µg
B	The volume of antibody-coupled magnetic beads	20 µl
C	Buffer solution	IP
D	**Incubation time (hour)**	**2, 4, 6, overnight**
E	Incubation temperature	RT
F	Antigen amount	500 µg
G	Amount of CK-MB protein	10 ng
H	Elution method	2X LD

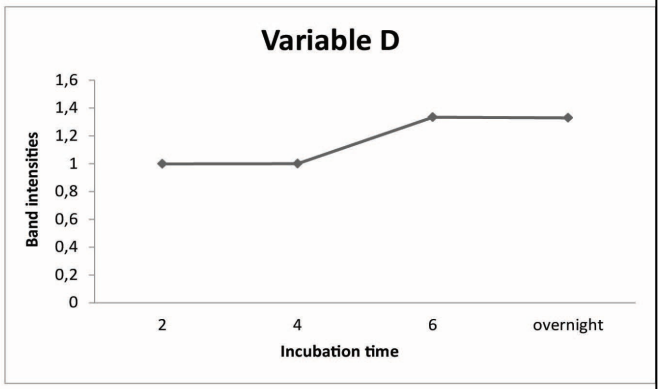

Variable E: The relationship between the incubation temperature and the amount of captured antigen was inversely proportional. The maximum yield in captured antigen was obtained at 4 ºC.

		Experimental setup
	Constants and variables	
A	The amount of antibody coupled to 1 mg beads	6 µg,
B	The volume of antibody-coupled magnetic beads	80 µl
C	Buffer solution	IP
D	Incubation time (hour)	1
E	**Incubation temperature**	**4ºC, RT, 30 ºC, 37ºC**
F	Antigen amount	500 µg
G	Amount of CK-MB protein	10 ng
H	Elution method	2X LD

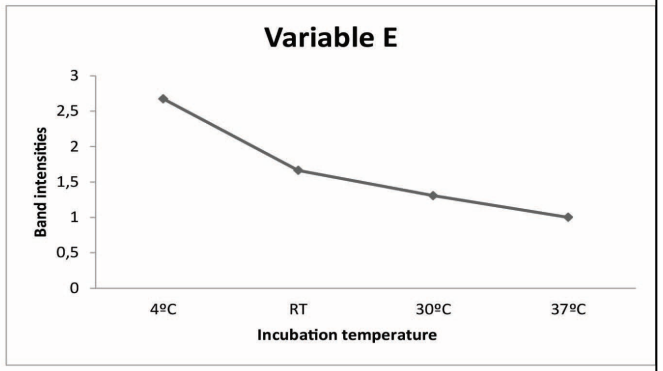

Figure F.4. E-SERPA optimization results for Variable D and E

Variable G: Optimization experiment with different concentrations of CK-MB protein was performed to measure the sensitivity of E-SERPA assay. SDS-PAGE were performed with the eluates and the gel was stained by silver staining method. In addition, the optimization experiment was performed again and the eluates was analyzed by nLC-MS/MS.

	Constants and variables	Experimental setup
A	The amount of antibody coupled to 1 mg beads	6 µg
B	The volume of antibody-coupled magnetic beads	20 µl
C	Buffer solution	IP
D	Incubation time (hour)	1
E	Incubation temperature	RT
F	Antigen amount	500 µg
G	**Amount of CK-MB protein (ng)**	**200, 100, 50, 10, 5, 3, 1**
H	Elution method	2X LD

Amount of CK-MB protein	Accession	Description	Coverage [%]	# Peptides	# PSMs	MW [kDa]	calc. pI	# Protein Groups	# AAs
1 ng	H0YJG0	Creatine kinase B-type (Fragment)	**4**	1	1	20,1	6,7	1	179
5 ng	P06732	Creatine kinase M-type	**3**	1	1	43,1	7,25	1	381
10 ng	P06732	Creatine kinase M-type	**14**	4	5	43,1	7,25	1	381
20 ng	P06732	Creatine kinase M-type	**18**	7	10	43,1	7,25	1	381

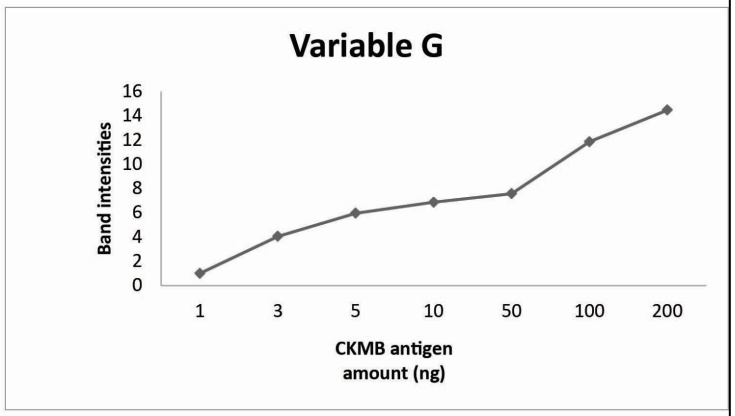

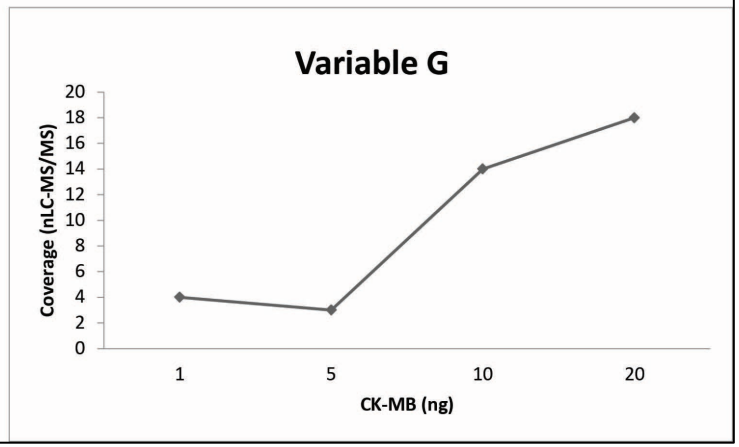

Figure F.5. E-SERPA optimization results for Variable G

Variable H: Optimization experiment with different elution methods was performed to obtain antigens (TAAs) with maximum yield. Afte elution proteins were digested using in-solution digestion kit. TAAs were identified by nLC-MS/MS and results were evaluated according to the number of identified proteins.

E1	10 µL elution buffer. In-solution digestion.
E2	100 µL elution buffer. Precipitated. In-solution digestion.
E3	40 µL 1% formic acid. Speedvac. In-solution digestion.

		Experimental setup
	Constants and variables	
A	The amount of antibody coupled to 1 mg beads	6 µg
B	The volume of antibody-coupled magnetic beads	50 µl
C	Buffer solution	IP
D	Incubation time (hour)	overnight
E	Incubation temperature	4°C
F	Antigen amount	2 mg
H	**Elution method**	**E1, E2, E3, OPT1, OPT2, OPT3.**

OPT1	(Ps) 50 mM Ambic, 10 mM iodoacetamide at 95°C. In-solution digestion without beads.
OPT2	(PsT) 50 mM Ambic, 10 mM iodoacetamide at 95°C. In-solution digestion without beads.
OPT3	(PsT) 50 mM Ambic, 10 mM iodoacetamide at 95°C. In-solution digestion with beads.

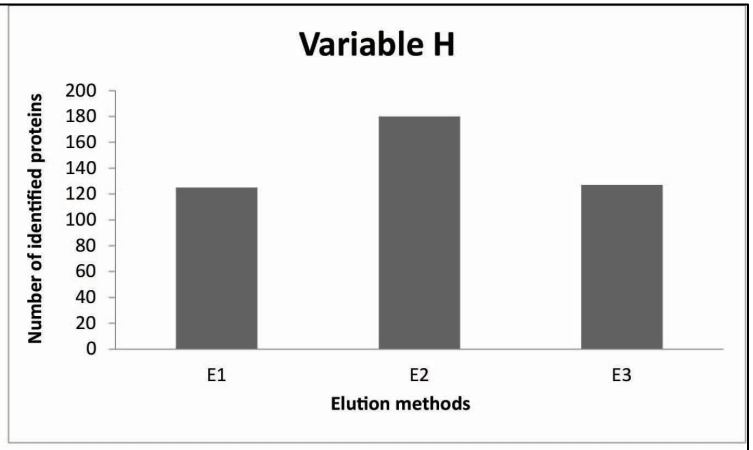

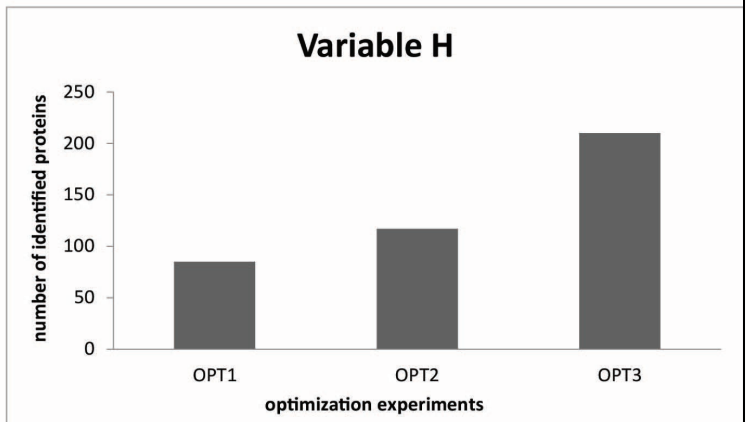

Figure F.6. E-SERPA optimization results for elution methods (Variable H)

Appendices G. The lists of identified proteins of tumour vs control E-SERPA analysis

Table G.1. The list of identified proteins in Ps

No.	Master	Accession	Description	Coverage [%]	# Peptides	# Unique Peptides	MW [kDa]	Calc. pI
1	MP	A0N5G5	Rheumatoid factor D5 light chain (Fragment)	15	1	1	12,8	8,97
2	MP	Q0ZCH9	Immunglobulin heavy chain variable region (Fragment	25	2	1	13,4	8,46
3	MP	Q6NS95	IGL@ protein	21	3	1	25,1	6,67
4	MP	P01861	Ig gamma-4 chain C region	31	6	1	35,9	7,36
5	MP	A2KBB9	Anti-(ED-B) scFV (Fragment)	19	3	2	25,1	8,12
6	MP	Q6GMV8	Uncharacterized protein	21	3	1	24,9	6,67
7	MP	Q6PIL8	IGK@ protein	43	7	1	25,8	6,55
8	MP	P01620	Ig kappa chain V-III region SIE	31	2	1	11,8	8,48
9	MP	A0A087X130	Ig kappa chain C region	41	6	1	25,1	6,32
10	MP	B4DPP6	cDNA FLJ54371, highly similar to Serum albumin	2	1	1	70,3	6,09
11	MP	Q6N093	Putative uncharacterized protein DKFZp686I04196 (Fragment)	32	10	4	46	7,59
12	MP	A0A087WYE1	Ig gamma-1 chain C region	38	13	7	52,1	7,55
13	MP	A0A087WVW2	Ig gamma-3 chain C region	21	8	2	57,1	8,1
14	MP	Q96SA9	Anti-streptococcal/anti-myosin immunoglobulin kappa light chain variable region (Fragment)	32	2	2	11,5	8,85
15	MP	P01625	Ig kappa chain V-IV region Len	16	1	1	12,6	7,93
16	MP	A2NB45	Cold agglutinin FS-1 L-chain (Fragment)	33	2	2	12,4	8,48
17	MPC	H0YA55	Serum albumin (Fragment)	3	1	1	51,5	6,95
18	MPC	V9HW68	Epididymis luminal protein 214	39	13	7	51,7	7,75
19	MPC	A0A075B6N8	Ig gamma-3 chain C region (Fragment)	29	8	2	41,3	7,9
20	MPC	Q8N355	IGL@ protein	21	3	1	24,8	6,37
21	MPC	A0A087X1V9	Protein IGKV2-28	36	2	2	11	5,24
22	MPC	Q6PJF2	IGK@ protein	43	7	1	25,5	6,55
23	MPC	A2KBC0	Anti-(ED-B) scFV (Fragment)	19	3	2	25,2	8,12
24	MPC	A2KBC6	Anti-FactorVIII scFv (Fragment)	19	3	2	25	8,41
25	MPC	P01622	Ig kappa chain V-III region Ti	31	2	1	11,8	8,5
26	MPC	A2KBC7	Anti-IFN-G scFv (Fragment)	19	3	2	25	7,72
27	MPC	B1N7B8	Cryocrystalglobulin CC1 kappa light chain variable region (Fragment)	17	1	1	11,8	7,99

Table G.1 (Continues). The list of identified proteins in Ps

No.	Master	Accession	Description	Coverage [%]	# Peptides	# Unique Peptides	MW [kDa]	Calc. pI
28	MPC	P04206	Ig kappa chain V-III region GOL	31	2	1	11,8	9,25
29	MPC	A2KBC8	Anti-TeTox scFv (Fragment)	19	3	2	25,1	7,71
30	MPC	Q56G89	Serum albumin	2	1	1	69	6,2
31	MPC	S4R460	Protein IGHV3OR16-9	31	2	1	10,4	7,97
32	MPC	B4DPR2	cDNA FLJ50830, highly similar to Serum albumin	2	1	1	59,5	7,17
33	MPC	A2KBC5	Anti-HCS scFv (Fragment)	19	3	2	25,2	8,05
34	MPC	P01617	Ig kappa chain V-II region TEW	33	2	2	12,3	6
35	MPC	Q9UL91	Myosin-reactive immunoglobulin heavy chain variable region (Fragment)	25	2	1	12,8	5,36
36	MPC	A2KBC1	Anti-(ED-B) scFV (Fragment)	19	3	2	25,1	8,12
37	MPC	Q6N089	Putative uncharacterized protein DKFZp686P15220	38	13	7	51,7	7,93
38	MPC	Q9UL78	Myosin-reactive immunoglobulin light chain variable region (Fragment)	31	2	1	11,6	8,29
39	MPC	A8K9P0	cDNA FLJ78413, highly similar to Homo sapiens albumin, mRNA	2	1	1	69,2	6,28
40	MPC	V9HW34	Epididymis luminal protein 213	43	7	1	25,6	6,55
41	MPC	B7WNR0	Serum albumin	3	1	1	56,2	7,14
42	MPC	A2KBC4	Anti-TN-C scFv (Fragment)	19	3	2	25,1	8,41
43	MPC	Q8NF17	FLJ00385 protein (Fragment)	21	8	2	56,1	7,59
44	MPC	A2KBC3	Anti-(ED-B) scFV (Fragment)	19	3	2	25,1	7,71
45	MPC	C9JKR2	Albumin, isoform CRA_k	3	1	1	47,3	6,35
46	MPC	A0A087WV47	Ig gamma-1 chain C region	39	13	7	51,1	7,55
47	MPC	D6RHD5	Serum albumin	3	1	1	52	6,84
48	MPC	A2KBC2	Anti-(ED-B) scFV (Fragment)	19	3	2	25,2	7,71
49	MPC	F6KPG5	Albumin (Fragment)	2	1	1	66,5	6,04
50	MPC	Q6N030	Putative uncharacterized protein DKFZp686I15212	21	8	2	57	8,05
51	MPC	P01623	Ig kappa chain V-III region WOL	31	2	1	11,7	8,91
52	MPC	P01860	Ig gamma-3 chain C region	29	8	2	41,3	7,9
53	MPC	A0A087X079	Ig gamma-1 chain C region	38	13	7	51,9	8,07
54	MPC	Q5EBM2	Uncharacterized protein	21	8	2	56,8	6,86
55	MPC	P02768	Serum albumin	2	1	1	69,3	6,28
56	MPC	A0A087WXL8	Ig gamma-3 chain C region	21	8	2	56,9	8,25

Table G.2. The list of identified proteins in PsT

No.	Master	Accession	Description	Coverage [%]	# Peptides	# Unique Peptides	MW [kDa]	Calc. pI
1	MP	Q6P5S8	IGK@ protein 1	48	11	1	25,8	6,33
2	MP	Q9HCC1	Single chain Fv (Fragment)	37	3	1	12,2	8,47
3	MP	P01621	Ig kappa chain V-III region NG9 (Fragment)	9	1	1	10,7	6,52
4	MP	P04406	Glyceraldehyde-3-phosphate dehydrogenase	4	1	1	36	8,46
5	MP	Q6N093	Putative uncharacterized protein DKFZp686I04196	40	13	6	46	7,59
6	MP	B7Z1K5	cDNA FLJ55956, highly similar to Tubulin alpha-6 chain	3	1	1	57,7	5,07
7	MP	I4AY87	Macrophage migration inhibitory factor (Fragment)	8	1	1	12,5	7,88
8	MP	B4DR52	Histone H2B	5	1	1	18	10,32
9	MP	A0A087WTX5	Ig kappa chain C region	44	10	1	25,6	7,97
10	MP	Q8N355	IGL@ protein	44	7	1	24,8	6,37
11	MP	Q6N094	Putative uncharacterized protein DKFZp686O01196	40	16	1	52,6	8,18
12	MP	Q14473	Beta-globin gene from a thalassemia patient	18	3	3	18,9	6,79
13	MP	A2IPI6	HRV Fab 027-VL (Fragment)	14	1	1	12,4	9,41
14	MP	Q6NS95	IGL@ protein	40	6	1	25,1	6,67
15	MP	B2R6F3	Splicing factor arginine/serine-rich 3	13	1	1	19,3	11,65
16	MP	H6VRG1	Keratin 1	2	1	1	66,1	8,12
17	MP	Q0ZCH9	Immunglobulin heavy chain variable region (Fragment)	41	4	1	13,4	8,46
18	MP	P01717	Ig lambda chain V-IV region Hil	18	1	1	11,5	6,51
19	MP	P01612	Ig kappa chain V-I region Mev	15	1	1	11,9	6,57
20	MP	V9HW43	Epididymis secretory protein Li 102	5	1	1	22,8	6,4
21	MP	S6BGE0	IgG H chain	29	7	1	32,2	7,85
22	MP	P01620	Ig kappa chain V-III region	46	4	1	11,8	8,48
23	MP	P01767	Ig heavy chain V-III region BUT	26	2	1	12,4	9,25
24	MP	A0A087WVW2	Ig gamma-3 chain C region	23	10	2	57,1	8,1
25	MP	A2NB45	Cold agglutinin FS-1 L-chain (Fragment)	33	2	2	12,4	8,48
26	MP	B4DPP6	cDNA FLJ54371, highly similar to Serum albumin	29	13	13	70,3	6,09
27	MP	A0A5E4	Uncharacterized protein	37	6	0	24,7	5,94
28	MP	P01602	Ig kappa chain V-I region HK102 (Fragment)	14	1	1	12,8	6,51
29	MP	Q9UL88	Myosin-reactive immunoglobulin heavy chain variable region (Fragment)	15	1	1	14,1	9,63
30	MP	A0A087WVN6	Protein IGKV1-27	35	2	2	10,4	8,47
31	MP	V9HW68	Epididymis luminal protein 214	50	19	0	51,7	7,75

Table G.2 (Continues). The list of identified proteins in PsT

No.	Master	Accession	Description	Coverage [%]	# Peptides	# Unique Peptides	MW [kDa]	Calc. pI
32	MP	D1MGQ2	Alpha-2 globin chain	11	1	1	15,2	8,68
33	MP	A8K486	Peptidyl-prolyl cis-trans isomerase	5	1	1	18	6,9
34	MP	P01616	Ig kappa chain V-II region MIL	21	1	1	12	9,29
35	MP	P01861	Ig gamma-4 chain C region	37	8	2	35,9	7,36
36	MP	P01613	Ig kappa chain V-I region Ni	30	2	2	12,2	5,36
37	MP	A2KBC2	Anti-(ED-B) scFV (Fragment)	31	6	3	25,2	7,71
38	MP	Q0ZCH6	Immunglobulin heavy chain variable region (Fragment)	7	1	1	14,3	6,55
39	MP	P01625	Ig kappa chain V-IV region Len	37	3	3	12,6	7,93
40	MP	A0A024RDS2	Periostin, osteoblast specific factor, isoform CRA_c	2	1	1	93,3	7,53
41	MP	Q8NEJ1	Uncharacterized protein	39	6	1	25	7,69
42	MP	B4DI63	cDNA FLJ59205, highly similar to Mimecan	7	2	2	40,5	7,99
43	MP	P04430	Ig kappa chain V-I region BAN	17	1	1	11,8	8,44
44	MP	P10909	Clusterin	3	1	1	52,5	6,27
45	MP	Q9UL85	Myosin-reactive immunoglobulin kappa chain variable region (Fragment)	25	2	2	11,8	8,51
46	MP	P16104	Histone H2AX	6	1	1	15,1	10,74
47	MP	A0N5G5	Rheumatoid factor D5 light chain (Fragment)	23	2	2	12,8	8,97
48	MP	P63261	Actin, cytoplasmic 2	20	6	6	41,8	5,48
49	MP	Q8IYE1	Coiled-coil domain-containing protein 13	2	1	1	80,8	8,84
50	MP	P62805	Histone H4	19	2	2	11,4	11,36
51	MPC	Q99878	Histone H2A type 1-J	7	1	1	13,9	10,89
52	MPC	F8VS66	Tubulin alpha-1C chain	12	1	1	14,4	5,47
53	MPC	F8VRK0	Tubulin alpha-1B chain (Fragment)	31	1	1	5,3	4,88
54	MPC	P04264	Keratin, type II cytoskeletal 1	2	1	1	66	8,12
55	MPC	B3VL86	Mutant beta-globin	23	3	3	14,9	6,77
56	MPC	A0A024RDT5	Periostin, osteoblast specific factor, isoform CRA_a	2	1	1	87	7,81
57	MPC	Q5ZEY3	Glyceraldehyde-3-phosphate dehydrogenase (Fragment)	16	1	1	9,2	9,72
58	MPC	Q8N532	TUBA1C protein	5	1	1	36,6	7,96
59	MPC	A2KBC7	Anti-IFN-G scFv (Fragment)	31	6	3	25	7,72
60	MPC	A8K9P0	cDNA FLJ78413, highly similar to Homo sapiens albumin, mRNA	29	13	13	69,2	6,28
61	MPC	C0IMJ3	Periostin isoform thy6	2	1	1	87,2	7,94

Table G.2 (Continues). The list of identified proteins in PsT

No.	Master	Accession	Description	Coverage [%]	# Peptides	# Unique Peptides	MW [kDa]	Calc. pI
62	MPC	P01860	Ig gamma-3 chain C region	32	10	2	41,3	7,9
63	MPC	F8VRZ4	Tubulin alpha-1A chain (Fragment)	13	1	1	12,2	5,77
64	MPC	A2KBC5	Anti-HCS scFv (Fragment)	31	6	3	25,2	8,05
65	MPC	Q9BQE3	Tubulin alpha-1C chain	3	1	1	49,9	5,1
66	MPC	B4DM82	Peptidyl-prolyl cis-trans isomerase	7	1	1	14,1	8,47
67	MPC	B7Z6G1	cDNA FLJ50671, highly similar to Periostin	5	1	1	30,5	5,26
68	MPC	L0R4T3	Histone H2B	13	1	1	7,3	8,88
69	MPC	Q9UBV6	Beta-globin (Fragment)	52	3	3	6,7	5,17
70	MPC	B2R5B6	Histone H2A	7	1	1	14,1	10,9
71	MPC	Q9BWU5	Mutant hemoglobin beta chain (Fragment)	30	3	3	11,5	7,05
72	MPC	Q4ZGM8	Hemoglobin alpha-2 globin mutant (Fragment)	15	1	1	10,8	9,04
73	MPC	F8VWV9	Tubulin alpha-1B chain (Fragment)	19	1	1	8,9	5,12
74	MPC	Q0QET7	Glyceraldehyde-3-phosphate dehydrogenase (Fragment)	6	1	1	24,6	8,51
75	MPC	H0YC35	Clusterin (Fragment)	4	1	1	33,5	5,74
76	MPC	A4UCT1	Glyceraldehyde-3-phosphate dehydrogenase (Fragment)	8	1	1	17,3	8,6
77	MPC	E9NGZ5	Hemoglobin beta globin chain (Fragment)	30	3	3	11,5	6,37
78	MPC	A0A087X2D0	Serine/arginine-rich-splicing factor 3	22	1	1	10,3	5,14
79	MPC	B3VL31	Beta globin (Fragment)	30	3	3	11,5	6,68
80	MPC	Q53GA7	Tubulin alpha 6 variant (Fragment)	3	1	1	49,8	5,14
81	MPC	A2KBC6	Anti-FactorVIII scFv (Fragment)	31	6	3	25	8,41
82	MPC	Q6V0K9	Mutant hemoglobin beta chain (Fragment)	30	3	3	11,5	6,68
83	MPC	H6VRF9	Keratin 1	2	1	1	66	7,8
84	MPC	Q96A08	Histone H2B type 1-A	7	1	1	14,2	10,32
85	MPC	H6VRG3	Keratin 1	2	1	1	66,1	7,8
86	MPC	P20671	Histone H2A type 1-D	7	1	1	14,1	10,9
87	MPC	B4DN58	cDNA FLJ53765, highly similar to Tubulin alpha chain	8	1	1	20	4,48
88	MPC	A0A075B6N8	Ig gamma-3 chain C region (Fragment)	32	10	2	41,3	7,9
89	MPC	Q9BWV6	Mutant beta globin	29	3	3	12,2	6,05
90	MPC	Q1KLZ0	HCG15971, isoform CRA_a	20	6	6	41,7	5,48
91	MPC	P06899	Histone H2B type 1-J	7	1	1	13,9	10,32
92	MPC	Q93079	Histone H2B type 1-H	7	1	1	13,9	10,32
93	MPC	B3KT06	cDNA FLJ37398 fis, clone BRAMY2027467, highly similar to Tubulin alpha-ubiquitous chain	4	1	1	46,3	5,14

Table G.2 (Continues). The list of identified proteins in PsT

No.	Master	Accession	Description	Coverage [%]	# Peptides	# Unique Peptides	MW [kDa]	Calc. pI
94	MPC	Q9BX83	Hemoglobin alpha 1 globin chain (Fragment)	15	1	1	10,7	7,72
95	MPC	A9YUX2	Truncated beta-globin	51	3	3	7	8,22
96	MPC	Q53GK6	Beta actin variant (Fragment)	20	6	6	41,7	5,48
97	MPC	P68363	Tubulin alpha-1B chain	3	1	1	50,1	5,06
98	MPC	Q9GZL9	Beta-globin (Fragment)	28	3	3	12,5	6,37
99	MPC	Q9UL78	Myosin-reactive immunoglobulin light chain variable region (Fragment)	46	4	1	11,6	8,29
100	MPC	Q8IWL5	CLU (Fragment)	9	1	1	16,3	6,01
101	MPC	O60814	Histone H2B type 1-K	7	1	1	13,9	10,32
102	MPC	V9GZN0	Histone H2A gene (lambda-HHG55) (Fragment)	19	1	1	5	11,9
103	MPC	Q71U36	Tubulin alpha-1A chain	3	1	1	50,1	5,06
104	MPC	Q8N257	Histone H2B type 3-B	7	1	1	13,9	10,32
105	MPC	A0A024QZZ7	Histone H2B	7	1	1	13,9	10,32
106	MPC	U3PXP0	Alpha globin chain (Fragment)	29	1	1	5,7	7,52
107	MPC	B5ANL9	Beta globin chain (Fragment)	36	3	3	9,5	6,79
108	MPC	A3KPC7	Histone H2A	7	1	1	13,9	10,89
109	MPC	A0A0A0MS15	Protein IGHV3-49 (Fragment)	8	1	1	13	8,62
110	MPC	Q3LR79	Hemoglobin beta (Fragment)	30	3	3	11,5	5,77
111	MPC	I6L9F7	Histone H2B (Fragment)	7	1	1	15,1	10,24
112	MPC	F8VQQ4	Tubulin alpha-1A chain (Fragment)	7	1	1	24,2	5,29
113	MPC	P62807	Histone H2B type 1-C/E/F/G/I	7	1	1	13,9	10,32
114	MPC	B4DW52	cDNA FLJ55253, highly similar to Actin, cytoplasmic 1	21	6	6	38,6	5,35
115	MPC	Q53G99	Beta actin variant (Fragment)	20	6	6	41,7	5,59
116	MPC	P57053	Histone H2B type F-S	7	1	1	13,9	10,37
117	MPC	E7ERK6	Clusterin (Fragment)	6	1	1	23,7	5,15
118	MPC	C9J5S7	Peptidyl-prolyl cis-trans isomerase	7	1	1	13,2	6,77
119	MPC	Q99880	Histone H2B type 1-L	7	1	1	13,9	10,32
120	MPC	P33778	Histone H2B type 1-B	7	1	1	13,9	10,32
121	MPC	Q5EBM2	Uncharacterized protein	23	10	2	56,8	6,86
122	MPC	A8JZY9	cDNA FLJ78587	3	1	1	50,1	5,06
123	MPC	Q8NF17	FLJ00385 protein (Fragment)	24	10	2	56,1	7,59
124	MPC	B4E335	cDNA FLJ52842, highly similar to Actin, cytoplasmic 1	21	6	6	39,2	5,59
125	MPC	D9YZU5	Hemoglobin, beta	22	3	3	16	7,28

Table G.2 (Continues). The list of identified proteins in PsT

No.	Master	Accession	Description	Coverage [%]	# Peptides	# Unique Peptides	MW [kDa]	Calc. pI
126	MPC	B3KPS3	cDNA FLJ32131 fis, clone PEBLM2000267, highly similar to Tubulin alpha-ubiquitous chain	4	1	1	46,2	5,12
127	MPC	H0YLK8	Clusterin (Fragment)	4	1	1	34,7	6,1
128	MPC	P01617	Ig kappa chain V-II region TEW	33	2	2	12,3	6
129	MPC	Q14484	Beta-globin (Fragment)	52	3	3	6,7	4,88
130	MPC	A0A087X1V9	Protein IGKV2-28	36	2	2	11	5,24
131	MPC	P23527	Histone H2B type 1-O	7	1	1	13,9	10,32
132	MPC	Q5NV90	V2-17 protein (Fragment)	20	1	1	10,4	4,59
133	MPC	Q8IUL9	Hemoglobin beta chain variant Hb.Sinai-Bel Air (Fragment)	30	3	3	11,5	6,05
134	MPC	B1ALD9	Periostin	2	1	1	90,1	7,94
135	MPC	Q53G76	Beta actin variant (Fragment)	20	6	6	41,7	5,48
136	MPC	Q7Z532	Osteoglycin OG	8	2	2	33,9	5,48
137	MPC	Q5TBF5	Mimecan (Fragment)	9	2	2	30,4	8,34
138	MPC	E1B2D1	Hemoglobin alpha-1 globin chain variant (Fragment)	15	1	1	10,8	8,48
139	MPC	C8C504	Beta-globin	22	3	3	16	8,06
140	MPC	Q96QV6	Histone H2A type 1-A	7	1	1	14,2	10,86
141	MPC	A8K0R3	Osteoglycin (Osteoinductive factor, mimecan), isoform CRA_a	8	2	2	33,9	5,63
142	MPC	E7EUT5	Glyceraldehyde-3-phosphate dehydrogenase	5	1	1	27,9	6,95
143	MPC	B2R5B3	Histone H2A	7	1	1	14,1	11,06
144	MPC	D5FZW3	Beta globin (Fragment)	78	3	3	4,5	5,83
145	MPC	A8K9J7	Histone H2B	7	1	1	14	10,32
146	MPC	B3VL05	Beta globin (Fragment)	30	3	3	11,5	6,68
147	MPC	Q9BTM1	Histone H2A.J	7	1	1	14	10,9
148	MPC	P0C0S5	Histone H2A.Z	7	1	1	13,5	10,58
149	MPC	P02768	Serum albumin	29	13	13	69,3	6,28
150	MPC	B4E3A4	cDNA FLJ57283, highly similar to Actin, cytoplasmic 2	21	6	6	39,8	5,38
151	MPC	V9H1D9	Alpha globin	12	1	1	13,6	8,24
152	MPC	Q8IUE6	Histone H2A type 2-B	7	1	1	14	10,89
153	MPC	Q99877	Histone H2B type 1-N	7	1	1	13,9	10,32
154	MPC	F5H5D3	Tubulin alpha-1C chain	3	1	1	57,7	5,07
155	MPC	Q08AJ9	Histone H2A	7	1	1	14,1	11,05
156	MPC	Q9UP81	Mutant beta-globin	36	3	3	9,7	8,19
157	MPC	Q16778	Histone H2B type 2-E =3	7	1	1	13,9	10,32
158	MPC	S6BGD6	IgG L chain	39	6	1	24,8	7,24
159	MPC	Q52MT0	Beta globin (Fragment)	30	3	3	11,5	6,37
160	MPC	P0C0S8	Histone H2A type 1	7	1	1	14,1	10,9

Table G.2 (Continues). The list of identified proteins in PsT

No.	Master	Accession	Description	Coverage [%]	# Peptides	# Unique Peptides	MW [kDa]	Calc. pI
161	MPC	Q0D2M2	HIST1H2BC protein	7	1	1	13,8	10,39
162	MPC	A0A087WXL8	Ig gamma-3 chain C region	23	10	2	56,9	8,25
163	MPC	F8VVB9	Tubulin alpha-1B chain (Fragment)	6	1	1	27,4	5,2
164	MPC	E9M4D4	Hemoglobin alpha-1 globin chain (Fragment)	15	1	1	10,8	8,48
165	MPC	Q9BXA2	Beta-globin (Fragment)	54	3	3	6,5	4,64
166	MPC	F8W6P5	Hemoglobin subunit beta (Fragment)	36	3	3	9,7	6,79
167	MPC	E9M263	Hemoglobin beta chain (Fragment)	56	3	3	6,2	4,64
168	MPC	Q8WVW5	Putative uncharacterized protein (Fragment)	20	6	6	40,5	6,14
169	MPC	P62937	Peptidyl-prolyl cis-trans isomerase A	5	1	1	18	7,81
170	MPC	Q8IZI0	Hemoglobin beta chain variant Hb-I_Toulouse (Fragment)	30	3	3	11,5	5,71
171	MPC	Q0Z944	Beta globin (Fragment)	30	3	3	11,5	6,37
172	MPC	H6VRG0	Keratin 1	2	1	1	65,9	7,8
173	MPC	A2KBC8	Anti-TeTox scFv (Fragment)	31	6	3	25,1	7,71
174	MPC	A2KBC3	Anti-(ED-B) scFV (Fragment)	31	6	3	25,1	7,71
175	MPC	Q7L7L0	Histone H2A type 3	7	1	1	14,1	11,05
176	MPC	Q99879	Histone H2B type 1-M	7	1	1	14	10,32
177	MPC	F8WE65	Peptidyl-prolyl cis-trans isomerase	8	1	1	13	6,77
178	MPC	Q6MZQ6	Putative uncharacterized protein DKFZp686G11190	40	16	1	52	8,06
179	MPC	Q71V99	Peptidyl-prolyl cis-trans isomerase	5	1	1	18	7,9
180	MPC	Q16777	Histone H2A type 2-C	7	1	1	14	10,9
181	MPC	U6A216	Mutant hemoglobin alpha 1 globin chain (Fragment)	15	1	1	10,7	8,48
182	MPC	Q6N030	Putative uncharacterized protein DKFZp686I15212	23	10	2	57	8,05
183	MPC	A2KBC4	Anti-TN-C scFv (Fragment)	31	6	3	25,1	8,41
184	MPC	Q6FI13	Histone H2A type 2-A	7	1	1	14,1	10,9
185	MPC	P01623	Ig kappa chain V-III region WOL	46	4	1	11,7	8,91
186	MPC	B2RE56	Peptidyl-prolyl cis-trans isomerase	5	1	1	18	7,81
187	MPC	Q5QNW6	Histone H2B type 2-F	7	1	1	13,9	10,32
188	MPC	U3KQK0	Histone H2B	5	1	1	18,8	10,54
189	MPC	A2MYD4	V2-7 protein (Fragment)	20	1	1	10,3	5,01
190	MPC	H6VRF8	Keratin 1	2	1	1	66	8,12
191	MPC	Q4TZM4	Hemoglobin beta chain (Fragment)	32	3	3	11	6,52
192	MPC	A0A087WV47	Ig gamma-1 chain C region	50	19	0	51,1	7,55
193	MPC	Q2TSD0	Glyceraldehyde-3-phosphate dehydrogenase	4	1	1	36	8,46
194	MPC	F8WE04	Heat shock protein beta-1	5	1	1	20,4	9,06

Table G.2 (Continues). The list of identified proteins in PsT

No.	Master	Accession	Description	Coverage [%]	# Peptides	# Unique Peptides	MW [kDa]	Calc. pI
195	MPC	F8VX09	Tubulin alpha-1B chain (Fragment)	20	1	1	8,3	5,33
196	MPC	I1VZV6	Hemoglobin alpha 1	11	1	1	15,3	9,03
197	MPC	Q0VAS5	Histone H4	19	2	2	11,3	11,03
198	MPC	A0A087WU91	Protein IGHV3-49	8	1	1	12,3	8,92
199	MPC	Q71UI9	Histone H2A.V	7	1	1	13,5	10,58
200	MPC	Q93077	Histone H2A type 1-C	7	1	1	14,1	11,05
201	MPC	C9J0D1	Histone H2A	7	1	1	13,2	9,99

Table G.3. The list of identified proteins in PsC

No.	Master	Accession	Description	Coverage [%]	# Peptides	# Unique Peptides	MW [kDa]	calc. pI
1	MP	A2NB45	Cold agglutinin FS-1 L-chain (Fragment)	33	2	2	12,4	8,48
2	MP	D9YZU5	Hemoglobin, beta	65	7	7	16	7,28
3	MP	B4DPP6	cDNA FLJ54371, highly similar to Serum albumin	33	14	14	70,3	6,09
4	MP	P01717	Ig lambda chain V-IV region Hil	18	1	1	11,5	6,51
5	MP	P01616	Ig kappa chain V-II region MIL	21	1	1	12	9,29
6	MP	B2R7Q9	cDNA, FLJ93562	3	1	1	59,6	4,82
7	MP	S6BGE0	IgG H chain	29	7	1	32,2	7,85
8	MP	A0A087WVW2	Ig gamma-3 chain C region	21	8	2	57,1	8,1
9	MP	V9HW43	Epididymis secretory protein Li 102	5	1	1	22,8	6,4
10	MP	A0A087WVN6	Protein IGKV1-27	35	2	2	10,4	8,47
11	MP	P01861	Ig gamma-4 chain C region	31	6	1	35,9	7,36
12	MP	A0A087WZW8	Protein IGKV3-11	41	8	0	25,6	6,01
13	MP	P16104	Histone H2AX	6	1	1	15,1	10,74
14	MP	Q0ZCH9	Immunglobulin heavy chain variable region (Fragment)	41	4	1	13,4	8,46
15	MP	V9HW68	Epididymis luminal protein 214	43	16	3	51,7	7,75
16	MP	Q8N355	IGL@ protein	29	5	3	24,8	6,37
17	MP	C3VMY8	Alpha B crystallin	22	2	2	20,1	7,08
18	MP	Q9UL85	Myosin-reactive immunoglobulin kappa chain variable region (Fragment)	17	1	1	11,8	8,51
19	MP	Q6P528	ASPN protein	5	1	1	43,9	6,48
20	MP	A0N5G5	Rheumatoid factor D5 light chain (Fragment)	23	2	1	12,8	8,97
21	MP	A0A024R5Z7	Annexin	5	1	1	38,6	7,75
22	MP	Q6NS95	IGL@ protein	21	3	1	25,1	6,67
23	MP	P01620	Ig kappa chain V-III region SIE	31	2	2	11,8	8,48
24	MP	Q96K68	cDNA FLJ14473 fis, clone MAMMA1001080, highly similar to Homo sapiens SNC73 protein (SNC73) mRNA OS=Homo sapiens PE=2 SV=1	9	2	1	53,1	6,86
25	MP	Q9UL88	Myosin-reactive immunoglobulin heavy chain variable region (Fragment)	15	1	1	14,1	9,63
26	MP	Q6N093	Putative uncharacterized protein DKFZp686I04196 (Fragment)	32	10	4	46	7,59
27	MP	A0A087WTX5	Ig kappa chain C region	43	8	1	25,6	7,97
28	MP	D1MGQ2	Alpha-2 globin chain	49	4	4	15,2	8,68

Table G.3 (Continues). The list of identified proteins in PsC

No.	Master	Accession	Description	Coverage [%]	# Peptides	# Unique Peptides	MW [kDa]	calc. pI
29	MP	A5A3E0	POTE ankyrin domain family member F	1	1	1	121,4	6,2
30	MP	P01613	Ig kappa chain V-I region Ni	16	1	1	12,2	5,36
31	MP	H6VRG1	Keratin 1	4	2	2	66,1	8,12
32	MP	S6BAP0	IgG H chain	21	5	1	24	8,54
33	MP	P01625	Ig kappa chain V-IV region Len	24	2	2	12,6	7,93
34	MPC	Q8WVW5	Putative uncharacterized protein (Fragment)	4	1	1	40,5	6,14
35	MPC	Q9BXN1	Asporin	6	1	1	43,4	7,08
36	MPC	H0YKS4	Annexin (Fragment)	9	1	1	19,5	5,96
37	MPC	H6VRF9	Keratin 1	4	2	2	66	7,8
38	MPC	Q5NV90	V2-17 protein (Fragment)	20	1	1	10,4	4,59
39	MPC	Q96DE1	Putative uncharacterized protein (Fragment)	10	1	1	17,7	5,3
40	MPC	Q53G76	Beta actin variant (Fragment)	4	1	1	41,7	5,48
41	MPC	B3KUD3	cDNA FLJ39583 fis, clone SKMUS2004897, highly similar to ACTIN, ALPHA SKELETAL MUSCLE OS=Homo sapiens PE=2 SV=1	5	1	1	37,8	5,73
42	MPC	P63267	Actin, gamma-enteric smooth muscle	4	1	1	41,9	5,48
43	MPC	A0A087WV47	Ig gamma-1 chain C region	43	16	3	51,1	7,55
44	MPC	F8WE04	Heat shock protein beta-1	5	1	1	20,4	9,06
45	MPC	A2MYD4	V2-7 protein (Fragment)	20	1	1	10,3	5,01
46	MPC	Q9BTM1	Histone H2A.J	7	1	1	14	10,9
47	MPC	H0YMD0	Annexin (Fragment)	7	1	1	25,3	5,97
48	MPC	B4E3A4	cDNA FLJ57283, highly similar to Actin, cytoplasmic 2	4	1	1	39,8	5,38
49	MPC	Q96FU6	ACTG1 protein (Fragment)	10	1	1	18,4	5,35
50	MPC	H6VRF8	Keratin 1	4	2	2	66	8,12
51	MPC	Q93077	Histone H2A type 1-C	7	1	1	14,1	11,05
52	MPC	B3KPP5	cDNA FLJ32030 fis, clone NTONG2000040, highly similar to Actin, alpha cardiac	9	1	1	20,9	5,66
53	MPC	B4E335	cDNA FLJ52842, highly similar to Actin, cytoplasmic 1	5	1	1	39,2	5,59
54	MPC	V9HVZ7	Epididymis luminal protein 176	7	1	1	25	5,66
55	MPC	H0YLE2	Annexin A2 (Fragment)	36	1	1	5,3	4,5
56	MPC	P01622	Ig kappa chain V-III region Ti	31	2	2	11,8	8,5
57	MPC	B2R5B6	Histone H2A	7	1	1	14,1	10,9
58	MPC	P04264	Keratin, type II cytoskeletal 1	4	2	2	66	8,12
59	MPC	Q99878	Histone H2A type 1-J	7	1	1	13,9	10,89

Table G.3 (Continues). The list of identified proteins in PsC

No.	Master	Accession	Description	Coverage [%]	# Peptides	# Unique Peptides	MW [kDa]	calc. pI
60	MPC	A4UCT3	Beta-actin (Fragment)	12	1	1	14,7	5,12
61	MPC	Q53G99	Beta actin variant (Fragment)	4	1	1	41,7	5,59
62	MPC	Q5TBF2	Asporin	9	1	1	27,7	5,66
63	MPC	Q9BYX7	Putative beta-actin-like protein 3	4	1	1	42	6,33
64	MPC	H0YN28	Annexin (Fragment)	12	1	1	16,1	5,17
65	MPC	A3KPC7	Histone H2A	7	1	1	13,9	10,89
66	MPC	A8K3K1	cDNA FLJ78096, highly similar to Homo sapiens actin, alpha, cardiac muscle (ACTC), mRNA	4	1	1	42	5,39
67	MPC	A0A087X1V9	Protein IGKV2-28	36	2	2	11	5,24
68	MPC	H6VRG3	Keratin 1	4	2	2	66,1	7,8
69	MPC	A0A075B6N8	Ig gamma-3 chain C region (Fragment)	29	8	2	41,3	7,9
70	MPC	Q6MZV6	Putative uncharacterized protein DKFZp686L19235	9	2	1	51,6	5,77
71	MPC	Q6PJ43	ACTG1 protein (Fragment)	6	1	1	29,4	5,69
72	MPC	P04206	Ig kappa chain V-III region GOL	31	2	2	11,8	9,25
73	MPC	B7Z6P1	cDNA FLJ53662, highly similar to Actin, alpha skeletal muscle	5	1	1	38,6	5,38
74	MPC	Q53GK6	Beta actin variant (Fragment)	4	1	1	41,7	5,48
75	MPC	V9GZN0	Histone H2A gene (lambda-HHG55) (Fragment)	19	1	1	5	11,9
76	MPC	U6A216	Mutant hemoglobin alpha 1 globin chain (Fragment)	69	4	4	10,7	8,48
77	MPC	P0C0S5	Histone H2A.Z	7	1	1	13,5	10,58
78	MPC	Q1KLZ0	HCG15971, isoform CRA_a	4	1	1	41,7	5,48
79	MPC	B4E2Z7	cDNA FLJ61562, highly similar to Asporin	9	1	1	27,5	5,99
80	MPC	H0YMM1	Annexin (Fragment)	11	1	1	16,4	5,91
81	MPC	Q5T8M8	Actin, alpha skeletal muscle	6	1	1	32	5,41
82	MPC	H6VRG0	Keratin 1	4	2	2	65,9	7,8
83	MPC	Q5EBM2	Uncharacterized protein	21	8	2	56,8	6,86
84	MPC	Q6S8J3	POTE ankyrin domain family member E	1	1	1	121,3	6,2
85	MPC	H0YNA0	Annexin (Fragment)	20	1	1	9,1	4,7
86	MPC	F8VZY2	Cysteine/serine-rich nuclear protein 2 (Fragment)	13	1	1	12,6	7,99
87	MPC	F8W1G8	Cysteine/serine-rich nuclear protein 2 (Fragment)	17	1	1	9,5	8,16
88	MPC	H0YL33	Annexin (Fragment)	11	1	1	16,4	5,17
89	MPC	P01860	Ig gamma-3 chain C region	29	8	2	41,3	7,9
90	MPC	C9J0D1	Histone H2A	7	1	1	13,2	9,99
91	MPC	Q96QV6	Histone H2A type 1-A	7	1	1	14,2	10,86

Table G.3 (Continues). The list of identified proteins in PsC

No.	Master	Accession	Description	Coverage [%]	# Peptides	# Unique Peptides	MW [kDa]	calc. pI
92	MPC	P68032	Actin, alpha cardiac muscle 1	4	1	1	42	5,39
93	MPC	Q6N030	Putative uncharacterized protein DKFZp686I15212	21	8	2	57	8,05
94	MPC	P01623	Ig kappa chain V-III region WOL	31	2	2	11,7	8,91
95	MPC	P02511	Alpha-crystallin B chain	22	2	2	20,1	7,33
96	MPC	P63261	Actin, cytoplasmic 2	4	1	1	41,8	5,48
97	MPC	H0YMU9	Annexin	7	1	1	25,6	5,97
98	MPC	G8FSY7	Beta actin (Fragment)	7	1	1	25,7	6,39
99	MPC	Q13707	ACTA2 protein (Fragment)	5	1	1	36,8	5,35
100	MPC	H0YNP5	Annexin (Fragment)	9	1	1	19,7	5,21
101	MPC	P0C0S8	Histone H2A type 1	7	1	1	14,1	10,9
102	MPC	B3KWQ3	cDNA FLJ43573 fis, clone RECTM2001691, highly similar to Actin, cytoplasmic 2	6	1	1	28,2	5,34
103	MPC	Q9H175	Cysteine/serine-rich nuclear protein 2	3	1	1	59,6	4,77
104	MPC	B7ZAP6	cDNA, FLJ79260, highly similar to Actin, cytoplasmic 2	5	1	1	33,1	5,64
105	MPC	Q71UI9	Histone H2A.V	7	1	1	13,5	10,58
106	MPC	B2R5B3	Histone H2A	7	1	1	14,1	11,06
107	MPC	B4DNH8	Annexin	8	1	1	21,7	6,35
108	MPC	Q7L7L0	Histone H2A type 3	7	1	1	14,1	11,05
109	MPC	B3KRQ1	Annexin	9	1	1	20,9	5,16
110	MPC	Q6FI13	Histone H2A type 2-A	7	1	1	14,1	10,9
111	MPC	Q16777	Histone H2A type 2-C	7	1	1	14	10,9
112	MPC	E9M4D4	Hemoglobin alpha-1 globin chain (Fragment)	69	4	4	10,8	8,48
113	MPC	B4DW52	cDNA FLJ55253, highly similar to Actin, cytoplasmic 1	5	1	1	38,6	5,35
114	MPC	Q9UL83	Myosin-reactive immunoglobulin light chain variable region (Fragment)	17	1	1	11,8	8,68
115	MPC	A0A087WXL8	Ig gamma-3 chain C region	21	8	2	56,9	8,25
116	MPC	A6NMY6	Putative annexin A2-like protein	5	1	1	38,6	6,95
117	MPC	F1BXA6	Beta-actin (Fragment)	15	1	1	12,2	6,05
118	MPC	P62736	Actin, aortic smooth muscle	4	1	1	42	5,39
119	MPC	B4DVQ0	cDNA FLJ58286, highly similar to Actin, cytoplasmic 2	5	1	1	37,3	5,71
120	MPC	P68133	Actin, alpha skeletal muscle	4	1	1	42	5,39
121	MPC	H0YM50	Annexin (Fragment)	6	1	1	28,4	5,83
122	MPC	P02768	Serum albumin	33	14	14	69,3	6,28
123	MPC	B4DUI8	cDNA FLJ52761, highly similar to Actin	5	1	1	37,3	5,55

Table G.3 (Continues). The list of identified proteins in PsC

No.	Master	Accession	Description	Coverage [%]	# Peptides	# Unique Peptides	MW [kDa]	calc. pI
124	MPC	Q5T8M7	Actin, alpha skeletal muscle	5	1	1	37,8	5,58
125	MPC	K4ENJ5	Beta actin (Fragment)	16	1	1	11	5
126	MPC	V9HW65	Annexin	5	1	1	38,6	7,75
127	MPC	A5GZ75	Beta-actin (Fragment)	11	1	1	16,8	5,58
128	MPC	E9PR44	Alpha-crystallin B chain (Fragment)	22	2	2	20	7,03
129	MPC	B3KW67	cDNA FLJ42347 fis, clone UTERU2003399, highly similar to Actin, gamma-enteric smooth muscle OS=Homo sapiens PE=2 SV=1	4	1	1	41,8	5,48
130	MPC	Q562R1	Beta-actin-like protein 2	4	1	1	42	5,59
131	MPC	Q9BX83	Hemoglobin alpha 1 globin chain (Fragment)	69	4	4	10,7	7,72
132	MPC	K4EP00	Beta actin (Fragment)	16	1	1	11	4,88
133	MPC	Q8NF17	FLJ00385 protein (Fragment)	21	8	2	56,1	7,59
134	MPC	H0YN42	Annexin (Fragment)	6	1	1	28,8	5,78
135	MPC	Q8IUE6	Histone H2A type 2-B	7	1	1	14	10,89
136	MPC	P20671	Histone H2A type 1-D	7	1	1	14,1	10,9
137	MPC	P01617	Ig kappa chain V-II region TEW	33	2	2	12,3	6
138	MPC	Q08AJ9	Histone H2A	7	1	1	14,1	11,05
139	MPC	Q9UL78	Myosin-reactive immunoglobulin light chain variable region (Fragment)	31	2	2	11,6	8,29
140	MPC	H0YN52	Annexin (Fragment)	27	1	1	6,8	4,88

Table G.4. The list of identified proteins in Cs

No.	Master	Accession	Description	Coverage [%]	# Peptides	# Unique Peptides	MW [kDa]	calc. pI
1	MP	A0A087WVW2	Ig gamma-3 chain C region	4	2	1	57,1	8,1
2	MP	B4DPP6	cDNA FLJ54371, highly similar to Serum albumin	6	2	2	70,3	6,09
3	MP	Q8TCD0	Uncharacterized protein	20	3	3	26,2	8,06
4	MP	Q7Z351	Putative uncharacterized protein DKFZp686N02209	9	3	2	52,8	8,48
5	MP	A0A075B6Z2	Protein TRAJ56 (Fragment)	38	1	1	2,2	10,29
6	MPC	Q6N096	Putative uncharacterized protein DKFZp686I15196	9	3	2	50,9	8,06
7	MPC	A0A0A0MS07	Ig gamma-1 chain C region (Fragment)	14	3	2	32	8,03
8	MPC	A0A087WV47	Ig gamma-1 chain C region	9	3	2	51,1	7,55
9	MPC	A0A087WYE1	Ig gamma-1 chain C region	9	3	2	52,1	7,55
10	MPC	F6KPG5	Albumin (Fragment)	6	2	2	66,5	6,04
11	MPC	Q6PYX1	Hepatitis B virus receptor binding protein (Fragment) 1	12	3	2	38,1	8,03
12	MPC	A0A087X010	Ig gamma-1 chain C region	9	3	2	50,8	8,18
13	MPC	A0A087WTX5	Ig kappa chain C region	20	3	3	25,6	7,97
14	MPC	Q5EBM2	Uncharacterized protein	4	2	1	56,8	6,86
15	MPC	Q6PIL8	IGK@ protein	20	3	3	25,8	6,55
16	MPC	B4DPR2	cDNA FLJ50830, highly similar to Serum albumin	7	2	2	59,5	7,17
17	MPC	A0A087WWV8	Protein IGKV1-8	21	3	3	25,6	8,5
18	MPC	Q6N095	Putative uncharacterized protein DKFZp686K03196	9	3	2	52,3	8,57
19	MPC	A0A087X130	Ig kappa chain C region	21	3	3	25,1	6,32
20	MPC	A8K9P0	cDNA FLJ78413, highly similar to Homo sapiens albumin, mRNA	6	2	2	69,2	6,28
21	MPC	V9HW68	Epididymis luminal protein 214	9	3	2	51,7	7,75
22	MPC	Q0KKI6	Immunoblobulin light chain (Fragment)	22	3	3	24	8,06
23	MPC	Q5EFE5	Anti-RhD monoclonal T125 gamma1 heavy chain	9	3	2	52,3	8,35
24	MPC	Q6N089	Putative uncharacterized protein DKFZp686P15220	9	3	2	51,7	7,93
25	MPC	Q6N093	Putative uncharacterized protein DKFZp686I04196 (Fragment)	5	2	1	46	7,59
26	MPC	Q68CN4	Putative uncharacterized protein DKFZp686E23209	5	2	1	51,5	7,56
27	MPC	Q6MZV7	Putative uncharacterized protein DKFZp686C11235	9	3	2	52,1	7,58
28	MPC	Q8NF17	FLJ00385 protein (Fragment)	4	2	1	56,1	7,59
29	MPC	Q6MZX7	Putative uncharacterized protein DKFZp686M24218	5	2	1	52,4	7,77
30	MPC	P01860	Ig gamma-3 chain C region	6	2	1	41,3	7,9

Table G.4 (Continues). The list of identified proteins in Cs

No.	Master	Accession	Description	Coverage [%]	# Peptides	# Unique Peptides	MW [kDa]	calc. pI
31	MPC	Q6N030	Putative uncharacterized protein DKFZp686I15212	4	2	1	57	8,05
32	MPC	Q6MZU6	Putative uncharacterized protein DKFZp686C15213	5	2	1	51,1	7,71
33	MPC	S6B291	IgG H chain	9	3	2	50,8	7,77
34	MPC	Q7Z3Y4	Uncharacterized protein	20	3	3	25,7	7,59
35	MPC	V9HW34	Epididymis luminal protein 213	20	3	3	25,6	6,55
36	MPC	A0A087WYC5	Ig gamma-1 chain C region	9	3	2	52,4	8,21
37	MPC	Q6MZQ6	Putative uncharacterized protein DKFZp686G11190	9	3	2	52	8,06
38	MPC	Q6N094	Putative uncharacterized protein DKFZp686O01196	9	3	2	52,6	8,18
39	MPC	Q6P5S8	IGK@ protein	20	3	3	25,8	6,33
40	MPC	A0A0A0MS08	Ig gamma-1 chain C region (Fragment)	10	3	2	43,9	6,96
41	MPC	P02768	Serum albumin	6	2	2	69,3	6,28
42	MPC	P01859	Ig gamma-2 chain C region	7	2	1	35,9	7,59
43	MPC	A0A087WXL8	Ig gamma-3 chain C region	4	2	1	56,9	8,25
44	MPC	A0A087WZW8	Protein IGKV3-11	21	3	3	25,6	6,01
45	MPC	P01834	Ig kappa chain C region	45	3	3	11,6	5,87
46	MPC	P01857	Ig gamma-1 chain C region	12	3	2	36,1	8,19
47	MPC	Q56G89	Serum albumin	6	2	2	69	6,2
48	MPC	Q6GMX0	Uncharacterized protein	20	3	3	25,8	7,97
49	MPC	A0A087X079	Ig gamma-1 chain C region	9	3	2	51,9	8,07
50	MPC	P01861	Ig gamma-4 chain C region	7	2	1	35,9	7,36
51	MPC	Q5EFE6	Anti-RhD monoclonal T125 kappa light chain	21	3	3	25,7	8,43
52	MPC	Q6N097	Putative uncharacterized protein DKFZp686H20196	9	3	2	52,7	8,48
53	MPC	A0N4V7	HCG2039797 (Fragment)	38	1	1	2,2	9,74
54	MPC	Q6GMX6	IGH@ protein	9	3	2	51,1	8,69
55	MPC	Q6PJF2	IGK@ protein	20	3	3	25,5	6,55
56	MPC	A0A075B6N8	Ig gamma-3 chain C region (Fragment)	6	2	1	41,3	7,9
57	MPC	A8K008	cDNA FLJ78387	9	3	2	51,6	8,16
58	MPC	A0A087WYL9	Ig kappa chain C region	21	3	3	25,6	8,5
59	MPC	A0A087X1C7	Ig gamma-1 chain C region	9	3	2	50,5	8,44

Table G.5. The list of identified proteins in CsT

No.	Master	Accession	Description	Coverage [%]	# Peptides	# Unique Peptides	MW [kDa]	calc. pI
1	MP	Q6GMX3	IGL@ protein	8	1	1	24,7	6,89
2	MP	A6NNU8	Nuclear receptor subfamily 0 group B member 1	9	1	1	11,8	8,31
3	MP	B4DPP6	cDNA FLJ54371, highly similar to Serum albumin	12	5	5	70,3	6,09
4	MP	F5H2R5	Rho GDP-dissociation inhibitor 2 (Fragment)	19	1	1	9,8	4,59
5	MP	E7DVW7	Membrane bound O-acyltransferase domain containing 4	3	1	1	49,7	8,47
6	MP	Q8TCD0	Uncharacterized protein	27	4	4	26,2	8,06
7	MP	Q68CN4	Putative uncharacterized protein DKFZp686E23209	10	4	2	51,5	7,56
8	MP	A0A075B6Z2	Protein TRAJ56 (Fragment)	38	1	1	2,2	10,29
9	MP	Q7Z351	Putative uncharacterized protein DKFZp686N02209	26	8	6	52,8	8,48
10	MP	A2NB46	Cold agglutinin FS-2 L-chain (Fragment)	17	1	1	11,9	9,01
11	MP	P63261	Actin, cytoplasmic 2	9	2	2	41,8	5,48
12	MP	Q99504	Eyes absent homolog 3	2	1	1	62,6	5,21
13	MP	Q8TC57	Meiosis 1 arrest protein	4	1	1	59,3	6,87
14	MP	Q68DX3	FERM and PDZ domain-containing protein 2	1	1	1	144,2	6,74
15	MP	B4DR52	Histone H2B	9	1	1	18	10,32
16	MP	Q9HB96	Fanconi anemia group E protein	2	1	1	58,7	5,24
17	MP	Q9BWT3	Poly(A) polymerase gamma	1	1	1	82,8	9,14
18	MPC	P0CG05	Ig lambda-2 chain C regions	18	1	1	11,3	7,24
19	MPC	Q6PYX1	Hepatitis B virus receptor binding protein (Fragment)	35	8	6	38,1	8,03
20	MPC	Q6N095	Putative uncharacterized protein DKFZp686K03196	26	8	6	52,3	8,57
21	MPC	A0A087X010	Ig gamma-1 chain C region	27	8	6	50,8	8,18
22	MPC	I6L9F7	Histone H2B (Fragment)	11	1	1	15,1	10,24
23	MPC	Q6GMW3	IGL@ protein	8	1	1	24,6	6,37
24	MPC	Q53G76	Beta actin variant (Fragment)	9	2	2	41,7	5,48
25	MPC	Q8WVW5	Putative uncharacterized protein (Fragment)	9	2	2	40,5	6,14
26	MPC	Q6PJG0	Uncharacterized protein	8	1	1	24,6	7,3
27	MPC	S6BAP8	IgG L chain	9	1	1	22,8	7,99
28	MPC	Q6PIL8	IGK@ protein	28	4	4	25,8	6,55
29	MPC	G3GAU4	Anti-H1N1 influenza HA kappa chain variable region (Fragment)	17	1	1	11,6	7,96
30	MPC	B4E335	cDNA FLJ52842, highly similar to Actin, cytoplasmic 1	10	2	2	39,2	5,59

Table G.5 (Continues). The list of identified proteins in CsT

No.	Master	Accession	Description	Coverage [%]	# Peptides	# Unique Peptides	MW [kDa]	calc. pI
1	MPC	Q1KLZ0	HCG15971, isoform CRA_a	9	2	2	41,7	5,48
32	MPC	Q6GMV8	Uncharacterized protein	8	1	1	24,9	6,67
33	MPC	A0A024QZZ7	Histone H2B	12	1	1	13,9	10,32
34	MPC	Q8N355	IGL@ protein	8	1	1	24,8	6,37
35	MPC	A0A075B6K9	Ig lambda-2 chain C regions (Fragment)	18	1	1	11,3	7,24
36	MPC	Q6PJR7	Beta-2-microglobulin	14	1	1	14,7	6,73
37	MPC	Q5EFE6	Anti-RhD monoclonal T125 kappa light chain	28	4	4	25,7	8,43
38	MPC	Q93079	Histone H2B type 1-H	12	1	1	13,9	10,32
39	MPC	S6C4S2	IgG L chain	9	1	1	22,8	8,07
40	MPC	Q96T53	Ghrelin O-acyltransferase	3	1	1	49,7	8,47
41	MPC	Q53GK6	Beta actin variant (Fragment)	9	2	2	41,7	5,48
42	MPC	A0A087WYC5	Ig gamma-1 chain C region	26	8	6	52,4	8,21
43	MPC	V9HW68	Epididymis luminal protein 214	26	8	6	51,7	7,75
44	MPC	A0A075B6L1	Ig lambda-7 chain C region (Fragment)	18	1	1	11,3	8,29
45	MPC	A0A087WWV8	Protein IGKV1-8	28	4	4	25,6	8,5
46	MPC	B4DPR2	cDNA FLJ50830, highly similar to Serum albumin	15	5	5	59,5	7,17
47	MPC	O60814	Histone H2B type 1-K	12	1	1	13,9	10,32
48	MPC	P0CF74	Ig lambda-6 chain C region	18	1	1	11,3	7,24
49	MPC	Q6IN99	IGL@ protein	8	1	1	24,9	6,74
50	MPC	Q8N5F4	IGL@ protein	8	1	1	24,9	5,34
51	MPC	F6KPG5	Albumin (Fragment)	13	5	5	66,5	6,04
52	MPC	Q99880	Histone H2B type 1-L	12	1	1	13,9	10,32
53	MPC	A0A087WV47	Ig gamma-1 chain C region	26	8	6	51,1	7,55
54	MPC	Q6N093	Putative uncharacterized protein DKFZp686I04196 (Fragment)	11	4	2	46	7,59
55	MPC	A2NUT2	Lambda-chain (AA -20 to 215)	8	1	1	24,6	7,62
56	MPC	Q6MZV7	Putative uncharacterized protein DKFZp686C11235	26	8	6	52,1	7,58
57	MPC	B4DW52	cDNA FLJ55253, highly similar to Actin, cytoplasmic 1	10	2	2	38,6	5,35
58	MPC	S6BGF9	IgG L chain	9	1	1	22,7	8
59	MPC	P23527	Histone H2B type 1-O	12	1	1	13,9	10,32
60	MPC	P01623	Ig kappa chain V-III region WOL	17	1	1	11,7	8,91
61	MPC	U3KQK0	Histone H2B	9	1	1	18,8	10,54
62	MPC	S6C4Q9	IgG L chain	9	1	1	22,8	6,76
63	MPC	S6B2B0	IgG L chain	9	1	1	23,1	8,53

Table G.5 (Continues). The list of identified proteins in CsT

No.	Master	Accession	Description	Coverage [%]	# Peptides	# Unique Peptides	MW [kDa]	calc. pI
64	MPC	S6B291	IgG H chain	26	8	6	50,8	7,77
65	MPC	Q99877	Histone H2B type 1-N	12	1	1	13,9	10,32
66	MPC	Q7Z3Y4	Uncharacterized protein	28	4	4	25,7	7,59
67	MPC	A0M8Q6	Ig lambda-7 chain C region	18	1	1	11,3	8,28
68	MPC	A8K9J7	Histone H2B	12	1	1	14	10,32
69	MPC	Q567P1	IGL@ protein	8	1	1	24,8	7,3
70	MPC	Q6PIQ7	IGL@ protein	8	1	1	25	7,97
71	MPC	P06899	Histone H2B type 1-J	12	1	1	13,9	10,32
72	MPC	P0CG06	Ig lambda-3 chain C regions	18	1	1	11,2	7,24
73	MPC	Q6N089	Putative uncharacterized protein DKFZp686P15220	26	8	6	51,7	7,93
74	MPC	Q5EFE5	Anti-RhD monoclonal T125 gamma1 heavy chain	26	8	6	52,3	8,35
75	MPC	P62807	Histone H2B type 1-C/E/F/G/I	12	1	1	13,9	10,32
76	MPC	Q7Z2U7	Uncharacterized protein	8	1	1	25	6,38
77	MPC	Q8TCJ5	Putative uncharacterized protein DKFZp667J0810 (Fragment)	18	1	1	11,3	7,24
78	MPC	S6BAR0	IgG L chain	9	1	1	23,1	7,69
79	MPC	B4E3A4	cDNA FLJ57283, highly similar to Actin, cytoplasmic 2	10	2	2	39,8	5,38
80	MPC	Q0D2M2	HIST1H2BC protein	12	1	1	13,8	10,39
81	MPC	S6AWE6	IgG L chain	9	1	1	22,9	8,43
82	MPC	P01620	Ig kappa chain V-III region SIE	17	1	1	11,8	8,48
83	MPC	A0A087WYE1	Ig gamma-1 chain C region	26	8	6	52,1	7,55
84	MPC	B4DVQ0	cDNA FLJ58286, highly similar to Actin, cytoplasmic 2	10	2	2	37,3	5,71
85	MPC	A0A087WTX5	Ig kappa chain C region	28	4	4	25,6	7,97
86	MPC	A0A087X130	Ig kappa chain C region	28	4	4	25,1	6,32
87	MPC	V9HW34	Epididymis luminal protein 213	28	4	4	25,6	6,55
88	MPC	A8K9P0	cDNA FLJ78413, highly similar to Homo sapiens albumin, mRNA	13	5	5	69,2	6,28
89	MPC	P57053	Histone H2B type F-S	12	1	1	13,9	10,37
90	MPC	Q0KKI6	Immunoblobulin light chain (Fragment)	30	4	4	24	8,06
91	MPC	Q8N257	Histone H2B type 3-B	12	1	1	13,9	10,32
92	MPC	Q9UL78	Myosin-reactive immunoglobulin light chain variable region (Fragment)	17	1	1	11,6	8,29
93	MPC	Q8NEJ1	Uncharacterized protein	8	1	1	25	7,69
94	MPC	Q6PJF2	IGK@ protein	28	4	4	25,5	6,55

Table G.5 (Continues). The list of identified proteins in CsT

No.	Master	Accession	Description	Coverage [%]	# Peptides	# Unique Peptides	MW [kDa]	calc. pI
95	MPC	Q6MZQ6	Putative uncharacterized protein DKFZp686G11190	26	8	6	52	8,06
96	MPC	A0N4V7	HCG2039797 (Fragment)	38	1	1	2,2	9,74
97	MPC	S6BGD6	IgG L chain	8	1	1	24,8	7,24
98	MPC	Q5FWF9	IGL@ protein	8	1	1	24,8	5,59
99	MPC	S6B286	IgG L chain	9	1	1	22,9	8,44
100	MPC	Q6N097	Putative uncharacterized protein DKFZp686H20196	26	8	6	52,7	8,48
101	MPC	Q6GMX6	IGH@ protein	26	8	6	51,1	8,69
102	MPC	P01834	Ig kappa chain C region	61	4	4	11,6	5,87
103	MPC	P02768	Serum albumin	13	5	5	69,3	6,28
104	MPC	Q6N094	Putative uncharacterized protein DKFZp686O01196	26	8	6	52,6	8,18
105	MPC	S6C4R7	IgG L chain	9	1	1	22,5	8,24
106	MPC	Q2TAI9	PAPOLG protein (Fragment)	2	1	1	58,1	8,32
107	MPC	P01859	Ig gamma-2 chain C region	14	4	2	35,9	7,59
108	MPC	Q16778	Histone H2B type 2-E	12	1	1	13,9	10,32
109	MPC	A0A0A0MS08	Ig gamma-1 chain C region (Fragment)	31	8	6	43,9	6,96
110	MPC	B3KX03	cDNA FLJ44410 fis, clone TUTER2002729, moderately similar to Mus musculus DNA segment, Chr 6, Miriam Meisler 5, expressed (D6Mm5e) OS=Homo sapiens PE=2 SV=1	8	1	1	31,6	8,25
111	MPC	A0A075B6L0	Ig lambda-3 chain C regions (Fragment)	18	1	1	11,3	7,24
112	MPC	P04206	Ig kappa chain V-III region GOL	17	1	1	11,8	9,25
113	MPC	B4E1N9	cDNA FLJ53430, highly similar to Homo sapiens FERM and PDZ domain containing 2 (FRMPD2), transcript variant 3, mRNA (Fragment) OS=Homo sapiens PE=2 SV=1	2	1	1	93,5	7,56
114	MPC	Q53T17	Putative uncharacterized protein PAPOLG (Fragment)	2	1	1	53,2	6,89
115	MPC	A8K008	cDNA FLJ78387	26	8	6	51,6	8,16
116	MPC	Q6IPQ0	IGL@ protein	8	1	1	24,8	6,76
117	MPC	Q5QNW6	Histone H2B type 2-F	12	1	1	13,9	10,32
118	MPC	Q6GMX4	IGL@ protein	8	1	1	24,8	6,89
119	MPC	A0A087X079	Ig gamma-1 chain C region	26	8	6	51,9	8,07
120	MPC	Q99879	Histone H2B type 1-M	12	1	1	14	10,32

Table G.5 (Continues). The list of identified proteins in CsT

No.	Master	Accession	Description	Coverage [%]	# Peptides	# Unique Peptides	MW [kDa]	calc. pI
121	MPC	Q6P5S8	IGK@ protein	28	4	4	25,8	6,33
122	MPC	P01622	Ig kappa chain V-III region Ti	17	1	1	11,8	8,5
123	MPC	A0A087WZW8	Protein IGKV3-11	28	4	4	25,6	6,01
124	MPC	A0A087WYL9	Ig kappa chain C region	28	4	4	25,6	8,5
125	MPC	A0A5E4	Uncharacterized protein	8	1	1	24,7	5,94
126	MPC	Q6N096	Putative uncharacterized protein DKFZp686I15196	26	8	6	50,9	8,06
127	MPC	Q6GMX0	Uncharacterized protein	28	4	4	25,8	7,97
128	MPC	Q05DB9	PAPOLG protein (Fragment)	2	1	1	57	8,75
129	MPC	P01857	Ig gamma-1 chain C region	37	8	6	36,1	8,19
130	MPC	C6KXN3	Lambda light chain of human immunoglobulin surface antigen-related protein (Fragment)	8	1	1	24,7	5,54
131	MPC	B1APR7	Eyes absent homolog 3	3	1	1	45,5	5,85
132	MPC	A0A087X1C7	Ig gamma-1 chain C region	27	8	6	50,5	8,44
133	MPC	Q53G99	Beta actin variant (Fragment)	9	2	2	41,7	5,59
134	MPC	S6BAN6	IgG L chain	9	1	1	22,9	8,31
135	MPC	P33778	Histone H2B type 1-B	12	1	1	13,9	10,32

Table G.6. The list of identified proteins in CsC

No.	Master	Accession	Description	Coverage [%]	# Peptides	# Unique Peptides	MW [kDa]	calc. pI
1	MP	Q7Z351	Putative uncharacterized protein DKFZp686N02209	17	6	3	52,8	8,48
2	MP	Q8TCD0	Uncharacterized protein	20	3	3	26,2	8,06
3	MP	F8W6M1	Tubulin polyglutamylase TTLL11	1	1	1	87,6	8,87
4	MP	Q14473	Beta-globin gene from a thalassemia patient	13	2	2	18,9	6,79
5	MP	A0A087WVW2	Ig gamma-3 chain C region	9	4	1	57,1	8,1
6	MP	B2RBD5	cDNA, FLJ95457, highly similar to Homo sapiens tubulin, beta, 4 (TUBB4), mRNA	4	1	1	50,4	4,93
7	MP	B4DI63	cDNA FLJ59205, highly similar to Mimecan	3	1	1	40,5	7,99
8	MP	B4DPP6	cDNA FLJ54371, highly similar to Serum albumin	12	5	5	70,3	6,09
9	MP	Q96BY6	Dedicator of cytokinesis protein 10	1	1	1	249,4	7,14
10	MP	A0A075B6Z2	Protein TRAJ56 (Fragment)	38	1	1	2,2	10,29
11	MPC	B5ANL9	Beta globin chain (Fragment	26	2	2	9,5	6,79
12	MPC	Q6MZQ6	Putative uncharacterized protein DKFZp686G11190	17	6	3	52	8,06
13	MPC	Q0Z944	Beta globin (Fragment)	22	2	2	11,5	6,37
14	MPC	B3VL31	Beta globin (Fragment)	22	2	2	11,5	6,68
15	MPC	Q9UBV6	Beta-globin (Fragment)	38	2	2	6,7	5,17
16	MPC	Q53G92	Tubulin, beta, 4 variant (Fragment)	4	1	1	50,3	4,93
17	MPC	Q4W4X9	Dopamine receptor interacting protein 2 (Fragment)	3	1	1	80,1	7,46
18	MPC	Q5EBM2	Uncharacterized protein	9	4	1	56,8	6,86
19	MPC	B4DF07	cDNA FLJ59487, highly similar to Dedicator of cytokinesis protein 10	2	1	1	116	8,15
20	MPC	Q9GZL9	Beta-globin (Fragment)	20	2	2	12,5	6,37
21	MPC	V9HW68	Epididymis luminal protein 214	18	6	3	51,7	7,75
22	MPC	A0A087WYC5	Ig gamma-1 chain C region	17	6	3	52,4	8,21
23	MPC	D5FZW3	Beta globin (Fragment)	56	2	2	4,5	5,83
24	MPC	A9YUX2	Truncated beta-globin	37	2	2	7	8,22
25	MPC	Q5EFE6	Anti-RhD monoclonal T125 kappa light chain	21	3	3	25,7	8,43
26	MPC	Q9BWV6	Mutant beta globin	21	2	2	12,2	6,05
27	MPC	A0A075B6N8	Ig gamma-3 chain C region (Fragment)	12	4	1	41,3	7,9
28	MPC	Q14484	Beta-globin (Fragment)	38	2	2	6,7	4,88
29	MPC	Q6PJF2	IGK@ protein	20	3	3	25,5	6,55
30	MPC	A0N4V7	HCG2039797 (Fragment)	38	1	1	2,2	9,74
31	MPC	D9YZU5	Hemoglobin, beta	16	2	2	16	7,28

Table G.6 (Continues). The list of identified proteins in CsC

No.	Master	Accession	Description	Coverage [%]	# Peptides	# Unique Peptides	MW [kDa]	calc. pI
32	MPC	Q6V0K9	Mutant hemoglobin beta chain (Fragment)	22	2	2	11,5	6,68
33	MPC	A0A087WWV8	Protein IGKV1-8	21	3	3	25,6	8,5
34	MPC	A0A087X010	Ig gamma-1 chain C region	18	6	3	50,8	8,18
35	MPC	Q6PYX1	Hepatitis B virus receptor binding protein (Fragment)	24	6	3	38,1	8,03
36	MPC	Q6N095	Putative uncharacterized protein DKFZp686K03196	17	6	3	52,3	8,57
37	MPC	Q3LIC8	Putative uncharacterized protein Nbla10300 (Fragment)	5	1	1	53,1	5,97
38	MPC	Q7Z3Y4	Uncharacterized protein	20	3	3	25,7	7,59
39	MPC	S6B291	IgG H chain	18	6	3	50,8	7,77
40	MPC	Q6N030	Putative uncharacterized protein DKFZp686I15212	9	4	1	57	8,05
41	MPC	P01860	Ig gamma-3 chain C region	12	4	1	41,3	7,9
42	MPC	Q9BV28	TUBB3 protein (Fragment)	4	1	1	45,6	5
43	MPC	Q8NF17	FLJ00385 protein (Fragment)	9	4	1	56,1	7,59
44	MPC	Q6MZV7	Putative uncharacterized protein DKFZp686C11235	18	6	3	52,1	7,58
45	MPC	Q4ZG60	Putative uncharacterized protein DOCK10	4	1	1	62,3	6,19
46	MPC	Q6N089	Putative uncharacterized protein DKFZp686P15220	18	6	3	51,7	7,93
47	MPC	Q5EFE5	Anti-RhD monoclonal T125 gamma1 heavy chain	17	6	3	52,3	8,35
48	MPC	B4DEY4	cDNA FLJ59486, highly similar to Dedicator of cytokinesis protein 10	3	1	1	97,8	8,02
49	MPC	Q52MT0	Beta globin (Fragment)	22	2	2	11,5	6,37
50	MPC	Q0KKI6	Immunoblobulin light chain (Fragment)	22	3	3	24	8,06
51	MPC	B3VL86	Mutant beta-globin	17	2	2	14,9	6,77
52	MPC	A8K9P0	cDNA FLJ78413, highly similar to Homo sapiens albumin, mRNA	12	5	5	69,2	6,28
53	MPC	V9HW34	Epididymis luminal protein 213	20	3	3	25,6	6,55
54	MPC	A0A087X130	Ig kappa chain C region	21	3	3	25,1	6,32
55	MPC	A0A087WTX5	Ig kappa chain C region	20	3	3	25,6	7,97
56	MPC	A8K0R3	Osteoglycin (Osteoinductive factor, mimecan), isoform CRA_a	3	1	1	33,9	5,63
57	MPC	A0A0A0MS07	Ig gamma-1 chain C region (Fragment)	28	6	3	32	8,03
58	MPC	A0A087W	Ig gamma-1 chain C	18	6	3	51,1	7,55

Table G.6 (Continues). The list of identified proteins in CsC

No.	Master	Accession	Description	Coverage [%]	# Peptides	# Unique Peptides	MW [kDa]	calc. pI
		V47	V47 region					
9	MPC	A0A087WYE1	Ig gamma-1 chain C region	17	6	3	52,1	7,55
60	MPC	F6KPG5	Albumin (Fragment)	13	5	5	66,5	6,04
61	MPC	Q9BXA2	Beta-globin (Fragment)	39	2	2	6,5	4,64
62	MPC	A0A087WYL9	Ig kappa chain C region	21	3	3	25,6	8,5
63	MPC	H0YFC5	Dedicator of cytokinesis protein 10 (Fragment)	12	1	1	22,2	8,44
64	MPC	Q3LR79	Hemoglobin beta (Fragment)	22	2	2	11,5	5,77
65	MPC	Q6PIL8	IGK@ protein	20	3	3	25,8	6,55
66	MPC	B3VL05	Beta globin (Fragment)	22	2	2	11,5	6,68
67	MPC	Q13509	Tubulin beta-3 chain	4	1	1	50,4	4,93
68	MPC	Q8IUL9	Hemoglobin beta chain variant Hb.Sinai-Bel Air (Fragment)	22	2	2	11,5	6,05
69	MPC	Q4TZM4	Hemoglobin beta chain (Fragment)	23	2	2	11	6,52
70	MPC	Q6N094	Putative uncharacterized protein DKFZp686O01196	17	6	3	52,6	8,18
71	MPC	Q8NHH1	Tubulin polyglutamylase TTLL11	2	1	1	58	9,2
72	MPC	Q7Z532	Osteoglycin OG	3	1	1	33,9	5,48
73	MPC	Q6P5S8	IGK@ protein	20	3	3	25,8	6,33
74	MPC	A0A087X079	Ig gamma-1 chain C region	18	6	3	51,9	8,07
75	MPC	A0A087WU58	Tubulin polyglutamylase TTLL11 (Fragment)	7	1	1	13,6	9,29
76	MPC	C8C504	Beta-globin	16	2	2	16	8,06
77	MPC	A8K008	cDNA FLJ78387	18	6	3	51,6	8,16
78	MPC	Q8IZI0	Hemoglobin beta chain variant Hb-I_Toulouse (Fragment)	22	2	2	11,5	5,71
79	MPC	Q5TBF5	Mimecan (Fragment)	3	1	1	30,4	8,34
80	MPC	Q6GMX0	Uncharacterized protein	20	3	3	25,8	7,97
81	MPC	P01857	Ig gamma-1 chain C region	25	6	3	36,1	8,19
82	MPC	Q68DA4	Putative uncharacterized protein DKFZp781A1532	2	1	1	135,6	7,68
83	MPC	P02768	Serum albumin	12	5	5	69,3	6,28
84	MPC	F8W6P5	Hemoglobin subunit beta (Fragment)	26	2	2	9,7	6,79
85	MPC	Q6N096	Putative uncharacterized protein DKFZp686I15196	18	6	3	50,9	8,06
86	MPC	E9NGZ5	Hemoglobin beta globin chain (Fragment)	22	2	2	11,5	6,37
87	MPC	A0A087WZW8	Protein IGKV3-11	21	3	3	25,6	6,01
88	MPC	E9M263	Hemoglobin beta chain (Fragment)	40	2	2	6,2	4,64

Table G.6 (Continues). The list of identified proteins in CsC

No.	Master	Accession	Description	Coverage [%]	# Peptides	# Unique Peptides	MW [kDa]	calc. pI
89	MPC	P01834	Ig kappa chain C region	45	3	3	11,6	5,87
90	MPC	A0A0A0MS08	Ig gamma-1 chain C region (Fragment)	21	6	3	43,9	6,96
91	MPC	A0A087X1C7	Ig gamma-1 chain C region	18	6	3	50,5	8,44
92	MPC	Q6N097	Putative uncharacterized protein DKFZp686H20196	17	6	3	52,7	8,48
93	MPC	A0A087WXL8	Ig gamma-3 chain C region	9	4	1	56,9	8,25
94	MPC	Q6GMX6	IGH@ protein	18	6	3	51,1	8,69
95	MPC	Q9BWU5	Mutant hemoglobin beta chain (Fragment)	22	2	2	11,5	7,05
96	MPC	Q9UP81	Mutant beta-globin	26	2	2	9,7	8,19

PUBLICATIONS AND WORKS

Ceylan Y., Akpınar G., Doger E., Kasap M., Guzel N., **Karaosmanoglu K**., Kopuk S.Y., Yucesoy I., Proteomic Analysis in Endometrial Cancer and Endometrial Hyperplasia Tissues by 2D-DIGE Technique, *J Gynecol Obstet Hum Reprod*, 2020, **49**(2), 101652.

Cevik S., Akpinar G., Yildizli A., Kasap M., **Karaosmanoglu K**., Unyayar S., Comparative Physiological and Leaf Proteome Analysis between Drought-tolerant Chickpea *Cicer reticulatum* and Drought-sensitive Chickpea *C. arietinum*, *J Biosci*, 2019, **44**, 20.

Yoneten K.K., Kasap M., Akpinar G., Kanli A., Karaoz E., Comparative Proteomics Analysis of Four Commonly Used Methods for Identification of Novel Plasma Membrane Proteins, *The Journal of Membrane Biology*, 2019, **252**(6), 587-608.

Yoneten K.K., Kasap M., Akpinar G., Gunes A, Gurel B, Utkan N.Z., Comparative Proteome Analysis of Breast Cancer Tissues Highlights the Importance of Glycerol-3-phosphate Dehydrogenase 1 and Monoacylglycerol Lipase in Breast Cancer Metabolism, 2019, *Cancer Genomics& Proteomics*, **16**(5), 377-397.

Coskun A., Baykal A.T., Senal M.O., Kazan D., Kaya E., Emiroglu R., Yilmaz S., Dundar H.Z., Akgoz M., Berber I., Aktas H., Bilsel G., **Karaosmanoglu K**., Cetiner B., Arslan C., Yurtsever I., Yazıcı C., Proteomic Analysis of Liver Preservation Solutions Prior to Liver Transplantation, *Current Proteomics*, 2018, **15**(5), 1-17.

Kanli A., Kasap M., **Yoneten K.K**., Akpinar G., Gulkac M.D., Identification of Differentially Regulated Deceitful Proteins in SH-SY5Y Cells Engineered with Tet-regulated Protein Expression System, *Journal of Cellular Biochemistry*, 2017, **119**(7), 6065-6071.

Guzel N., Kasap M., Kanli A., Akpinar G., Gulkac M.D., **Karaosmanoglu K**., Exogenous Expressions of FTO Wild-Type and R316Q Mutant Proteins Caused an Increase in HNRPK Levels in 3T3-L1 Cells as Demonstrated by DIGE Analysis, *Hindawi BioMed Research International*, 2017, **2017**, 8216180.

Budeyri G.N., Avci F.G., **Yoneten K.K**., Alaybeyoglu B., Ozkirimli E., Sayar N.A., Kazan D., Sariyar AKBULUT B., Response of Escherichia coli to Prolonged Berberine Exposure, *Microb Drug Resist*, 2017, **23**(5), 531-544.

Kasap M., Karadenizli A., Akpınar G., Uzuner H., Ayimugu A., **Karaosmanoğlu K**., Er D.K., Comparative Analysis of Proteome Patterns of *Francisella tularensis* Isolates from Patients and the Environment, *Curr Microbiol*, 2017, **74**(2), 230-238.

Pinar O., **Karaosmanoğlu K**., Sayar N.A., Kula C., Kazan D., Sayar A.A., Assessment of Hazelnut Husk as a Lignocellulosic Feedstock for the Production of fermentable Sugars and Lignocellulolytic Enzymes, *3 Biotech*, 2017, **7**(6), 367.

Coskun A., Baykal A.T., Kazan D., Akgoz M., Senal M.O., Berber I., Titiz I., Bilsel G., Kilercik H., **Karaosmanoglu K**., Cicek M., Yurtsever I., Yazıcı C., Proteomic Analysis of Kidney Preservation Solutions Prior to Renal Transplantation, *PLoS One*, 2016, **11**(12), e0168755.

Ozgul S., Kasap M., Akpinar G., Kanli A., Guzel N., **Karaosmanoglu K**., Baykal A. T., Iseri P., Linking a compound-heterozygous Parkin mutant (Q311R and A371T) to Parkinson's disease by using proteomic and molecular approaches, *Neurochemistry International*, 2015, **85-86**, 1–13.

Karaosmanoğlu K., Sayar N.A., Kurnaz Aksan I., Sariyar Akbulut B., Assessment of Berberine as a Multi-target Antimicrobial: A Multi-omics Study for Drug Discovery and Repositioning, *OMICS A Journal of Integrative Biology*, 2013, **18**(1), 42-53.

Karaosmanoglu K., Kasap M., Akpinar G., Gurel B., Utkan N.Z., Comparative Proteome Analysis Of Breast Cancer Tissues To Investigate Breast Cancer Metabolism, *Molecular Biology of the Cell*, Meeting abstract, 2019.

Karaosmanoglu K., Gunes A., Kasap M., Utkan N.Z., Akpinar G., Guler S.A, Tissue proteome analysis of hormone receptor-positive breast cancer, *Molecular Biology of the Cell*, Meeting abstract, 2017, **28**.

Karaosmanoglu K., Akbulut B., Kurnaz A.I., Response of *Escherichia coli* to Berberine, *The FEBS Journal*, Supplement 1, Meeting abstract, 2012, **279**, 232-232.

Coskun A., Kazan D., Akgoz M., **Karaosmanoglu K**., et al., Proteomic Evaluation of Preservation Solutions Prior to Kidney Transplantation, *The FEBS Journal*, Supplement 1, Meeting abstract, 2012, **279**, 235-235.

Ozbalci C., **Karaosmanoglu K**., Kurnaz A.I., Akbulut B. Comparative Transcriptome and Proteome Analysis for the Effect of Berberine, *The FEBS Journal*, Supplement 1, Meeting abstract, 2010, **277**, 184-185.

BIOGRAPHY

She was born in 1986 in Istanbul. She completed his primary, secondary and high school education in Istanbul. She went to Istanbul University, Faculty of Life Sciences, Department of Biology in 2005 and graduated in 2009. She completed her master's degree at Marmara University, Institute of Life Sciences, Department of Bioengineering, between 2009 and 2012. She started her doctoral education at Marmara University in 2013. She has not completed her doctoral education at Marmara University and applied to Kocaeli University for research assistant position and finally has started her doctoral education at Kocaeli University, Faculty of Technology, Department of Biomedical Engineering in 2014. She has been working as a research assistant at Kocaeli University since 2014.